DOCTORAL THESIS

FAULT DIAGNOSIS TOOLS IN MULTIVARIATE STATISTICAL PROCESS AND QUALITY CONTROL

UNIVERSITAT POLITÈCNICA DE VALÈNCIA

Santiago Vidal Puig

Supervisor:

Dr. Alberto J. Ferrer Riquelme

UNIVERSIDAD POLITÉCNICA DE VALENCIA

DEPARTAMENTO DE ESTADÍSTICA
E INVESTIGACIÓN OPERATIVA
APLICADAS Y CALIDAD

FAULT DIAGNOSIS TOOLS IN MULTIVARIATE STATISTICAL PROCESS AND QUALITY CONTROL

SANTIAGO VIDAL PUIG

Valencia 2015

Director: Dr. Alberto José Ferrer Riquelme

Agradecimientos

En primer lugar debo agradecer, a todos aquellos que habéis creído en mí, por el apoyo que me habéis dado y que sin duda ha sido clave para poder concluir esta Tesis. En especial, a mi familia y a mis amigos sin los cuales todo hubiera sido, sin duda, más difícil. También agradezco a mis compañeros del Departamento de Estadística por su apoyo personal y humano.

De manera especial y sincera también debo agradecer al Profesor Alberto Ferrer Riquelme, mi director de tesis, por la dedicación, apoyo y confianza que me ha dado a lo largo de este extenso trabajo y especialmente por haberme guiado desde mis inicios en investigación.

A todos muchas gracias!

Para vosotros!

Abstract

An accurate fault diagnosis of both, faults sensors and real process faults have become more and more important for process monitoring (minimize downtime, increase safety of plant operation and reduce the manufacturing cost). Quick and correct fault diagnosis is required in order to put back on track our processes or products before safety or quality can be compromised. In the study and comparison of the fault diagnosis methodologies, this thesis distinguishes between two different scenarios, methods for multivariate statistical quality control (MSQC) and methods for latent-based multivariate statistical process control: (Lb-MSPC). In the first part of the thesis the state of the art on fault diagnosis and identification (FDI) is introduced. The second part of the thesis is devoted to the fault diagnosis in multivariate statistical quality control (MSQC). The rationale of the most extended methods for fault diagnosis in supervised scenarios, the requirements for their implementation, their strong points and their drawbacks and relationships are discussed. The performance of the methods is compared using different performance indices in two different process data sets and simulations. New variants and methods to improve the diagnosis performance in MSQC are also proposed. The third part of the thesis is devoted to the fault diagnosis in latent-based multivariate statistical process control (Lb-MSPC). The rationale of the most extended methods for fault diagnosis in supervised Lb-MSPC is described and one of our proposals, the Fingerprints contribution plots (FCP) is introduced. Finally the thesis presents and compare the performance results of these diagnosis methods in Lb-MSPC. The diagnosis results in two process data sets are compared using a new strategy based in the use of the overall sensitivity and specificity.

Resumen

La realización de un diagnóstico preciso de los fallos, tanto si se trata de fallos de sensores como si se trata de fallos de procesos, ha llegado a ser algo de vital importancia en la monitorización de procesos (reduce las paradas de planta, incrementa la seguridad de la operación en planta y reduce los costes de producción). Se requieren diagnósticos rápidos y correctos si se quiere poder recuperar los procesos o productos antes de que la seguridad o la calidad de los mismos se pueda ver comprometida. En el estudio de las diferentes metodologías para el diagnóstico de fallos esta tesis distingue dos escenarios diferentes, métodos para el control de estadístico multivariante de la calidad (MSQC) y métodos para el control estadístico de procesos basados en el uso de variables latentes (Lb-MSPC). En la primera parte de esta tesis se introduce el estado del arte sobre el diagnóstico e identificación de fallos (FDI). La segunda parte de la tesis está centrada en el estudio del diagnóstico de fallos en control estadístico multivariante de la calidad. Se describen los fundamentos de los métodos más extendidos para el diagnóstico en escenarios supervisados, sus requerimientos para su implementación sus puntos fuertes y débiles y sus posibles relaciones. Los resultados de diagnóstico de los métodos es comparado usando diferentes índices sobre los datos procedentes de dos procesos reales y de diferentes simulaciones. En la tesis se proponen nuevas variantes que tratan de mejorar los resultados obtenidos en MSQC. La tercera parte de la tesis está dedicada al diagnóstico de fallos en control estadístico multivariante de procesos basados en el uso de modelos de variables latentes (Lb-MSPC). Se describe los fundamentos de los métodos mas extendidos en el diagnóstico de fallos en Lb-MSPC supervisado y se introduce una de nuestras propuestas, el fingerprint contribution plot (FCP). Finalmente la tesis presenta y compara los resultados de diagnóstico de los métodos propuestos en

Lb-MSPC. Los resultados son comparados sobre los datos de dos procesos usando una nueva estrategia basada en el uso de la sensitividad y especificidad promedia.

Resum

La realització d'un diagnòstic precís de les fallades, tant si es tracta de fallades de sensors com si es tracta de fallades de processos, ha arribat a ser de vital importància en la monitorització de processos (reduïx les parades de planta, incrementa la seguretat de l'operació en planta i reduïx els costos de producció) . Es requerixen diagnòstics ràpids i correctes si es vol poder recuperar els processos o productes abans de que la seguretat o la qualitat dels mateixos es puga veure compromesa. En l'estudi de les diferents metodologies per al diagnòstic de fallades esta tesi distingix dos escenaris diferents, mètodes per al control estadístic multivariant de la qualitat (MSQC) i l mètodes per al control estadístic de processos basats en l'ús de variables latents (Lb-MSPC). En la primera part d'esta tesi s'introduïx l'estat de l'art sobre el diagnòstic i identificació de fallades (FDI). La segona part de la tesi està centrada en l'estudi del diagnòstic de fallades en control estadístic multivariant de la qualitat. Es descriuen els fonaments dels mètodes més estesos per al diagnòstic en escenaris supervisats, els seus requeriments per a la seua implementació els seus punts forts i febles i les seues possibles relacions. Els resultats de diagnòstic dels mètodes és comparat utilitzant diferents índexs sobre les dades procedents de dos processos reals i de diferents simulacions. En la tesi es proposen noves variants que tracten de millorar els resultats obtinguts en MSQC. La tercera part de la tesi està dedicada al diagnòstic de fallades en control estadístic multivariant de processos basat en l'ús de models de variables latents (Lb-MSPC). Es descriu els fonaments dels mètodes més estesos en el diagnòstic de fallades en MSPC supervisat i s'introdueix una nova proposta, el fingerprint contribution plot (FCP). Finalment la tesi presenta i compara els resultats de diagnòstic dels mètodes proposats en MSPC. Els resultats són comparats sobre les dades de dos processos utilitzant una nova estratègia basada en l'ús de la sensibilitat i especificitat mitjana.

CONTENTS

Justification, Objectives and Contributions

Justification

For centuries the only way to learn about malfunctions and their location was by biological senses (changes in shape or color, unusual sounds, unusual vibrations and fumes). Later, the great advances in the development of new measuring devices served to provide more exact information about important physical variables. However, these devices (sensors) also proved prone to malfunction raising the dilemma of false alarms. The existence of fault sensors became even more critical in automatic control of machines or processes, where the effects of such malfunctions finally derived into more devastating real process faults.

An accurate fault diagnosis of both, faults sensors and real process faults have become more and more important for process monitoring (minimize downtime, increase safety of plant operation and reduce the manufacturing cost). Nowadays the speed of computers has made it realistic to capture faults while they are developing before they lead to significant disruptions. Quick and correct fault diagnosis is required in order to put back on track our processes or products before safety or quality can be compromised.

According to this, an essential part of process monitoring is the fault diagnosis stage. There is a wide range of fault diagnosis and identification strategies. They can be based on a fundamental understanding of the process (mechanistic models) or based on the past experience with the process (data driven models). It must be noted that accurate detailed mechanistic models of processes are difficult and time consuming to develop what supposes that most of the process monitoring methods applied to industrial processes are

based on data driven measures. This thesis is going to focus precisely in data driven methods for fault diagnosis in monitoring multivariate processes.

Even though we have only considered data driven diagnosis methods, it is noteworthy that the literature still provides an extensive list of different methodologies proposed to perform fault diagnosis. Unfortunately, these approaches have been introduced by emphasizing their positive or negative virtues generally on an individual basis so it is not clear for the practitioner which method should be used in each particular context. Another highlight is the lack of proposals in the literature concerning to an efficient way of comparing the diagnosis performance of these methods what make us to consider that appropriate methodologies to accomplish this objective are required.

In the study and comparison of the fault diagnosis methodologies, this thesis distinguishes between two different scenarios:

- Methods for multivariate statistical quality control (MSQC)

  These methods only perform reasonably well in data poor environments with a reduced number of mildly correlated quality and/or process variables and a well-conditioned covariance matrix. The proposed diagnosis methods for this scenario work in the scale of the original measured variables and aim to the suspected responsible variables. After that, the process engineers must diagnose the root cause based on the list of suspected variables.

  The MSQC fault diagnosis methods prove unsuccessful to cope with situations involving large number of variables with high collinearity as it is usual in data rich environments typical of chemical, pharmaceutical and food industry processes.

- Methods for latent-based multivariate statistical process control: (Lb-MSPC)

These methods are appropriate in data rich environments involving large number of variables (hundreds of process variables), measured on-line (sensors with high collinearity), high sampling rate (seconds-hours) and missing data problems. The proposed diagnosis methods for this scenario are based on the projection to latent structures models such as principal component analysis (PCA) (Jackson 1991 and Jolliffe 2002) and Partial least squares (PLS) (Wold 1985 and Wold *et al.* 1987).

The fault diagnosis methods in Lb-MSPC studied in this thesis are the supervised methods. These methods aim directly to the root cause of the faults and they do not provide just only a long list of suspected variables. It is remarkable that fault diagnosis in Lb-MSPC is not so straightforward as in MSQC as it works in a latent variable space and there are also hundreds or thousands of measured variables. It must also be noted that only if there is availability of information on the faults (historical data) it is feasible to accomplish the objective of the supervised methods.

Objectives

The detailed objectives of this thesis are the following:

- Clarify the relationships and the requirements for the implementation in practice of the most important data driven diagnosis methods in MSQC and Lb-MSPC and highlight their key weaknesses and strengths.
- Develop new efficient ways of comparing the performance of the different diagnosis methods.
- Test and compare the performance of different diagnosis methods in MSQC.
- Propose and test new improved variants of the diagnosis methods in MSQC.
- Test and compare the performance of different diagnosis methods in Lb-MSPC
- Propose and test new diagnosis methods in Lb-MSPC.

With the previous goals in mind the thesis is structured as follows:

In the first part of the document, Chapter 1 introduces the state of the art on fault diagnosis and identification (FDI). After a general overview of the FDI, chapter looks in more detail the detection and diagnosis in multivariate process monitoring based in data driven methods. This chapter also presents a glossary for fault detection and diagnosis. Chapter 2 presents the material and the process data sets and simulations used for testing the diagnosis methods.

The second part of the document (Chapters 3 to 6) is devoted to the fault diagnosis in multivariate statistical quality control (MSQC). Chapter 3 presents the most extended methods for fault diagnosis in supervised MSQC. The chapter describes the rationale of the different methods and shows the requirements for their implementation, their strong points and their drawbacks and establishes the relationships between them. Chapter 4 presents the performance indices and compares the performance results of the diagnosis methods in multivariate statistical quality control (MSQC) described in Chapter 3. The diagnosis results in a four variables simulation are explored with a partial least square (PLS) model and compared using an analysis of variance (ANOVA). Chapter 5 presents new proposed variants in some of the MSQC diagnosis methods described in Chapter 3 that try to improve their diagnosis efficiency according to the nature of the shortcomings detected in Chapter 4. Chapter 6 presents and compare the performance results of the improved diagnosis methods in MSQC described in chapter 5. The diagnosis results in a seven variables simulation are compared using an analysis of variance (ANOVA).

The third part of the document (Chapters 7 to 9) is devoted to the fault diagnosis in latent-based multivariate statistical process control (Lb-MSPC). Chapter 7 presents some of the most extended methods for fault diagnosis in supervised Lb-MSPC. This chapter describes the rationale of these methods and shows the requirements for their

implementation, their strong points and their drawbacks. Chapter 8 introduces one of our proposals, the Fingerprints contribution plots (FCP). Chapter 9 presents and compares the performance results of the diagnosis methods in Lb-MSPC described in Chapters 7 and 8. The diagnosis results in two process data sets are compared using a new strategy based in the use of the overall sensitivity and specificity.

Finally, the fourth part of the document is devoted to the conclusions of this work. Chapter 10 presents the conclusions of this dissertation and the future directions of the current work.

Contributions

The main contributions of this work are:

- The comparison study of the performance of the most extended data driven fault diagnosis methods in MSQC and Lb-MSPC. These methods are tested and compared under a wide number of different simulated scenarios and real process data bases.
- The development of new efficient ways of comparing the performance of the different diagnosis methods. A strategy based in the use of the overall sensitivity and specificity is applied to the comparison of the Lb-MSPC performance results. A classical analysis of variance (ANOVA) is applied to the comparison of the MSQC performance results.
- The comparison of the performance of different diagnosis methods in MSQC: Alt´s method (1985) Doganaksoy, Faltin and Tucker´s method (1991), Hayter and Tsui´s method (1994), Modifications to the Doganoksoy, Faltin and Tucker´s method, Murphy´s method (1987), Hawkin´s method (1991,1993), Montgomery

and Runger´s method (1996), Mason, Tracy and Young´s method (1995, 1997) and Step-down method (1958).

- The development of new improved variants of the diagnosis methods in MSQC: two variants of the Mason Tracy and Young method: MTY1 and MTY2; three variants of the Hawkins´ method: T2-recursive (T2RH), T2-pre-filtered and recursive (T2FRH) and Hawkins' one single variable method (HSVM); four variants of the Montgomery and Runger´s method: recursive methodology (RM), sequential extraction methodology (MUSE), pre-filtered and recursive methodology (FRM) and pre-filtered and sequential extraction methodology (FMUSE) ; finally, two variants of the Murphy´s method: T2-Murphy method (T2M) and pre-filtered T2-Murphy (FT2M).
- The development of a new supervised diagnosis method in Lb-MSPC: The fingerprints contribution plot method (FCP) (Vidal-Puig and Ferrer 2008). This method incorporates the historical information of the different types of faults to the contribution plot (most classical unsupervised method in Lb-MSPC).
- The comparison of the performance of different diagnosis methods in Lb-MSPC: Fault signature proposed by Yoon S., MacGregor, J.F. (2001), SPE fault reconstruction proposed by Dunia R., Qin S.J. (1998), combined index fault reconstruction proposed by Yue H., Qin S.J. (2001) and discriminant partial least squares (PLS-DA) (Barker *et al.* 2003 and Wold *et al.* 2009)
- The implementation in Matlab of all the diagnosis methods and variants applied in this study.

The following written contributions have arisen as a result of the work performed:

Refereed Journal Papers

- Vidal-Puig S. and Ferrer A. (2014). "A comparative study of different methodologies for fault diagnosis in multivariate quality control". *Communications in Statistics-Simulation and Computation.* Vol 45 num 5 986-1005 (ISSN 0361- 0918) .

Conference Presentations

- "Estrategias para el diagnóstico de fallos en la monitorizacion de procesos multivariantes: estudio de revisión". *Proceedings of the XXVIII Congreso Nacional de Estadística e Investigación Operativa 2004 (SEIO) Cadiz, Spain.*

- "Fault diagnosis in the on-line monitoring of a pasteurisation process: a comparative study of different strategies". *Proceedings of the 5th Annual Conference of the European Network for Business and Industrial Statistics 2005 (ENBIS) Newcastle, UK.*

- "Diagnóstico de fallos basado en una estrategia combinada: PLS Discriminante SIMCA" *XXX Congreso Nacional de Estadística e Investigación Operativa" 2007 (SEIO) Valladolid, Spain*

- "Fingerprints contribution plot: A new approach for fault diagnosis in multivariate statistic process control" *11th International Conference on Chemometrics in Analytical Chemistry (CAC 2008) Montpellier, France.*

- "A comparative study of different methodologies for fault diagnosis in multivariate quality control ". *Proceedings of the 28th Quality and Productivity Research Conference 2011 (QPRC) Roanoke, Virginia, USA.*

- "A comparative study of different methodologies for supervised fault diagnosis in multivariate statistical process control". *Proceedings of the 12th Annual Conference of the European Network for Business and Industrial Statistics 2013 (ENBIS) Linz, Austria*

Part I

Introduction

Chapter 1: State of the art

The objective of this chapter is to review the state of the art in multivariate statistical process monitoring and fault diagnosis. Section 1.1 reviews the diverse fault diagnosis approaches. Section 1.2 introduces the abundant terminology related to fault diagnosis. It presents a glossary of terms that are frequently used in the field of fault diagnosis. The last section of this chapter (Section 1.3) is dedicated to describe the statistical process control (SPC) methodology.

1.1 Fault diagnosis and isolation approaches

Something that call our attention and can be somewhat misleading for new practitioners is that there are many different approaches to fault diagnosis and isolation (FDI) problem. Because each of them has their strengths and weaknesses, some practical applications may even combine multiple approaches. In this section, we highlight some of the major differentiating factors between the different techniques. These approaches are surveyed and conveniently classified in Venkatasubramanian *et al.* (2003). Figure 1.1 shows a classification of fault diagnosis methods based in Venkatasubramanian´s proposal with some minor changes.

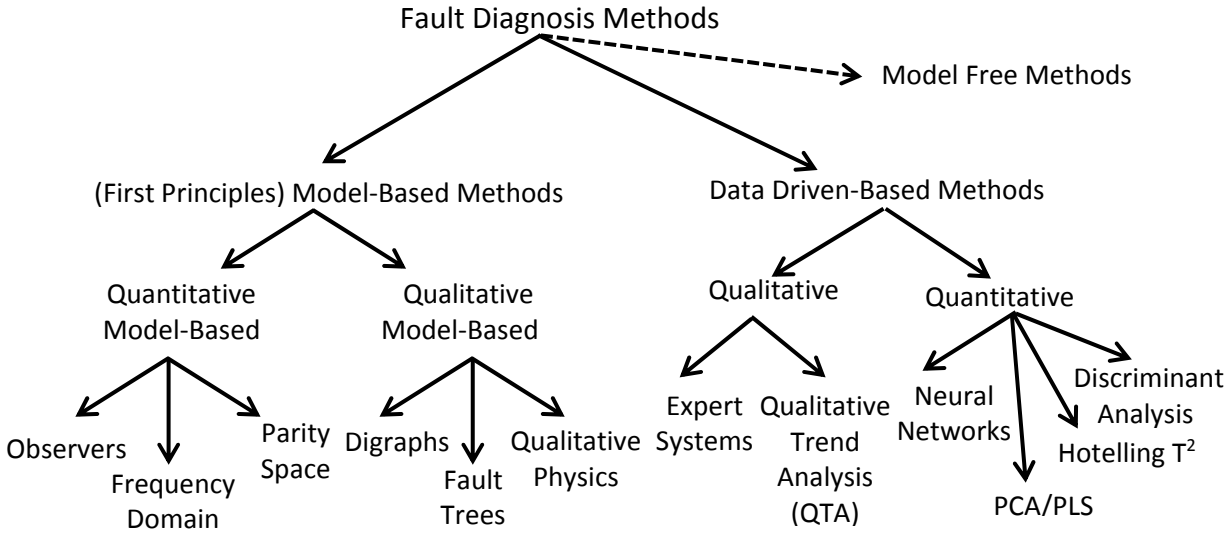

FIGURE 1.1: Classification of fault diagnosis methods

In the proposed classification (Figure 1.1), the diagnostic systems are divided based on the *a priori* knowledge used. The basic *a priori* knowledge that is needed for fault diagnosis is the set of failures and the relationships between the observations and the failures. The *a priori* domain knowledge may be developed from a fundamental understanding of the process (model-based knowledge) or it may proceed from past experience with the process (process history-based knowledge).

In the case of the model-based knowledge there are quantitative and qualitative models. In quantitative models this understanding is expressed in terms of mathematical functional relationships between the inputs and outputs of the systems. In qualitative model equations, these relationships are expressed in terms of qualitative functions centered around different units in a process.

In process history based-knowledge (data driven models) only the availability of large amount of historical data can be transformed and presented as a priori knowledge to a diagnostic system. This is known as the feature extraction process from the process history data. The extraction process can mainly proceed as either quantitative or qualitative feature extraction.

Finally, a third category which includes model free methods (Gertler 1998) can be added to complete this classification. The model free methods do not utilize the mathematical model of the plant and range from physical redundancy, special sensors, limit-checking or spectrum analysis.

For an overall overview of the wide variety of solutions to the FDI problem a short review of all of them based on Venkatasubramanian *et al.* (2003) classification is presented in the following sections.

1.1.1 First principles model-based methods

These methods are developed from a fundamental understanding of the physics of the process using first-principles knowledge. “First principles” models are often engineering design models, reflecting physical laws such as mass balance, energy balance, heat transfer relations, and so on. Or, even qualitative models such as causal fault propagation models can be considered as “first principles” models if they are based on physical laws

or device implementation knowledge, rather than primarily on data. These models are also often referred to as using “deep knowledge”.

1.1.1.1 Quantitative model-based methods

These methods use an explicit mathematical model of the monitored plant. Most of the model based fault detection and diagnosis methods rely on the concept of the *analytical redundancy* where sensory measurements are compared to analytically computed values of the respective variable. Such computations use present and/or previous measurements of other variables and the mathematical plant model describing their nominal relationship to the measured variable. The resulting differences called residuals are indicative of the presence of faults in the system. Another class of model based methods relies directly on parameter estimation.

The generation of residuals needs to be followed by residual evaluation, in order to arrive at detection and isolation decisions. To facilitate fault isolation, the residual generators are usually designed for isolation enhanced residuals, exhibiting structural or directional properties.

The most important residual generation methods are:

- *Kalman filter*: The innovation (prediction error) of the Kalman filter can be used as a fault detection residual. However fault isolation is somewhat awkward with the Kalman filter.
- *Diagnostic observers*: The basic idea is to estimate the outputs of the system from the measurements by using observers in a deterministic setting (Patton and Chen 1997). Depending on the circumstances, one may use linear (O´Reilly 1983) or nonlinear (Frank 1987) full or reduced order, fixed or adaptive observers.

- *Parity relations*: They are rearranged and usually transformed variants of input-output or state space models of the plant (Gertler and Singer 1990). The basic idea is to check the parity (consistency) of the plant models with sensor outputs (measurements) and known process inputs.

In general the advantages of using quantitative model-based approach is that we will have some control over the behavior of the residuals through the use of enhanced residuals (directional or structured residuals). However, several factors such as system complexity, high dimensionality, process nonlinearity and the lack of good data often render it very difficult even impractical to develop an accurate mathematical model for the system. In addition to the difficulties related to modelling they do not support an explanation facility that enable users to understand how conclusions are reached, to be convinced that these conclusions are reasonable.

1.1.1.2 Qualitative model-based methods

They are based on various forms of qualitative knowledge used in fault diagnosis. The need for a reasoning tool which can qualitatively model a system, capture the causal structure of the system in a more profound manner than the conventional expert systems lead to development of methodologies to qualitatively represent knowledge, and to reason from them. These methods can be classified into digraphs, fault trees and qualitative physics methods

- *Causal model approaches using digraphs:* Diagnosis is concerned with deducing the structure from the behavior. This kind of deduction needs reasoning about the cause and effects relationships in the process. Cause-effect relations or models can be represented in the form of signed digraphs (SDG) that lead from the 'cause' nodes to the 'effect' nodes. SDGs provide a very efficient way of representing

qualitative models graphically and have been the most widely used form of causal knowledge for process fault diagnosis. Iri *et al*. (1979) were the first to use SDG for fault diagnosis.

- *Fault trees approaches:* Fault trees are used in analyzing system reliability and safety. Fault tree is a logic tree that propagates primary events or faults to the top level event or a hazard. The tree usually has layers of nodes. At each node different logic operations like AND and OR are performed for propagation. Fault-trees have been used in a variety of risk assessment and reliability analysis studies.
- *Qualitative physics approaches:* They are based on common sense reasoning about physical systems and have been an area of major interest to artificial intelligence community.

In general we can say that causal models are a very good alternative when the quantitative models are not available but functional dependencies are understood. Abstraction hierarchies help to focus the attention of the diagnostic system quickly to problem areas. They can also provide an explanation of the path of propagation of a fault. They suffer from resolution problems resulting from the ambiguity in qualitative reasoning.

1.1.2 Data driven based methods

1.1.2.1 Qualitative data-driven methods

Two of the important methods that employ qualitative feature extraction are the expert systems and qualitative trend analysis (QTA).

- *Expert system approaches:* Rule-based feature extraction has been widely used in expert systems for many applications. An expert system is generally a very specialized system that solves problems in a narrow domain of expertise. They can be used where fundamental principles are lacking but there is an abundance

of experience despite not enough detail is available to develop accurate quantitative models. Initial attempts at the application of expert systems for fault diagnosis can be found in the work of Henley (1984), Chester *et al.* (1984), Rich *et al.* (1989) and Niida (1985). There are a number of other researchers who have worked on application of expert systems for fault diagnosis problems. However in all the applications, the limitations of an expert system approach is obvious. knowledge based systems developed from expert rules are very system specific and they are difficult to update. The advantage though is in the easy development and transparent reasoning.

- *Qualitative trend analysis approaches*: This method works by representing sensor trends as a sequence of certain basic shapes (called primitives) and matching the current sensor-trends against the sensor-trends for various faults stored in a database. Trend analysis and prediction are important components of process monitoring and supervisory control. Trend modelling can be used to explain the various important events that happen in a process, do fault diagnosis and predict future states. Cheung and Stephanopoulos (1990) have built a formal framework for the representation of process trends. Other interesting results on qualitative trend analysis can be found in the work of Janusz and Venkatasubramanian (1991), Rengaswamy and Venkatasubramanian (1995) and Rengaswamy *et al*. (2001).

1.1.2.2 Quantitative data-driven methods

The statistical feature extraction approaches include methods based on statistical pattern classifiers, methods based on the multivariate Hotelling´s T^2 statistic and methods that use projection to latent structures models such as principal component analysis (PCA) or partial least squares (PLS).

- *Neural networks approaches (NNs):* A neuronal network is a computer architecture in which processors are connected in a manner suggestive of connections between neurons. The NNs can learn by trial and error and adjust its behaviour accordingly. NNs has been conceptualized by some authors as non-parametric statistical techniques (Smith, 1993) or as non-linear regression techniques (Sarle,1994). In general, neural networks that have been used for fault diagnosis can be classified along two dimensions: (i) the architecture of the network such as sigmoidal, radial basis and so on; and (ii) the learning strategy such as supervised and unsupervised learning. The most popular supervised learning strategy in neural networks has been the back-propagation algorithm. In chemical engineering, Watanabe *et al.* (1989), Venkatasubramanian and Chan (1989), Ungar *et al.* (1990) and Hoskins *et al.* (1991) were among the first researchers to demonstrate the usefulness of neural networks for fault diagnosis. About its limitations it must be noted that due to the procedural nature of neural network development they lack the explanation and adaptability properties. They have also the limitation of their generalization capability outside of the training data despite this problem can be alleviated avoiding decision in case there are no similar training patterns in that region. They also have problems when multiple faults are considered.

- *Discriminant analysis:* Fault diagnosis is cast in a classical statistical pattern recognition framework. Distance classifiers use distance metrics to calculate the distance of a given pattern from the means of various classes and classify the pattern to the class from which it is closest.

- *Multivariate statistical approaches based on the Hotelling´s T^2 statistic:* A wide variety of methods specially fitted for multivariate statistical quality control (MSQC) have been proposed: Doganaksoy *et al.* (1991), Hayter and Tsui´s (1994), Murphy (1987), Hawkins (1991,1993), Runger and Montgomery (1996), Mason, Tracy and Young (1995, 1997) and Roy (1958). Most of these methods are based on computed terms that are equivalent to different decomposition terms of the Hotelling´s T^2 statistic. These methods work in the original measured variable space. The problem with these methods is that they perform reasonably well only in scenarios of limited number of mildly correlated variables as it is the common case in statistical quality control. In addition to this, in multivariate statistical process control (MSPC), where there is a large list of process and quality variables involved with high correlations among them, the covariance matrix becomes close to singular or ill conditioned and, consequently, all these methods present difficulties in the inversion of the covariance matrix.

- *Multivariate statistical approaches based on PCA/PLS models* (Lb-MSPC): The successful applications of latent based multivariate statistical methods to fault diagnosis such as Principal Component Analysis (PCA) and Partial Least Squares (PLS) have been extensively reported in the literature. Overview of using PCA and PLS in process analysis, control and fault diagnosis was given by

MacGregor et al. (1991), MacGregor *et al.* (1994), MacGregor and Kourti (1995), Kourti and MacGregor (1996) and Nomikos and MacGregor (1995). In unsupervised fault diagnosis MacGregor *et al.* (1994) and Miller *et al.* (1993) suggested the use of contribution plots on scores and square prediction error (*SPE*). This tool indicates which variables are likely the contributors to inflated *SPE* or scores due to the presence of a fault. In supervised fault diagnosis, Dunia and Qin (1998) and Yue and Qin (2001) looked at PCA from a geometric point of view and presented a fault reconstruction methodology that analyzed the fault subspace for process and sensor fault detection and diagnosis. Alcala and Qin (2009) proposed a reconstruction-based contributions approach. Raich and Cinar (1996) proposed an integral statistical methodology combining PCA and discrimination analysis techniques based on angle discriminants for fault diagnosis. Yoon and MacGregor (2001) proposed to extract fault signatures that are vectors of movement of the fault in both the model space (PCA/PLS) and the residual space. The directions of these vectors are then compared to the corresponding vector directions of known faults in a fault library. Another important tools for classification is PLSDA (partial least squares discriminant analysis) (Sjöström *et al.* 1985). This classification tool is based on partial least square models in which the dependent variable is chosen to represent the class membership. Another widely used multi-model approach for fault diagnosis is the SIMCA (Soft Independent Modeling of Class Analogies) (Wold 1983) where a principal component analysis (PCA) is fitted to data from each class of fault.

1.1.3 Model free methods

These methods include the following techniques:

- *Physical redundancy*: Multiple sensors are installed to measure the same physical quantity. Any serious discrepancy between the measurements indicates a sensor fault. It involves extra hardware cost, extra weight and only would serve to diagnose sensor faults
- *Special sensors*: They may be installed for detection and diagnosis.
- *Limit checking*: Plant measurements are compared by computer to preset limits. Exceeding the threshold indicates a fault situation. This approach suffers from two serious drawbacks: Test thresholds need to be set quite conservatively and the effect of a single component may propagate into many plant variables, setting of multitude of alarms and making isolation extremely difficult.
- *Spectrum analysis*: Most plant variables exhibit a typical frequency spectrum under normal operating conditions; any deviation from this is an indication of abnormality. Certain types of faults may even have their characteristic signatures in the spectrum facilitating fault isolation.

1.2 Glossary for fault detection and diagnosis

This section presents a glossary of terms that are frequently used in the field of fault diagnosis and that in some cases are diversely interpreted and may involve contradictions. According to Gertler (1998) definitions:

> **Faults:** departures from an acceptable range of an observed variable or a calculated parameter associated with a process and consequently they are

deviations from the normal behavior in the process or its instrumentation. This defines a fault as a process abnormality or symptom. The underlying cause of this abnormality is called the basic event or the root cause. The basic event is also referred to as malfunction or failure. We distinguish between **Jump- fault** (step function) and **Drift-fault** (ramp function). The faults cannot be handled adequately by the controllers. Faults are unknown inputs which we wish to detect and isolate. We can classify the faults in the following categories:

- **Process Faults**: changes (abrupt or gradual) in some plant parameters. Such faults may include surface contaminations, clogging, partial or total loss of power, plant leaks and loads.
- **Sensor Faults**: discrepancies between the measured and the actual values of individual plant variables. Gross error detection or sensor validation refers to the identification of faulty or failed sensors in the process. Data reconciliation or rectification is the task of providing estimates for the true values of the sensor readings.
- **Actuator Faults**: discrepancies between the input command of an actuator and its actual output

Disturbances: nuisances which we wish to ignore. They can be managed by standard process controllers (PI controllers, model predictive controllers).

Fault detection: indication that something is going wrong in the monitored system and that a fault has occurred.

Fault isolation: determination of the exact location of the fault or the component which is faulty, identifying the measured variables most relevant to diagnosing

the fault. The purpose of this procedure is to focus the plant operator´s and engineer´s attention on the subsystems more pertinent to the diagnosis of the fault.

Fault identification: determination of the magnitude of the fault.

Fault diagnosis: **i**solation and identification task together. Statistical fault diagnosis aims to the most suspected variables responsible for the fault. Following this, process engineers proceed to the fault diagnosis of the root causes.

Process recovery or **intervention**: removal of the effect of the fault. In the case of a sensor problem, a sensor reconstruction technique can be applied to the process to restore in-control operations.

While detection and isolation is an absolute must in any practical system, the identification may not justify the extra effort it requires. In case that only detection and isolation is considered we can talk about FDI (fault detection and isolation) systems (Gertler 1998). On the contrary another authors prefer FDI as an acronym for fault detection and identification systems. The two tasks, detection and diagnosis, may be performed in parallel or sequentially. It is most common the sequential strategy where the detection task is running permanently and the diagnostic task is triggered only upon the detection of the presence of a fault

Regarding the performance efficiency of the diagnosis systems:

Sensitivity for a fault f_i: proportion of the real faults (f_i) that are correctly classified by the diagnosis method. it must be noted that in fault detection the term fault sensitivity is also used to describe the ability of the different techniques to detect faults of reasonably small size.

Specificity for a fault f_i: proportion of the real "no f_i faults" that are correctly classified by the diagnosis method as "no f_i fault" .

Reaction Speed: ability of the technique to detect faults with reasonably small delay after their arrival.

Robustness: ability of the technique to operate in the presence of noise, disturbances and modeling errors with few false alarms.

Isolation performance: ability of the diagnosis system to distinguish faults, depends on the physical properties of the plants, size of the faults, noise, disturbances, and model errors and on the design of the diagnosis algorithm. Multiple simultaneous faults are more difficult to isolate than single faults. Further, some faults may be non-isolable from one another because they act in an undistinguishable way.

Regarding the availability or not of faults data sets used for implementing the fault diagnosis algorithms:

Unsupervised fault diagnosis: there is no information about the different types of fault. So when a fault is detected, in the diagnosis stage it is decided which variables are involved in the fault and then the process engineers have to search for the root causes of the fault.

Supervised fault diagnosis: there exist data sets for the different types of fault. In the diagnosis stage it can aim directly to the root cause so it can be much helpful to process engineers.

1.3 Statistical process control

The aim of Statistical Process Control *(*SPC) is to monitor the performance of a process along time in order to verify whether the process behaves as it is expected to do (*i.e.* if it is in-control or not), and to detect any unusual (special) event that may occur. It will detect the anomalies (special causes) at an early stage (**fault detection**) and will help to identify the causes of the anomalies (**fault diagnosis**). Significant improvements in the process performance can be achieved by eliminating these causes (or implementing them if they are beneficial). As it can be seen, the diagnosis of the faults, which is the principal topic of this thesis, is an important stage in SPC.

1.3.1 Statistical process control – Detection

The fault detection is the first stage in the SPC. It is an indication that something is going wrong in the monitored system or that there is statistical evidence that a fault has occurred in the process. The basic tools for fault detection in the SPC are the control charts. These charts require to take data periodically (process or quality variables) from the monitored process and plot the evolution of different statistics in special charts. These charts allow the process operators to detect the signals of the existence of a fault more easily.

At this point, it is worth noting the difference between the common and special variation cause since it is important to distinguish among them in order to implement an SPC scheme:

Common causes are the usual, historical, quantifiable variation in a system. These causes produce a stable predictable pattern in the variability of the measured

parameter. If only common causes are present, the process is considered " in statistical control".

Special causes are unusual, not previously observed and non-quantifiable variation. They are associated to faults or anomalies and when they are present the process is considered out of statistical control, and consequently, there is no a stable predictable pattern in the variability of the measured parameter. When a process is out of control then the anomalies must be diagnosed and measures to correct and prevent their reappearance (if harmful) taken.

In industrial processes where process and quality variables are measured there are different charts and strategies for fault detection in statistical process control: univariate charts for univariate statistical process control (*USPC)***,** multivariate charts for *c*lassical multivariate statistical process control (*MSPC*), and megavariate charts for *Lb-MSPC* on latent variable models.

It must be noted that the methods for fault diagnosis are influenced by the different charts and strategies used for the fault detection.

1.3.1.1 Univariate statistical process control (USPC)

In order to implement an USPC scheme, industries have used some univariate control charts to monitor one or a few quality variables or key process variables that are suspected to be related in some way to the final product quality. The USPC most used charts in the literature have been the Shewhart, Cumulative sum (CUSUM) and EWMA charts.

In the following, a brief overview of such control charts is given.

Average run length (ARL)

The average run length (ARL) is defined as the average number of points that will be plotted on a control chart before and out-of-control condition is indicated when one or several points exceed the stated control limits.

There are two types of ARL: the *in-control* ARL that is measured when the process is actually in control and consequently the detected fault corresponds to a false alarm and the *out-control* ARL that is measured when the process is actually out of control and consequently the detected fault corresponds to a real alarm.

The ARL is useful to compare the performance of SPC control charts in terms of fault detection.

Shewhart charts

This type of chart was developed by Shewhart (1931). Figure 1.2 shows a typical example. This chart contains a center line (green line), which represents the in-control average value of the sample statistic of the variable to be monitored. Additionally, two lines (blue and red lines) are depicted and represent the *Upper Control Limit* (*UCL*) and *Lower Control Limit* (*LCL*). The values of such control limits are chosen in such a way that when the process is under control, an expected fraction α of the statistics values lies beyond the control limits assuming the sample statistic is normally distributed. Hence, a $100\times(1-\alpha)$ percentage of the sample statistic values plotted are expected to fall within the confidence region limited by the upper and lower control limits.

One of the most common Shewhart control charts is the $\bar{x} - s$ control chart, which is designed from two different charts. The $\bar{x}$ chart uses the sample mean to monitor the process mean whereas the s chart uses the sample standard deviation to monitor the process standard deviation at each sampling time point.

In a first stage an historic data set generated when the process is in control is analyzed. After checking the normal distribution and purging the abnormal data of this data set, the in-control mean (μ_{ref}), the standard deviation (σ_{ref}) and the upper (*UCL*) and lower (*LCL*) control limits ($\mu_{ref} \pm 3\sigma_{ref}$) for the chart of the monitored parameter ($\bar{x}$ or s), are calculated. The existence of outliers would cause wider control limits, thereby reducing the detection capability of the charts. Hence, a previous step consisting of detecting potential outliers in data needs to be taken prior to the estimation of the control limits. The process is considered out of control when the statistic sample mean of a new observation lays out of the bounds defined by the control limits or according to some additional rules that attempt to distinguish abnormal from natural patterns based on several criteria such as: the absence of points near the centerline, the absence of points near the control limits, or other abnormal patterns (systematic, repetition, trend patterns). It is worth noting that there are many situations in industry in which the sample size is 1, hence, control charts for individual measurements are used.

As it can be seen in Figure 1.2 the Shewhart chart performs a sequential test on the mean for every sample taken from the process. In each observation it is checked if the mean for the monitored variable stay in μ_{ref} or on the contrary there is enough statistical evidence to reject this hypothesis. It is known that even when a process is *in control*, that is, no special causes are present in the system, there is approximately a 0.27% probability of a point exceeding *3-sigma* control limits so it means that this chart has a type I risk α=0.0027. For a Shewhart control chart using *3-sigma* limits, this *false alarm* occurs on average once every 1/0.0027 = 370.4 observations. Therefore, the *in-control* ARL of a Shewhart chart is 370.4. Meanwhile, if a special cause does occur, it may not be of sufficient magnitude for the chart to produce an immediate *alarm condition*. If a special cause occurs, one can describe that cause by measuring the change in the mean and/or

variance of the process in question. When those changes are quantified, it is possible to determine the *out-of-control* ARL for the chart.

It turns out that Shewhart charts are quite good at detecting large changes in the process mean or variance (jump faults), as their *out-of-control* ARLs are fairly short in these cases. However, for smaller changes (such as a 1- or 2-sigma change in the mean) or drift faults, the Shewhart chart does not detect these changes efficiently. Figure 1.3 shows that this chart has not many chances to quickly detect a 1-sigma change in the mean since the resulting *out-of-control* ARL is large in size. For instance, using one point beyond the limits as the out-of-control rule, in the case of a change in mean from an *in-control* normal distribution (μ_{ref}=5; σ_{ref}=1) to an *out-of-control* normal distribution (μ_{new}=6; σ_{ref}=1), the resulting *out-of-control* ARL is equal to 1/P = 44 where P=0.0229 is the out-of-control probability for one single observation. It means that on average 44 observations will be required to detect this small shift in mean and consequently, this lack of sensitivity to detect small shifts in the mean urges to use other monitoring strategies to detect these types of faults. Other types of control charts have been developed to overcome these problems, such as the CUSUM and EWMA charts which detect smaller changes more efficiently than the Shewhart Chart by making use of information from observations collected prior to the most recent data point.

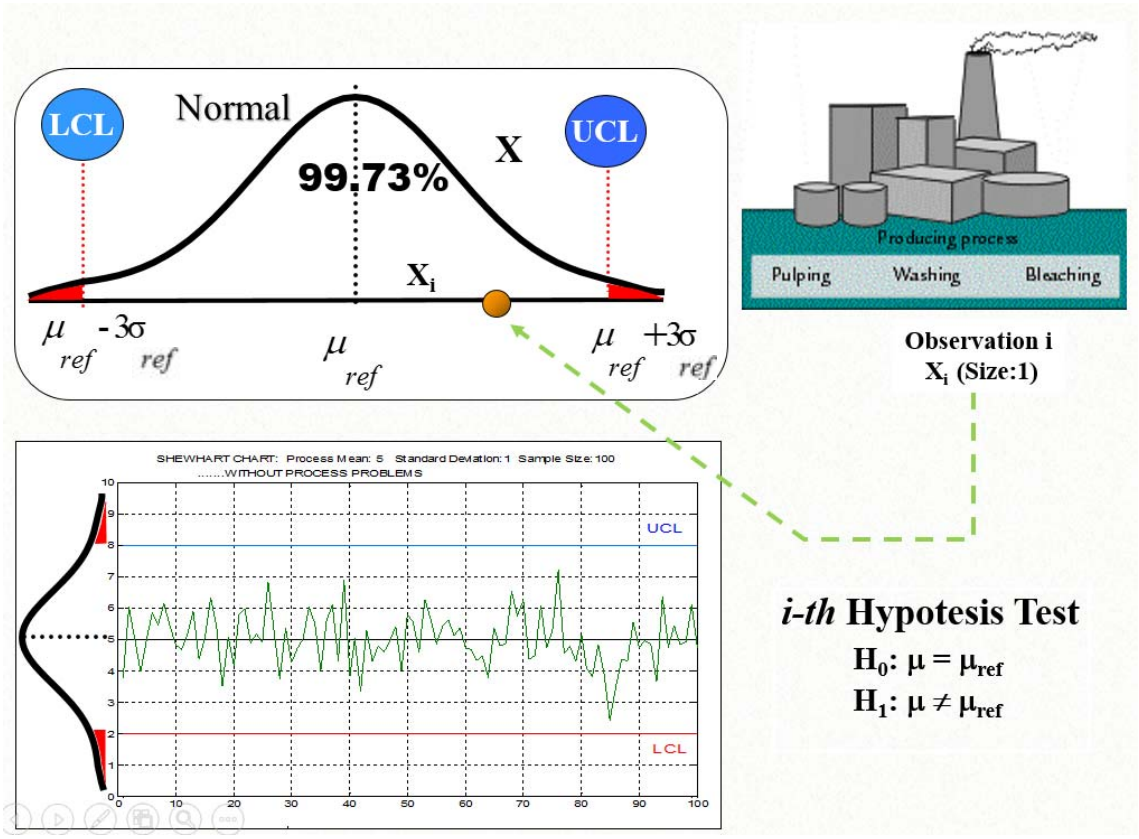

FIGURE 1.2: Shewhart monitoring chart for an in-control N/(μ_{ref}=5; σ_{ref}=1)

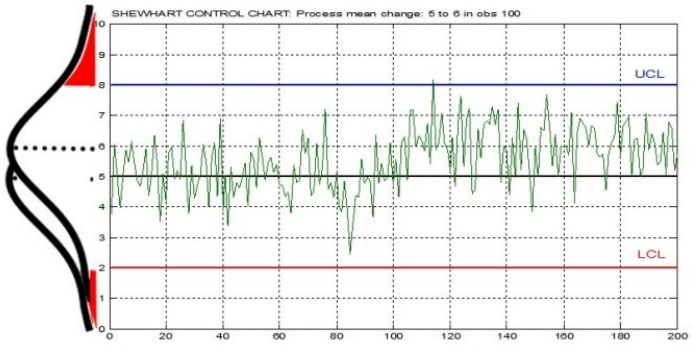

FIGURE 1.3: Change from an in-control N/(μ_{ref}=5; σ_{ref}=1) to an out of-control N(μ_{new}=6; σ_{ref}=1) at t=100 in a Shewhart monitoring chart

CUSUM charts

The CUSUM chart was originally designed by Page (1961). The basic idea is to plot at each stage *t* the CUSUM of past and present deviations of the selected sample statistic z_t over its target (in-control) value θ_{ref}:

$$S_t = \sum_{i=1}^{t} (z_i - \theta_{ref}) \tag{1.1}$$

CUSUM charts are more effective (smaller out-of-control ARLs) than Shewart charts for detecting persistent shifts in the process parameter θ, since the former accumulates information of several samples. When the process is under control, the CUSUM statistic S_i will fluctuate around 0 as a random walk. In the case there is a shift in θ the CUSUM control chart will signal an upward or downward trend. Care should be taken in the interpretation of the trends since it may happens that the process parameter θ is on target but the CUSUM value S_i is far from 0, giving the appearance that there has been a process shift. Control limits in the shape of a V-mask were proposed in the original CUSUM control chart to identify statistically significant changes in the slope. An alternative to the V-mask based CUSUM control chart is the so-called tabular CUSUM. This involves two statistics S_i^+ and S_i^-, which are the sum of deviations above the target (referred as one-sided upper CUSUM) and below the target (referred as one-sided lower CUSUM), respectively.

Both statistics are expressed as:

$$\begin{aligned} S_t^+ &= \max\{0, z_t - (\theta_{ref} + D) + S_{t-1}^+\} \\ S_t^- &= \max\{0, (\theta_{ref} - D) - z_t + S_{t-1}^-\} \end{aligned} \tag{1.2}$$

where D is the '*reference value*' to detect a change in the process parameter. This is usually set to the difference between the target value θ_{ref} and the out-of-control value θ_{new} that we are aiming to detect quickly. The starting value of the aforementioned statistic is $S_t^+ = S_t^- = 0$. When any of the two statistic exceeds a stated threshold H, the

process is considered to be out of control. ARL based methods are often used to find the appropriate values of the parameters *H* and *D*. The proper selection of both parameters is crucial for the good performance of the control chart in terms of fault detection (Hawkins Olwell 1988).

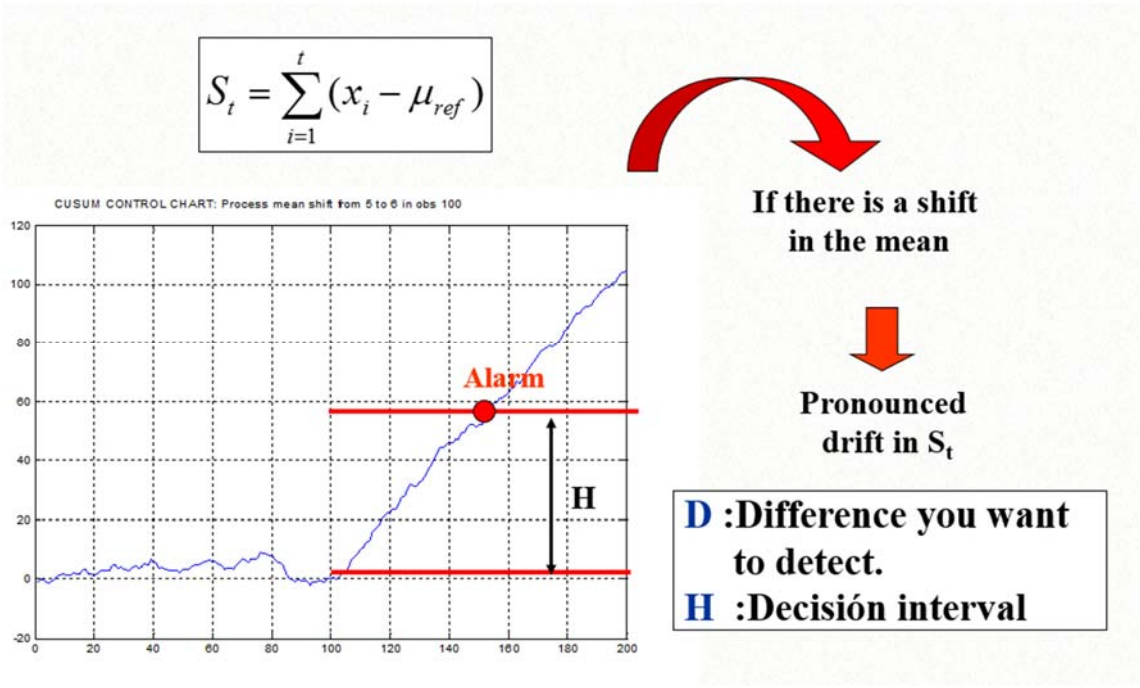

FIGURE 1.4: : Change from an in-control N/(μ_{ref}=5; σ_{ref} =1) to an out of-control N(μ_{new}=6; σ_{ref} =1) at *t*=100 in a CUSUM monitoring chart

Figure 1.4 shows an example for a change in mean with a sample of size 1 and $\theta_{ref} = \mu_{ref}$. It can be seen that the slope for the monitored statistic S_t is more pronounced after the fault at t =100.

EWMA charts

The Exponentially Weighted Moving Average (EWMA) chart was first introduced by Roberts (1959). The control statistic to be charted is an EWMA of present and past values of the selected sample statistic z_t.

$$E_t = \lambda z_t + (1 - \lambda) E_{t\text{-}1} \qquad (1.3)$$

Where λ is a smoothing constant ($0 < \lambda \leq 1$). Considering that the initial value E_0 is equal to the process target θ_{ref}, Equation 1.3 can be expressed as:

$$E_t = (1-\lambda)^t E_0 + \lambda \sum_{i=1}^{t} (1-\lambda)^{t-i} z_i \tag{1.4}$$

The latter expression shows the weight $\lambda(1-\lambda)^{t-i}$ decreasing geometrically with the time at which the observation were registered. Hence, the parameter λ determines the memory of EWMA, *i.e.* the rate of weighting of past information. When $\lambda = 1$, the chart becomes a Shewhart control chart. On the contrary if λ is close to zero, the EWMA performs like a CUSUM. The selection of the parameter λ should be chosen based on the magnitude of the shift to be detected. Usual values for this parameter are $0.05 \leq \lambda \leq 0.25$.

As commented before, the goal of this chart is to improve the detection of small shifts in the monitored process parameter. Typically, this chart has two control limits (red lines depicted in Figure 1.5), upper (*UCL*) and lower (*LCL*) control limits, which define the region where the process can be considered under control. When one or more values of E_t exceed the control limits, the process is considered to be out of control. The central line represented in Figure 1.5 is the process target θ_{ref}. The EWMA control limits are estimated as

$$\begin{aligned} UCL &= \theta_{ref} + L\sigma_Z \sqrt{\frac{\lambda}{(2-\lambda)}\left[1-(1-\lambda)^{2t}\right]} \\ LCL &= \theta_{ref} - L\sigma_Z \sqrt{\frac{\lambda}{(2-\lambda)}\left[1-(1-\lambda)^{2t}\right]} \end{aligned} \tag{1.5}$$

where L is the width of the control limits and σ_z is the standard deviation of the sample statistic z_t. Usually, the parameter L is typically set to values between 2.6 and 3. For further details, readers are referred to Hunter (1986).

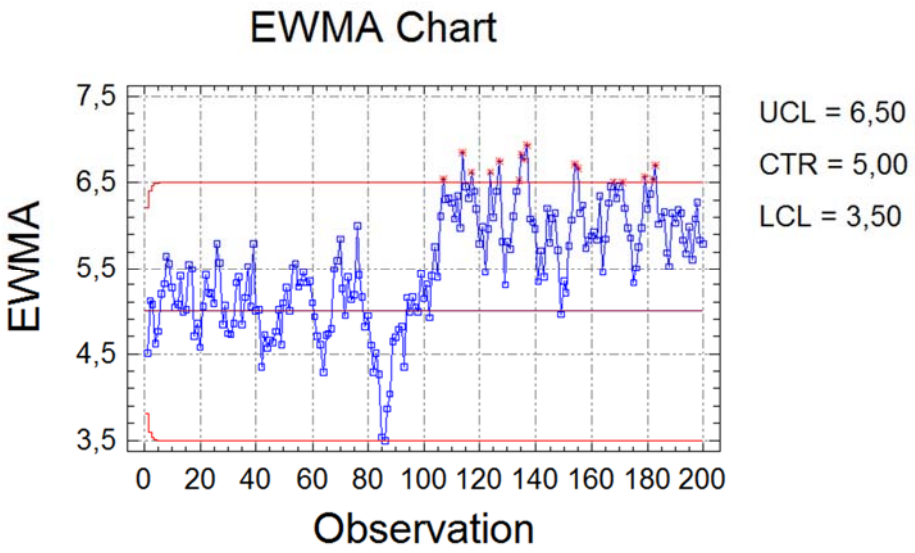

FIGURE 1.5: : Change from an in-control N/(μ_{ref}=5; σ_{ref}=1) to an out-of-control N(μ_{new}=6; σ_{ref}=1) in EWMA Monitoring Chart at t=150

Figure 1.5 shows that EWMA charts give better results than Shewhart charts in the detection of slight changes of mean and that, consequently, provides a smaller *out-of-control* ARL.

1.3.1.2 Classical multivariate statistical process control (MSPC)

USPC: Limitations

Quality is often a multivariate property and univariate control charts ignore correlation. This phenomenon can be appreciated from Figure 1.6 where two quality variables are monitored using two different univariate control charts and a two-dimensional control chart that is built by aligning one univariate control chart perpendicular to the other. Assume that the control limits of the univariate control charts are set to a 99% confidence level. As observed, the bivariate observation lies within the in-control region limited by the *UCL* and *LCL* when USPC is used to monitor both variables. The ellipsoid shown at the top-left in Figure 1.6 represents the control limits associated with the in-control bivariate process behaviour at 99% confidence level. It can be seen that the observation lies outside the in-control region represented by the ellipsoid,

which indicates that the quality of the product is actually deviating from historical normal records. Nonetheless the abnormality is not detected by the USPC. This support the claim that a monitoring scheme needs to capture the time-varying correlation among variables to be capable of detecting severe abnormalities affecting the multivariate data structure. This is the role of the multivariate control charts introduced in the following.

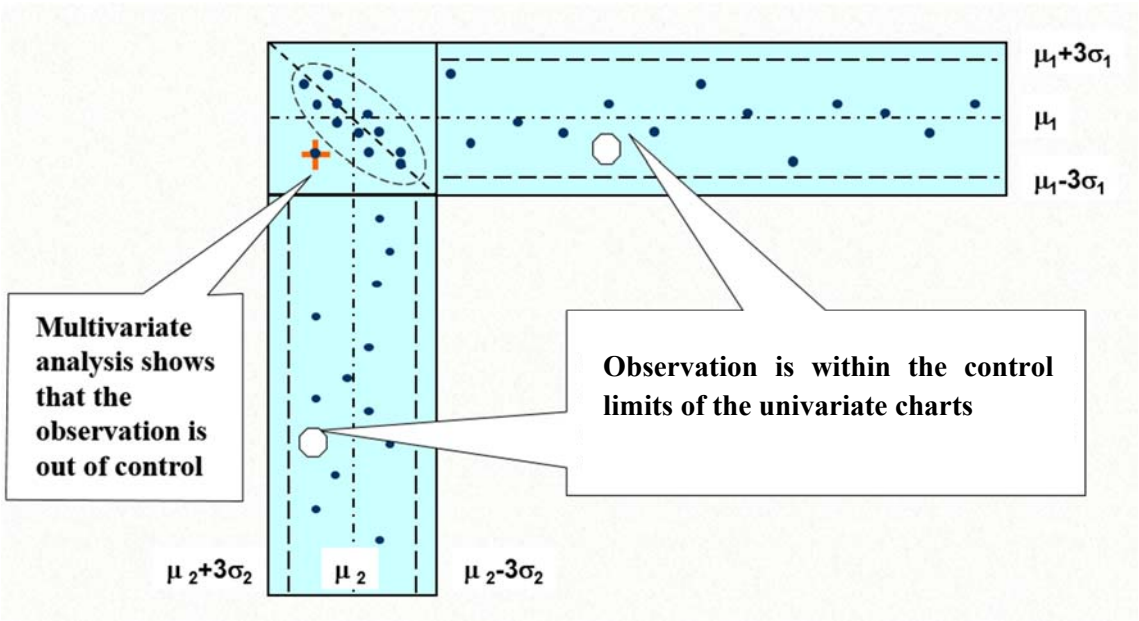

FIGURE 1.6: Univariate control chart limitations

Multivariate charts

There are different types of charts that may be used in MSPC such as Hotelling´s T^2, MCUSUM and MEWMA. In the case of the Hotelling´s T^2, the monitored statistic is based on the estimated Mahalanobis´s distance. Let $\mathbf{x}_i$ represent a K-dimensional vector of measurements made on a process at sampling time i. Let us assume that when the process is in control, the $\mathbf{x}_i$ are independent and follow a multivariate normal distribution with a Kx1 mean vector $\boldsymbol{\mu}_{ref}$ and a $K \times K$ covariance matrix Σ, *i.e.* $\mathbf{x} \sim N_K(\boldsymbol{\mu}_{ref}, \Sigma)$.

For the multivariate normal distribution, the probability density function (pdf) is

$$f(\boldsymbol{x})=k\mathrm{e}^{-\frac{1}{2}(\mathbf{x}-\boldsymbol{\mu}_{\mathrm{ref}})^{\mathrm{T}}\boldsymbol{\Sigma}^{-1}(\mathbf{x}-\boldsymbol{\mu}_{\mathrm{ref}})}=k\mathrm{e}^{-\frac{1}{2}D^2} \quad (1.6)$$

This density function gives the ”likelihood” or “prior probability” of the observation. From this expression the Mahalanobis´s squared distance of the observation is defined as:

$$D^2_{\mathrm{Mahalanobis}}=(\mathbf{x}-\boldsymbol{\mu}_{\mathrm{ref}})^{\mathrm{T}}\boldsymbol{\Sigma}^{-1}(\mathbf{x}-\boldsymbol{\mu}_{\mathrm{ref}}) \quad (1.7)$$

It must be noted that this is a stastistical distance and that the larger the likelihood the shorter the Mahalanobis´ square distance.

Figure 1.7 shows a normal distribution bivariate case with a positive correlation, where the different ellipses show the set of observations with a similar Mahalanobis´ distance. It can be seen that this Mahalanobis´ distance is not a Euclidean but a probabilistic distance *i.e.* the green dot observation is further from a probabilistic point of view of the red dot observation (mean) than the blue dot observation despite there is the same Euclidean distance in both cases.

The Hotelling´s T^2 statistic (Jackson 1985, Mason, Tracy and Young 1992) is defined as the *estimated* Mahalanobis´ squared distance from the *K*-dimensional sample observation $\mathbf{x}_i$ to its sample mean vector $\bar{\mathbf{x}}$:

$$T_i^2=(\mathbf{x}_i-\bar{\mathbf{x}})^T\mathbf{S}^{-1}(\mathbf{x}_i-\bar{\mathbf{x}}) \quad (1.8)$$

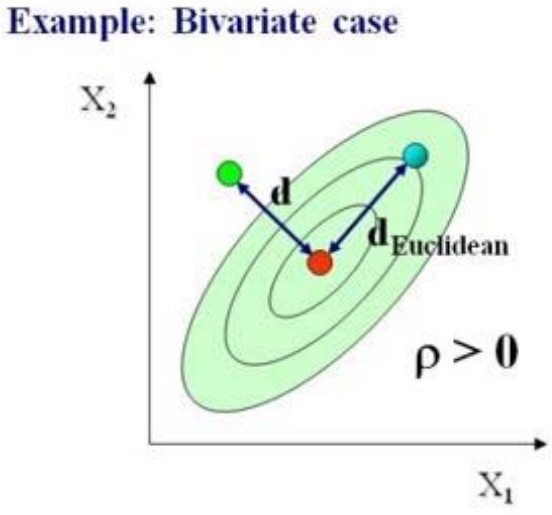

FIGURE 1.7: Mahalanobis´ distance

where $\bar{\mathbf{x}}$ and $\mathbf{S}$ are, respectively, the sample mean vector and covariance matrix calculated from a reference (in-control), historical data set having N multivariate observations. When the sample observation $\mathbf{x}_i$ is independent of the estimates $\bar{\mathbf{x}}$ and $\mathbf{S}$, the distribution of Hotelling´s T^2 is given by an F-Snedecor distribution:

$$\frac{N(N-K)}{K(N+1)(N-1)}T^2 \sim F_{(K,N-K)} \tag{1.9}$$

This Hotelling´s T^2 statistic is most frequently monitored in a Shewhart chart. But it must be noted that CUSUM and EWMA variants can also be implemented with this statistic. In such case we will obtain the MCUSUM and MEWMA charts that are the multivariate extensions of these charts described in Section 1.3.1.1.

1.3.1.3 MSPC on latent variable models

Classical SPC Limitations

The classical tools of SPC (USPC and classical MSPC) are extremely inefficient in the megavariate context of the XXI century processes (Ferrer 2014). Among the reasons of such inefficiency are the high dimensionality of the covariance matrices, the high degree of collinearity that is caused by the correlation structure among process and quality variables, the common presence of missing data and the existence of a low noise-signal ratio in the data. In this context analyzing each variable separately, as if they were independent variables, makes the interpretation and the diagnostic of the problems with the univariate strategy a very difficult, not to say impossible, task. The ill-conditioned covariance matrix is a problem in the computation of the inverse of the covariance matrix, which makes that the Hotelling´s T^2 statistic (traditionally used in classical MSPC) becomes unstable. Indeed, in the case that there are more variables than observations the covariance matrix becomes singular and, as a result of this, the Hotelling´s T^2 statistic cannot be calculated. In addition, Hotelling´s T^2 statistic is also affected by the existence

of missing data, since when there are missing data the computation of this statistic is not possible and it supposes that the information contained in the rest of the measured variables is not finally used.

It is in this context where the use of statistical techniques based on the projection to latent structures, such as Principal Component Analysis (PCA) (Jackson 1991), and the Partial Least Squares, (PLS) (Geladi and Kowalski 1986, Wold *et al.* 1987) becomes an interesting option. These techniques are relatively robust to the presence of missing data and can successfully cope with large ill conditioned covariance matrices. These techniques allow to implement the Megavariate Statistical Process Control (Mega-SPC) (Ferrer 2007). The PCA and PLS compress the multidimensional data in a small number of latent variables which explain the majority of the variability in the measured variables and its relationships. It is in this new subspace of notably reduced dimension, where it can be explained most of the variability of the measured variables and its relationships, and where the classical techniques of the SPC work without problems. This approach allows the process operators to indirectly control a multitude of process variables through the monitoring of a small number of latent variables, and the prediction of the quality parameters from the recorded information of the process making use of inferential models known as *soft sensors.*

Latent variable models

- **Principal component analysis (PCA)**

  In a situation where N observations in K measured process variables and M quality variables are registered in normal operation conditions of the process, the information can be organized in two data matrices, process variables data matrix $\mathbf{X}$ ($N \times K$) and quality variables data matrix $\mathbf{Y}$ ($N \times M$). These matrices usually are mean

centered and scaled to unit variance. The PCA can be used to decompose both matrices making **Z**=**X** or **Z**=**Y** in a set of matrices of range equal to 1 according to the following expression:

$$\mathbf{Z} = \sum_{a=1}^{A} \mathbf{t}_a \mathbf{p}_a^{\mathrm{T}} + \mathbf{E} = \hat{\mathbf{Z}} + \mathbf{E} \tag{1.10}$$

where the loading vectors $\boldsymbol{p}_a$ are the directions which maximize the variance in the subspace **Z** and define the latent subspace of dimension A ($A \leq$ range of **Z**); the score vectors $\mathbf{t}_a = \mathbf{Z}\,\mathbf{p}_a$ are the new latent variables, projection of the N observations in the A-dimensional latent subspace spanned by the principal directions; and $\hat{\mathbf{Z}}$ is the prediction of matrix **Z** from only the first A principal components. The latent variables are orthogonal and can be sorted according to the percentage of explained variance. The vectors $\mathbf{p}_a$ and $\mathbf{t}_a$ are the *a-th* eigenvectors of matrices $\mathbf{Z}^{\mathrm{T}}\mathbf{Z}$ and $\mathbf{Z}\mathbf{Z}^{\mathrm{T}}$, respectively. The number of components can be determined by crossvalidation (Wold 1978) in such a way that the matrix of the model residuals **E** does not include a significant predictive component. Note than other criteria than crossvalidation may be more appropriate in Lb-MSPC (Camacho and Ferrer 2014).

The quadratic error in the prediction of the observation *i-th* is given by the following expression:

$$SPE_i = \sum_{k=1}^{K} \mathbf{e}_{ik}^2 = (\mathbf{z}_i - \hat{\mathbf{z}}_i)^T (\mathbf{z}_i - \hat{\mathbf{z}}_i) \tag{1.11}$$

This represents the euclidean distance of the observation $\mathbf{z}_i$ to its own projection in the *A-th* dimensional latent subspace and, consequently, it is an index of the goodness of fit of that observation to the latent model. The model of the in-control process is defined by the directions $\mathbf{p}_a$, the mean vector $\boldsymbol{\mu}_{\mathrm{ref}}$ of the original variables

and the covariance matrix of the latent variables (diagonal matrix including the variances of the A latent variables considered in the model). For each new observation $\mathbf{z}_{new}$, the monitoring consists on computing the scores $\mathbf{t}_{a,new}$ and the SPE_{new}, and compare them to the region for an in-control process in the corresponding multivariate control charts.

The *scores* t_a are linear combinations of the process variables and, as a consequence of the central limit theorem, can be approximately modelled by a multivariate normal distribution. Hotelling´s T^2 charts on only A components are used to monitor the scores. To distinguish this statistic from the normal Hotelling´s T^2 statistic which uses all the components, we will use the notation T_A^2.

$$T_A^2 = \sum_{a=1}^{A} \frac{t_{a,new}^2}{s_a^2} = \sum_{a=1}^{A} \frac{\mathbf{p}_a^T(\mathbf{z}_{new} - \boldsymbol{\mu}_{ref})}{s_a^2} \qquad (1.12)$$

where s_a^2 is the variance of the *a-th* latent variable.

The upper control limit of the T_A^2 chart can be obtained by different approaches but it is frequent to use the expression given by Tracy *et al.* (1992)

$$UCL_{T_A^2} = \frac{(N^2 - 1)A}{N(N - A)} F_{1-\alpha}(A, N - A) \qquad (1.13)$$

where $F_{1-\alpha}(A, N - A)$ is the (1-α)×100 percentile of the F- Snedecor distribution with (A, N-A) degrees of freedom.

The upper control limit for the *SPE* can be calculated from approximated solutions that are based on cuadratic forms or obtained from a historic data reference in-control distribution. Box (1954) demonstrated that the distribution of the *SPE* is well approximated by a non-central chi-square distribution $g \cdot \chi^2_{(h)}$ where g (scale parameter) and h (freedom degree) depend on the eigenvalues (λ_{A+1}, λ_{A+2} ….λ_K) of

the covariance matrix of the residuals **E**. Nomikos and Macgregor (1995) use this approach and proceed to estimate the parameters of the non-central chi-square by the methods of the moments. That is to say, they equal the mean and the variance of the *SPE* calculated on the reference in-control data set (obtained under normal operating conditions, NOC) to the expected values for the chi-square distribution (gh and $2g^2h$ respectively). Thus, the following expression for the *SPE* control limit with a type I risk α is obtained:

$$SPE_\alpha = \frac{\nu}{2m}\chi^2_{\frac{2m^2}{\nu},\alpha} \tag{1.14}$$

where $\chi^2_{\frac{2m^2}{\nu},\alpha}$ is the (1-α) × 100 percentile for a chi-square distribution with $\frac{2m^2}{\nu}$ degree of freedom. Another approximation is used by Jackson and Mudholkar (1979):

$$SPE_\alpha = \theta_1\left[\frac{z_\alpha\sqrt{2\theta_2 h_0^2}}{\theta_1} + \frac{\theta_2 h_0(1-h_0)}{\theta_1^2}\right]^{1/h_0} \tag{1.15}$$

where $\theta_k = \sum_{j=A+1}^{K}(\lambda_j)^k$ and $h_0 = 1 - \left(2\theta_1\theta_3 \Big/ 3\theta_2^2\right)$ and z_α is the (1-α)×100 percentile for a standard normal distribution.

The T_A^2 chart checks if the new observation is inside the normal operation region (inside statistical control limits) of the projected subspace and the *SPE* chart analyses if the distance from the new observation to its projection in the model latent variables subspace is similar to the case of the in-control observations. As it can be seen in Figure 1.8 abnormal variations which break the correlation structure of the model would lead to abnormally large values of the *SPE* whilst abnormal variations that keep

the correlation structure of the model would lead to abnormally large values of the T^2_A statistic.

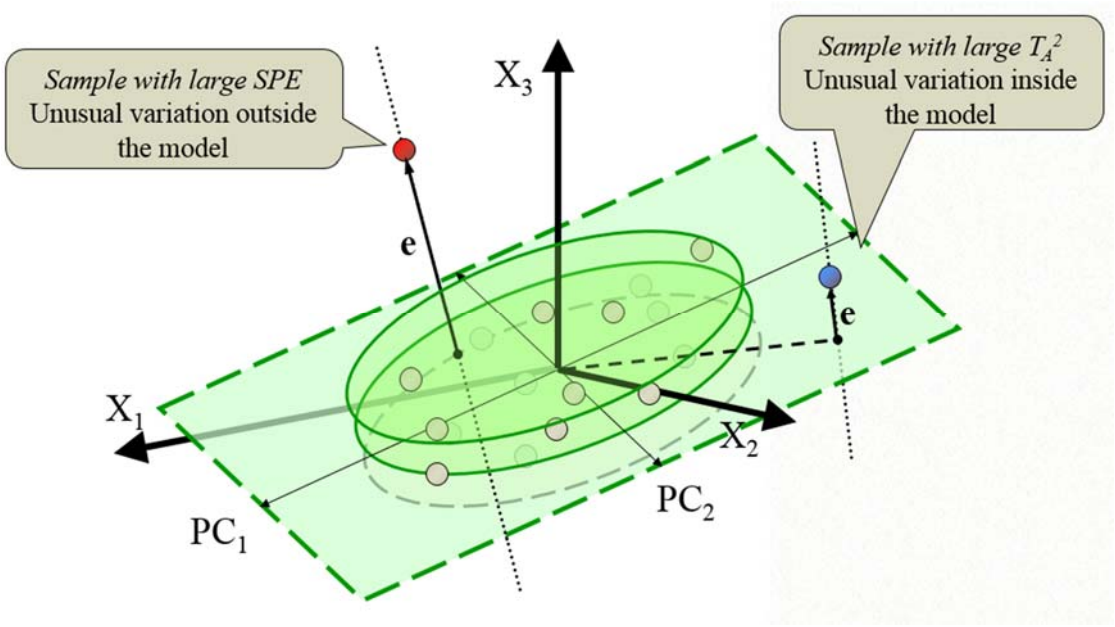

FIGURE 1.8: Faults associated to abnormal values of the *SPE* and T^2_A

Process monitoring with PCA will proceed as described in Figure 1.9: first the statistics *SPE* and T^2_A for the new observation are computed, then the *SPE* is checked against the corresponding threshold. If the statistic *SPE* exceed the threshold then a fault is detected and we proceed to the diagnosis. In this case the detected fault has broken the correlation structure of the model. On the contrary if the *SPE* is in-control then it continues by checking the T^2_A statistic against its threshold. If this statistic exceeds the corresponding threshold then a fault is detected. In this case the fault keeps the correlation structure of the model but the process seems to have moved to a different operational point. In case that both statistics (*SPE* and T^2_A) fall within their control limits then the process is considered in control.

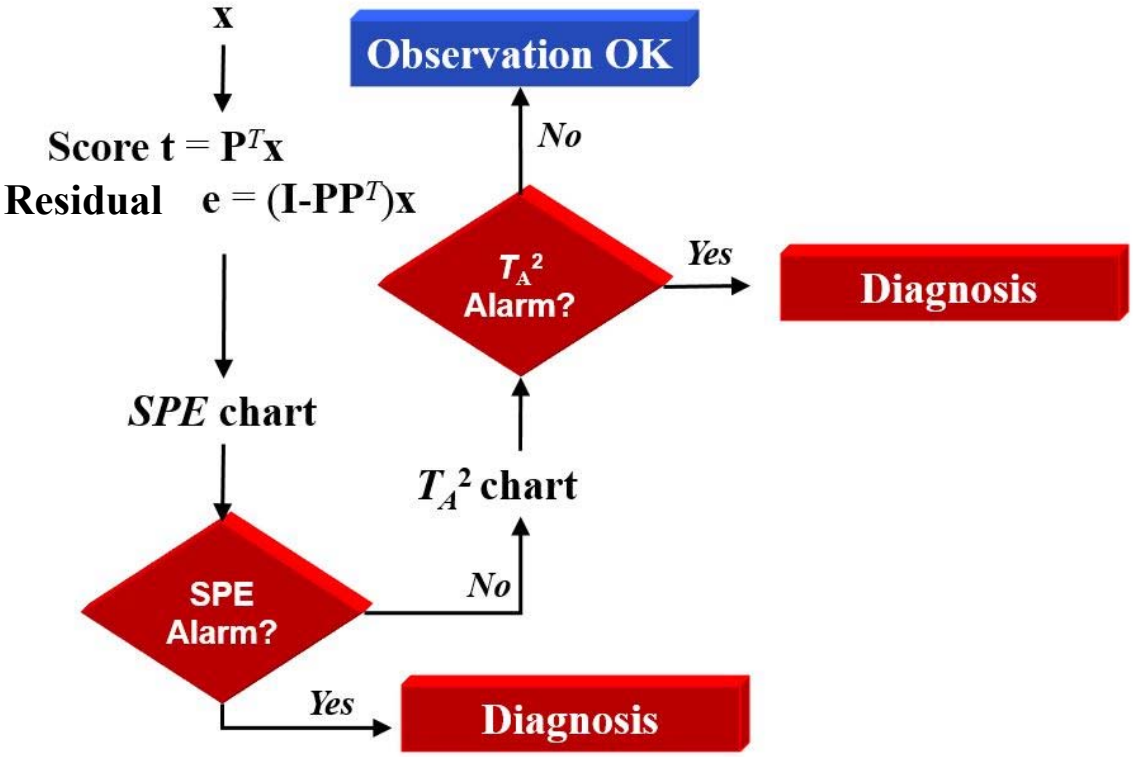

FIGURE 1.9 Process monitoring with PCA

- **Hotelling´s T^2_A and *SPE* statistics versus Hotelling´s T^2 statistic**

Equation 1.16 shows that the Hotelling ´s T^2 statistic expressed in terms of the latent variables of a *PCA* model with A latent components has two parts: the T^2_A that uses the first A major latent components and the $T^2_{Hawkins}$ that uses the K-A minor latent components (which are not extracted).

$$T^2 = \sum_{a=1}^{A} \frac{t^2_{a,new}}{s^2_a} + \sum_{a=A+1}^{K} \frac{t^2_{a,new}}{s^2_a} = T^2_A + T^2_{Hawkins} \qquad (1.16)$$

It must be noted that the variances s^2_a of the minor latent components are close to zero and can be the cause of large values in the Hotelling ´s T^2 statistic that are not necessarily related to the presence of a fault. The MSPC based on latent variable models

uses the Hotelling´s T^2 statistic on the first A latent components (T^2_A) and consequently do not present that problem.

The other monitored statistic in MSPC based on latent variable models is the square prediction error *SPE*. This statistic expressed in terms of the latent variables has the following expression: $SPE = \sum_{a=A+1}^{K} t_a^2$. It can be appreciated that this statistic does not present the problems associated to the T^2_{Hawkins} as their terms are not divided by small variances.

The consequence of the above is that the Lb-MSPC based on latent variables (T^2_A and *SPE*) have a smaller number of false alarms than the MSPC based on the Hotelling´s T^2 statistic (classical MSPC).

- **Partial least squares (PLS):**

  The partial least squares PLS model uses the joint information contained in the process (matrix **X**) and quality (matrix **Y**) variables measured under normal operation conditions (NOC) to create an in-control PLS model of the process. The PLS model simultaneously reduces the dimension of the matrix **X** and **Y** and proceed to select the latent variables in **X** that not only explain the variability associated to the process variables but that serves to make a better prediction of the quality variables. This model provides online predictions of the quality of the process using process data and before laboratory results may be obtained. The PLS model can be expressed as:

$$\begin{gathered} \mathbf{t}_a = \mathbf{X}_{a-1}\mathbf{w}_a; \mathbf{X}_a = \mathbf{X}_{a-1} - \mathbf{t}_a\mathbf{p}_a^T \\ \mathbf{X} = \sum_{a=1}^{A} \mathbf{t}_a\mathbf{p}_a^T + \mathbf{E} \\ \mathbf{Y} = \sum_{a=1}^{A} \mathbf{u}_a\mathbf{c}_a^T + \mathbf{F} = \sum_{a=1}^{A} \mathbf{t}_a\mathbf{c}_a^T + \mathbf{G} \end{gathered} \tag{1.17}$$

Where $\mathbf{w}_a$ and $\mathbf{c}_a$ are the directions in the space spanned by the matrices **X** and **Y**, respectively, which maximize the covariance among the latent variables associated to both subspaces, $\mathbf{t}_a$ and $\mathbf{u}_a$. The directions $\mathbf{p}_a$ are the ones which permit a better reconstruction of the matrix **X** while maintaining the orthogonality between the *score vector* $\mathbf{t}_a$ and the loading vector $\mathbf{w}_a$. In this model the new latent variables in the space **X**, $\mathbf{t}_a = \mathbf{X}_{a-1}\,\mathbf{w}_a$ represents the projection of the *N* observations in the directions of major variance of the space **X** which are more correlated to the most important variables of **Y**.

The number of components to extract are obtained by crossvalidation (Wold 1978, Bro *et al.* 2008). For each observation ($\mathbf{x}_i$, $\mathbf{y}_i$), two *SPE* can be calculated, one in the **X** space ($SPE_{\mathbf{X}_i}$) and the other in the **Y** space ($SPE_{\mathbf{Y}_i}$):

$$\begin{aligned} SPE_{\mathbf{X}_i} &= \sum_{k=1}^{K} e_{ik}^2 = \left(\mathbf{x}_i - \hat{\mathbf{x}}_i\right)^T \left(\mathbf{x}_i - \hat{\mathbf{x}}_i\right) \\ SPE_{\mathbf{Y}_i} &= \sum_{m=1}^{M} g_{ik}^2 = \left(\mathbf{y}_i - \hat{\mathbf{y}}_i\right)^T \left(\mathbf{y}_i - \hat{\mathbf{y}}_i\right) \end{aligned} \tag{1.18}$$

New observations are monitored in a similar way to the PCA through the use of control charts constructed from the in-control model obtained from a data set collected under normal operation conditions (NOC). As in the PCA, the monitored statistics in PLS are the T_A^2 and the *SPE*. In this case, the T_A^2 monitors the variation in the process variables which have a more important influence in the quality variables.

- **NIPALS algorithm:**

In PCA and PLS the components are usually computed in an iterative scheme using the NIPALS algorithm (Geladi and Kowalski 1986). This algorithm is specially

indicated in the case of a megavariate context with large ill-conditioned data matrices. In these cases the use of non-iterative algorithms (like singular value decomposition, SVD) is not recommended, not only because they would be more time consuming but these methods would experiment difficulties in the calculation of some components due to the presence of a high collinearity (created by the eigenvalues close to zero). Another advantage of the NIPALS algorithm is that it performs well despite the presence of missing data (Nelson *et al.* 1996). Some authors have studied different methods to estimate the scores when there are missing data in the observations (Arteaga and Ferrer 2002, Nelson *et al.* 1996) and the uncertainty associated to the scores and *SPE* computed with these type of observations (Arteaga and Ferrer 2003, Nelson 2002).

- **PCA and PLS further applications:**

The good performance of these monitoring techniques in continuous processes and its superiority in relation to the standard USPC have been proved in many real industrial processes (Dayal *et al.* 1994, Kourti and MacGregor 1996, Tano *et al.* 1995). Nomikos and MacGregor (1995) adapted the multivariate statistical method based on projection to latent structures PCA and PLS, developed for monitoring continuous processes, to the case of batch processes using PCA Multiway Principal Component Analysis (MPCA) and Multi-way Partial Least Squares (MPLS) (Wold *et al.* 1987, Geladi 1989). The basic idea of these techniques consists on unfolding the tridimensional matrix (batch - variable - time) into a two dimensions matrix **X,** where each row corresponds to the trajectory of each process variables along the batch duration. Applications of these techniques can be found at Kourti *et al.* (1996), Ferrer (2002) and Zarzo *et al.* (2002a y 2002b). The batch-MSPC scheme can be extended

to processes that can be split in blocks. These blocks can correspond to different physical units, stages or phases of the process or extra information about the process, initial conditions of temperature and pressure, quality of the raw materials or suppliers, different labour teams, and so on. All these blocks of information in addition to the quality variables can be used in a unique SPC scheme throw the use of the multi-block projection methods (Wold *et al.* 1987). These methods permit to establish monitoring charts for each block of variables and for the process as a whole and reduce the complexity of the implementation for fault detection and diagnosis in these situations. Examples of these methods can be found at Kourti *et al* (1996), Kourti and MacGregor (1996), MacGregor *et al.* (1994), Qin *et al.* (2001), Westerhuis *et al.* (1998a) and Wold *et al.* (1996).

1.3.2- Statistical process control - Diagnosis

Section 1.1 reviews the diverse approaches to perform fault diagnosis that is the main goal of this research work. In particular we are especially interested in the FDI process history-based approaches with a quantitative feature extraction using statistical methods based on latent variable models (PCA/PLS) or multivariate statistics (Hotelling´s T^2 statistic). Particularly, these approaches are frequently used for fault diagnosis applications in process industries. The reasons are that they are easy to implement, require very little modelling effort and a priori knowledge, and make use of the vast amount of data usually registered in actual processes due to communication and information technologies.

In the SPC the fault diagnosis stage is triggered by the detection of a fault and it is aimed to determine the root cause of the problem. The final objective is the process recovery or the reconstruction of the sensor measurements if it results to be a sensor fault.

The latter may be an important issue if the variable is involved in a process loop. In this case the sensor fault, if not attended or reconstructed, might finally provoke a more serious process fault. As it can be seen in Figure 1.10 there are two general approaches based on the availability or not of data sets corresponding to the different types of fault.

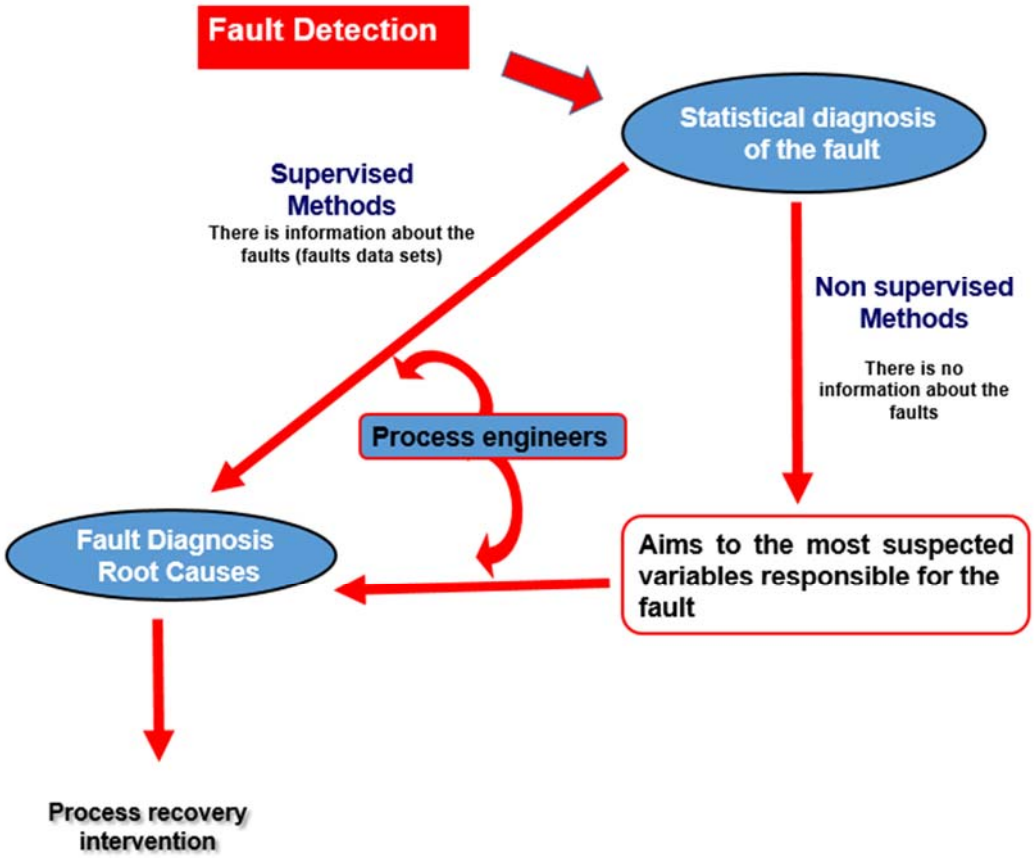

FIGURE 1.10 Fault diagnosis scheme

There are diagnosis methodologies that are based on the use of fault data sets and that are classified as supervised methods. The main advantage of these methods is that they can aim directly to the root cause of the problems and consequently ease the work of the process engineers. The main problem in applying these methodologies is precisely the difficulty of obtaining these fault data sets. If no fault data sets are available, then only the unsupervised methods can be used. These methods just aim to the list of variables that

can be involved in the root cause of the fault. Then, process engineers will have to determine the probable root cause of the problem.

In addition, the diagnosis procedure is related to the adopted strategy for fault detection. Thus, the performance of the different diagnosis methodologies may be in part conditioned to an appropriate selection of the best joint strategy for detection and diagnosis taking into account the type of process and the nature of the relationships existing among the measured variables. We consider three possible scenarios:

Scenario 1: Data poor environments with uncorrelated quality variables

This is the scenario where the USPC is the most appropriate tool for monitoring the process. The univariate charts are appropriate as there is no extra information to consider about the correlation among the monitored variables. The selection of the appropriate monitoring chart, Shewhart, CUSUM or EWMA is depending on the nature of the faults as it was explained in Section 1.3.1.1. For small size faults the CUSUM and EWMA charts have a better performance (smaller *out of control* ARL) than the Shewhart chart.

In this scenario the fault diagnosis strategy is reduced to detect which charts are giving signals for the isolation of the set of observation variables that are out of control. Following this, the process engineer has to assign a root cause to the detected problem in the process.

Nowadays, the boom in affordable measure devices and technological advances in the industry and communications accounts for the abundance of data rich environments (with many process variables measured on line). As the number of the measured variables increases it becomes hard to find a situation where variables remain uncorrelated. Due to the lack of applicability in modern industrial processes, this scenario 1 is not going to be addressed in our research.

Scenario 2: Data poor environments with mildly correlations among variables

This is a good scenario for using multivariate statistical quality control (MSQC) methods. These methods are defined in the space of the original measured variables and have good performance when there is a reduced number of mildly correlated quality and/or process variables with a well-conditioned covariance matrix. The Hotelling´s T^2 statistic is the multivariate statistic most frequently used in the detection stage. As commented in Section 1.1.2.2 there is a wide variety of unsupervised methods proposed for fault diagnosis in MSQC. The diagnosis in these methods is mostly based on the use of different computed terms that are equivalent to the decomposition terms of the Hotelling´s T^2 statistic. The terms that becomes statistically significant aim to the original measured variables which contributes to a major extent to the abnormal value of Hotelling´s T^2 statistic and provide the information about what variables are responsible for the fault and to diagnose the root causes. The second part of this thesis (Part II) is focused in this group of unsupervised methods used in MSQC. All these methods are described in full detail in Chapter 3.

Scenario 3: Data rich environments

In this scenario it is common to have hundreds of process variables measured with on-line sensors. It is frequent a high sampling rate (seconds-hours). It is a common feature the high-dimensional and collinear data with missing data problems. In this context the USPC and classical MSPC do not work and there is room for a new type of approaches such as the latent variable models, that take into consideration that the process is driven by only a few underlying common cause events.

Once a fault has been detected we need to know the original measured variables responsible for the detected fault (unsupervised method). This is even more important for

the Lb-MSPC that uses latent variables that differ from the measured ones. After this, the process engineers will have to look for the root causes for process recovery. The diagnosis procedure depends on the context: unsupervised vs supervised methods.

- **Unsupervised methods: contribution plots**

This methodology, proposed by MacGregor *et al.* (1994) and Miller *et al.* (1993), and is an excellent and widespread option when there is no information about the different types of fault. In the case of the *SPE* for a new observation with $SPE = \sum_{k=1}^{K} (x_k - \hat{x}_k)^2$ the contribution of the variable x_k to the *SPE* is given by the expression:

$$\text{Cont}\,(SPE; x_k) = (x_k - \hat{x}_k)^2 \qquad (1.19)$$

An alternative to the definition of the contribution of the original variables to the *SPE* is to use the square root of these contributions:

$$\text{Cont}\,(SPE; x_k)^* = \sqrt{\text{Cont}\,(SPE; x_k)} = (x_k - \hat{x}_k). \qquad (1.20)$$

The advantage of this definition is that these contributions maintain the sign of the differences. These contributions will be used in Chapter 8 as part of a novel fault diagnosis approach called the fingerprint contribution plot methodology (FCP).

On the other hand the contributions of the variable x_k to individual score "*a*" is equal to $p_{a,k}\,(x_k - \bar{x}_k)$. As it is common that more than one score may have high values, Kourti and Macgregor (1996) suggested that an overall average contribution per variable is calculated using the normalized scores with high values and keeping only the contributions with the same sign as the score. These contributions are calculated with the following expression:

$$\text{Cont}\,(T_A^2;a,x_k)=\frac{t_a}{s_a^2}\,p_{a,k}(x_k-\bar{x}_k)=\frac{t_a}{\lambda_a}\,p_{a,k}(x_k-\bar{x}_k) \qquad (1.20)$$

If Cont $(T_A^2;a,x_k)$ is negative it is set equal to zero and then the total contribution of variable x_k is calculated as:

$$CONT_k=\sum_{a=1}^{K}\text{Cont}\,(T_A^2;a,x_k) \qquad (1.21)$$

This contributions arranged in the corresponding bar charts are known as contribution plots and are excellent tools for a quickly identification of the observation variables that are related to the detected fault.

- **Supervised methods**

In the last 20 years several supervised approaches have been proposed for diagnosis in MSPC based on latent variable models (Lb_MSPC). As commented in Section 1.1.2.2, different methodologies based on fault reconstruction (Dunia and Qin 1998, Yue and Qin 2001, Alcala and Qin 2009), on fault signature extraction (Yoon and MacGregor 2001) in addition to different classification techniques based on the use of PLSDA (partial least squares discriminant analysis) (Sjöström *et al.* 1985) or SIMCA modelling (Wold 1983), were successfully applied to fault diagnosis. A good state of the art review of these methods and applications developed during the last two decades can be found in Qin (2012), Russell *et al.* (2012) and MacGregor and Cinar (2012). Some studies on diagnosis performance in data driven diagnosis methodologies can be found at Yin *et al.* (2012) and Russell *et al.* (2012).

The third part of this thesis (Part III) is focused in this group of supervised methods which use latent variable models for diagnosis. In Chapter 7 we will proceed to describe the methods under comparison in full detail.

Chapter 2: Material and data sets

The objective of this chapter is to introduce the material and all the process data bases and simulations that have been used to compare the fault diagnosis performance of the different proposed strategies. We have worked with processes of diverse nature and with varied data sets that can affect the different strategies in different ways. Section 2.1 and 2.2 describe the hardware and software used for this research. Section 2.3 is dedicated to describe the process data sets and simulations. They include data from a pasteurization process in pilot plant and a distillation process, and data sets from simulations

2.1 Hardware

All computations carried out along this thesis have been performed with an Intel (R) Core (TM) i7-4500U CPU @ 1.80 GHz 2.40 GHz

2.2 Software

The software package used in this thesis is:

- Matlab 7.4 and R2010a (©The Mathworks, Inc.,Natick, MA, USA).

All functions, algorithms and scripts used in this thesis are own code implemented in Matlab code.

2.3 Process and simulations data sets

2.3.1 Process data sets

2.3.1.1 Pasteurization process

This data set is used in the comparison of the performance of different methods proposed for fault diagnosis in Chapter 6 (MSQC) and Chapters 7 to 9 (MSPC).

Plant description

The process plant trainer PCT23 MKII of ARMFIELD is a bench mounted process plant trainer with multiple streams both interacting and noninteracting. The process plant incorporates a miniature three-stage plate heat exchanger (recycle, heating and cooling) heated from a hot water circulator, two independent feed tanks, a holding tube with product divert valve and two variable-speed peristaltic pumps. The equipment incorporates electrical fault simulation and control,

FIGURE 2.1: Picture of the PCT23 MKII plant

The process mimics an industrial high temperature short time pasteurisation process. In this process the product stream has to be kept at a predetermined temperature for a minimum time, usually for bacteriological purposes. This is achieved by the use of a holding tube, which delays the product stream, thus posing particular process control problems. The unit includes a wide range of instrumentation for temperature and flow measurement.

An electrical console provides measurement and control of the process plant and allows a variety of control techniques including manual operation, on/off control, control from an external signal and control from a programmable logic controller (PC or PLC). The equipment incorporates electrical fault simulation.

Process description

A pasteurization process works as follows: First the product flows into the system. This product is heated by water flowing along it, of which we can control the temperature and the flow speed. Next the heated product goes through a curved pipe (holding tube). To pasteurize the product it needs to be above a certain temperature for a certain time. This is the time the products needs to pass through the holding tube. This tube is coated with thermal insulated material so that the loss of heat is reduced to the minimum. When it comes out of the holding tube there is a diverter valve where the temperature is measured and the system decides whether the product is good or not. If the temperature of the product is still above the required temperature, we know that it is good. If it is not, it is thrown away or used to refill the feed tank. Now the good product is used to preheat the new product flowing in. Next the temperature is measured again and the system decides whether or not it needs to be cooled down more using cold water.

A flow diagram of the process is shown in Figure 2.2:

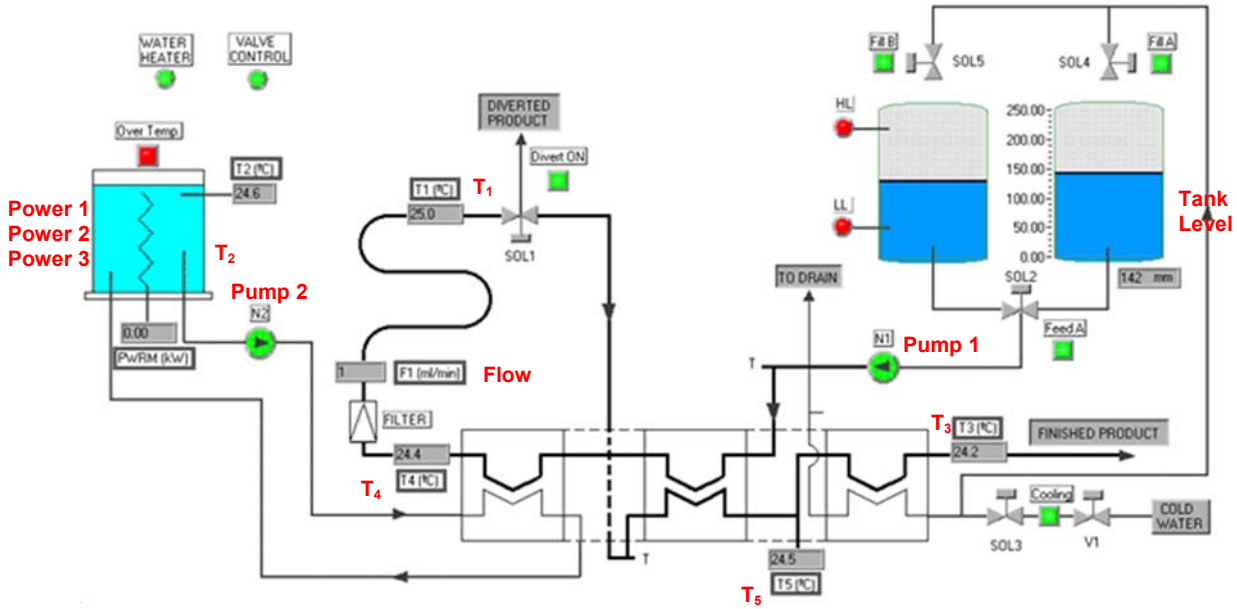

FIGURE 2.2: Flow diagram of the pasteurization process

Components of the process unit

- Feed tanks: they store and feed the system with the fluid to be pasteurized
- Product feed pump (N1): This is a peristaltic pump that makes the product circulate through the system.
- Hot water tank: This tank contains the hot water after passing the heat exchanger. It is used to increase the temperature of the product undergoing pasteurization. The water is on a closed system and after passing the heat exchanger return to the hot water tank so it can be heated again until it reaches a predetermined temperature. There is a peristaltic pump (N2) that circulates the water through the system. The speed of the pump depends on the temperatures in the hot water tank and the required outlet temperature at the heat exchanger. The more outlet temperature the more speed in the pump N2 as it is needed more heat to transfer. On the other side the more is the temperature in the hot water tank the less speed is required in the pump N2 for a fixed heat transfer. The tank has a low level sensor that warns when the heat resistance is not covered by water and a thermostat that shut off the plant if hot water tank goes up higher than 65ºC. The electrical resistance has a maximum heating power of 1,92[kW].
- Heat exchanger: The plant has a heat exchanger divided in three sections. In the first section from left to right the fluid to be pasteurized is heated. In the second section the fresh feed is preheated, for energetic reasons, by the already pasteurized product. In the third section the pasteurized product can be cooled using cold water (external source).
- Holding tube with a thermal insulating coat.
- Divert valves: It is a solenoid valve that is placed at the holding tube outlet.

Process variables

There are 13 variables involved in this process described in Table 2.1. Clearly some of these variables are highly correlated. For example, a high temperature before going into the holding tube, T^a_4, implies a high temperature after flowing through the holding tube, T^a_1.

TABLE 2.1 Variables measured in the pasteurization model

Variable	Description
Tank Level	Level of the water in the tank at the beginning of the process. If it drops below a certain limit, the tank is refilled.
T^a_1	Temperature of the product after flowing through the holding tube. This temperature defines whether or not we have a good product.
T^a_2	Temperature of the heating water. This is the water which has to heat the product.
T^a_3	Temperature of the final product. This is the temperature of the product when it leaves the system.
T^a_4	The temperature of the product immediately after heating, *i.e.* before entering the holding tube..
T^a_5	Temperature of the product after preheating the new product. This temperature defines whether or not the product needs further cooling down.
Flow	Speed with which the product flows through the system.
SPFlow	Setpoint of the flow.
Power 1 **Power 2** **Power 3**	These variables measure the power used to heat the heating water.
Pump 1	Percentage that pump 1 is opened. Pump 1 controls the flow speed of the product.
Pump 2	Percentage that pump 2 is opened. Pump 2 controls the flow speed of the heating water.

Process loops controls

The pasteurization process is an automatic process. This means that it changes by itself to correct things when it is not producing good product. The process contains three control loops. There is a setpoint for the temperature of the heating water, T^a_2. If this temperature is not good, the power of the heater is adjusted. There is a second setpoint for the temperature right after the product comes out of the holding tube, T^a_1. If this temperature is not good, the speed with which the heating water is flowing is adjusted by

changing the working of Pump 2. Finally, there is a third setpoint for the flow. If the product does not flow through the system at the right speed, Pump 1 is adjusted.

Reference and faults data sets

Several data sets under different conditions (normal operating (NOC) and faulty conditions) were registered. The arrangements for the reference data set are the following: the setpoint for the temperature of the heating water is 60C^{o} and the product assumed to be good if the temperature T_1 is larger than 48C^{o}, while the setpoint for T^{a}_1 is 50C^{o}. While taking this reference data, the product produced was good. Add to it we also registered data sets in which we initialized several faults shown in Table 2.2.

TABLE 2.2 List of possible faults

Fault
Set Point T_1
Failure in Pump 1 (Feeding)
Decay of 30% in Pump 1 (Feeding)
Sensor Flow
Sensor T_1 (Down)
Sensor T_1 (Up)
Sensor T_2 (Down)
Sensor T_3 (Up)
Sensor T_4 (Down)
Sensor T_4 (Up)
Sensor T_5 (Down)
Sensor T_5 (Up)
Failure of the valve which divert the wrong product
Set Point Flow (Down to 110)
Set Point Flow (Up to 200)

2.3.1.2 Distillation process

A simulink nonlinear model of a binary distillation column developed by Skogestad (1996) and modified by Villaba (2012) to obtain a more realistic one was used. Simulink

is an environment for multidomain simulation and model-based design for dynamic and embedded systems.

This data set is used in the comparison of the performance of different methods proposed for fault diagnosis in Chapters 7 to 9 (MSPC).

Process description

Distillation is a process of separating the component substances from a liquid mixture by selective evaporation and condensation. Distillation may result in essentially complete separation (nearly pure components), or it may be a partial separation that increases the concentration of selected components of the mixture. In either case the process exploits differences in the volatility of mixture's components.

Among the different types of distillation processes the selected model is based in a *fractionation* design. Industrial distillation is typically performed in large, vertical cylindrical columns known as "distillation or fractionation towers" or "distillation columns". The distillation towers have liquid outlets at intervals up the column which allow for the withdrawal of different fractions or products having different boiling points or boiling ranges. By increasing the temperature of the product inside the columns, the components are separated. The "lightest" products (those with the lowest boiling point) exit from the top of the columns and the "heaviest" products (those with the highest boiling point) exit from the bottom of the column. A schematic representation of this type of processes (Wikipedia) is shown in Figure 2.3.

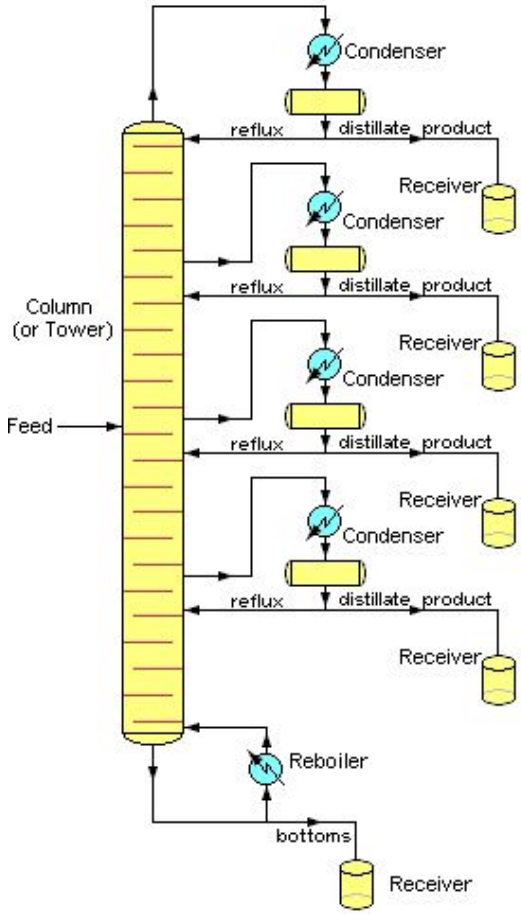

FIGURE 2.3: Scheme representation of a continuous fractional distillation tower separating one feed mixture stream into four distillate and one bottoms fractions

The feed is introduced more or less centrally into a vertical cascade of stages. Vapour rising in the section above the feed (called the absorption, enriching or rectifying section) is washed with liquid to remove or absorb the less volatile component. Since no extraneous material is added, as in the case of absorption, the washing liquid in this case is provided by condensing the vapour issuing from the top, which is rich in more volatile component. The liquid returning to the tower is called reflux, and the material permanently removed is the distillate, which may be a vapour or a liquid rich in the more volatile component. In the section below the feed (stripping or exhausting section), the liquid is stripped of the more volatile component by vapour produced at the bottom by partial vaporization of the bottom liquid in the reboiler. The liquid removed rich in less volatile component, is the residue, or bottoms. Inside the tower, the liquids and vapours

are always at their bubble and dew points, respectively, so that the highest temperatures are reached at the bottom and the lowest at the top. The entire device is called a fractionator.

Process variables and model assumptions

The model used corresponds to a fractionator of a mixture of two components (methanol and ethanol) operating at constant pressure, constant relatively volatility and constant molar flows.

The scheme of the process is shown in Figure 2.4. The controlled variables are product compositions, the column pressure (p) and the liquid holdups in the reflux drum and reboiler (M_D and M_B), respectively. The five manipulated variables are product flow rates at the top (D) and at the bottom (B) and internal flow rates at the top (L,V_T) and at the bottom (V_B) of the column. The feed stream is assumed to come from an upstream unit. Thus, the feed flow rates (F) cannot be manipulated, but it can be measured and used for feedforward control. Other disturbances are temperature (T_F) and composition (z_F) of the feed. Figure 2.4 shows the location of this controlled and manipulated variables in the binary distillation column.

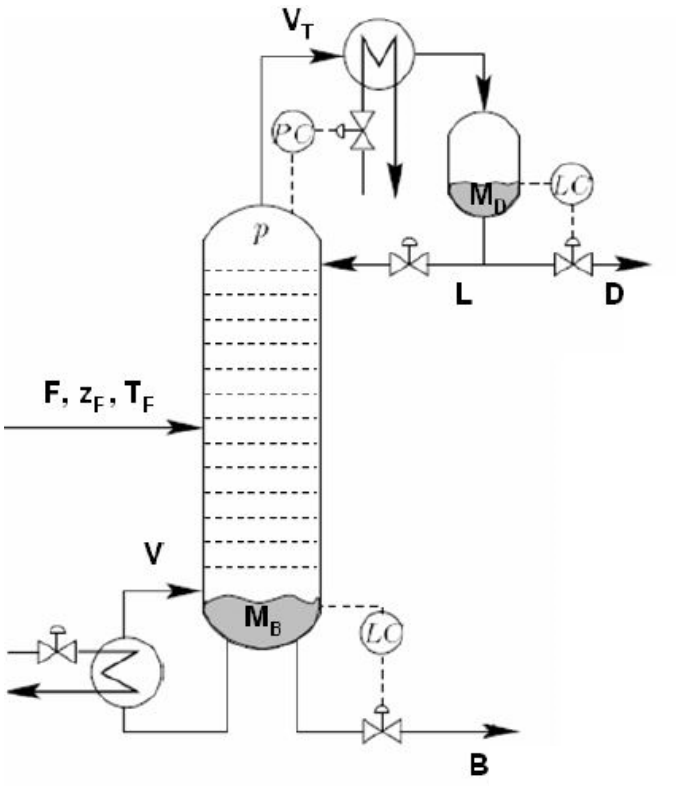

FIGURE 2.4: Controlled and manipulated variables in the binary distillation column

In the fault diagnosis methods we have considered the following process variables:

TABLE 2.3 List of the 48 process variables used in fault diagnosis

Variable	Explanation	Units
T_F	Feed Temperature	ºC
z_F	Feed composition	Molar Composition
Fv	Reflux Flow	L/h
D	Distillate flow	L/h
V	Boilup flow (vapour)	L/h
B	Bottom flow	L/h
L	Liquid Flow	L/h
T_1 to T_{41}	41 try temperatures	ºC

Process loops controls

The multiloop control strategy for the distillation column consisted of three decentralized single input single output (SISO) loops for level and pressure involving the outputs

1) Distillate holdup level (M_D) controlled by distillate flow (D)

2) Bottom holdup level (M_B) controlled by bottom flow (B)

3) Column pressure (p) controlled by condenser vapour flow (V_T)

There is also a control on the product composition.

Faults

Some of the faults were related to changes in the feed parameters (F, z_F and T_F) and the other types of faults were related to failures in the PI controllers.

2.3.2 Simulations data sets

This data set is used in the comparison of the performance of different methods proposed for fault diagnosis in Chapters 4 and 6 (MSQC).

Simulations were run for the case of four and seven measured variables. In order to compare the proposed methods several faults consisting of small, medium or large shifts in the mean of one or more variables under different scenarios of correlation matrices were simulated. Different correlation structures where the covariance matrix condition numbers tend to increase. Reference data sets for each of the correlation structures were obtained using the algorithm proposed by Arteaga and Ferrer (2010). For every correlation structure 102 different types of faults were considered. The faults consisted in small, medium or large shifts in the mean of one, two or three variables. The shifts involving several means happened in both the same or opposite directions. For each type of fault, observations were also simulated using the algorithm proposed by Arteaga and Ferrer (2010).

Part II

Fault diagnosis in multivariate statistical quality control (MSQC)

The first part, including Chapters 3 to 6, is concerned with the Multivariate Statistical Quality Control (MSQC). In this part we are going to consider data poor environments (scenario 2 described in Section 1.3.2) where the MSQC is the preferred option for monitoring the process. These methods are defined in the space of the original measured variables and have performed reasonably well when there is a reduced number of mildly correlated quality and/or process variables with a well-conditioned covariance matrix.

Our research in this part has produced the following results:

Journal publications

- S.Vidal and A.Ferrer (2014).“A comparative study of different methodologies for fault diagnosis in multivariate quality control” *Communications in Statistics-Simulation and Computation* . Vol 45 num 5 986-1005 (ISSN 0361- 0918)

Conferences

- “A comparative study of different methodologies for fault diagnosis in multivariate quality control “. *Proceedings of the 28th Quality and Productivity Research Conference 2011 (QPRC) Roanoke, Virginia, USA.*
- “Fault diagnosis in the on-line monitoring of a pasteurisation process: a comparative study of different strategies”. *Proceedings of the 5th Annual Conference of the European Network for Business and Industrial Statistics 2005 (ENBIS) Newcastle, UK.*
- “Estrategias para el diagnóstico de fallos en la monitorizacion de procesos multivariantes: estudio de revisión”. *Proceedings of the XXVIII Congreso Nacional de Estadística e Investigación Operativa 2004 (SEIO) Cadiz, Spain.*

Chapter 3: Fault diagnosis methods in MSQC

This chapter gives a description of the most common methods used for fault diagnosis in unsupervised MSQC. The chapter describes the rationale of the different methods and shows the requirements for their implementation, their strong points and their drawbacks, and establishes the relationships between them.

3.1 Introduction

Industrial quality control usually involves a vector of measurements of either several critical to quality or critical to process parameters rather than a single characteristic. Typically, when these measurements are mutually correlated, a more efficient statistical process monitoring scheme is obtained by using multivariate control charts rather than separate univariate control charts. Among the most popular multivariate control charts is the one based on Hotelling´s T^2 statistic (Jackson 1985, Mason *et al.* 1992) that was described in Section 1.3.1.2. This statistic is defined as the estimated Mahalanobis squared distance from the K-dimensional sample observation $\mathbf{x}_i$ to its sample mean vector $\bar{\mathbf{x}}$ calculated from a reference (in-control) historical data set. A major advantage of the above statistic is that it is the optimal single-test statistic for a general multivariate shift in the mean vector (Hawkins 1991). However, it has several practical drawbacks: a) it is not optimal for more structured mean shifts (*i.e.* mean shifts in only selected variables); b) it is not specific to a shift in mean as it is also affected by changes in the covariance matrix; c) it is not immediately interpretable, (*i.e.* if following a signal, it does not provide information on which specific variable or set of variables is out of control).

In an attempt to improve the interpretability of T^2-based fault diagnostics several approaches have been proposed in multivariate quality control literature. The Step-down method of Roy (1958) assumes that there is *a priori* ordering among the means of the variables and tests subsets sequentially using this ordering to determine the sequence. Murphy (1987) suggests a method based on a discriminant distance using Hotelling´s T^2 statistic. Mason, Tracy and Young (1995, 1997) introduce a procedure for decomposing Hotelling´s T^2 statistic into orthogonal components. Hawkins (1991, 1993) uses regression adjustments for each individual variable. Runger and Montgomery (1996) define a distance to measure the contribution of a variable to the value of Hotelling´s T^2

statistic. Doganaksoy, Faltin and Tucker (1991) propose to rank the variables most likely to have changed according to their relative contribution to Hotelling´s T^2 statistic using a univariate t statistic as a criterion. Hayter and Tsui (1994), using a different procedure than Hotelling´s T^2 statistic as a trigger mechanism for out-of-control detection, propose to build exact simultaneous confidence intervals for each of the variable means. Li *et al.* (2008) suggest a modification of Mason, Tracy and Young´s method based on the use of bayesian networks for reducing computational cost and improving the diagnosability. The problem with this method is that it can only be applied when *a priori* relationships among process variables and the interrelationships between process variables and quality variables are known.

To sum up there is a long list of proposed methods for fault diagnosis in MSQC and some of them are interrelated. Indeed, Mason, Tracy and Young (1995) show that some of these methods: the standardized t–based ranking technique of Doganaksoy, Faltin and Tucker, the regression-adjusted variables of Hawkins, the step-down procedure of Roy and the T^2 discriminant distance procedure of Murphy, are imbedded in the partitioning of Hotelling´s T^2.

In the different sections of this chapter we provide a full description of these methods and their interrelationships.

3.2 Fault diagnosis methodologies

In the following it is assumed that after a previously established statistical monitoring chart detects a new signal, this new observation $\mathbf{x}_{new}$ is used to diagnose the cause of the fault. It must be noted that most of the compared methods use the Hotelling´s T^2 statistic for the detection of out-of-control observations whilst some like Hawkins´ method, Hayter and Tsui´s method and the Step-down method use their own detection trigger mechanism. It is also assumed that $\mathbf{x}_i$ represent a K-dimensional vector of measurements made on a

process at sampling time *i*. and when the process is in control, the $\mathbf{x}_i$ are independent and follow a multivariate normal distribution with a *K*x1 mean vector $\boldsymbol{\mu}_{ref}$ and a *K*x*K* covariance matrix Σ, *i.e.* $\mathbf{x} \sim N_K(\boldsymbol{\mu}_{ref}, \Sigma)$. So that $\mu_{k,ref}$ is the in-control mean value for the k^{th} variable, and $\mu_{k,new}$ is the mean value of the k^{th} variable after the change (fault). In practice $\boldsymbol{\mu}_{ref}$ and Σ are estimated from the sample vector $\bar{\mathbf{x}}_{ref}$ and sample covariance matrix $\mathbf{S}$ using in-control data.

3.2.1 Alt´s Method

This was the first methodology proposed for the detection and diagnosis of faults in multivariate processes. The diagnosis is based on the use of univariate Shewhart charts with a Type I risk calculated according to Bonferroni´s method (Sankoh *et al.* 1997). This method is equivalent to the use of simultaneous confidence intervals for the difference of means in the *K* measured variables. These confidence intervals can be used as a guide to find out the most suspected variables for the detected mean change.

The Type I risk for the individual tests (univariate chart) in the classical approaches would be equal to the desired overall Type I risk (α). But this approach does not adjust appropriately the Type I risk of the individual tests as it does not take into account the likely correlation amongst the measured variables. If the correlation among variables is 1 then the Type I risk (α) would be appropriate for the individual tests whereas if the correlation is 0 then it would be more appropriate to use a Type I risk (α/K) where *K* is the number of variables. Moreover if the correlation *r* amongst the variables is $0 < r < 1$, then a Type I risk (α/q) defined by $\alpha/K < \alpha/q < \alpha$ and $1 < q < K$ would be the best selection.

Alt´s method proposes the use of a Type I risk (α/K) in the individual tests. When applied this method to an intermediate situation with a correlation r, $0 < r < 1$, the overall

Type I risk (false alarm rate) is too conservative so there will be problems of lack of power or situations where faults are successfully detected but no variables can be diagnosed as responsible for the faults.

3.2.2 Doganaksoy, Faltin and Tucker´s method (DFT)

The diagnostic method proposed by Doganaksoy Faltin and Tucker (1991) is triggered by an out of control signal from a Hotelling´s T^2 chart. The measured variables are ranked according to the univariate t statistic for the difference of two means:

$$t_k = \frac{x_{k,\text{new}} - \bar{x}_{k,\text{ref}}}{\left[s_{kk}^2 \left(1 + \frac{1}{N} \right) \right]^{1/2}} \quad \text{For } k = 1 \text{ to } K \tag{3.1}$$

where $x_{k,\text{new}}$ is the value of the k^{th} variable in the new observation; $\bar{x}_{k,\text{ref}}$ is the estimated mean of the k^{th} variable in the in-control reference data set; s_{kk}^2 is the estimated variance of the k^{th} variable in the in-control reference data set and N is the size of the reference data set.

This ranking is a valuable guide to diagnose the source of the change. Bonferroni's type of simultaneous confidence intervals for $\mu_{k,\text{ref}} - \mu_{k,\text{new}}$ (k = 1,…, K) are used to provide signals on individual variables. Variables for which the Bonferroni intervals do not enclose zero are highly suspect.

The implementation of this approach is as follows: An observation is considered out of control when Hotelling´s T^2 statistic for the new observation exceeds the control limit (threshold) at the nominal confidence level CL_{nom}. Then, for each variable the smallest

confidence level CL_{ind} that would yield an individual confidence interval for $\mu_{k,\text{ref}} - \mu_{k,\text{new}}$ ($k = 1,..., K$) that contains the zero is calculated as (see Appendix 3.1):

$$CL_{\text{ind}} = \left|2T(t_{\text{computed}}; N-1) - 1\right| \tag{3.2}$$

where t_{computed} is the calculated value of the univariate t statistic for a variable and T(t ; d) is the cumulative distribution function of the t distribution with d degrees of freedom. Variables with larger CL_{ind} values are the ones with relatively larger univariate t statistics which require closer investigation. For each interval the confidence level according to Bonferroni's proposal $CL_{\text{Bonf}} = 1 - \alpha_{\text{Bonf}}$ is computed:

if $CL_{\text{sim}} = 1 - \alpha_{\text{sim}}$ is the desired nominal confidence level and α_{sim} the desired overall Type I risk in multiple testing, then

α_{sim} = P(At least one significant individual test | no change in the means) =

1-P(No significant individual test | no change in the means) $= 1 - (1 - \alpha_{\text{Bonf}})^K$ and

$$\Rightarrow \alpha_{\text{Bonf}} = 1 - (1 - \alpha_{\text{sim}})^{1/K} \approx \frac{\alpha_{\text{sim}}}{K} \text{ and } CL_{\text{Bonf}} = CL_{\text{sim}}^{1/K} \approx \frac{K + CL_{\text{sim}} - 1}{K}$$

Then, the variables with $CL_{\text{ind}} > CL_{\text{Bonf}}$ are classified as being those which are most likely to have changed. Consequently, the proposed method is correspondent to work out the p-value of each individual two sample comparisons, and signalling those variables which p-value is lower than α_{Bonf}.

The methodology advices to use a smaller confidence level in diagnosis than in detection. The reason for this recommendation is that frequently this method does not succeed in finding out any variable to which assign the detected fault as p-value > α_{Bonf}.

This situation is a consequence of the existence of correlation among the variables which increases the problem of lack of power in diagnosis.

This methodology is similar to the Alt´s method but it incorporates the *t* ranking statistics which help to cope with situations where no variable is finally identified as responsible for the detected signal.

3.2.3 Modifications to the Doganoksoy, Faltin and Tucker´s method

As commented in Section 3.2.1 the Bonferroni test (Sankoh *et al.* 1997) is the simplest multiplicity adjustment procedure to ensure an overall Type I risk in multiple testing (*K*-dimensional measured variables). This method assumes independence throughout the different tests. Therefore, this proposal is too conservative when there are many tests and/or the tests are highly correlated. Being too conservative in the Type I risk derives in less sensitive tests (*i.e.* lack of power). In this thesis we consider some variants of the DFT methodology focused in reducing the risk of being too conservative when applying multiple hypothesis tests. Bonferroni's test will be replaced by different stepwise procedures proposed by Holm (1979), Hochberg (1988) and Hommel (1988). These approaches are based on the fact that of the *K* null hypotheses tested, the only ones to protect against rejection (at a given step) are those not yet rejected. Bonferroni's test will also be replaced by two *ad hoc* procedures to take advantage of the correlation information amongst the measured variables. All these methods proved to be less conservative than the Bonferroni´s approach.

Holm´s procedure

It is a step down approach which conducts the testing in a decreasing order of statistical significance of the ordered hypotheses, starting from the lower (*i.e.* last) *p*-value (highest statistical significance). In each test the $\alpha_{\text{Holm}} = 1-(1-\alpha_{\text{sim}})^{1/K^*}$, where K^*= *K* for the 1st test, K^*= *K*-1 for the 2nd test and K^*=1 for the *K*th test. Significance testing

continues until a null hypothesis is accepted. Then, all remaining (untested) null hypotheses are accepted without further testing.

The implementation of Holm´s procedure is as follows: Let ($\alpha_{ind,1}$,…, $\alpha_{ind,K}$) be the ordered *p*-values and H_{01}, H_{02}, ... , H_{0K} the corresponding ordered null hypotheses for the *K* measured means. Then, if $\alpha_{ind,K} < \frac{\alpha_{sim}}{K}$, reject H_{0K} and go to the next step, otherwise stop and accept all the remaining null hypotheses. In the next step, if $\alpha_{ind,,(K-1)} < \frac{\alpha_{sim}}{K-1}$, reject $H_{0(K-1)}$ and go to the next step, otherwise stop and accept all the remaining null hypotheses. In general, if $\alpha_{ind,k} < \frac{\alpha_{sim}}{k}$, reject H_{0k} otherwise stop and accept all the remaining null hypotheses H_{0j}, $j \leq k$.

The final adjusted *p*-values are $\alpha_{adj\ ind,k} = max\{K\alpha_{ind,K}, (K-1)\ \alpha_{ind,K-1},..., k\ \alpha_{ind,k}\}$, $k=1,2,.....K$.

Hochberg´ s procedure

It is a step up approach which conducts the testing in an increasing order of statistical significance of the (ordered) hypotheses starting from the higher *p*-value (lowest statistical significance). Significance testing continues until a null hypothesis is rejected. Then all remaining (untested) null hypotheses are rejected without further testing.

The implementation of Hochberg´s procedure is as follows: Let ($\alpha_{ind,1}$,…, $\alpha_{ind,K}$) be the ordered *p*-values and H_{01}, H_{02},..., H_{0K} the corresponding ordered null hypotheses for the *K* measured means. Then, if $\alpha_{ind,1} > \frac{\alpha_{sim}}{1}$, accept H_{01} and go to the next step, otherwise stop and reject the remaining all null hypotheses. In general, if $\alpha_{ind,k} > \frac{\alpha_{sim}}{k}$, accept H_{0k}, otherwise stop and reject all the remaining null hypotheses H_{0j} for $j>k$.

The final adjusted *p*-values are $\alpha_{\text{adj ind},k}=min\{\alpha_{\text{ind},1}, 2\alpha_{\text{ind},2},..., k\alpha_{\text{ind},k}\}$, $k=1,2,..., K$.

Hommel´ s procedure

It is a step up approach. The implementation of Hommel´s procedure is as follows: Let ($\alpha_{\text{ind},1}$,……,$\alpha_{\text{ind},K}$) be the ordered *p*-values as in the Hochberg´s procedure and H_{01}, H_{02}, ...,H_{0K} the corresponding ordered null hypotheses for the *K* measured means. Then, find out the largest *m* for $\alpha_{\text{ind},1}>\alpha_{\text{sim}}$; $\alpha_{\text{ind},1}>\alpha_{\text{sim}}$, $\alpha_{\text{ind},2}>\alpha_{\text{sim}}/2$; $\alpha_{\text{ind},1}>\alpha_{\text{sim}}$, $\alpha_{\text{ind},2}>2\alpha_{\text{sim}}/3$, $\alpha_{\text{ind},3}>\alpha_{\text{sim}}/3$; ... ; $\alpha_{\text{ind},1}>\alpha_{\text{sim}}$, $\alpha_{\text{ind},2}>\alpha_{\text{sim}}(m-1)/m$, $\alpha_{\text{ind},3}>\alpha_{\text{sim}}(m-2)/m$, ..., $\alpha_{\text{ind},m}>\alpha_{\text{sim}}/m$. Then reject H_{0k} for which $\alpha_{\text{ind},k}<\alpha_{\text{sim}}/m$

The adjusted *p*-values are $\alpha_{\text{adj ind},k}=m\ \alpha_{\text{ind},k}$, $k=1,2,.....K$.

Ad hoc procedures

The first procedure, proposed by Tukey, Ciminera and Heyse (1985), suggests the adjustments: $p_{ak}=1-(1-p_k)^{\sqrt{K}}$ and $\alpha_k=1-(1-\alpha_{\text{sim}})^{1/\sqrt{K}}$, where p_k and p_{ak} are, respectively, the observed and adjusted *p*-values for the k^{th} variable, and α_k is the adjusted critical α-level for the k^{th} hypothesis for $k=1,\ldots, K$. In the second procedure, proposed by Dubey (1985), Armitage and Parmar (1986), and Sankoh, Huque and Dubey (1997), the following adjustments were suggested: $p_{ak}=1-(1-p_k)^{m_k}$ and $\alpha_k=1-(1-\alpha_{sim})^{1/m_k}$, where $m_k=K^{1-r_k}$ and $r_k=(K-1)^{-1}\sum_{j\neq k}^{K} r_{jk}$, r_{jk} being the correlation coefficient between the j^{th} and the k^{th} variable.

These variants signal the variables where adjusted *p*-values, p_{ak} , are lower than α_{sim} or, equivalently, those variables whose non-adjusted *p*-values are lower than α_k.

3.2.4 Hayter and Tsui´s method

This procedure (Hayter and Tsui 1994), operates by calculating a set of simultaneous confidence intervals for each one of the *k* variables mean (μ_k) with an overall coverage probability of 1-α, assuming a known correlation structure. This method is similar to the bar plot of normalized errors of the variables discussed in Kourti and MacGregor (1996) or the multivariate profile charts proposed by Fuchs and Benjamini (1994). In Hayter and Tsui´s method the process is deemed to be out of control whenever any of these confidence intervals do not contain its in-control value, $\mu_{k,\text{ref}}$, and the identification of the errant variable or variables is immediate. For a known covariance structure $\sum$ and a chosen Type I risk α, the experimenter first evaluates the critical point C_α by simulation. This critical point is defined by:

$$P\left(\frac{\left|x_k - \mu_{k,\text{ref}}\right|}{\sigma_{kk}} \le C_\alpha ; for \quad 1 \le k \le K\right) = 1 - \alpha \tag{3.3}$$

Then, following any new observation $\mathbf{x}_{\text{new}} = \{x_{1,\text{new}}, ...x_{k,\text{new}}, ..., \mathrm{x}_{K,\text{new}}\}$, simultaneous confidence intervals for the mean of each of the *k* measured variables (μ_k) are obtained:

$$[x_{k,\text{new}} - \sigma_{kk} C_\alpha ; x_{k,\text{new}} + \sigma_{kk} C_\alpha] \tag{3.4}$$

These confidence intervals assume a known variance and they are calculated for a fixed $(1-\alpha)$ confidence level. The process is considered out of control if at least one interval does not contain the corresponding reference value $\mu_{k,\text{ref}}$. This is equivalent to consider that a new observation $\mathbf{x}_{\text{new}}$ is out of control when:

$$M = \underset{1 \le k \le K}{\text{Max}} \frac{\left|x_{k,\text{new}} - \mu_{k,\text{ref}}\right|}{\sigma_{kk}} > C_\alpha \tag{3.5}$$

The variables x_k whose confidence intervals do not contain $\mu_{k,\text{ref}}$ are identified as those responsible for the signal.

It must be noted that this method uses the *M* statistics for fault detection instead of the traditional Hotelling´s T^2 statistic. The *M* statistic is more sensitive to faults which move the mean in the direction of the principal axes of the correlation structure of the process than those which move the mean in counter-correlation directions. On the contrary, as it was shown in Figure 1.7 and will be explained in Section 3.2.8 the Hotelling´s T^2 statistic behaviour is just the opposite, resulting more sensitive to the faults that move the process mean in counter-correlation directions than to mean changes in directions which are close to the principal axes.

An essential point of this method is the critical point evaluation. For *K* measured variables the value of the C_α is determined as follows. For K=2 the critical point can be obtained from existing tables. For K=3 or K= 4 it can be obtained by approximation from existing tables or by numerical integration. For $K \geq 5$ it can be obtained by simulation methods or by the use of non-parametric methods.

- **Simulation method**

  This method assumes that the observed vector $\mathbf{x}_i$ follows a multivariate normal distribution. A large number (N=100.000) of observation vectors $\mathbf{x}_1, \mathbf{x}_2, \ldots, \mathbf{x}_N$ from a $\mathrm{N}_K(\mathbf{0}, \boldsymbol{\Sigma})$ distribution are generated using the sample correlation matrix **R** from the in-control data as an estimation of $\boldsymbol{\Sigma}$. Then the *M* statistic for each vector $\mathbf{x}_i = (x_{1,i}, x_{2,i}, \ldots, x_{K,i})$ is computed: $M_i = \underset{1 \leq k \leq K}{\text{Max}} |x_{k,i}|$ for $i = 1, 2, \ldots, N$. The $(1-\alpha)^{th}$ percentile of the sample $\{M_1, M_2, \ldots, M_N\}$ is a good estimation for the C_α. The empirical cumulative distribution $\widehat{\mathrm{F}}(M)$ provides an estimation of the C_α for different levels of the Type I risk α.

- **Non-parametric methods**

This approach is recommended when the multivariate normality hypothesis does not hold and a reference data set with at least 500 in-control process observations is available. The sample mean $\bar{\mathbf{x}}$ and the sample covariance matrix **S** are calculated from the reference data set. Then the *M* statistic for each observation vector of the reference data set $\mathbf{x}_i = (x_{1,i}, x_{2,i}, ..., x_{K,i})$ is computed.

$$M_i = \underset{1 \le k \le K}{\text{Max}} \left| \frac{x_{k,i} - \bar{x}_k}{s_{kk}} \right| \quad \text{for } i = 1, 2, ..., N \tag{3.6}$$

The $(1-\alpha)^{th}$ percentile of the sample $\{M_1, M_2, \ldots, M_N\}$ is a good estimation for the C_α.

3.2.5 Murphy´s Method

Murphy´s method (Murphy 1987) is an approach based on a discriminant distance. This considers a reference population Π_0 when the process is in control where the observations follow a $N_K(\boldsymbol{\mu}_{ref}; \boldsymbol{\Sigma})$ distribution; and a new population Π after a change in the process, where the observations follow a $N_K(\boldsymbol{\mu}; \boldsymbol{\Sigma})$ distribution.

Once an out-of-control observation is detected by the Hotelling´s T^2 statistic, the method searches for the subset of variables which better discriminates between these two populations. Given a partition of the *K* variables in two subsets: k_1 variables $\mathbf{x}^{(1}$ and k_2 variables $\mathbf{x}^{(2}$, where $K = k_1 + k_2$, in discriminant analysis, the true squared distance between the populations Π and Π_0 is defined as $\Delta_K^2 = (\boldsymbol{\mu} - \boldsymbol{\mu}_{ref})^T \boldsymbol{\Sigma}^{-1} (\boldsymbol{\mu} - \boldsymbol{\mu}_{ref})$, and the reduced squared distance as $\Delta_{k_1}^2 = (\boldsymbol{\mu}^{(1} - \boldsymbol{\mu}_{ref}^{(1})^T \boldsymbol{\Sigma}_1^{-1} (\boldsymbol{\mu}^{(1} - \boldsymbol{\mu}_{ref}^{(1})$ where $\boldsymbol{\mu}^{(1}$ and $\boldsymbol{\mu}_{ref}^{(1}$ refer to the mean population vector of $\mathbf{x}^{(1}$. Then testing H_0: $\Delta_K^2 - \Delta_{k_1}^2 = 0$ is equivalent to testing that the k_1 subset of variables discriminates just as well as the full set of *K* variables. Under the assumption that the null hypothesis H_0 is true and the reference data set is large,

the D statistic, $D = T_K^2 - T_{k_1}^2$, follows a $\chi_{k_2}^2$, where T_K^2 is the overall Hotelling´s T^2 statistic (full squared distance): $T_K^2 = (\bar{\mathbf{x}} - \mathbf{x}_{\text{new}})^T \mathbf{S}^{-1} (\bar{\mathbf{x}} - \mathbf{x}_{\text{new}})^T$ and $T_{k_1}^2$ is the Hotelling´s T^2 statistic based on the subset of k_1 variables $\mathbf{x}^{(1}$ (reduced squared distance): $T_{k_1}^2 = (\bar{\mathbf{x}}^{(1} - \mathbf{x}_{new}^{(1})^T \mathbf{S}_1^{-1} (\bar{\mathbf{x}}^{(1} - \mathbf{x}_{new}^{(1})^T$ where $\bar{\mathbf{x}}$ and $\bar{\mathbf{x}}^{(1}$ refer to the sample mean vector corresponding to all variables and the subset of k_1 variables respectively using the reference (in-control) data, $\mathbf{S}$ is the estimated covariance matrix of $\mathbf{x}$ and $\mathbf{S}_1$ is the estimated covariance matrix of $\mathbf{x}^{(1}$. If D is large, the hypothesis that the k_1 subset caused the signal is rejected; if it remains small then it is accepted. No *a priori* ordering is assumed in this method and all the possible subsets can be tested. The subset of variables which best discriminates between these two groups is considered the responsible for the observed out-of-control signal and corresponds to the smallest value of the D statistic

The number of partitions to be considered grows exponentially as the number of variables increase. In order to reduce the computational work, Murphy (1987) proposed the following algorithm that reduces the number of terms to be computed:

1) Given a new observation $\mathbf{x}_{\text{new}} = (x_{1,\text{new}}, x_{2,\text{new}}, ..., x_{K,\text{new}})$ it computes $T_K^2(\mathbf{x}_{\text{new}})$.

If $T_K^2(\mathbf{x}_{\text{new}}) \leq \chi_K^2(1-\alpha)$, the process is considered in control and the algorithm ends.
If $T_K^2(\mathbf{x}_{\text{new}}) > \chi_K^2(1-\alpha)$, the process is considered out of control and the algorithm goes to 2)**.**

2) Compute the K terms $T_1^2(\mathbf{x}_{\text{new}})$ and the K differences $D_{K-1}(i) = T_K^2(\mathbf{x}_{\text{new}}) - T_1^2(x_{i,\text{new}})$ for i =1, 2, ..., K.
Then, select the minimum difference $D_{K-1}(r) = \underset{i}{\text{Min}}\, D_{K-1}(i)$ and check for statistical significance.
If $D_{K-1}(r) > \chi_{K-1}^2(1-\alpha)$ the algorithm ends and only variable r is considered responsible for the detected out-of-control.
If $D_{K-1}(r) \leq \chi_{K-1}^2(1-\alpha)$ the algorithm goes to 3).

3) Computes the K-1 differences $D_{K-2}(r, j) = \mathrm{T}_K^2(\mathbf{x}_{\text{new}}) - \mathrm{T}_{r,j}^2(x_{r,\text{new}}, x_{j,\text{new}}) \; \forall j$: $1 \leq j \neq r \leq K$.

Then select the minimum difference $D_{K-2}(r,j) = \underset{j \neq r}{\text{Min}} D_{K-2}(r,j)$ and check for statistical significance.

If $D_{K-2}(r,j) > \chi^2_{K-2}(1-\alpha)$, the algorithm ends and the set of variables (*r, j*) is considered responsible for the detected out-of-control.
If $D_{K-2}(r,j) \leq \chi^2_{K-2}(1-\alpha)$, the algorithm goes to 4).

4) The algorithm continues with differences of decreasing order in an iterative way until it arrives to the end. If the algorithm arrives to the first order difference $D_{K\text{-}(K\text{-}1)}$ and this difference is not statistically significant, then it is concluded that all the variables are responsible of the observed change in the mean of the process.

3.2.6 Hawkins´ Method

Given a new observation $\mathbf{x}_{\text{new}}$, the detection and diagnosis in Hawkins' methodology is based on the perturbation vector $\mathbf{z}_{\text{new}}$, whose k^{th} component is the standardized perturbation resulting when the k^{th} variable is regressed onto all the other variables of $\mathbf{x}_{\text{new}}$.

$$z_{k,\text{new}} = \frac{\left(x_{k,\text{new}} - \mu_{k,\text{ref}}\right) - \sum_{k \neq j} \beta_{kj}\left(x_{j,\text{new}} - \mu_{j,\text{ref}}\right)}{\sigma_{k|1.2.3..k-1.k+1.....K}} \tag{3.7}$$

where $\sigma_{k|1.2.3...k-1.k+1...K}$ is the standard deviation of the conditional distribution of x_k given all other variables of **x**. Note that if $\boldsymbol{\mu}_{\text{new}}$ differs from $\boldsymbol{\mu}_{\text{ref}}$ only in its k^{th} component, then the optimal test for a shift is one based on $z_{k,\text{new}}$, the k^{th} component of vector $\mathbf{z}_{\text{new}}$. These $z_{k,\text{new}}$ perturbations follow a N(0,1) when the process is in control. Hawkins (1993) proposes an easy way of estimating $\hat{\mathbf{z}}_{\text{new}}$ by using the vector of scaled residuals. Let $\mathbf{y}_{\text{new}} = \mathbf{S}^{-1}(\mathbf{x}_{\text{new}} - \bar{\mathbf{x}}_{\text{ref}})$ where $\mathbf{S}$ is the estimated covariance matrix, then the k^{th} component of $\mathbf{y}_{\text{new}}$ is the regression residual when variable x_k is regressed on all other variables, scaled by factor $s^2_{k|1.2.3...k-1.k+1...K}$. (see Appendix 3.2)

When the process is in control $\mathbf{y}_{\text{new}} \sim \text{N}(\mathbf{0}, \mathbf{S}^{-1})$ and then $\hat{\mathbf{z}}_{\text{new}}$ is just a rescaling of $\mathbf{y}_{\text{new}}$ (see Appendix 3.2):

$$\hat{\mathbf{z}}_{\text{new}} = [\mathbf{diag}(\mathbf{S}^{-1})^{-1/2}]\mathbf{y}_{\text{new}} = \mathbf{A}(\mathbf{x}_{\text{new}} - \bar{\mathbf{x}}_{\mathbf{ref}}) \tag{3.8}$$

where the transformation matrix $\mathbf{A} = \mathbf{diag}(\mathbf{S}^{-1})^{-1/2}\mathbf{S}^{-1}$. Thus, when the process is in control $\hat{\mathbf{z}} \sim \text{N}(\mathbf{0}; \mathbf{B})$ where $\mathbf{B} = \left(\mathbf{diag}(\mathbf{S}^{-1})^{-1/2}\right)\mathbf{S}^{-1}\left(\mathbf{diag}(\mathbf{S}^{-1})^{-1/2}\right)$ is the covariance matrix for the vector of scaled residuals $\hat{\mathbf{z}}_{\text{new}}$.

The original proposal consists of monitoring the process using separate control charts for all of the $\hat{z}_{k,\text{new}}$. If the control chart for one of the $\hat{z}_{k,\text{new}}$ signals while charts of others do not, then that indicates that it is $\hat{z}_{k,\text{new}}$ that has shifted (Hawkins 1993). Note that the original proposal does not make any correction either for multiple testing or correlation among the scaled residuals. So it is necessary to adjust the Type I risk with an appropriate selection of the number of standard deviations (*nd*) when calculating the upper control limits of the monitoring charts.

A variant of Hawkins´ methodology to detect faults which affect one single variable (Hawkins' one single variable method) is considered. In this variant, the algorithm identifies as responsible the variable with the largest significant residual. Rewriting the Hotelling T^2 statistic in terms of the residuals $\hat{z}$:

$$\begin{aligned} T^2 &= (\mathbf{x} - \bar{\mathbf{x}}_{\text{ref}})^T \mathbf{S}^{-1}(\mathbf{x} - \bar{\mathbf{x}}_{\text{ref}}) = (\mathbf{x} - \bar{\mathbf{x}}_{\text{ref}})^T \mathbf{y} = (\mathbf{x} - \bar{\mathbf{x}}_{\text{ref}})^T \mathbf{diag}(\mathbf{S}^{-1})^{1/2} \hat{\mathbf{z}}_{\text{new}} \\ &= \sum_{k=1}^{K} \text{T}_{x_k}^2 \end{aligned} \tag{3.9}$$

This relationships gives a decomposition of the Hotelling´s T^2 statistic into K variable specific terms $T_{x_k}^2$ according to Hawkins (1991), where each term $T_{x_k}^2$

$$T_{x_k}^2 = (x_k - \bar{x}_{k,\text{ref}}) \cdot \hat{z}_{\text{k}} \cdot s_{k|1.2.3...k-1.k+1...K}^{-1} \tag{3.10}$$

is formed by two parts:

- Hawkins´ statistic $\hat{z}_{k,}$ which measures the deviation of the observation from the conditional distribution of the variable x_k on all the other variables $x_k \mid x_1 x_2 \ldots x_{k-1} x_{k+1} \ldots x_K$.
- $x_k - \bar{x}_{k,\text{ref}}$ which measures the deviation from the marginal distribution of the variable x_k .

The terms of this particular decomposition of the Hotelling´s T^2 statistic ($T^2_{x_k}$) are not orthogonal and do not follow a chi-squared distribution.

3.2.7 Runger and Montgomery´s method

This methodology (Runger and Montgomery 1996) tries to establish the contribution of a variable to the value of Hotelling´s T^2 statistic used for monitoring the process when a control chart signals. The contribution c_k for variable $x_{k,\text{new}}$ is the required change in the single variable x_k which gives a minimum value of the expression:

$$\left[\frac{\mathbf{x}_{\text{new}} - c_k \mathbf{e}_k}{\left(\mathbf{e}_k^T \mathbf{S}^{-1} \mathbf{e}_k\right)^{1/2}}\right]^T \mathbf{S}^{-1} \left[\frac{\mathbf{x}_{\text{new}} - c_k \mathbf{e}_k}{\left(\mathbf{e}_k^T \mathbf{S}^{-1} \mathbf{e}_k\right)^{1/2}}\right] \tag{3.11}$$

where $\mathbf{e}_k$ is the unit vector in the direction of the k^{th} coordinate axis and $\left(\mathbf{e}_k^T \mathbf{S}^{-1} \mathbf{e}_k\right)^{1/2}$ is a scale factor so that c_k can be interpreted as a measure of a Euclidean distance.

Variables that require large changes (c_k) aim to the responsible variables. Given a partition of the K variables in two subsets: k_1 with K-1 variables $\mathbf{x}^{(1} = (x_1 x_2 \ldots x_{k-1} x_{k+1} \ldots x_K)$ and k_2 with 1 variable $\mathbf{x}^{(2} = x_k$,authors proved that the squared contribution c_k^2 is equivalent to the Murphy´s D difference.

$$c_k^2 = D = T_K^2 - T_{k_1}^2 \tag{3.12}$$

where $T_{k_1}^2$ is Hotelling´s T^2 statistic based on a subset $\mathbf{x}^{(1}$ made up of K-1 variables after excluding the k^{th} variable. A large contribution c_k^2 corresponds to a large D statistic, therefore, we reject that the k_1 subset of variables causes the signal, highlighting the variable x_k as responsible for the shift. Tracy, Mason and Young (1995) show that

$$D \sim \frac{N+1}{N} F_{1,N-1}^2$$

3.2.8 Mason, Tracy and Young´s method (MTY)

3.2.8.1 MTY´s decomposition

The MTY´s method (Mason, Tracy and Young 1995, 1997) decomposes the overall Hotelling´s T^2 statistic into independent components, each reflecting the contribution of the different variables to the statistic. The Hotelling´s T^2 statistic for a new observation may be iteratively decomposed according to Rencher *(1*993) as (see Appendix 3.3) :

$$T^2 = T_{K-1}^2 + T_{K|1,2,\ldots K-1}^2 \tag{3.13}$$

where:

- T_{K-1}^2 is the Hotelling´s T^2 statistic on the first K-1 variables.

Then if $\mathbf{x}_{\text{new}}^T = (\mathbf{x}_{\text{new}}^{(K-1}{}^T, x_{K,\text{new}})$ so that $\mathbf{x}_{\text{new}}^{(K-1}$ is a K-1 dimensional vector, the component T_{K-1}^2 may be calculated according to the expression:

$$T_{K-1}^2 = (\mathbf{x}_{\text{new}}^{(K-1} - \overline{\mathbf{x}}^{(K-1)})^T \mathbf{S}_{\mathbf{XX}}^{-1} (\mathbf{x}_{\text{new}}^{(K-1} - \overline{\mathbf{x}}^{(K-1)}) \tag{3.14}$$

where $\mathbf{S}_{\mathbf{XX}}$ is the sub-matrix of the sample covariance matrix $\mathbf{S}$ that corresponds to the first K-1 variables with $(K\text{-}1)\times(K\text{-}1)$ dimensions.

- $T^2_{K|1,2.....K-1}$ is the squared value of the *K*-th component of the new observation after being adjusted by the estimated mean ($\bar{x}_{K|1,2...K-1}$) and standard deviation ($s_{K|1,2....K-1}$) of the conditional distribution, $x_K \mid x_1 x_2 \ldots x_{K-1}$. Note that in this case this term is equal to the squared value of the Hawkins´ statistics z_K^2 (see Appendix 3.7)

$$T^2_{K|1,2...,K-1} = \left(\frac{x_{K,\text{new}} - \bar{x}_{K|1,2...K-1}}{s_{K|1,2....K-1}} \right)^2 = \hat{z}_K^2 \tag{3.15}$$

This expression shows that this type of component is close to zero when the value of the variable *K* in the new observation becomes a reasonable value (in terms of likelihood) for the conditional distribution $x_K \mid x_1 x_2 \ldots x_{K-1}$ so that it follows the correlation structure observed in the reference data set. In this case it is supposed that the reference data set is large enough so that the estimated mean of the conditional distribution may be considered as the true population mean.

In order to calculate this conditional component, the estimated mean $\bar{x}_{K|1,2...K-1}$ is computed according to the expression obtained in Appendix 3.4.

$$\bar{x}_{K|1,2.....K-1} = \bar{x}_K + \hat{\boldsymbol{\beta}}_K^T (\mathbf{x}_{\text{new}}^{(K-1} - \bar{\mathbf{x}}^{(K-1)}) \tag{3.16}$$

where: $\bar{x}_K$ is the sample mean of the *K*-th variable in the reference data set.

$\hat{\boldsymbol{\beta}}_K = \mathbf{S}_{\mathbf{XX}}^{-1}\mathbf{s}_{\mathbf{xX}}$ is the estimated coefficients vector in the regression of the *K*-th variable on the *K*-1 first variables.

The estimated standard deviation of $x_{K|1,2...K-1}$ is calculated with the following expression (see Appendix 3.5):

$$s^2_{K|1,2.....K-1} = s^2_{xx} - \mathbf{s}_{\mathbf{xX}}^T \mathbf{S}_{\mathbf{XX}}^{-1} \mathbf{s}_{\mathbf{xX}} \tag{3.17}$$

where $\mathbf{S} = \begin{bmatrix} \mathbf{S}_{\mathbf{XX}} & \mathbf{s}_{\mathbf{xX}} \\ \mathbf{s}_{\mathbf{xX}}^T & s^2_{xx} \end{bmatrix}$

Each decomposition iteratively leads to one unconditional component and *K*-1 conditional components, as given by the expression:

$$T^2 = T_1^2 + T_{2|1}^2 + T_{3|1,2}^2 + ... + T_{K|1,2,....K-1}^2 = T_1^2 + \sum_{k=1}^{K-1} T_{k+1|1,2.....k}^2 \qquad (3.18)$$

Since this method does not assume any special order in the variables, there are *K!* different decompositions of the T^2, each one with *K* independent components. As commented in Section 3.2.8.2 then, all the components are compared against its corresponding component distribution thresholds, and the variables with significant components are identified as responsible for the detected fault. In this thesis, the computational scheme proposed by Mason, Tracy and Young (MTY) (Section 3.2.8.4) is implemented.

3.2.8.2 Interpretation of the significant components

As shown in equation 3.18 and Appendix 3.4 there are two types of components:

a) The *unconditional components* $T_k^2 = \left(\frac{x_{k,\text{new}} - \bar{x}_{k,\text{ref}}}{s_{kk}} \right)^2$ measure the "marginal" contribution of the variable x_k to the statistic T^2 and, therefore, record changes in variable magnitudes but does not account for the correlation structure in the data. Assuming normality, these components T_k^2 are distributed as $T_k^2 \sim \frac{N+1}{N} F_{1,N-1}$, (see Appendix 3.6) where *N* is the number of observations of the reference data set. The component T_k^2 is the squared univariate *t* statistics for the variable x_k and detect when the value of one of the observation variables is out of the normal operational range. A significant component means that the observation is placed

out of the *K*-dimensional volume delimited by the univariate control limits at a particular statistical significance level of the *K* observation variables.

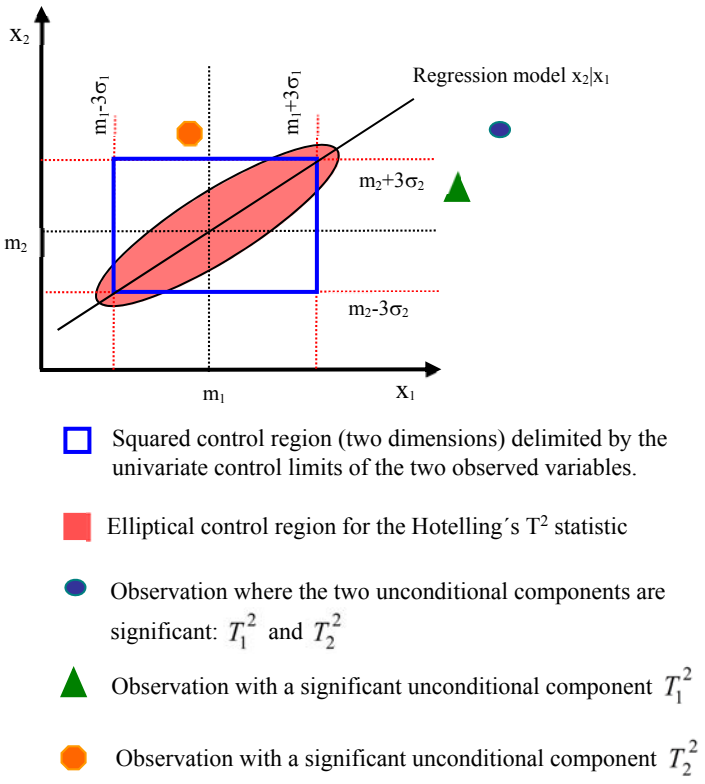

FIGURE 3.1: Observations with significant unconditional terms

Figure 3.1 shows different situations where the unconditional components for a two variables (x_1 and x_2) case become significant. All the observations in Figure 3.1 have a significant Hotelling´s T^2 statistic since they fall outside the squared control region (in blue).

Figure 3.2 shows the existence of two zones (in red) where the observations have significant unconditional components (fall outside the blue region) while the observations have non-significant Hotelling´s T^2 statistics (are within the elliptical control region).

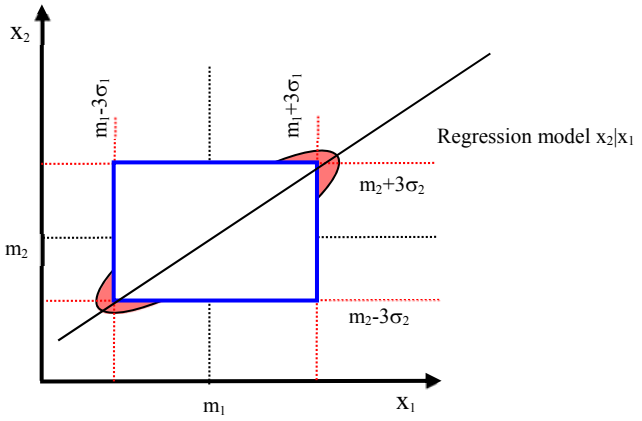

FIGURE 3.2: Observations with significant unconditional components and non-significant Hotelling´s T^2 statistic

b) The *conditional components* for a particular order and subset of variables can be expressed as $T^2_{k|1,2....k-1} = \left(\frac{x_{k,new} - \bar{x}_{k|1,2...k-1}}{s_{k|1,2....k-1}} \right)^2$ for k=2,..., K. These components measure the contribution of variables $x_{k,new}$ to the value of the T^2 statistic after being adjusted by a regression onto a subset of the other variables and, therefore, they are useful to record events that break the in-control correlation structure (Figure 3.3).

The conditional components are distributed as (see Appendix 3.6):

$$T^2_{k|1,2,....M} \sim \frac{(N+1)(N-1)}{N(N-M-1)} F_{1,N-M-1} \qquad (3.19)$$

where N is the number of observations of the reference data set and M the number of variables conditioning the distribution of the components.

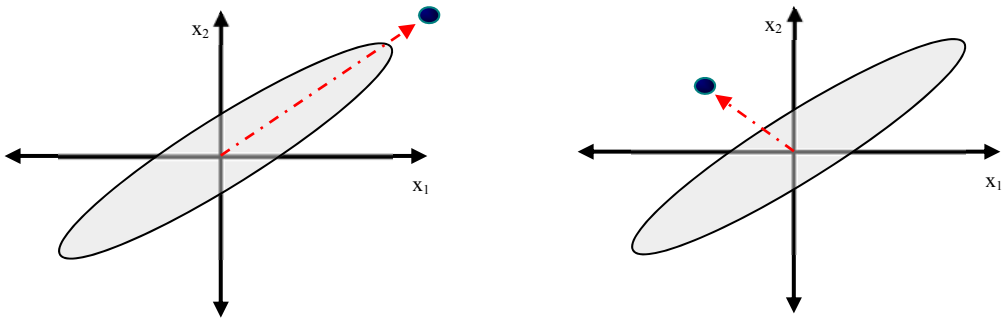

a) A change that keeps the correlation structure between x_1 and x_2

b) A change that breaks the correlation structure between x_1 and x_2

FIGURE 3.3: Faults that keep (a) or break (b) the correlation structure that is present in the reference data set

In an example of two variables:

$$T^2_{2|1} = \left(\frac{x_2 - \bar{x}_{2|1}}{s_{2|1}}\right)^2 = \left(\frac{e}{c \cdot s_{res}}\right)^2 \approx \left(\frac{e}{s_{res}}\right)^2 = \text{Squared standardized residual} \quad (3.20)$$

where:

e : Residual of the observation in the linear regression model $x_2|x_1$

s_{res} : Standard deviation of the residuals of the regression model $x_2|x_1$.

$c = \sqrt{\frac{N-M-1}{N-1}}$: Constant which adjusts the degrees of freedom between $s_{2|1}$ (the estimation of the standard deviation for the conditional distribution $x_2|x_1$ and s_{res} (see Appendix 3.5). For a large number of observations and one explicative variable this coefficient is close to 1.

Figure 3.4 shows the existence of two zones where the Hotelling´s T^2 statistics becomes significant whilst the univariate control charts do not. The Hotelling´s T^2 signals due to the abnormal values in the conditional components of the MTY decomposition. The abnormal value in these components is accounted for the large residuals *"e"* of the new observation in the regression model $x_2|x_1$ or the regression model $x_1|x_2$.

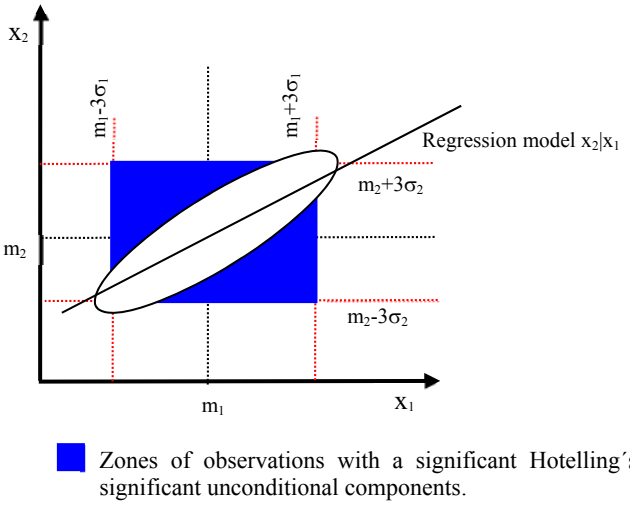

FIGURE 3.4 : Zones of observations with a statistically significant Hotelling´s T^2 statistic and where no unconditional component becomes significant

This situation is an indication that the correlation structure between x_1 and x_2 of the in-control process conditions may be broken.

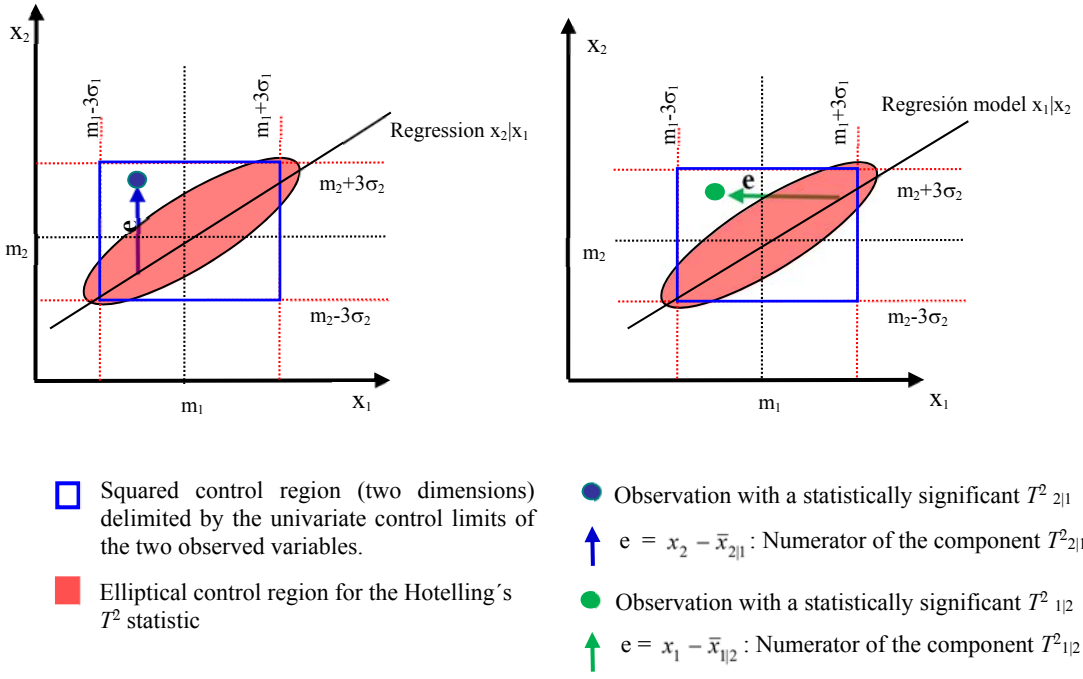

FIGURE 3.5: Residuals in the regressions model $x_2|x_1$ and $x_1|x_2$

Figure 3.5 shows that the abnormal large residuals are always associated to the zones where the conditional components signal. The same observation has

been considered in the two plots. In this case the two conditional components $T^2_{1|2}$ and $T^2_{2|1}$ signal for this observation.

Figure 3.6 shows the values for x_2 and x_1 in a new observation (x_1, x_2) that would be acceptable (no statistically significant Hotelling´s T^2 statistic) and that will not cause a signal in MTY conditional components. If the value for x_1 is out of the limits for acceptable values in $x_1|x_2$ distribution, then the conditional component $T^2_{1|2}$ will be statistically significant. Similarly, if the value for x_2 is out of limits for acceptable values in $x_2|x_1$ distribution, then the conditional component $T^2_{2|1}$ will be statistically significant. As the values for the variables x_1 and x_2 in the new observation (Figure 3.5) are both out of the limits, then the two conditional components $T^2_{1|2}$ and $T^2_{2|1}$ will be statistically significant.

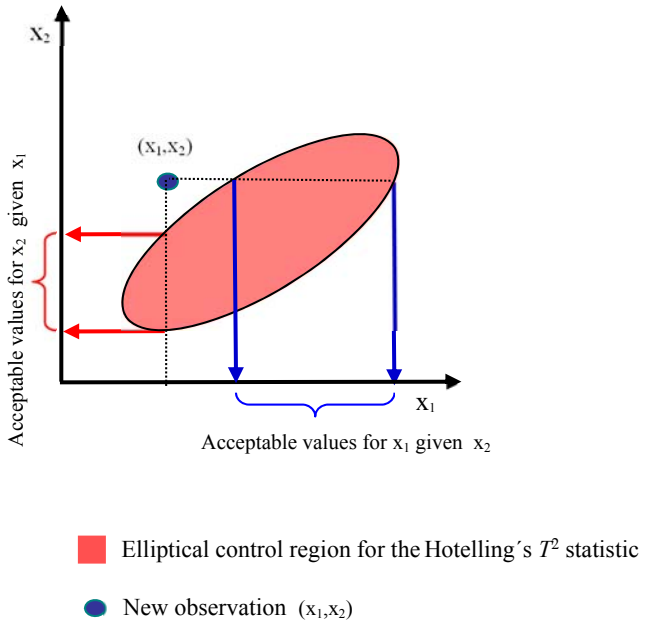

FIGURE 3.6: Acceptable values for the conditional distributions: $x_1|x_2$ and $x_2|x_1$

3.2.8.3 Computing the components

As an illustration see an example of Mason, Tracy and Young decomposition for *3*-variables:

$$T^2 = T_1^2 + T_{2|1}^2 + T_{3|1.2}^2$$
$$T^2 = T_1^2 + T_{3|1}^2 + T_{2|1.3}^2$$
$$T^2 = T_2^2 + T_{1|2}^2 + T_{3|2.1}^2$$
$$T^2 = T_2^2 + T_{3|2}^2 + T_{1|2.3}^2$$
$$T^2 = T_3^2 + T_{1|3}^2 + T_{2|3.1}^2$$
$$T^2 = T_3^2 + T_{2|3}^2 + T_{1|3.2}^2$$

Since this method does not assume any special order in the variables, there are *K!* different decompositions of the T^2, each one with *K* independent components. The total number of components in all the decompositions are $K \times K!$. Without considering the redundant components the total number of components to compute is $K \times 2^{(K-1)}$.

Number of components to compute: $K \times 2^{K-1} = 3 \times 2^{3-1} = 12$

Components to compute: $T_1^2,\ T_2^2,\ T_3^2,\ T_{1|2}^2,\ T_{1|3}^2,\ T_{2|1}^2, T_{2|3}^2, T_{3|1}^2, T_{3|2}^2, T_{1|2.3}^2, T_{2|1.3}^2, T_{3|1.2}^2$

In this case components such as $T_{3|1.2}^2$ and $T_{3|2.1}^2$ are redundant because the regression result does not depend on the order of the explicative variables. But it is not the same for the pair of components $T_{1|2}^2, T_{2|1}^2$ since the change in the dependent variable supposes the use of a different direction for measuring the residuals of the observations in the estimation of the regression model. As the number of the measured variables grows up the number of non-redundant components to be computed increases exponentially as can be seen in Table 3.1. Mason *et al.* (1997) propose a method to reduce the number of components to compute without losing diagnosis power. This algorithm is described in Section 3.2.8.4.

TABLE 3.1 Number of MTY´s components for different number of variables

Nº Variables	**Nº Components**	**Nº Variables**	**Nº Components**
n=3	12	**n=8**	1024
n=4	32	**n=9**	2304
n=5	80	**n=10**	5120
n=6	192	**n=20**	10485760
n=7	448	**n=30**	16106127360

3.2.8.4 MTY' s algorithm:

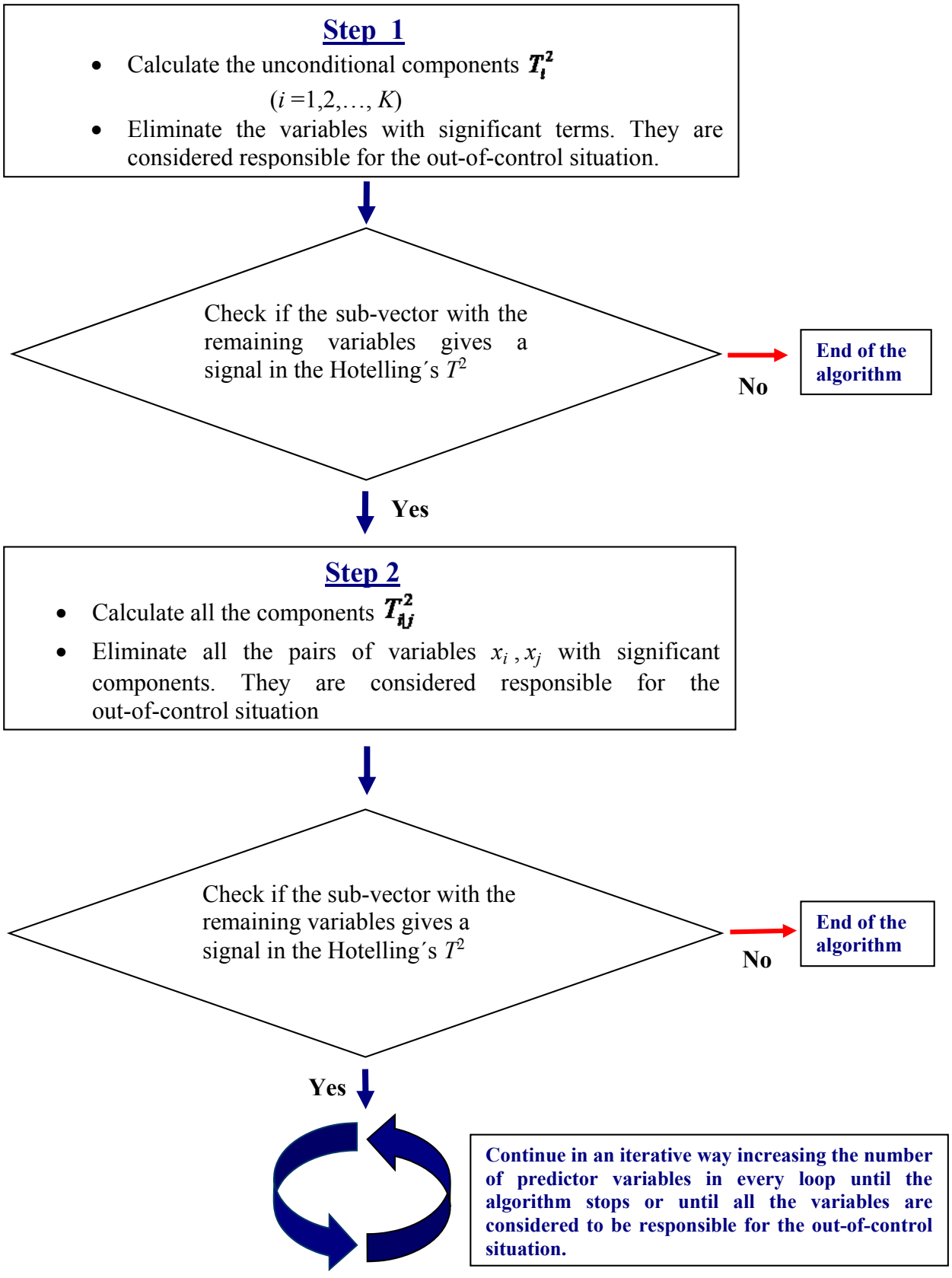

3.2.8.5 Additional aspects of the MTY´s method

There are some aspects, such as, collinearity or a bad model specification that can affect the diagnosis performance of this method

Collinearity

The conditional component for the variable x_K on the other *K-1* variables may be expressed as:

$$T^2_{K|1,2....K-1} = \frac{\left(x_K - \bar{x}_{K|1,2...K-1}\right)^2}{s^2_{KK}\left(1 - r^2_{K|1,2....K-1}\right)} \tag{3.21}$$

where $r^2_{K|1,2....K-1}$ is the square value of the multiple correlation coefficient between x_K and the other variables x_1, x_2 ..., x_{K-1}.

The denominator of the expression shows that collinearity (*i.e* multiple correlation coefficient close to one) will lead to large values in the conditional components. So, the reason for an abnormal value may be a collinearity problem instead of a large discrepancy between the predicted and the measured value for the variable as it is happens in a real fault.

Model misspecification

The MTY decomposition components are calculated on the residuals of different regression models estimated from all the possible subsets that we can select with the measured variables of the process. Large residuals would lead to large decomposition components and it may be interpreted that the relationships between the measured variables in the process are different to the ones prevailing in the reference data set. But there is another explanation for large residuals as they can also be caused by a model misspecification. So a better knowledge of the functional relationships among the variables or a better model specification will improve the sensibility for detection and diagnosis of the faults in the MTY methodology. It is convenient to use all the theoretical

knowledge and the expert opinion of process engineers to select the most suitable process variables to monitor the process and its more appropriate functional shape (linear, logarithm, inverse, …). Data exploration methods may also be useful for this task. To improve the sensibility of the T^2 in the detection of faults Mason *et al* (1999) propose in the case of sharp changes, to look for a better description of the functional relationship in the phase I. If some autocorrelation is detected it can be incorporated into the regression models. In the case of small consistent changes they recommend the use of *T*-components charts on some selected conditional components which may facilitate the observation of drifts in the residuals.

3.2.9 Step-down method

The step-down methodology proposed by Roy (1958) and Wierda (1993) assumes a certain *a priori* ordering among subsets that can be formed with the *K* measured variables. According to the ordering, the step-down procedure uses partitions of the mean vector of the new observation $\boldsymbol{\mu}_{new}$ and the mean vector of the reference data $\boldsymbol{\mu}_{ref}$ into *Q* subvectors: $\boldsymbol{\mu}_{1,new}$, $\boldsymbol{\mu}_{2,new}$, …, $\boldsymbol{\mu}_{q,new}$ …, $\boldsymbol{\mu}_{Q,new}$ and $\boldsymbol{\mu}_{1,ref}$, $\boldsymbol{\mu}_{2,ref}$, …, $\boldsymbol{\mu}_{q,ref}$ …, $\boldsymbol{\mu}_{Q,ref}$, respectively.

Then, it sequentially tests $H_0^{(1}: \boldsymbol{\mu}_{1,new} = \boldsymbol{\mu}_{1,ref}$ versus $H_1^{(1}: \boldsymbol{\mu}_{1,new} \neq \boldsymbol{\mu}_{1,ref}$; then $H_0^{(2}: \boldsymbol{\mu}_{2,new} = \boldsymbol{\mu}_{2,ref}$ versus $H_1^{(2}: \boldsymbol{\mu}_{2,new} \neq \boldsymbol{\mu}_{2,ref}$ given $\boldsymbol{\mu}_{1,new} = \boldsymbol{\mu}_{1,ref}$; then $H_0^{(3}: \boldsymbol{\mu}_{3,new} = \boldsymbol{\mu}_{3,ref}$ versus $H_1^{(3}: \boldsymbol{\mu}_{3,new} = \boldsymbol{\mu}_{3,ref}$ given $\boldsymbol{\mu}_{1,new} \neq \boldsymbol{\mu}_{1,ref}$ and $\boldsymbol{\mu}_{2,new} = \boldsymbol{\mu}_{2,ref}$; and so on.

The test statistics associated with testing these sub-hypotheses, G_q^2, are independently distributed under H_0, where $G_q^2 = \dfrac{T_q^2 - T_{q-1}^2}{1 + (T_{q-1}^2/(N-1))}$, $q = 1...Q$, T^2_q is the MTY

unconditional T^2 term for the first L_q variables with $L_q = \sum_{i=1}^{q} k_i$, k_i is the number of elements of subset *i*, and $T_0^2 = 0$.

Under H_0 assumption it follows that $G_q^2 \sim \frac{(N-1)k_q}{N-L_q} F(k_q, N-L_q)$ and it is possible to use separated control charts for monitoring them with a critical value *(i.e.* upper control limit, *UCL*) for the sub-hypothesis *q* given by:

$$UCL_q = \frac{(N-1)k_q}{N-L_q} F_{\alpha_q}(k_q, N-L_q) \text{ for } q=1,2,...,Q \tag{3.22}$$

where $F_{\alpha_q}(k_q, N-L_q)$ is the $(1-\alpha_q)\times 100$ percentile of the $F(k_q, N-L_q)$ distribution. The overall type I risk is:

$$\alpha = 1 - \prod_{q=1}^{Q}(1-\alpha_q) \tag{3.23}$$

In the different tests for each subset of hypothesis, the variables used in the precedent tests are used as covariates taking into account the correlation structure among the variables. The process is considered out of control if at least one G_q^2 exceeds the corresponding threshold UCL_q.

Key drawbacks of this methodology are: a) it assumes the existence of an *a priori* order among the different types of faults; and b) it is impossible to implement this methodology when there are faults that share common measured variables.

Additional aspects on the Step-down method:

- The Step-down methodology signals the first of the ordered *Q* subsets of variables to be considered as responsible for the detected signal. Nothing can be concluded about the subset of means to be tested in the sequence after we encounter the first test with a null hypothesis rejection result.

- The probability of a correct diagnosis increases when the real change takes place in the last subsets of variables as it is in the last tests where the correlation structure among variables is fully taken into account. So it is advisable to put in the first order positions the variables with less probability of suffering changes and employ a minor Type I risk α_q for testing these subsets.
- If more information about the *a priori* distributions of the mean is available, it is recommended to adapt the order of the variable subsets to be tested according to this available information. It is not advisable to employ this methodology when there is no information about an *a priori* order for the means subsets.

Appendix 3.1

The resulting confidence interval for the difference of means would contain the zero if $s_{x_{k,\text{new}}-\bar{x}_{k,\text{ref}}} t_{N-1}^{\alpha/2} > \left|x_{k,\text{new}} - \bar{x}_{k,\text{ref}}\right| \Rightarrow t_{N-1}^{\alpha/2} > \left|t_{\text{Computed}}\right|$. Then, according to Figure 3.7, the p-value is equal to α_{ind} for each individual test,

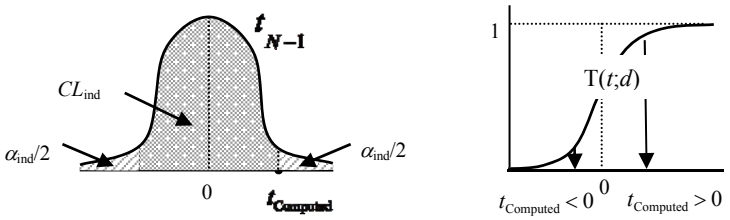

FIGURE 3.7: density probability function (left) and cumulative distribution function (right)for t_{N-1}

If $t_{\text{computed}} > 0 \Rightarrow T(t_{\text{computed}}; N-1) = 1 - \dfrac{\alpha_{\text{ind}}}{2}$

$$CL_{\text{ind}} = 1 - \alpha_{\text{ind}} = 1 - 2(1 - T(t_{\text{computed}}; N-1)) = 2T(t_{\text{computed}}; N-1) - 1$$

If $t_{\text{computed}} < 0 \Rightarrow T(t_{\text{computed}}; N-1) = \dfrac{\alpha_{\text{ind}}}{2}$

$$CL_{\text{ind}} = 1 - \alpha_{\text{ind}} = 1 - 2T(t_{\text{computed}}; N-1) = -(2T(t_{\text{computed}}; N-1) - 1)$$

and then, $CL_{\text{ind}} = \left|2T(t_{\text{computed}}; N-1) - 1\right|$

Appendix 3.2

The elements of the inverse of the estimated covariance matrix $\mathbf{S}^{-1}$ can be expressed in terms of the regression coefficients and the residual variances of the regression of each variable k^{th} onto all the other variables: the diagonal elements $\mathbf{S}^{-1}(i,i) = \left(s^2_{i|1.2.3...i-1.i+1...K}\right)^{-1}$

and the others elements $\mathbf{S}^{-1}(i,j) = \dfrac{-\hat{\beta}_{i,j}}{s^2_{i|1.2.3...i-1.i+1...K}}$ with $i \neq j$

where:

$$s^2_{i|1.2.3..i-1.i+1..K} = s^2_{ii} - \sum_{j \neq i} \hat{\beta}_{ij} s^2_{ij} \qquad (A\ 3.1)$$

Let demonstrate this for the bivariate case (x_1, x_2) and *N* observations.

Regression of x_2 on x_1

RSS (Residual Sum of Squares) = $\sum_{\text{obs}=1}^{N} (x_{2.\text{obs}} - \hat{\beta}_0 - \hat{\beta}_1 x_{1.\text{obs}})^2 \qquad (A\ 3.2)$

In order to get the least square estimation of the parameters β_0, β_1 we differentiate with respect both estimators and set the derivatives to zero:

$$\frac{\partial \text{RSS}}{\partial \hat{\beta}_0} = -2 \sum_{\text{obs}=1}^{N} (x_{2.\text{obs}} - \hat{\beta}_0 - \hat{\beta}_1 x_{1.\text{obs}}) = 0 \Rightarrow \text{n}\hat{\beta}_0 = \sum_{\text{obs}=1}^{N} x_{2.\text{obs}} - \hat{\beta}_1 \sum_{\text{obs}=1}^{N} x_{1.\text{obs}}$$

$$\hat{\beta}_0 = \bar{x}_2 - \hat{\beta}_1 \bar{x}_1 \qquad (A\ 3.3)$$

$$\frac{\partial \text{RSS}}{\partial \hat{\beta}_1} = -2 \sum_{\text{obs}=1}^{N} x_{1,\text{obs}} (x_{2.\text{obs}} - \hat{\beta}_0 - \hat{\beta}_1 x_{1.\text{obs}}) = 0 \Rightarrow \hat{\beta}_0 \sum_{\text{obs}=1}^{N} x_{1,\text{obs}} + \hat{\beta}_1 \sum_{\text{obs}=1}^{N} \left(x_{1,\text{obs}}\right)^2 = \sum_{\text{obs}=1}^{N} x_{1,\text{obs}} \cdot x_{2.\text{obs}}$$

$$(\bar{x}_2 - \hat{\beta}_1 \bar{x}_1)(N\bar{x}_1) + \hat{\beta}_1 \sum_{\text{obs}=1}^{N} \left(x_{1,\text{obs}}\right)^2 = \sum_{\text{obs}=1}^{N} x_{1,\text{obs}} \cdot x_{2.\text{obs}} \Rightarrow \hat{\beta}_1 \left(\sum_{\text{obs}=1}^{N} \left(x_{1,\text{obs}}\right)^2 - N\bar{x}_1^2 \right) = \sum_{\text{obs}=1}^{N} x_{1,\text{obs}} \cdot x_{2.\text{obs}} - N\bar{x}_1 \bar{x}_2$$

$$\hat{\beta}_1 \left(\sum_{\text{obs}=1}^{N} \left(x_{1,\text{obs}}\right)^2 - N\bar{x}_1^2 \right) = \sum_{\text{obs}=1}^{N} x_{1,\text{obs}} \cdot x_{2.\text{obs}} - N\bar{x}_1 \bar{x}_2 \Rightarrow \hat{\beta}_1 \left(\sum_{\text{obs}=1}^{N} \left(x_{1,\text{obs}} - \bar{x}_1\right)^2 \right) = \sum_{\text{obs}=1}^{N} (x_{1,\text{obs}} - \bar{x}_1) \cdot (x_{2.\text{obs}} - \bar{x}_2)$$

$$\hat{\beta}_1 = \frac{\sum_{\text{obs}=1}^{N} (x_{1,\text{obs}} - \bar{x}_1) \cdot (x_{2.\text{obs}} - \bar{x}_2)}{\left(\sum_{\text{obs}=1}^{N} \left(x_{1,\text{obs}} - \bar{x}_1\right)^2 \right)} = \frac{s^2_{12}}{s^2_{11}} \qquad (A\ 3.4)$$

Replacing the least square estimation of the parameters $\hat{\beta}_0$ *(A 3.3)* in expression *(A 3.2)*

$$\text{RSS} = \sum_{\text{obs}=1}^{N} (x_{2.\text{obs}} - (\bar{x}_2 - \hat{\beta}_1 \bar{x}_1) - \hat{\beta}_1 x_{1.\text{obs}})^2 = \sum_{\text{obs}=1}^{N} \left[(x_{2.\text{obs}} - \bar{x}_2) - \hat{\beta}_1 (x_{1.\text{obs}} - \bar{x}_1) \right]^2$$

$$\text{RSS} = \sum_{\text{obs}=1}^{N} (x_{2.\text{obs}} - \bar{x}_2)^2 + \hat{\beta}_1^2 \sum_{\text{obs}=1}^{N} (x_{1.\text{obs}} - \bar{x}_1)^2 - 2\hat{\beta}_1 \sum_{\text{obs}=1}^{N} (x_{1.\text{obs}} - \bar{x}_1)(x_{2.\text{obs}} - \bar{x}_2) \qquad (A\ 3.5)$$

and replacing $\hat{\beta}_1$ *(A 3.4)* in *(A 3.5)*

$$\mathrm{RSS} = \sum_{\mathrm{obs}=1}^{N} (x_{2.\mathrm{obs}} - \bar{x}_2)^2 + \hat{\beta}_1 \sum_{\mathrm{obs}=1}^{N} (x_{1.\mathrm{obs}} - \bar{x}_1)(x_{2.\mathrm{obs}} - \bar{x}_2) - 2\hat{\beta}_1 \sum_{\mathrm{obs}=1}^{N} (x_{1.\mathrm{obs}} - \bar{x}_1)(x_{2.\mathrm{obs}} - \bar{x}_2)$$

$$\mathrm{RSS} = \sum_{\mathrm{obs}=1}^{N} (x_{2.\mathrm{obs}} - \bar{x}_2)^2 - \hat{\beta}_1 \sum_{\mathrm{obs}=1}^{N} (x_{2.\mathrm{obs}} - \bar{x}_2)(x_{1.\mathrm{obs}} - \bar{x}_1)$$

If we divide by *N*-1 degrees of freedom and generalizing to the regression of x_i on $x_1, x_2, ..., x_{i\text{-}1}, x_{i+1}, ..., x_K$

$$MSE = s^2_{2|1} = s^2_{22} - \hat{\beta}_1 s^2_{12} \Rightarrow s^2_{i|1.2.3..i-1.i+1..K} = s^2_{ii} - \sum_{j \neq i} \hat{\beta}_{ij} s^2_{ij}$$

$$\mathbf{S} = \begin{pmatrix} s^2_{11} & s^2_{12} \\ s^2_{12} & s^2_{22} \end{pmatrix} \Rightarrow \mathbf{S}^{-1} = \begin{pmatrix} \dfrac{s^2_{22}}{s^2_{11}s^2_{22} - s^4_{12}} & \dfrac{-s^2_{12}}{s^2_{11}s^2_{22} - s^4_{12}} \\ \dfrac{-s^2_{12}}{s^2_{11}s^2_{22} - s^4_{12}} & \dfrac{s^2_{11}}{s^2_{11}s^2_{22} - s^4_{12}} \end{pmatrix}$$

$$\mathbf{S}^{-1} = \begin{pmatrix} \dfrac{1}{s^2_{11} - \left(s^4_{12}/s^2_{22}\right)} & \dfrac{-s^2_{12}/s^2_{22}}{(s^2_{11}s^2_{22} - s^4_{12})/s^2_{22}} \\ \dfrac{-s^2_{12}/s^2_{11}}{(s^2_{11}s^2_{22} - s^4_{12})/s^2_{11}} & \dfrac{1}{s^2_{22} - \left(s^4_{12}/s^2_{11}\right)} \end{pmatrix} = \begin{pmatrix} \dfrac{1}{s^2_{11} - \hat{\beta}_2 s^2_{12}} & \dfrac{-\hat{\beta}_2}{s^2_{11} - \hat{\beta}_2 s^2_{12}} \\ \dfrac{-\hat{\beta}_1}{s^2_{22} - \hat{\beta}_1 s^2_{12}} & \dfrac{1}{s^2_{22} - \hat{\beta}_1 s^2_{12}} \end{pmatrix}$$

$$\mathbf{S}^{-1} = \begin{pmatrix} \dfrac{1}{s^2_{1|2}} & \dfrac{-\hat{\beta}_2}{s^2_{1|2}} \\ \dfrac{-\hat{\beta}_1}{s^2_{2|1}} & \dfrac{1}{s^2_{2|1}} \end{pmatrix} \quad \textit{(A 3.6)}$$

where $\hat{\beta}_1$ is the estimated coefficient of the regression of x_2 on x_1 and $\hat{\beta}_2$ is the estimated coefficient of the regression of x_1 on x_2.

Then we can use the expression *A* 3.6 of the inverse of the covariance matrix $\mathbf{S}^{-1}$ in the bivariate case to confirm that the k^{th} component of $\mathbf{y}_{\mathrm{new}} = \mathbf{S}^{-1}(\mathbf{x}_{\mathrm{new}} - \bar{\mathbf{x}}_{\mathrm{ref}})$ is the regression residual when variable x_k is regressed on all other variables, scaled by factor $s^2_{k|1.2.3...k-1.k+1...K}$:

$$\begin{pmatrix} y_{1,new} \\ y_{2,new} \end{pmatrix} = \cdot \begin{pmatrix} \frac{1}{s_{1|2}^2} & \frac{-\hat{\beta}_2}{s_{1|2}^2} \\ \frac{-\hat{\beta}_1}{s_{2|1}^2} & \frac{1}{s_{2|1}^2} \end{pmatrix} \cdot \begin{pmatrix} \bar{x}_{1,new} - \bar{x}_{.1,ref} \\ \bar{x}_{2,new} - \bar{x}_{2,ref} \end{pmatrix} = \begin{pmatrix} \frac{\left(x_{1,new} - \mu_{ref.1}\right) - \hat{\beta}_2\left(\bar{x}_{2,new} - \bar{x}_{2,ref}\right)}{s_{1|2}^2} \\ \frac{\left(x_{2,new} - \mu_{ref.2}\right) - \hat{\beta}_1\left(\bar{x}_{1,new} - \bar{x}_{.1,ref}\right)}{s_{2|1}^2} \end{pmatrix} = \begin{pmatrix} \frac{e_{1|2}}{s_{1|2}^2} \\ \frac{e_{2|1}}{s_{2|1}^2} \end{pmatrix}$$

where $e_{i|j}$ is the regression residual when variable x_i is regressed onto variable x_j.

Appendix 3.3

Verification of the Rencher´s decomposition for *k*=2

For a sample variance-covariance matrix: $\mathbf{S} = \begin{pmatrix} s_{11}^2 & s_{12}^2 \\ s_{12}^2 & s_{22}^2 \end{pmatrix}$ and a new observation $\mathbf{x}_i$, $\mathbf{x}_i = \begin{pmatrix} x_{i1} \\ x_{i2} \end{pmatrix}$. The Hotelling´s T^2 statistic for the new observation $\mathbf{x}_i$ is provided by:

$$T^2 = \begin{pmatrix} x_{i1} - \bar{x}_1 & x_{i2} - \bar{x}_2 \end{pmatrix} \frac{1}{s_{11}^2 s_{22}^2 - s_{12}^4} \begin{pmatrix} s_{22}^2 & -s_{12}^2 \\ -s_{12}^2 & s_{11}^2 \end{pmatrix} \begin{pmatrix} x_{i1} - \bar{x}_1 \\ x_{i2} - \bar{x}_2 \end{pmatrix}$$

Unfolding the expression:

$$T^2 = \frac{1}{s_{11}^2 s_{22}^2 - s_{12}^4} \left[s_{22}^2 \left(x_{i1} - \bar{x}_1\right)^2 - 2 s_{12}^2 \left(x_{i1} - \bar{x}_1\right)\left(x_{i2} - \bar{x}_2\right) + s_{11}^2 \left(x_{i2} - \bar{x}_2\right)^2 \right] \quad \textit{(A 3.7)}$$

And applying the Rencher´s decomposition (*Equation* 3.13) for *K*=2:

$$T^2 = T_1^2 + T_{2|1}^2$$

$$T_1^2 = \left(\frac{x_{i1} - \bar{x}_1}{s_{11}} \right)^2 \qquad T_{2|1}^2 = \left(\frac{x_{i2} - \bar{x}_{2|1}}{s_{2|1}} \right)^2 \quad \textit{(A 3.8)}$$

where

$$\left.\begin{aligned} \bar{x}_{2|1} &= \bar{x}_2 + \left[\frac{s_{12}^2}{s_{11}^2} \left(x_{i1} - \bar{x}_1\right) \right] \\ s_{2|1}^2 &= s_{22}^2 - \hat{\beta}_1 s_{12}^2 = s_{22}^2 - \frac{s_{12}^4}{s_{11}^2} = \left(\frac{s_{11}^2 s_{22}^2 - s_{12}^4}{s_{11}^2} \right) \end{aligned}\right\} \text{ Replacing in } \textit{(A 3.8)} \qquad T_{2|1}^2 = \frac{\left(x_{i2} - \bar{x}_2 - \frac{s_{12}^2}{s_{11}^2}\left(x_{i1} - \bar{x}_1\right) \right)^2}{\left(\frac{s_{11}^2 s_{22}^2 - s_{12}^4}{s_{11}^2} \right)}$$

$$T^2 = T_1^2 + T_{2|1}^2 = \left(\frac{x_{i1} - \bar{x}_1}{s_{11}} \right)^2 + \frac{\left(x_{i2} - \bar{x}_2 - \frac{s_{12}^2}{s_{11}^2}\left(x_{i1} - \bar{x}_1\right) \right)^2}{\left(\frac{s_{11}^2 s_{22}^2 - s_{12}^4}{s_{11}^2} \right)}$$

$$T_1^2 + T_{2|1}^2 = \frac{(x_{i1} - \bar{x}_1)^2}{s_{11}^2} + \frac{s_{11}^2}{s_{11}^2 s_{22}^2 - s_{12}^4}\left(x_{i2} - \bar{x}_2 - \frac{s_{12}^2}{s_{11}^2}(x_{i1} - \bar{x}_1) \right)^2$$

$$T_1^2 + T_{2|1}^2 = \frac{1}{s_{11}^2 s_{22}^2 - s_{12}^4}\left[\frac{(x_{i1} - \bar{x}_i)^2}{s_{11}^2}\left(s_{11}^2 s_{22}^2 - s_{12}^4\right) + s_{11}^2\left((x_{i2} - \bar{x}_2)^2 + \frac{s_{12}^4}{s_{11}^4}(x_{i1} - \bar{x}_1)^2 - 2\frac{s_{12}^2}{s_{11}^2}(x_{i1} - \bar{x}_1)(x_{i2} - \bar{x}_2) \right) \right]$$

$$T_1^2 + T_{2|1}^2 = \frac{1}{s_{11}^2 s_{22}^2 - s_{12}^4}\left[s_{22}^2 (x_{i1} - \bar{x}_1)^2 - \frac{s_{12}^4}{s_{11}^2}(x_{i1} - \bar{x}_1)^2 + s_{11}^2 (x_{i2} - \bar{x}_2)^2 + \frac{s_{12}^4}{s_{11}^2}(x_{i1} - \bar{x}_1)^2 - 2s_{12}^2 (x_{i1} - \bar{x}_1)(x_{i2} - \bar{x}_2) \right]$$

$$T_1^2 + T_{2|1}^2 = \frac{1}{s_{11}^2 s_{22}^2 - s_{12}^4}\left[s_{22}^2 (x_{i1} - \bar{x}_1)^2 - 2s_{12}^2 (x_{i1} - \bar{x}_1)(x_{i2} - \bar{x}_2) + s_{11}^2 (x_{i2} - \bar{x}_2)^2 \right] = T^2 \quad \textit{(A 3.9)}$$

So *(A 3.9)=(A 3.7)* and the Rencher´s decomposition expression is verified for *k*=2.

Appendix 3.4

Derivation of the expression:

$$\bar{x}_{K|1,2.....K-1} = \bar{x}_K + \hat{\boldsymbol{\beta}}^T (\mathbf{x}_i^{(K-1} - \bar{\mathbf{x}}^{(K-1)})$$

From the linear regression model:

$$\bar{x}_{K|1,2,...,K-1} = \hat{\beta}_0 + \hat{\boldsymbol{\beta}}^T \mathbf{x}_i^{(K-1} \qquad \textit{(A 3.10)}$$

As every linear regression model goes throw the centre of gravity of the data $\left(\bar{\mathbf{x}}^{(k-1}, \bar{x}_K\right)$

$$\bar{x}_K = \hat{\beta}_0 + \hat{\boldsymbol{\beta}}^T \bar{\mathbf{x}}^{(K-1} \Rightarrow \hat{\beta}_0 = \bar{x}_K - \hat{\boldsymbol{\beta}}^T \bar{\mathbf{x}}^{(K-1}$$

Replacing $\hat{\beta}_0$ en *(A 3.10)*:

$$\bar{x}_{K|1,2.....K-1} = \bar{x}_K - \hat{\boldsymbol{\beta}}^T \bar{\mathbf{x}}^{(K-1} + \hat{\boldsymbol{\beta}}^T \bar{\mathbf{x}}_i^{(K-1} = \bar{x}_K + \hat{\boldsymbol{\beta}}^T (\mathbf{x}_i^{(K-1} - \bar{\mathbf{x}}^{(K-1)})$$

Appendix 3.5

Checking of the expressions for *K*=2

$$\hat{\boldsymbol{\beta}}_K = \mathbf{S}_{\mathbf{XX}}^{-1} \mathbf{s}_{\mathbf{xX}} \qquad\qquad s_{K|1,2.....K-1}^2 = s_{xx}^2 - \mathbf{s}_{\mathbf{xX}}^T \mathbf{S}_{\mathbf{XX}}^{-1} \mathbf{s}_{\mathbf{xX}}$$

In the bidimensional case, using the linear regression model expressions for ($x_2|x_1$)

$$\hat{\beta} = \frac{s_{12}^2}{s_{11_1}^2} = \left(s_{11}^2\right)^{-1} s_{12}^2 = \mathbf{S_{XX}^{-1}} \mathbf{s_{xX}}$$

$$s_{2|1}^2 = s_{22}^2 (1 - r_{12}^2) = s_{22}^2 - s_{22}^2 \frac{s_{12}^4}{s_{11}^2 s_{22}^2} = s_{22}^2 - s_{21}^2 \left(s_{11}^2\right)^{-1} s_{12}^2 = s_{xx}^2 - \mathbf{s}_{\mathbf{xX}}^T \mathbf{S_{XX}^{-1}} \mathbf{s_{xX}}$$

$s_{2|1}^2$ is a biased estimator of $\sigma_{2|1}^2$ with $E(s_{2|1}^2) = \frac{N-M-1}{N-1}\sigma_{2|1}^2$ where M is the number of predictor variables (in this case 1). An unbiased estimator of $\sigma_{2|1}^2$ would be the Mean Square Error (MSE) in the regression $(x_2|x_1)$. So the relationship between $s_{2|1}^2$ and the MSE of the regression $(x_2|x_1)$ would be:

$$MSE = \frac{N-1}{N-M-1} s_{2|1}^2 \;\Rightarrow\; s_{2|1}^2 = \frac{N-M-1}{N-1} MSE = \sqrt{\frac{N-M-1}{N-1}} \sqrt{MSE} = c \cdot S_{res}$$

Appendix 3.6

Unconditional components distribution

For a new observation $\mathbf{x}_i$ where k variables are measured and the sample covariance matrix computed from a reference data set is **S**, the value of the unconditional component for the k-th variable, T_k^2, for that observation is provided by:

$$T_k^2 = \left(x_{ik} - \bar{x}_k\right)^T \left(s_{kk}^2\right)^{-1} \left(x_{ik} - \bar{x}_k\right) = \left(\frac{x_{ik} - \bar{x}_k}{s_{kk}}\right)^2$$

where $\bar{x}_k$ is the sample mean for the k-th variable calculated from N observations of a reference data set, x_{ik} is the value for the k-th variable in the new observation $\mathbf{x}_i$ and $\bar{x}_k \sim N(\mu_k; \frac{\sigma_k^2}{N})$.

If H_0 is true (*i.e.* there is not a change in the position of the distribution of the process), it follows that:

$$x_k \sim N(\mu_k; \sigma_{kk}^2)$$

$$\bar{x}_k - x_k \sim N\left(0; \sigma_{kk}^2 \frac{(N+1)}{N}\right)$$

$$\frac{\bar{x}_k - x_k}{\sigma_{kk}\sqrt{\frac{N+1}{N}}} \sim N(0;1)$$

Assuming normality,
$(N-1)\frac{s_{kk}^2}{\sigma_{kk}^2} \sim \chi_{N-1}^2$ so it follows $\frac{s_{kk}^2}{\sigma_{kk}^2} \sim \frac{\chi_{N-1}^2}{N-1}$

then

$$\frac{\bar{x}_k - x_k}{\frac{s_{kk}}{\sigma_{kk}}\sigma_{kk}\sqrt{\frac{N+1}{N}}} \sim \frac{N(0;1)}{\sqrt{\frac{\chi_{N-1}^2}{N-1}}} \sim t_{N-1}$$

and

$$\frac{\bar{x}_k - x_k}{s_{kk}} \sim t_{N-1}\sqrt{\frac{N+1}{N}}$$

Considering the squared of this expression:

$$\left(\frac{\bar{x}_k - x_k}{s_{kk}}\right)^2 \sim \frac{N+1}{N}\frac{(N(0;1))^2}{\left(\frac{\chi_{N-1}^2}{N-1}\right)} \sim \frac{N+1}{N}\frac{\left(\frac{\chi_1^2}{1}\right)}{\left(\frac{\chi_{N-1}^2}{N-1}\right)} \sim \frac{N+1}{N}F_{1,N-1}$$

So we finally get the distribution for the unconditional components:

$$T_k^2 \sim \frac{N+1}{N}F_{1,N-1}$$

Conditional components distribution

For the bivariate case: k =2

$$T^2 = T_1^2 + T_{2|1}^2$$

$$T_{2|1}^2 = \left(\frac{x_2 - \bar{x}_{2|1}}{s_{2|1}}\right)^2$$

$$\left.\begin{array}{l} x_2 \sim N(\mu_2; \sigma_{22}^2) \\ \bar{x}_{2|1} \sim N(\mu_{2|1}; \frac{\sigma_{2|1}^2}{N}) \end{array}\right\} \quad x_2 - \bar{x}_{2|1} \sim N(\mu_2 - \mu_{2|1}; \sigma_{22}^2 + \frac{\sigma_{2|1}^2}{N})$$

So that

$$\frac{x_2 - \bar{x}_{2|1} - (\mu_2 - \mu_{2|1})}{\sqrt{\sigma_{22}^2 + \frac{\sigma_{2|1}^2}{N}}} \sim N(0;1)$$

If H_0: $x_2 \in$ Conditional distribution $(x_2|x_1)$ is true $\rightarrow$ $\mu_2 = \mu_{2|1}$, $\sigma_{22} = \sigma_{2|1}^2$

then, $$\frac{x_2 - \bar{x}_{2|1}}{\sqrt{\sigma_{2|1}^2\left(1 + \frac{1}{N}\right)}} \sim N(0;1) \quad \rightarrow \quad \frac{x_2 - \bar{x}_{2|1}}{\sigma_{2|1}\sqrt{\frac{N+1}{N}}} \sim N(0;1)$$

In normal populations:

$$(N-1)\frac{s_{kk}^2}{\sigma_{kk}^2} \sim \chi_{N-1}^2 \rightarrow (N-M-1)\frac{MSE}{\sigma_{2|1}^2} \sim \chi_{N-M-1}^2 \rightarrow \frac{\sqrt{MSE}}{\sigma_{2|1}} \sim \sqrt{\frac{\chi_{N-M-1}^2}{(N-M-1)}}$$

where M is the number of predictor variables (in this case $M=1$)

$$\frac{x_2 - \bar{x}_{2|1}}{\frac{\sqrt{MSE}}{\sigma_{2|1}}\sigma_{2|1}\sqrt{\frac{N+1}{N}}} = \frac{x_2 - \bar{x}_{2|1}}{\sqrt{MSE}\sqrt{\frac{N+1}{N}}} \sim \frac{N(0;1)}{\sqrt{\frac{\chi_{N-M-1}^2}{(N-M-1)}}} \sim t_{N-M-1}$$

$$\frac{\left(x_2 - \bar{x}_{2|1}\right)^2}{MSE\left(\frac{N+1}{N}\right)} \sim F_{1,N-M-1} \rightarrow \quad \frac{\left(x_2 - \bar{x}_{2|1}\right)^2}{MSE} \sim \left(\frac{N+1}{N}\right)F_{1,N-M-1}$$

Taking into account the relationship between the MSE and $s_{2|1}^2$ (Appendix 3.6):

$$MSE = \frac{N-1}{N-M-1}s_{2|1}^2 \rightarrow \quad T_{2|1}^2 = \frac{\left(x_2 - \bar{x}_{2|1}\right)^2}{s_{2|1}^2} \sim \frac{(N-1)(N+1)}{(N-M-1)N}F_{1,N-M-1}$$

So, we finally get the distribution for the conditional components:

$$T_{2|1}^2 = \frac{(N-1)(N+1)}{(N-M-1)N}F_{1,N-M-1}$$

Appendix 3.7

$$T^2_{K|1,2....K-1} = \left(\frac{x_K - \bar{x}_{K|1,2...K-1}}{s_{K|1,2....K-1}} \right)^2 = \frac{\left[x_K - \left(\bar{x}_K + \hat{\boldsymbol{\beta}}^T (\mathbf{x}_i^{(K-1} - \bar{\mathbf{x}}^{(K-1)}) \right) \right]^2}{s^2_{K|1,2....K-1}}$$

$$= \frac{\left[(x_K - \bar{x}_K) - \hat{\boldsymbol{\beta}}^T (\mathbf{x}_i^{(K-1} - \bar{\mathbf{x}}^{(K-1)}) \right]^2}{s^2_{K|1,2....K-1}} = \hat{z}^2_K$$

Chapter 4: Diagnosis performance in MSQC (I)

In this chapter we proceed to compare the diagnosis performance of the different fault diagnosis methodologies in MSQC described in chapter 3. The methods are tested in a simulation procedure for 4 measured variables. In the simulation a wide variety of different types of fault with different correlation structures have been considered. The simulation tries to highlight the strong and weak points of the different methods.

4.1 Simulation procedure for 4 variables

4.1.1 Simulation data generation

In order to compare the methods described in chapter 3, several faults consisting of small, medium or large shifts in the mean of one (or more) variables under different scenarios of correlation matrices will be simulated. In the simulation, the different methodologies are applied to a case of four measured variables under eleven different correlation structures shown in Table 4.1 where the covariance matrix condition numbers tend to increase its value from C1 to C11. The standard deviations of the four variables were uniformly distributed between 0.3 and 0.4. Scenarios leading to unfeasible covariance matrices were discarded. Reference data sets of 50.000 observations for each of the 11 correlation structures were obtained using the algorithm proposed by Arteaga and Ferrer (2010). These reference data sets were used to adjust the Type I risk when the methodologies under comparison used a different detection trigger mechanism in the detection of the out-of-control observations other than Hotelling´s T^2 statistic (*i.e.* Hawkins´ method, Hayter and Tsui´s method and Step-down method). For every correlation structure 102 different types of faults were considered. The faults consisted in mean shifts in one, two or three variables. The size of the shifts were small (1.25 to 1.66 standard deviations), medium (2.5 to 3.33 standard deviations) or large (5 to 6.6 standard deviations). The shifts involving several means happened in both the same or opposite directions. For each type of fault, 500 observations using the algorithm proposed by Arteaga and Ferrer (2010) were simulated.

In this study we have only considered faults affecting the mean of the process and excluded faults affecting the covariance structure. The rationale for this decision is: i) this approach is most commonly used to address the performance of different diagnostic methods; ii) this allows the appropriate comparison of the methods described in chapter

3 especially as some of them are not suited for the detection of changes in the covariance matrix of the process.

TABLE 4.1. Correlation structures.

Correlation Structure	Correlation Values	Extreme Correlations (0.9)	Condition number $CN=\frac{\lambda_{max}}{\lambda_{min}}$
C1: Weak correlations	Weak correlation coefficients uniform distributed, U[-0.1 , +0.1]	No	1.57
C2: Moderate positive correlations	Moderate positive correlation coefficients uniformly distributed, U[+0.1 , +0.4]	No	3.24
C3: Moderate mixed correlations	Moderate mixed positive-negative correlations. Absolute correlation coefficients uniformly distributed, U[+0.1 , +0.4]	No	4.91
C4: Moderate negative correlations	Moderate negative correlation coefficients uniformly distributed, U[-0.1 , -0.4]	No	22.32
C5: Weak correlations with one extreme correlation	Weak correlation coefficients uniformly distributed, U[-0.1 , +0.1] with one coefficient +0.9	Yes	20.38
C6: Moderate positive correlations with one extreme correlation	Moderate positive correlation coefficients uniformly distributed, U[+0.1 , +0.4] with one coefficient +0.9	Yes	21.49
C7: Moderate mixed Correlations with one extreme correlation	Moderate mixed positive-negative correlations. Absolute correlation coefficients uniformly distributed, U[+0.1 , +0.4] with one coefficient +0.9	Yes	29.92
C8: Strong positive correlations	Strong positive correlation coefficients uniformly distributed, U[+0.5 , +0.8]	No	17.37
C9: Strong positive correlations with one extreme correlation	Strong positive correlation coefficients uniformly distributed, U[+0.5 , +0.8] with one coefficient +0.9	Yes	38.07
C10: Strong mixed correlations	Moderate strong positive-negative correlations. Absolute correlation coefficients uniformly distributed, U[+0.5 , +0.8]	No	17.91
C11: Strong mixed correlations with one extreme correlation	Moderate strong positive-negative correlations. Absolute correlation coefficients uniformly distributed, U[+0.5 , +0.8] with one coefficient +0.9	Yes	39.35

4.1.2 Performance indices

These faulty data sets were processed under the different proposed fault diagnosis methodologies and their performance were measured and compared according to several performance indices that were computed for every correlation structure and a particular type of fault. The considered performance indices were the following:

- PTC_0 : Proportion of observations correctly diagnosed

$$PTC_0 = \frac{\sum_{i=1}^{500} P_{0,i}}{500}$$

where P_0=1 if *all the variables* in the observation are correctly diagnosed, and P_0 = 0 on the contrary.

- $PTCv$: Proportion of faulty variables correctly diagnosed (i.e., true positives in variables)

$$PTC_v = \frac{\sum_{i=1}^{500} P_{v,i}}{500}$$

Where $P_{v,i} = N_{df,i}/N_{f,i}$ with $N_{df,i}$ equals to the number of correctly diagnosed faulty variables in the i^{th} observation, and $N_{f,i}$ equals to the number of faulty variables in the i^{th} observation.

- PWC_0 Proportion of observations with any non faulty variable wrongly diagnosed (i.e. false positives in observations)

$$PWC_0 = \frac{\sum_{i=1}^{500} W_{0,i}}{500}$$

where W_0=1 if there is any non-faulty variable in the observation wrongly classified, and W_0 = 0 on the contrary.

- $PWCv$: Proportion of non faulty variables wrongly diagnosed (i.e. false positives in variables)

$$PWC_v = \frac{\sum_{i=1}^{500} W_{v,i}}{500}$$

Where $W_{v,i} = NW_{df,i}/N_{nf,i}$ with $NW_{df,i}$ equals to the number of wrongly diagnosed non-faulty variables in the i^{th} observation, and $N_{nf,i}$ equals to the number of non-faulty variables in the i^{th} observation.

- PND : Proportion of faulty observations which are not detected as faults. This is related to the lack of detection power

$$PND = \frac{\sum_{i=1}^{500} P_{d,i}}{500}$$

where $P_{d,i}$=1 if the i^{th} observation is not detected as a faulty observation, and $P_{d,i}$ = 0 on the contrary.

- PNF : Proportion of detected faulty observations in which no variable is found as responsible. This is related with the lack of isolation power

$$PNF = \frac{\sum_{i=1}^{500} P_{f,i}}{500}$$

where $P_{f,i}$=1 if the i^{th} observation is detected as a faulty observation but no variable is found as responsible, and $P_{f,i}$ = 0 on the contrary.

4.1.3 Type I risk considerations

In order to check the accuracy and precision of the adjusted Type I risk for the 11 covariance matrices under different detection trigger mechanisms, 10 reference data sets under each correlation matrix were simulated and the real Type I risk for each data set were computed. In the methodologies based on Hotelling´s T^2 statistic the real Type I risk is centered in the desired value as it expected since the Type I risk level is adjusted from a theoretical distribution that takes into account the correlation between variables**.** Hawkins´ methodology assumes that the marginal distribution of the monitored residuals follows a standardized normal distribution. The overall Type I risk depends on the number of hypotheses tests and the Type I risk α of each of the hypotheses tests. In the case of four independent variables, the overall Type I risk is $1-(1-\alpha)^4$. For a desired overall rate of $\alpha_{overall} = 0.05$, $\alpha = 1-(1-\alpha_{overall})^{1/4} = 0.01274$ so the number of standard deviations to consider for a two-tail hypothesis test is 2.49σ.

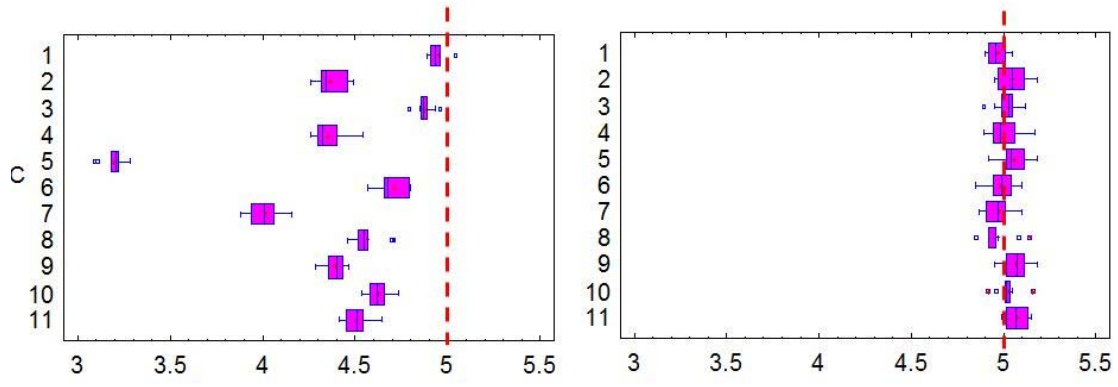

a) b)

FIGURE 4.1: Type I risk ($\alpha_{overall} \times 100$) for the 11 correlation structures:
a) Original Hawkins´ method; b) Adjusted Hawkins´ method

Figure 4.1 a) shows the Type I risk of Hawkins´ methodology after Bonferroni correction for the 11 correlation structures simulated. The underestimation of $\alpha_{overall}$ in most scenarios is due to the lack of independence between the monitored residuals. The **B** matrix of the Hawkins´ methodology (section 3.2.6) shows that the monitored standardized normal residuals are correlated and, consequently, it is necessary to adjust for the Type I risk in every case. Table 4.2 shows the selection of the number of standard deviation (*nd*) to use in the construction of the upper control limit (*UCL*) in Hawkins´ methodology in order to get an overall Type I risk, $\alpha_{overall}$=0.05 in the 11 correlation matrices situations of the simulation. The values of Table 4.2 were selected according to the results shown in Appendix 4.1 (Table 4.4) where the Type I risk for 20 different *nd* values were calculated in the 11 correlation matrix scenarios.

TABLE 4.2. Selected number of standard deviations (*nd*) to use in the construction of the UCL in Hawkins' methodology for an overall Type I risk, $\alpha_{overall}$=0.05, in the 11 correlation matrix scenarios

C	**1**	**2**	**3**	**4**	**5**	**6**	**7**	**8**	**9**	**10**	**11**
nd	2.49	2.44	2.48	2.44	2.31	2.47	2.41	2.46	2.44	2.46	2.45

The Type I risk corresponding to this *nd* selection was computed on new 10 test data sets for the corresponding 11 correlation matrix scenarios. Figure 5.1 b) shows that after the adjustment the objective of overall Type I risk of 5% is accomplished.

In the case of Hayter and Tsui´s and the Step-down´s methodologies the monitored statistic follows known theoretical distributions what makes easier to adjust them for the overall Type I risk ($\alpha_{overall}$=0.05).

4.2 Fault diagnosis performance comparison

In order to compare the methodologies first we started with an exploratory partial least squares (PLS) regression study over the data to investigate the relationships among the different methodologies and the proposed indices PTC_0, *PTCv*, PWC_0, *PWC*v, *PND* and *PNF*. In a second step, the results for the different performance indices obtained from the simulation study were analyzed with a multifactor analysis of variance (ANOVA)

4.2.1 PLS initial exploratory study

A PLS model is fitted for 6 response variables: PTC_0 , *PTCv*, *PWCo*, *PWCv*, *PND, PNF* and for 33 predictor variables: diagnosis method (14 methods), correlation scenario (11 different scenarios), number of faulty variables (1 to 3), size of the fault (small, medium or large faults), strength of correlation (low and high). The 14 methods are labeled according to Table 4.3.

In the step-down method, two *a priori* ordering among the different types of faults were considered: profile 1-1-1-1 (fault in x_1, fault in x_2, fault in x_3, fault in x_4) in M12 and profile 1-1-2 (fault in x_1, fault in x_2, fault in x_3 and x_4) in M13. A variant of Hawkins´ methodology (M14) to detect faults affecting one single variable (Hawkins' one single

variable method) was also considered. In this variant, the algorithm identifies as responsible the variable with the largest significant residual $\hat{z}_{k,\text{new}}$.

TABLE 4.3. List of diagnostic methods

Label	Method
M1	Hawkins
M2	Hayter and Tsui
M3	Doganaksoy, Faltin and Tucker (Bonferroni)
M4	Doganaksoy, Faltin and Tucker (Holm)
M5	Doganaksoy, Faltin and Tucker (Hochberg)
M6	Doganaksoy, Faltin and Tucker (Hommel)
M7	Doganaksoy, Faltin and Tucker (TCH)
M8	Doganaksoy, Faltin and Tucker (D/AP)
M9	Murphy
M10	Mason, Tracy and Young (MTY)
M11	Montgomery and Runger
M12	Step-down with profile (1-1-1-1)
M13	Step-down with profile (1-1-2)
M14	Hawkins' one single variable

The PLS results shows that the first two PLS components jointly explain a 45.1 % of the variability (R_Y^2) of the response variables with a predictive ability of 44.9% (Q^2). Figure 4.2 a) shows the $w*c_1$ /$w*c_2$ weighting plot corresponding to these PLS components for the most relevant factors. The size of the fault (*Sf)* accounts for the most of the first component. Large faults (Sf(3*)*) yield large values for PTC_v and PTC_o, so the larger the size of the fault the better the classification results. On the other hand, the lack of power indices *PND* and *PNF* are inversely related to the true classification percentages PTC_0 and *PTCv*, and the lower the size of the fault the higher the lack of the detection and isolation power. In Figure 4.2 b), the t_1/t_2 score plot shows three clusters along the first component which correspond to small Sf(1), medium Sf(2) and large Sf(3) size of faults. The first component has to do with the inverse relationship between *PND* and *PNF* with PTC_0 and *PTCv*. The Step-down methods (M12 and M13) and the M14 cannot be compared against the other methodologies in all the faults as they only cover some specific types of the faults and, consequently, these methods presented the worse results

in *PTCv*. The second component has to do with the false positives indices (*PWCv* and *PWC0)* in which Murphy´s (M9), Montgomery´s (M11) and Hawkins´ (M1) methods had the worst results.

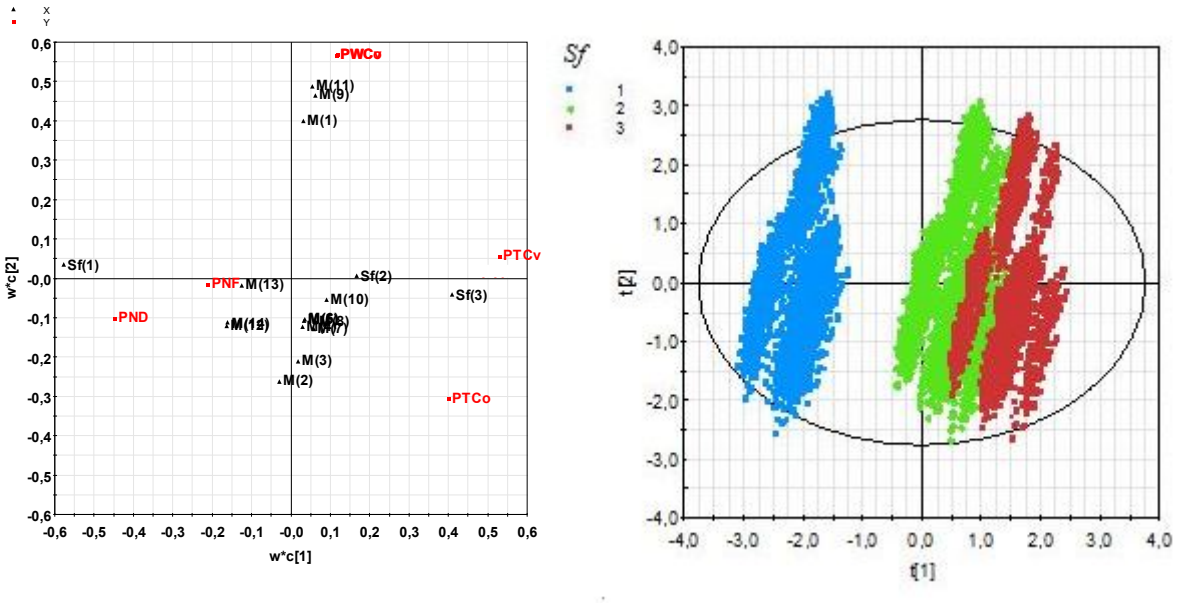

FIGURE 4.2 PLS model: a) w^*c_1 /w^*c_2 weighting plot b) t_1/t_2 score plot: small size (blue), medium size (green) and large size (red) faults

The PLS regression coefficients plots in Figure 4.3 allow to study the statistical significance of the predictor variables for the response variables *PTC0* , *PTCv*, *PWCo*, *PWCv*, *PND* and *PNF*.

- In *PTC0* the methods M1, M9, M11, M12, M13, M14 perform significantly worse than methods M2 to M8 and M10. The plot shows that *PTC0* improves with small correlation scenarios (C1 and C2), one single variable faults and large-sized faults.
- In *PTCv*, the methods M2, M12, M13 and M14 perform worse than the rest. There are no special problems with M1, M9, M11 which allows us to conclude that the bad performance in *PTC0* of these methods is mainly due to an excesive number of false positive diagnosis. The method with the best results in *PTCv* is the M10. The plot shows that *PTC v* improves in large-sized faults of one single variable.

In contrast to what happens in the PTC_0 it performs better in strong correlation scenarios.

- PWC_0 and PWC_v coefficients plots shows clearly that the problems with methods M1, M9, M11 is a problem of an excesive false positives and that the problem is associated to the high correlation scenarios.
- *PND* coefficient plot shows that only method M2 has special problems of lack of detection which is specially associated to small faults in small correlation scenarios.
- *PNF* coefficient plot shows that DFT and its variants (M3 to M8) are the only methods with lack of power in diagnosis. The ad hoc variants M7 and M8 perform better than methods M3 to M6. This problem is specially associated to small faults in high correlation scenarios.

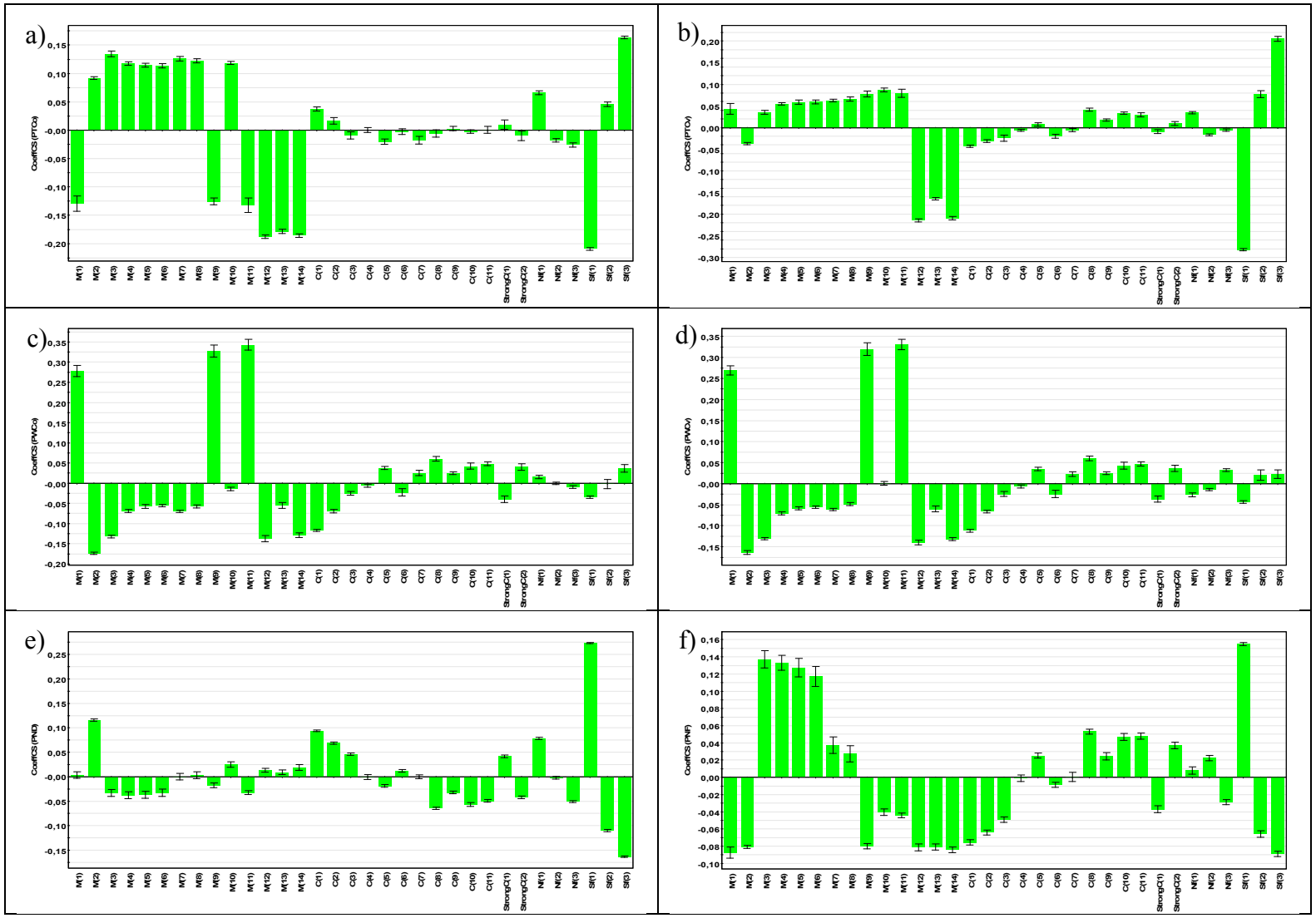

FIGURE 4.3: PLS Regression Coefficients Plot (CoeffCS): a) PTC_0, b) *PTCv*, c) *PWCo*, d) *PWCv*, e) *PND* and f) *PNF* (95% confidence level)

4.2.2 Interpretation of the ANOVA Results

In order to check for the statistical significance of the PLS results a multifactor analysis of variance (ANOVA) was performed considering the factors: number of faulty variables, N_f (3 levels: 1, 2 and 3 faulty variables); diagnosis method, M (14 levels, see Table 4.3); and correlation structure, C (11 levels, see Table 4.1). The ANOVA results (see Appendix 2) show that all the factors and most of their interactions are statistically significant (p-value< 0.05) for all the performance indices.

The mean and 95% least significance difference (LSD) intervals plots displayed in Figure 4.4 show similar results than those obtained from the PLS regression coefficients in Figure 4.3. MTY (M10), the *ad hoc* and Bonferroni variants of the DFT method (M3, M7, M8) have the best results in PTC_0. The MTY also presents the best results in PTC_v and a medium performance in PWC_0 and PWC_v. The Hawkins' (M1), Murphy's (M9) and Montgomery's (M11) methods exhibit serious problems of false positives in diagnosis, as it can be concluded from the large values in PWC_0 and PWC_v, yielding low performance in terms of correct diagnosis (PTC_0).

The interaction plots displayed in Figure 4.5 shows that one of the main reasons why the interaction between correlation structure and the diagnosis method is statistically significant is the different effect of the correlation structure in the performance in PTC_0, PWC_0 and PWC_v of the methods M1, M9, M11. The performance of these methods is much more more sensitive to changes in the correlation structure than the others**.**

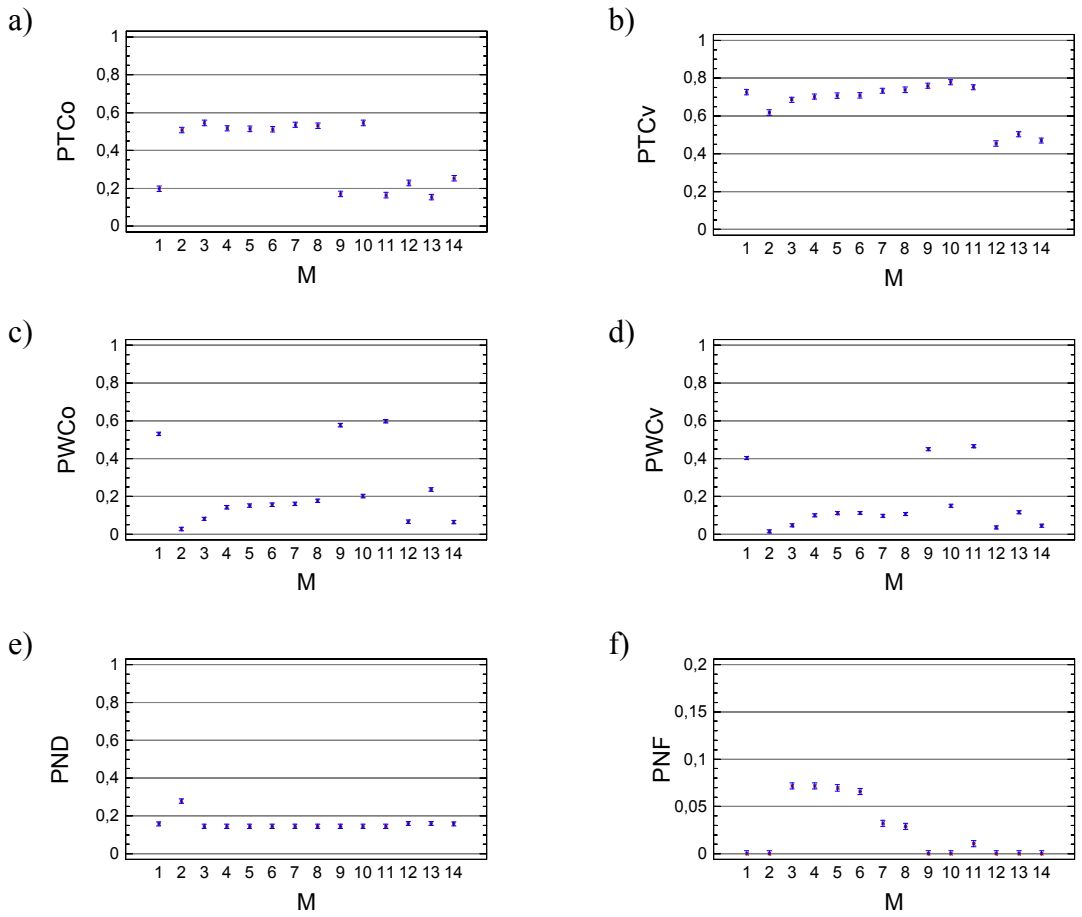

FIGURE 4.4: Means and 95% LSD intervals plot: a) PTC_0, b) PTC_v, c) PWC_0, d) PWC_v, e) *PND* , f) *PNF*.

Figure 4.6 shows the PTC_0, PTC_v,, PWC_0, PWC_v, *PND* and *PNF* for the methods M1, M9, M11. It can be appreciated that the PTC_0 drops, while PWC_0 and PWC_v rise, for correlation scenarios with a bad condition number (high correlations).

The interaction plots between the number of observation variables involved in the fault (*Nf*) and the fault diagnosis method displayed in Figure 4.7 show that although M12 and M14 are the best methods in PTC_0 for one single variable faults they do not perform well when the number of variables involved in the fault is 2 or 3. This account for their bad performance in PTC_0 as shown in Figure 4.7 a). By contrast methods M1,

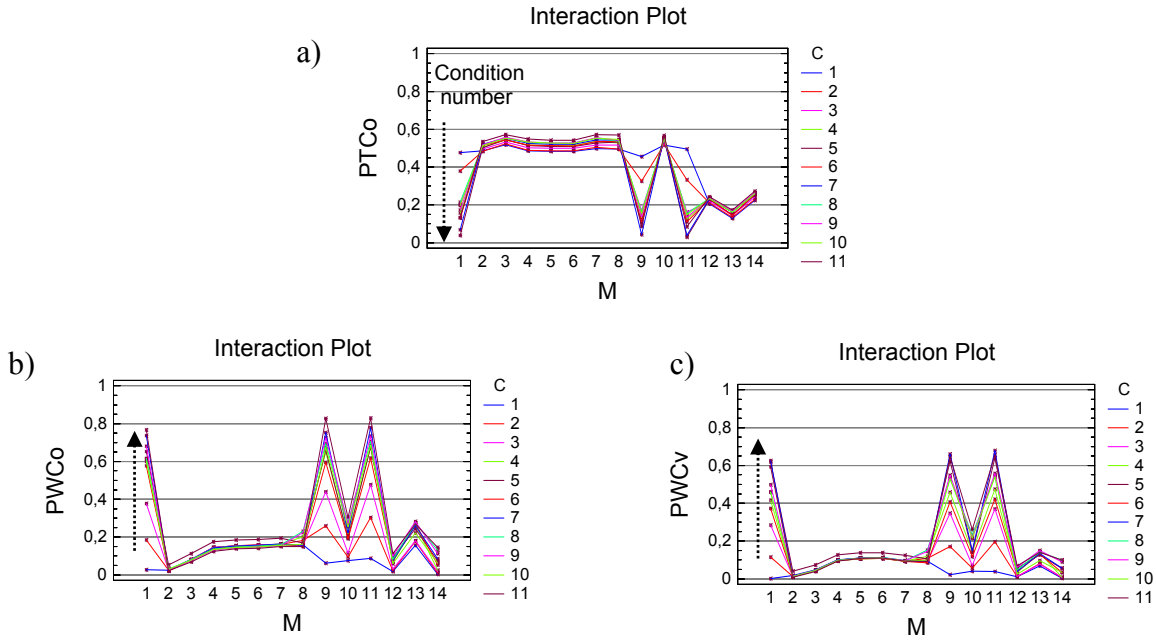

FIGURE 4.5 Interaction plots for diagnosis method × covariance structure:
a) PTC_0 , b) PWC_0 c) PWC_v
Arrows in the plots indicate the direction of increment of condition number of the correlation structures.

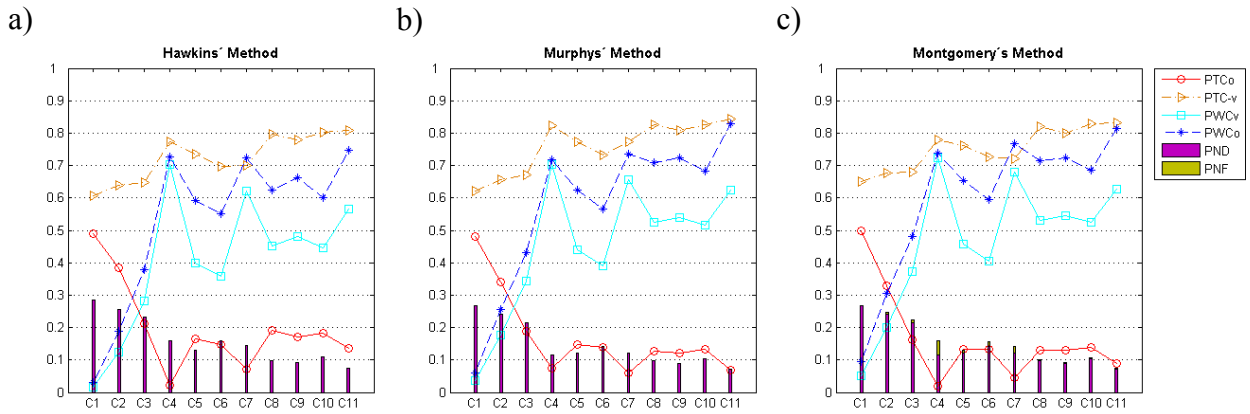

FIGURE 4.6 PTC_0 , PTC_v ,PWC_0 , PWC_v , *PND* and *PNF* under the different correlation structures
a) Hawkins', b) Murphy´s and c) Montgomery´s methods

M9, M11 and M13 perform badly in PTC_0 no matter the number of variables involved in the fault. Regarding PTC_v, Figure 4.7 b) shows that the M1 has the best performance for one single variable faults while the M10 gives the best diagnosis performance for to 2 and 3 variables faults. Methods M12, M13 and M14 perform badly for 2 and 3 variables faults. This explains their bad performance in PTC_v shown in Figure 4.7 b).

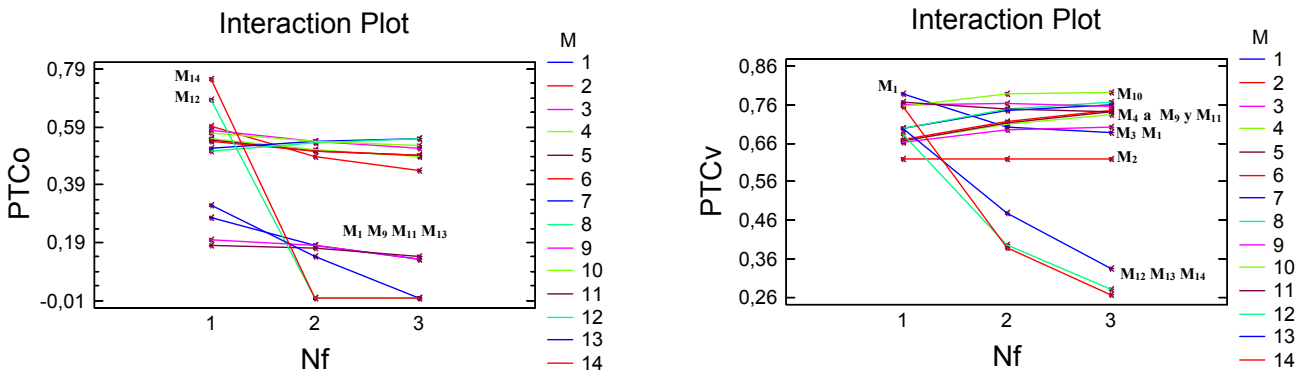

FIGURE 4.7 Interaction plots for diagnosis method × number of faults: a) PTC_0, b) PTC_v.

In the case of one single variable faults, Figure 5.9 a) shows that M14 (Hawkins´ one single fault method) and M12 (Step-down method with 1-1-1-1 subsets) perform better in PTC_0 than the rest of the methods. Figures 4.8 b) and c) shows that M12 and M14 present small values for PWC_0 and PWC_v. The good performance of these methods in diagnosing single variable faults can be explained by the fact that they are especially designed for this situation. On the contrary, these methods give bad results when the actual fault involves more than one variable as already shown in Figure 5.8. Another drawback in the Step-down method is the difficulty in implementing the monitoring plots when two different types of faults share a common out-of-control variable (i.e. if one type of fault supposes that the variables 1 and 2 become out of control and a second type of fault supposes that variable 1 and 3 become out of control).

If the size of the fault Sf (3 levels: small, medium and large) is introduced as a new factor in the ANOVA we observe an interesting result in Figure 4.9 whereby ANOVA interaction plots between the diagnosis method and the size of fault show that large and medium faults are particularly responsible for the excessive false positive rates in methods M1, M9 and M11

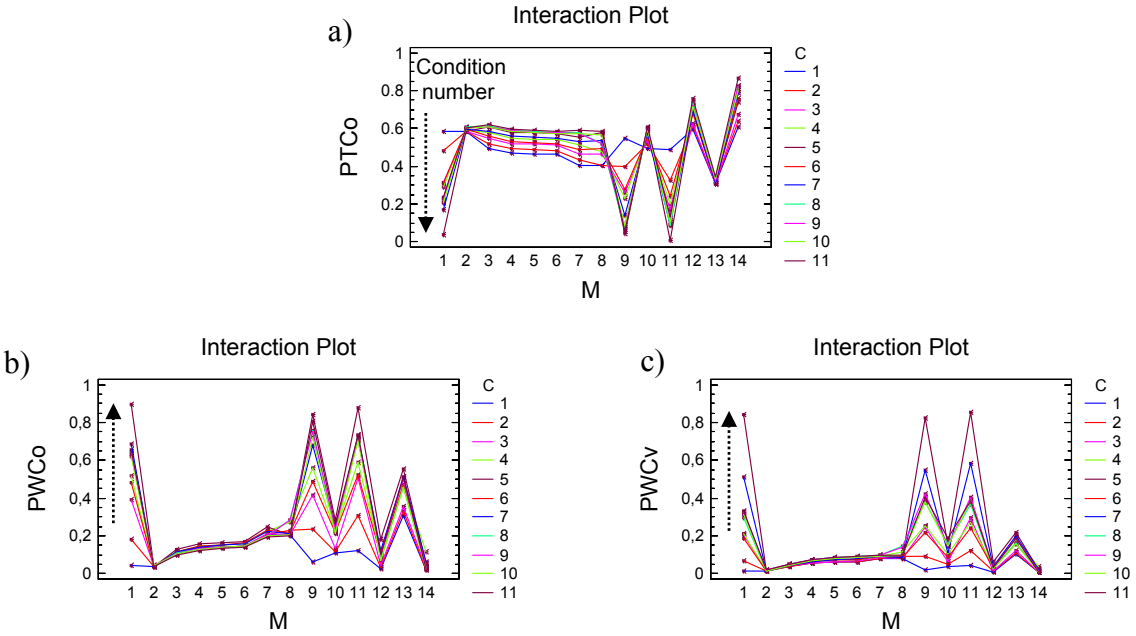

FIGURE 4.8 One single variable fault interaction plots: diagnosis method × covariance structure: a) PTC_0, b) PWC_0, c) PWC_v.

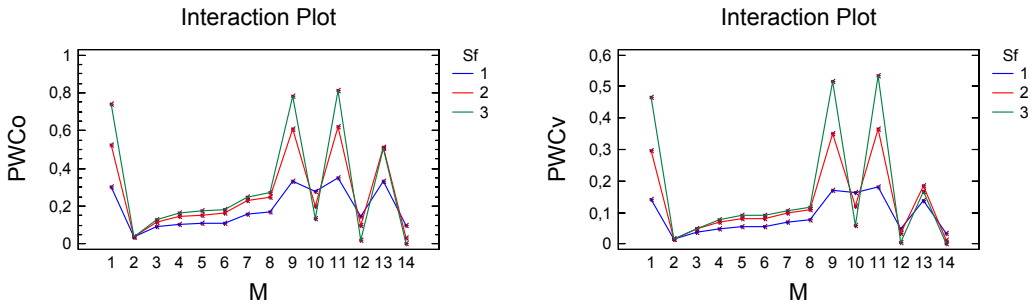

FIGURE 4.9 One single variable fault interaction plots: diagnosis method × fault size *a)* PWC_0, *b)* PWC_v

As it can be seen in Figures 4.10 a) the *PND* is equal on methods M3 to M11 since the detection on these methods is based on the Hotelling´s T^2 statistic. Methods M1, M12 and M13 have slightly larger *PND* in all the correlations structures. It can be appreciated that *PND* higher values are obtained in the weakest correlation structures C1, C2 and C3 for all the methodologies with the exception of the M2. The M2 presented a singular

behavior since the *PND* results become close similar in all the correlation structures. This method has the worst results in *PND*.

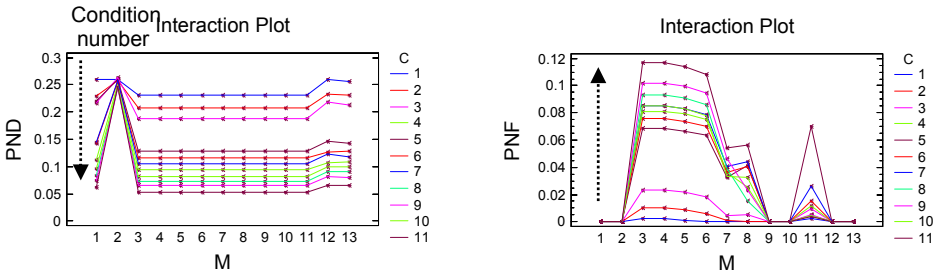

FIGURE 4.10 Interaction plots: diagnosis method × correlation structure: a) *PND* b) *PNF*

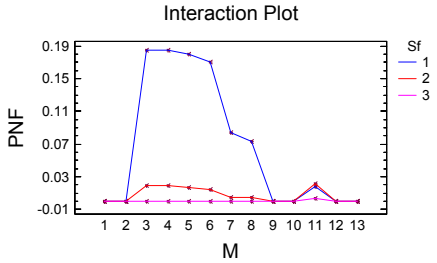

FIGURE 4.11: *PNF* Interaction plot: diagnosis method × fault size

Figure 5.11 b) and 5.5 f) shows that the DFT methods (from M3 to M8) give high values on *PNF*, thus indicating a lack of diagnostic power. Figure 5.12 shows that the bad *PNF* results are mainly associated to the small-sized faults, being particulary problematic in M3 to M6 methods. Among the DFT method and its variants the *ad hoc* variants (D/AP and TCH) (M7 and M8) have smaller values in *PNF* than M3, M4, M5 and M6.

4.3 Summary and Conclusions

The simulation results let us to conclude:

- The MTY method has a better diagnosis performance than the rest of the methods because it achieves better results in PTC_v while keeping a similar performance in PTC_0 to the other methods. Moreover, the MTY provides an easy interpretation of the significant terms and the relationships between variables and distinguishes

situations in which the correlation structure among the variables is broken from situations in which the correlation structure is still valid.

- Hawkins´, Murphy´s and Montgomery´s methods increase the number of false positives in the case of strong correlations and, consequently, yield a bad performance in PTC_0.
- DFT method and its variants showed problems of "lack of power in fault isolation" (*PNF*). The *ad hoc* methods D/AP and TCH showed a better power in fault isolation and PTC_0 values in the case of faults involving three variables or small faults, than the Bonferroni´s variant. The Holm´s, Hochberg´s and Hommel´s variants had the worst results in all the scenarios simulated.
- The step-down method with profile 1-1-1-1 and the Hawkins´method for faults in one single variable yielded the best results in the case of one single variable faults. The problem with these methods is that they cannot be used to diagnose faults in which there are more than one responsible variable.
- These results show that most of the compared methodologies have problems with false positives that have often not been reported in literature. Research is needed to introduce variants in these methods or improve the algorithms to reduce the impact of the *PWC* indices in the diagnosis performance of these methodologies and, consequently, improve their classification results. This is the goal of Chapter 5.

Appendix 4.1

Correlation Matrix Scenarios	Nº Standard Deviations									
	2.3	**2.31**	**2.32**	**2.33**	**2.34**	**2.35**	**2.36**	**2.37**	**2.38**	**2.39**
1	0.0824	0.0803	0.0783	0.0762	0.0744	0.0725	0.0706	0.0686	0.0668	0.0651
2	0.0722	0.0703	0.0685	0.0667	0.0651	0.0634	0.0618	0.0602	0.0587	0.0572
3	0.0813	0.0792	0.0772	0.0753	0.0734	0.0715	0.0696	0.0678	0.0659	0.0643
4	0.0716	0.0698	0.0682	0.0665	0.0649	0.0633	0.0617	0.0602	0.0585	0.057
5	0.0518	**0.0505**	0.0493	0.048	0.0469	0.0457	0.0446	0.0435	0.0425	0.0414
6	0.0772	0.0753	0.0734	0.0716	0.0697	0.068	0.0663	0.0646	0.0629	0.0613
7	0.0663	0.0646	0.063	0.0615	0.06	0.0585	0.0569	0.0554	0.054	0.0525
8	0.0754	0.0735	0.0718	0.0699	0.0682	0.0663	0.0647	0.063	0.0613	0.0596
9	0.0723	0.0707	0.069	0.0672	0.0656	0.0639	0.0623	0.0607	0.0592	0.0577
10	0.0752	0.0735	0.0717	0.07	0.0684	0.0667	0.0651	0.0633	0.0618	0.0602
11	0.0744	0.0726	0.0708	0.069	0.0673	0.0657	0.064	0.0624	0.0607	0.0592

Matriz Covar	Nº Standard Deviations									
	2.4	**2.41**	**2.42**	**2.43**	**2.44**	**2.45**	**2.46**	**2.47**	**2.48**	**2.49**
1	0.0634	0.0616	0.06	0.0584	0.0568	0.0554	0.0539	0.0524	0.051	**0.0496**
2	0.0557	0.0543	0.053	0.0516	**0.0503**	0.049	0.0477	0.0464	0.0451	0.0438
3	0.0626	0.0609	0.0592	0.0576	0.0561	0.0546	0.0532	0.0518	**0.0503**	0.0489
4	0.0555	0.0541	0.0527	0.0513	**0.0499**	0.0486	0.0472	0.0459	0.0447	0.0436
5	0.0403	0.0392	0.0382	0.0373	0.0364	0.0354	0.0345	0.0336	0.0329	0.032
6	0.0597	0.0582	0.0567	0.0553	0.0538	0.0524	0.0511	**0.0498**	0.0485	0.0472
7	0.0512	**0.0498**	0.0486	0.0473	0.0461	0.0448	0.0436	0.0425	0.0414	0.0402
8	0.0581	0.0565	0.0552	0.0537	0.0523	0.051	**0.0497**	0.0484	0.0471	0.0458
9	0.0562	0.0547	0.0533	0.0519	**0.0505**	0.0493	0.0479	0.0466	0.0453	0.044
10	0.0587	0.0573	0.0558	0.0544	0.0529	0.0515	**0.0502**	0.049	0.0478	0.0464
11	0.0576	0.0563	0.0548	0.0535	0.0521	**0.0506**	0.0491	0.0478	0.0466	0.0452

TABLE 4.4: Selection of the number of standard deviation (*nd*) to use in the construction of the UCL in Hawkins´ methodology in order to get an overall Type I risk, $\alpha_{overall}$ =0.05 in the 11 correlation matrix scenarios.
(The final selection is marked in bold font).

Appendix 4.2

Multifactor ANOVA

Dependent variable: PTCo
Factors:
Nf: Number of faults
M: Diagnostic Method
C: Correlation Structure

Analysis of Variance for PTCo - Type III Sums of Squares

Source	Sum of Squares	Df	Mean Square	F-Ratio	P-Value
MAIN EFFECTS					
A:Nf	39,8789	2	19,9395	242,13	0,0000
B:M	295,449	13	22,7268	275,98	0,0000
C:C	3,47592	10	0,347592	4,22	0,0000
INTERACTIONS					
AB	99,7702	26	3,83731	46,60	0,0000
AC	1,3626	20	0,0681298	0,83	0,6822
BC	48,0837	130	0,369874	4,49	0,0000
RESIDUAL	1276,93	15506	0,0823505		
TOTAL (CORRECTED)	2069,61	15707			

Analysis of Variance for PTCv - Type III Sums of Squares

Source	Sum of Squares	Df	Mean Square	F-Ratio	P-Value
MAIN EFFECTS					
A:Nf	6,61053	2	3,30527	42,84	0,0000
B:M	121,702	13	9,36166	121,33	0,0000
C:C	12,8711	10	1,28711	16,68	0,0000
INTERACTIONS					
AB	51,0124	26	1,96202	25,43	0,0000
AC	6,88896	20	0,344448	4,46	0,0000
BC	9,48221	130	0,0729401	0,95	0,6576
RESIDUAL	1196,38	15506	0,0771563		
TOTAL (CORRECTED)	1567,52	15707			

Analysis of Variance for PWCo - Type III Sums of Squares

Source	Sum of Squares	Df	Mean Square	F-Ratio	P-Value
MAIN EFFECTS					
A:Nf	3,36662	2	1,68331	51,63	0,0000
B:M	374,171	13	28,7824	882,80	0,0000
C:C	37,7596	10	3,77596	115,82	0,0000
INTERACTIONS					
AB	13,952	26	0,536615	16,46	0,0000
AC	6,33112	20	0,316556	9,71	0,0000
BC	120,106	130	0,923893	28,34	0,0000
RESIDUAL	505,548	15506	0,0326034		
TOTAL (CORRECTED)	1267,47	15707			

All F-ratios are based on the residual mean square error.

Analysis of Variance for PWCv - Type III Sums of Squares

Source	Sum of Squares	Df	Mean Square	F-Ratio	P-Value
MAIN EFFECTS					
A:Nf	12,258	2	6,12902	244,17	0,0000
B:M	241,267	13	18,559	739,35	0,0000
C:C	28,0647	10	2,80647	111,80	0,0000
INTERACTIONS					
AB	15,9675	26	0,614133	24,47	0,0000
AC	5,58864	20	0,279432	11,13	0,0000
BC	92,0882	130	0,708371	28,22	0,0000
RESIDUAL	389,228	15506	0,0251017		
TOTAL (CORRECTED)	948,837	15707			

All F-ratios are based on the residual mean square error.

Analysis of Variance for PND - Type III Sums of Squares

Source	Sum of Squares	Df	Mean Square	F-Ratio	P-Value
MAIN EFFECTS					
A:Nf	25.2997	2	12.6498	255.52	0.0000
B:M	12.3138	13	0.947218	19.13	0.0000
C:C	37.8173	10	3.78173	76.39	0.0000
INTERACTIONS					
AB	0.816611	26	0.0314081	0.63	0.9234
AC	9.03737	20	0.451868	9.13	0.0000
BC	4.76283	130	0.0366372	0.74	0.9881
RESIDUAL	767.65	15506	0.0495067		
TOTAL (CORRECTED)	873.571	15707			

All F-ratios are based on the residual mean square error.

Analysis of Variance for PNF - Type III Sums of Squares

Source	Sum of Squares	Df	Mean Square	F-Ratio	P-Value
MAIN EFFECTS					
A:Nf	0.23255	2	0.116275	27.12	0.0000
B:M	9.65712	13	0.742855	173.25	0.0000
C:C	2.03821	10	0.203821	47.53	0.0000
INTERACTIONS					
AB	0.36364	26	0.0139862	3.26	0.0000
AC	0.208887	20	0.0104443	2.44	0.0003
BC	4.35935	130	0.0335334	7.82	0.0000
RESIDUAL	66.4869	15506	0.00428782		
TOTAL (CORRECTED)	86.7313	15707			

All F-ratios are based on the residual mean square error.

Chapter 5: New proposed variants for MSQC fault diagnosis

As it was stated in Chapter 4, some methods for fault diagnosis employed in MSQC suffer from a high false positives rate in scenarios of strong correlations among variables, degrading their classification performance. In this chapter we propose some new variants to improve the diagnosis performance of these methods through the reduction of the number of false positives in Mason, Tracy and Young´s, Hawkins´, Murphy´s and Runger and Montgomery´s algorithms.

5.1 Variants of the Mason Tracy and Young Method (MTY)

Mason *et al.* (1995,1997) (Section 3.2.8) describe in their methodology that in the interpretation of new observations in which a conditional component, *i.e.* a pair-wise variables term, such as $T_{j|k}$ where $j \neq k$, becomes significant, it is concluded that the relationship between both variables x_j and x_k in the new observation is different to the relationship observed in the reference data set. Therefore, the two variables are suspected to be responsible of the detected problem as there is no reason to consider one of them more suspicious than the other.

In our opinion in scenarios with a certain number of variables involved, the last recommendation could lead to high false positive rates. For instance, if we are monitoring several observation variables and there is a problem in the process or a sensor that cause a change in the mean of only one single variable, the size of the change may not be large enough to cause the unconditional terms to be significant but many correlations of this variable with the others may be affected. Under this situation in the diagnosis there will be a *dominant variable* appearing in most of the significant conditional terms. In this case this variable must be considered the responsible for the fault and not the others.

According to this we are going to propose two variants of the MTY´s algorithm.

5.1.1 Variant 1: MTY1

The first variant of the algorithm proposes that when a dominant variable is detected it will be withdrawn from the set and considered as one of the responsible variables of the detected change. Then, the algorithm continues checking if the Hotelling´s T^2 statistic calculated on the remaining set of variables is significant.

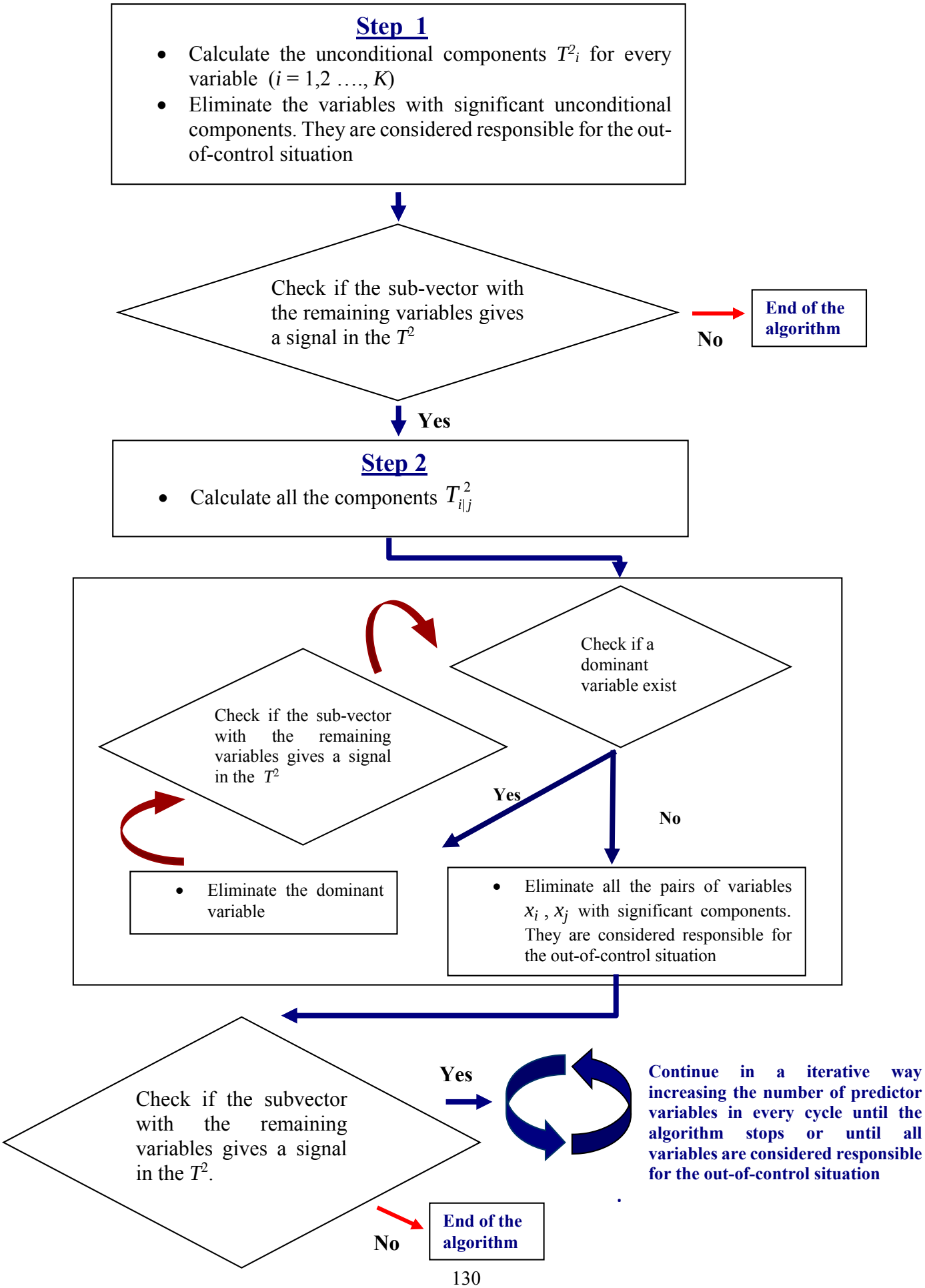
Step 1
Calculate the unconditional components T^2_i for every variable ($i = 1,2 \ldots, K$)
Eliminate the variables with significant unconditional components. They are considered responsible for the out-of-control situation
Check if the sub-vector with the remaining variables gives a signal in the T^2
No
End of the algorithm
Yes
Step 2
Calculate all the components $T^2_{i|j}$
Check if a dominant variable exist
Check if the sub-vector with the remaining variables gives a signal in the T^2
Yes
No
Eliminate the dominant variable
Eliminate all the pairs of variables x_i , x_j with significant components. They are considered responsible for the out-of-control situation
Check if the subvector with the remaining variables gives a signal in the T^2.
Yes
Continue in a iterative way increasing the number of predictor variables in every cycle until the algorithm stops or until all variables are considered responsible for the out-of-control situation
No
End of the algorithm

The procedure to be considered a dominant variable is as follows. Firstly, it is computed the number of times, *h*, the different variables appear in the significant conditional terms for each loop of the algorithm. Secondly, the variables are ranged according to this number *h*. Thirdly, the ratio between the two more frequent variables $h_{\text{first}}/h_{\text{second}}$ is worked out. Fourthly, if this ratio is larger than a threshold, the first variable is considered as a dominant variable. In our simulations we have used three threshold values 1.5, 2 and 3, to study the performance of the proposed variant. The larger is the selected threshold the higher is the resemblance of the proposed variant to the original *Mason et al´s* algorithm. The proposed algorithm is presented in detail as follows:

5.1.2 Variant 2: MTY2

In this variant, after computing the different significant conditional terms for the current loop of the algorithm, they are sorted by magnitude from the largest significant term to the smallest, selecting the variables in each term as suspicious if the term does not include any variable that has been already considered suspicious.

An example of how this variant will proceed to select the suspicious variables in a case with three significant terms in conditional terms with two variables follows: $T_{1|2} = 18.2$, $T_{2|3} = 10.5$ and $T_{4|5} = 9.5$, then variables x_1 and x_2 become suspicious because the most significant conditional term in the second loop includes these two variables. The significant conditional term $T_{2|3}$ depends on the variables x_2 and x_3. But in this case, given that the variable x_2 has already been considered as responsible in a previous term it is assumed that is x_2 which account for most of this significant conditional term and not x_3. The last significant term $T_{4|5}$ depends on the variables x_4 and x_5. As these

variables are not already considered suspicious in the previous significant terms, then the variables x_4 and x_5 are both considered as suspicious.

5.2 Variants of the Hawkins´ method (HM)

As commented in Section 3.2.6 the detection and diagnosis in Hawkins' methodology is based on the residual vector $\hat{\mathbf{z}}$, whose k^{th} component is the standardized residual when the k^{th} variable is regressed onto all the other variables of **x**.

When applying a univariate shewhart chart scheme for monitoring the individual K residuals, the overall Type I risk is overestimated as a consequence of the presence of correlation among the scaled residuals. So it makes necessary to adjust the Type I risk according to the actual correlation structure with an appropriate selection of the number of standard deviations (*nd*) when calculating the upper control limits of the monitoring charts. In section 3.2.6 a variant of Hawkins´ methodology to detect faults which affect one single variable (Hawkins' one single variable method) was considered. In this variant, the algorithm identifies as responsible the variable with the largest significant residual $\hat{z}_k$.

In order to reduce the false positives rate three new variants of Hawkins´ algorithm are proposed. Our reasoning to consider these variants are going to improve the performance of the Hawkins´ algorithm is based on the fact that all the computed Hawkins residuals $\hat{z}_k$ are affected by all the variables whose mean changes. The only way to reduce the effect in the regressions is the recursive extraction of the suspected variables. For instance, if there is a mean shift only in the variable x_1, z_1 is probably going to be

significant but also the other residuals $\hat{z}_k$ for other variables x_k that are obtained with x_1 acting as an outlier regressor.

5.2.1 Variant 1: Recursive Hawkins´ methodology (RH)

In this variant, Hawkins´ methodology is applied recursively, extracting one single variable as responsible in each loop. To extract a second suspected variable, the algorithm proceeds to compute again the $\hat{z}_k$ residuals from the remaining variables checking for their significance. The algorithm proceeds in recursive loops until the observation in the remaining variables does not cause signal in the monitoring statistics. In the case of a mean shift in e.g. x_1, the z_1 residual corresponding to variable x_1, which is the largest residual, is isolated and, then, when the Hawkins´ methodology is applied in a second loop all the regressions to compute the different residuals, where x_1 is now excluded, are going to fit well and no large residuals are going to be expected. This algorithm is expected to perform better than the original Hawkins proposal not only for one variable fault but for faults which include more variables.

5.2.2 Variant 2: Pre-Filtered Recursive Hawkins´ methodology (FRH)

When the number of variables involved in the fault increases, the impact in the regression residuals may be important and a way to reduce this impact is pre-filtering the most suspected variables before applying Hawkins´ methodology. Our proposal is to filter out those variables having significant unconditional terms from Mason *et al´s* procedure. These variables with values out of the normal operational range act as gross outliers in Hawkin´s regressors and affect the results notably.

The first step is the computation of the unconditional terms of Mason *et al´s* method and the selection of the variables which are out of their normal operational region as suspicious of being responsible of the fault. Once the suspicious variables are filtered out, the method applies Hawkins´ methodology in a recursive way to sequentially extract the variables. As shown in Section 3.2.8.1 and Appendix 3.8, Hawkins´ $\hat{z}_k$ residuals are equivalent to the square root of the higher order conditional terms of Mason *et al´s* methodology ($T^2_{k|1\ldots k\text{-}1,k+1\ldots K}$) and, therefore, applying Hawkins´ method in a recursive way is similar to compute the different conditional terms of Mason *et al´s* method. The difference is that in our proposal these terms are calculated from the larger order terms to the lower order terms (backward strategy) while Mason *et al´s* algorithm proceeds from lower order to larger order terms (forward strategy). We consider the backward strategy is more appropriate because in determining whether a variable is or not responsible for the fault it uses the information contained in the relation with all the remaining variables.

5.2.3 Variant 3: Hawkins´ variants with a Hotelling´s T^2 detection trigger mechanism

Hawkins´ methodology and the proposed variants RH and FRH need to be adjusted to a fixed Type I risk. In this third variant a Hotelling T^2 statistic is used to detect the out-of control and can be easily adjusted to the required Type I risk based on the assumed in-control Hotelling T^2 known distribution, yielding:

- **Variant 3.1** T^2-Recursive Hawkins (T2RH)
- **Variant 3.2** T^2-Pre-Filtered Recursive Hawkins (T2FRH)

In these variants the number of standard deviations (*nd*) to consider as threshold for the different $\hat{z}_k$ residuals tests is an adjustment parameter. In a first approach, for variant 3.2 we will use the Bonferroni approach considering two times the number of variables as the number of tests to consider. Also we will study the effect of changing the value of this parameter on the diagnosis performance. Additionally, when diagnosing the case of one variable faults they will be compared to Hawkins' one single variable method. In this methodology the variable detected by the algorithm as responsible is the one with the largest significant $\hat{z}_k$ residual so that this method can only be applied to diagnose one variable faults.

5.3 Variants of the Montgomery and Runger´s method

Four variants of the Montgomery and Runger´s algorithm (MR) are proposed

5.3.1 Variant 1: Recursive Montgomery and Runger´s methodology (RM)

When the Hotelling´s T^2 decomposition in Rencher (1993) is applied starting by the *k*-th variable, it follows that

$$T^2 = T^2_{(K-1)} + T^2_{k|1,2,..k\text{-}1..k+1..K} \tag{5.1}$$

where $T^2_{(K-1)}$ is the Hotelling´s T^2 statistic on the *K*-1 variables excluding in this particular case the *k*-th variable. Writing $T^2_{k_1} = T^2_{(K-1)}$ and from Equation 3.12 it follows:

$$T^2_{k|1,2,...k\text{-}1...k+1...K} = T^2 - T^2_{(K-1)} = T^2 - T^2_{k_1} = c^2_k = D_k = \hat{z}^2_k \tag{5.2}$$

According to this expression, the *D* statistics are equivalent to the conditional terms of maximum order of Mason *et al´s* methodology. These conditional terms are the squared residuals when each one of the *K* variables are regressed onto the remaining *K-1* variables

(see Appendix 3.8). All the statistics distances D_k are affected when one single mean changes as it happened in Hawkins´s methodology. A way to solve this problem is applying Montgomery´s methodology in a recursive way, eliminitating one significant single variable per cycle.

5.3.2 Variant 2: Montgomery and Runger´s method under a sequential extraction methodology (MUSE)

The statistics distances D_k are computed only one time and ranged from the smallest to the largest, then the suspected variables are extracted sequentially. After the selection of the first suspected variable it is checked whether the Hotelling´s T^2 for the remaining K-1 variables is significant or not. If it is significant the algorithm proceeds to extract a second suspected variable, otherwise the algorithm ends.

5.3.3 Variant 3: Pre-filtered recursive Montgomery and Runger´s methodology (FRM)

The first step is the computation of the unconditional terms of the Mason *et al´s* method and the selection of the variables which are out of their normal operational region as suspicious of being responsible of the fault. Once the suspicious variables are filtered out, the method applies the recursive Montgomery methodology (RM)

5.3.4 Variant 4: Pre-filtered Montgomery and Runger´s method under a sequential extraction methodology (FMUSE)

Once the suspicious variables according to the unconditional Mason *et al´s* terms are filtered out, the method applies the Montgomery´s method under a sequential extraction methodology.

5.4 Variants of the Murphy´s method

Two variants of the Murphy´s algorithm (M) are proposed.

5.4.1 Variant 1: T2-Hotelling Murphy´s methodology (T2M)

In this variant, the decision to proceed to the next loop is not based on the distribution of the statistic D_k. For each loop, it is checked whether the subvector with the remaining variables gives a signal in the Hotelling T^2 statistic or not.

5.4.2 Variant 2: Pre-filtered T2-Murphy´s methodology (FT2M)

In this method the Variant 1 of Murphy´s algorithm is applied after filtering out those variables having significant unconditional terms for Mason *et al´s* procedure.

Chapter 6: Diagnosis performance in MSQC (II)

In this chapter we proceed to compare the diagnosis performance of the new variants for Mason, Tracy and Young´s, Hawkins´, Murphy´s and Montgomery´and Runger´s algorithms proposed in Chapter 5. The methods are tested in a simulation procedure for 7 measured variables. A wide variety of different types of fault with different correlation structures have been considered. Finally the improved methods were used in the pasteurization process data set.

6.1 Simulation procedure for 7 Variables

6.1.1 Simulation data generation

In order to compare the new variants of the methods proposed in Chapter 5, we use a simulation for 7 variables in which the performance of these methods is measured for different types of faults and different correlation scenarios in the same way as we did in section 4.1 for a four variables simulation case. In this simulation, the different methodologies are applied under ten different correlation structures shown in Table 6.1 where the covariance matrix condition numbers tend to increase its value from C1 to C10. The standard deviations of the seven variables were uniformly distributed between 0.3 and 0.4. Scenarios leading to unfeasible covariance matrices were discarded. Reference data sets of 50.000 observations for each of the 10 covariance structures were obtained using the algorithm proposed by Arteaga and Ferrer (2010). These reference data sets were used to adjust the Type I risk when the methodologies under comparison used a different detection trigger mechanism in the detection of the out-of-control observations (Hawkins´ method and its variants). For every correlation structure 102 different types of faults were considered. The faults consisted in mean shifts in one, two or three variables. The size of the shifts were small (1.25 to 1.66 standard deviations), medium (2.5 to 3.33 standard deviations) or large (5 to 6.6 standard deviations). The shifts involving several means happened in both the same or opposite directions. For each type of fault, 500 observations using the algorithm proposed by Arteaga and Ferrer (2010) were simulated.

TABLE 6.1 Correlation structures.

Correlation Structure	Correlation Values	Extreme Correlations (0.9)	Condition Number $\frac{\lambda_{max}}{\lambda_{min}}$
C1: Weak correlations	Weak correlation coefficients uniform distributed, U[-0.1 , +0.1]	No	1.94
C2: Moderate positive correlations	Moderate positive correlation coefficients uniformly distributed, U[+0.1 , +0.4]	No	5.25
C3: Moderate negative correlations	Moderate negative correlation coefficients uniformly distributed, U[-0.1 , -0.3]	No	68.66
C4: Moderate mixed correlations	Moderate positive correlations mixed with three negative correlations Absolute correlation coefficients uniformly distributed, U[+0.1 , +0.4]	No	12.71
C5: Weak correlations with one extreme correlation	Weak correlation coefficients uniformly distributed, U[-0.1 , +0.1] with one coefficient +0.9	Yes	22.11
C6: Moderate positive correlations with one extreme correlation	Moderate positive correlation coefficients uniformly distributed, U[+0.1 , +0.4] with one coefficient +0.9	Yes	43.02
C7: Moderate mixed correlations with one extreme correlation	Moderate positive correlations mixed with three negative correlations. Absolute correlation coefficients uniformly distributed, U[+0.1 , +0.4] with one coefficient +0.9	Yes	2026.7
C8: Strong positive correlations	Strong positive correlation coefficients uniformly distributed, U[+0.5 , +0.8]	No	40.91
C9: Strong positive correlations with one extreme correlation	Strong positive correlation coefficients uniformly distributed, U[+0.5 , +0.8] with one coefficient +0.9	Yes	1244.1
C10: Strong mixed Correlations	Positive correlations coefficients uniformly distributed U [+0.3 +0.6] mixed with two negative correlations	No	542.29

6.1.2 Performance indices

These faulty data sets were processed under the different proposed fault diagnosis methodologies and their performance were measured and compared according to the indices described in Section 4.1.2: PTC_0, $PTCv$, PWC_0, $PWCv$, PND and PNF. In this section three additional new combined indices which try to measure the overall classification performance will be introduced:

- *TCI* (True Classification Index): which takes into account the joint results in PTC_0 and PTC_v and gives them an equal weight according to the following expression:

$$TCI = (PTC_0 + PTC_v)/2 \quad (6.1)$$

- *WCI* (Wrong Classification Index): which takes into account the joint results in PWC_0 and PWC_v and gives them an equal weight according to the following expression:

$$WCI = (PWC_0 + PWC_v)/2 \quad (6.2)$$

- *GCI* (Global Classification Index): which takes into account the joint results in PTC_0, PTC_v, PWC_0 and PWC_v and gives them an equal weight according to the following expression:

$$GCI = \left[(PTC_0 + PTC_v) - (PWC_0 + PWC_v)\right]/2 = TCI - WCI \quad (6.3)$$

6.1.3 Type I risk considerations

Among all the tested methods, only the Hawkins´ methodology and our proposed variants on this method require a Type I risk adjustment. The others methodologies and proposed variants use the Hotelling´s T^2 statistic in the detection step which follows an in-control known distribution. In order to check the accuracy and precision of the adjusted Type I risk for the 10 covariance matrices under different detection trigger mechanisms, 10 reference data sets under each correlation matrix were simulated and the real Type I risk for each data set were computed. In the methodologies based on the Hotelling´s T^2 the real Type I risk is centered in the desired value as it was expected since the Type I risk level is adjusted from a theoretical distribution that takes into account the correlations between variables.

In the Hawkins´ methodology it is assumed that the monitored residuals follow a unit variance normal distribution. The overall Type I risk depends on the number of hypotheses tests and the Type I risk α of each of the individual hypothesis tests. In the

case of seven variables the overall Type I risk for the recursive Hawkins´ methodology (RH) is $1-(1-\alpha)^7$. For a desired overall rate of $\alpha_{\text{overall}} = 0.05$, the $\alpha = 1-(1-\alpha_{\text{overall}})^{1/7} = 0.0073$ and the number of standard deviations to consider for a two-tale hypothesis test is 2.685 σ. The pre-filtered recursive Hawkins´ methodology (FRH) performs 7 hypotheses tests in the pre-filter step and 7 hypotheses tests in the first loop of the recursive procedure. The overall Type I risk for FRH is $1-(1-\alpha)^{14} = 0.05$. For a desired overall rate of $\alpha_{\text{overall}} = 0.05$, the $\alpha = 1-(1-\alpha_{\text{overall}})^{1/14} = 0.0036571$ so the number of standard deviations to consider for a two-tale hypothesis test is 2.92σ. In both cases it is necessary to adjust the Type I risk according to the selected correlation matrix because the Type I risk may be underestimated and these values of 2.685σ and 2.92σ can be considered a first tentative approach. In order to select the best number of standard deviation (*nd*) in every correlation scenario, the Type I risk corresponding to different *nd* selections in the neighborhood of the first tentative approach were calculated in Appendix 6.6 (Tables 1 and 2) and the best values for *nd* are shown in Table 6.2 and Table 6.3.

TABLE 6.2: Selected number of standard deviations (*nd*) to use in the construction of the UCL in Hawkins' methodology and its Variant 1 for an overall Type I risk ($\alpha_{\text{overall}} = 0.05$) in the 10 correlation matrix scenarios

C	**1**	**2**	**3**	**4**	**5**	**6**	**7**	**8**	**9**	**10**
nd	2.68	2.68	2.36	2.65	2.66	2.64	2.38	2.66	2.50	2.39

TABLE 6.3: Selected number of standard deviations (*nd*) to Use in the Construction of the UCL in the Variant 2 of the Hawkins' methodology for a prefixed Type I risk ($\alpha_{\text{overall}} = 0.05$) in the 10 correlation matrix scenarios

C	**1**	**2**	**3**	**4**	**5**	**6**	**7**	**8**	**9**	**10**
nd	2.74	2.81	2.79	2.84	2.77	2.81	2.77	2.83	2.75	2.77

As a final verification, the Type I risk corresponding to these *n* selections was computed on new 10 test data sets for the corresponding 10 correlation matrix scenarios**.** Figure 6.1 shows that after the adjustment the objective of overall Type I risk of 5% is accomplished for the proposed variants of the Hawkins´ methodology.

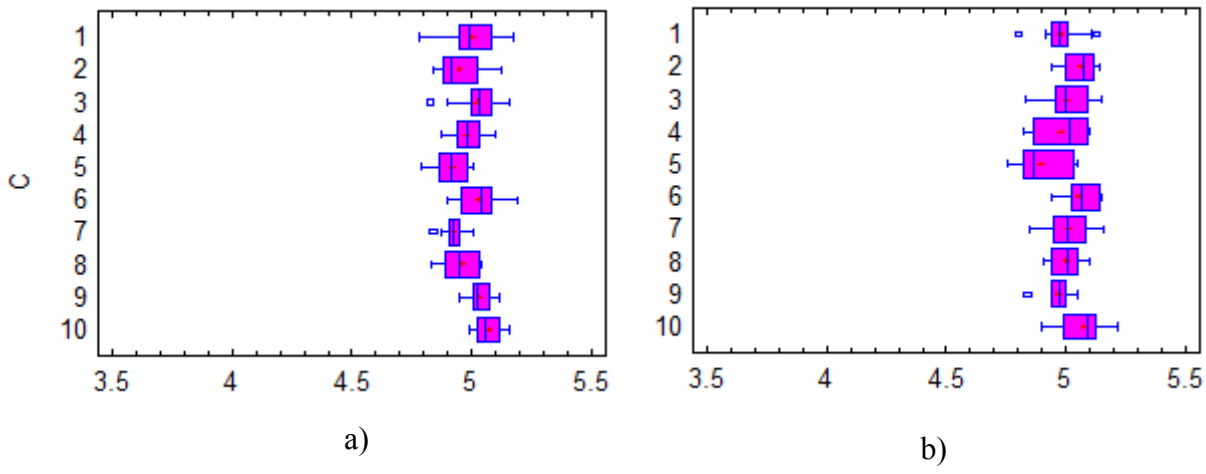

FIGURE 6.1: Type I risk ($\alpha_{overall} \times 100$) in the different correlation scenarios

a) Adjusted Recursive Hawkins´ Methodology (RH)
b) Adjusted Prefiltered Recursive Hawkins´ Methodology (FRH)

6.2 Fault diagnosis performance comparison

In order to study the performance of the proposed methodologies and variants under different correlation scenarios a multifactor analysis of variance (ANOVA) is carried out. Firstly, the original algorithms will be compared with the new proposed variants according to the PTC_0, PTC_v, PWC_0, PWC_v, *PND* and *PNF* indexes defined in section 4.1.2. Then, to conclude, a final ANOVA study is used to compare the best variants of each methodology

6.2.1 MTY´s Methodology

6.2.1.1 Significance level for the decomposition terms

In this methodology we have considered an overall type I risk α =5% for fault detection. But once a fault has been detected, it is necessary to select an appropriate significance level (α_{terms}) for the Hotelling´s T^2 decomposition terms. The analysis of variance (ANOVA) was performed considering the factors: α_{terms} (1% 5% and 10%); correlation structure, C (10 levels, see Table 6.1); number of faulty variables, N_f (3 levels: 1, 2 and 3 faulty variables) ; and size of the fault (3 levels: small, medium or large faults). The ANOVA results (see Appendix 6.1) show that all the factors and most of their interactions are statistically significant (p-value< 0.05) for all the performance indices.

Figure 6.2 shows the results on PTC_0, PTC_v, PWC_0, PWC_v, PND and PNF when applying α_{terms} = 1%, 5% and 10%. It shows that a change in the significance level for the Hotelling´s T^2 decomposition terms affects the MTY final classification results in all the indices. In PTC_0, using α_{terms} equal to 1% and 5% perform better than using a 10% and that in high correlation scenarios (C8 to C10) a 5% gives the best results. These results are consistent with the high PWC_0 obtained with α_{terms} equal to 10%. In PTC_v, the results with α_{terms} equal to 5% are close to the ones obtained with a 10% proving superior to the results with a 1%. Figure 6.2 also shows that there are situations of lack of power in the diagnosis (PNF) when α_{terms} is equal to 1%.

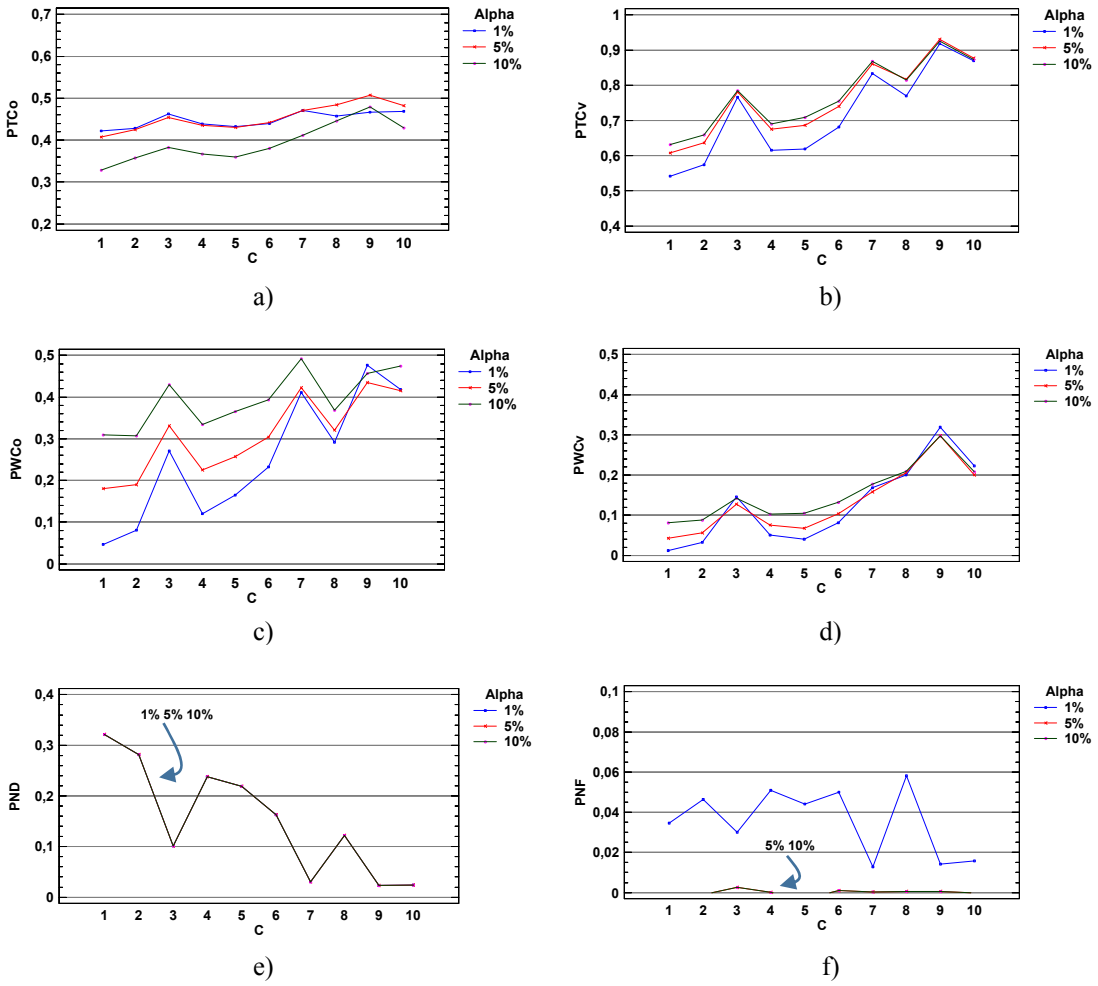

FIGURE 6.2: Interaction α_{terms} (α_1=0.01; α_2=0.05; α_3=0.10)× covariance structure for MTY´s Methodology
a) PTC_0, b) PTC_v, c) PWC_0, d) PWC_v, e) *PND* and f) *PNF*

Figure 6.3 shows that α_{terms} equal to 5% gives the best results in PTC_0, stay close to the results for PTC_v with α_{terms} equal to 10% and does not present problems of lack of power for 2 and 3 variables faults.

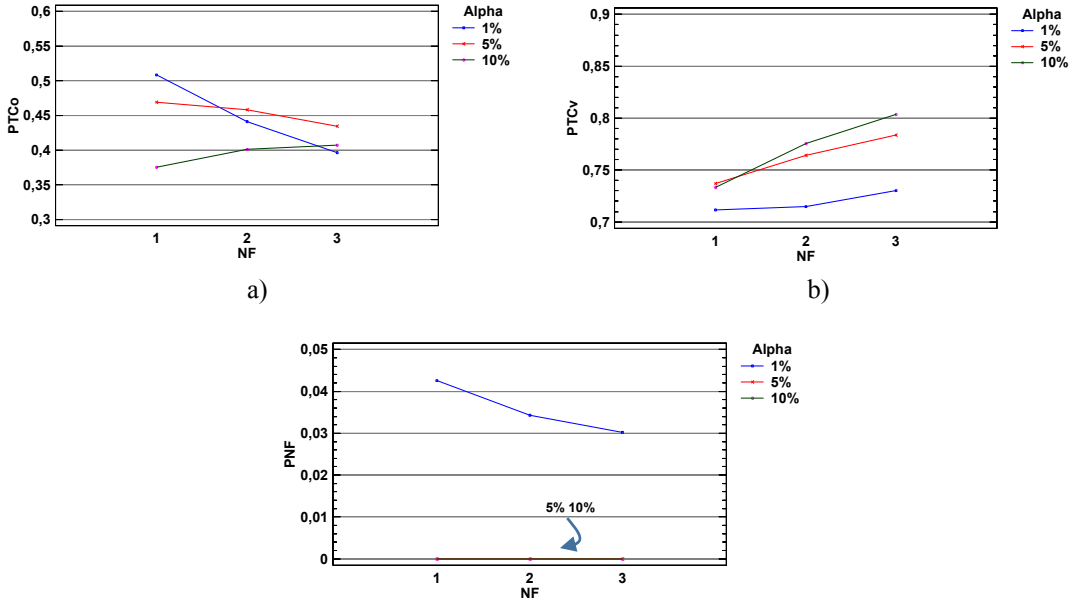

FIGURE 6.3: Interaction α_{terms} (α_1=0.01; α_2=0.05; α_3=0.10) × NF (Number of faulty variables) for MTY´s Methodology
a) PTC_0, b) PTC_v and c) PNF_z

Figure 6.4 shows that problems of lack of power is specially related to small-sized faults and α_{terms} equal to 1%. it also shows that performance in PTC_0 and PTC_v improves with the size of the fault.

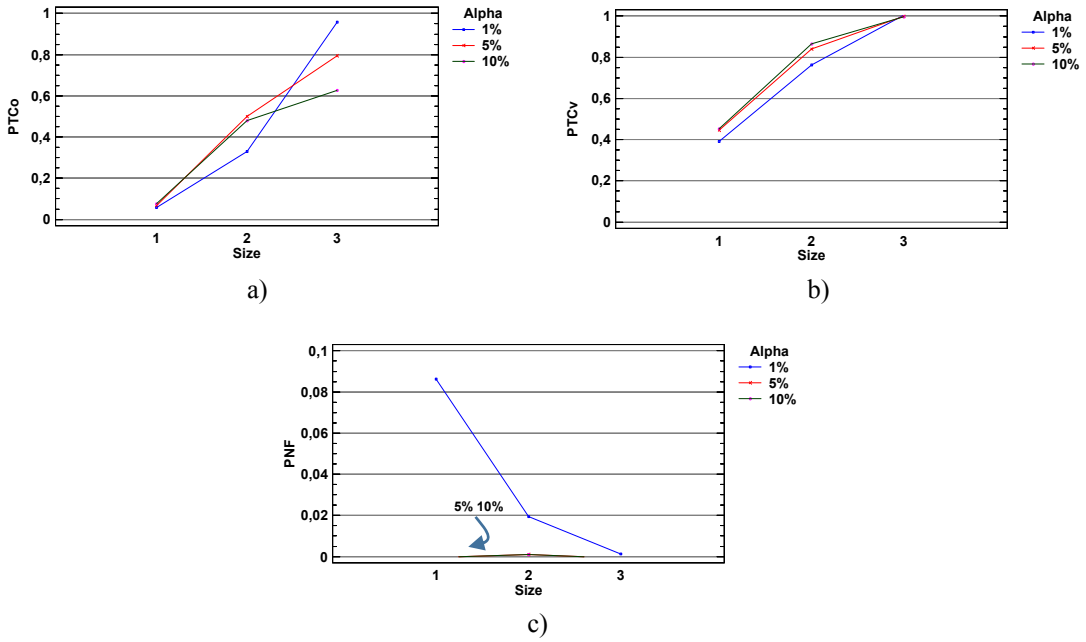

FIGURE 6.4: Interaction α_{terms} (α_1=0.01; α_2=0.05; α_3=0.10) × Size of fault (1-Small; 2-Medium; 3-Large) for MTY´s Methodology. a) PTC_0, b) PTC_v and c) PNF_z

The interaction plots for the combined indices in Figure 6.5 shows that the *TCI* achieves best results for α_{terms} equal to 5%, the *WCI* achieves best results for α_{terms} equal to 1% except for C9 and C10 where the best results were obtained for α_{terms} = 5%. The global index *GCI* gives the best results for α_{terms} equal to 1% for C1 to C6 and for α_{terms} equal to 5%. for the strongest correlations scenarios C7 to C10. The global index also presents the best results in 2 and 3 variables faults for α_{terms} equal to 5%.

According to all these results it can be concluded that in our simulation a significance level in the decomposition terms α_{terms} equal to 5% gives overall good classification performance.

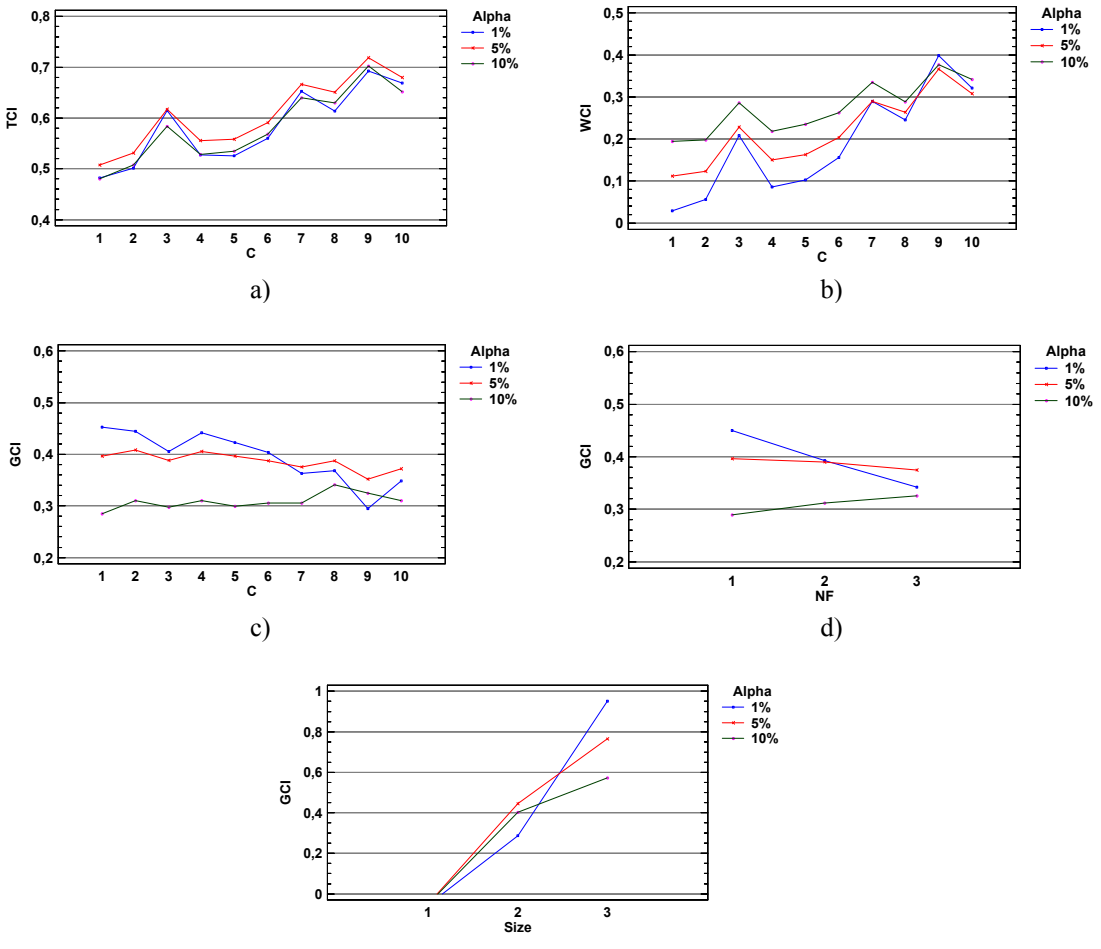

FIGURE 6.5: Interaction plots for the combined indices *TCI*, *WCI* and *GCI* in MTY´s Methodology
α_{terms} (α_1=0.01; α_2=0.05; α_3=0.10) × covariance structure ⇒ a) *TCI* , b) *WCI* , c) *GCI*
α_{terms} (α_1=0.01; α_2=0.05; α_3=0.10) × NF (Number of faulty variables) ⇒ d) *GCI*
α_{terms} (α_1=0.01; α_2=0.05; α_3=0.10) × Size of fault (1-Small; 2-Medium; 3-Large) ⇒ e) *GCI*

6.2.1.2 MTY´s variants performance

In the MTY1 (Variant 1 of the MTY´s algorithm explained in section 5.1.1) three different ratio h_{first}/h_{second} values for the condition of dominant variable: 1.5, 2 or 3 have been considered. The analysis of variance (ANOVA) was performed considering the factors: Method (4 levels: MTY, MTY1 h_{first}/h_{second} = 1%, 5% and 10%); correlation structure, C (10 levels, see Table 6.1); number of faulty variables, N_f (3 levels: 1, 2 and 3 faulty variables); and size of the fault (3 levels: small, medium or large faults). The ANOVA results (see Appendix 6.1) show that all the factors and most of their interactions are statistically significant (p-value< 0.05) for all the performance indices.

Figure 6.6 shows that the MTY1 outperforms the classification results yielded by the original MTY´s algorithm in the high correlation scenarios (C8 to C10). The good classification results were mainly a consequence of the improvement in the PTC_0 , PWC_0 and PWC_v indices. For C1 to C7 correlation scenarios, the results were only slightly better for the MTY1 than in the original MTY´s algorithm. Figure 6.6 also shows that the number of variables involved in the faults and the size of the fault have a similar effect in all these methods, and that the best classification results in our simulation were obtained with a ratio h_{first}/h_{second} equal to 1.5.

Figure 6.7 shows that the MTY2 (Variant 2 of the MTY´s algorithm explained in section 6.1.2) yields similar results in PTC_0 and PTC_v than the original MTY algorithm. The MTY2 reduces the PWC_0 and PWC_v indices in high correlation scenarios (C8-C10) but this improvement is not transferred to the PTC_0 index which stays close to the values of the original MTY. In other words, the method is successful in reducing the number of false positive variables but this reduction is not enough to increase the number of correctly diagnosed observations. Consequently, it can be concluded that the MTY1 outperforms the results yielded by the MTY2.

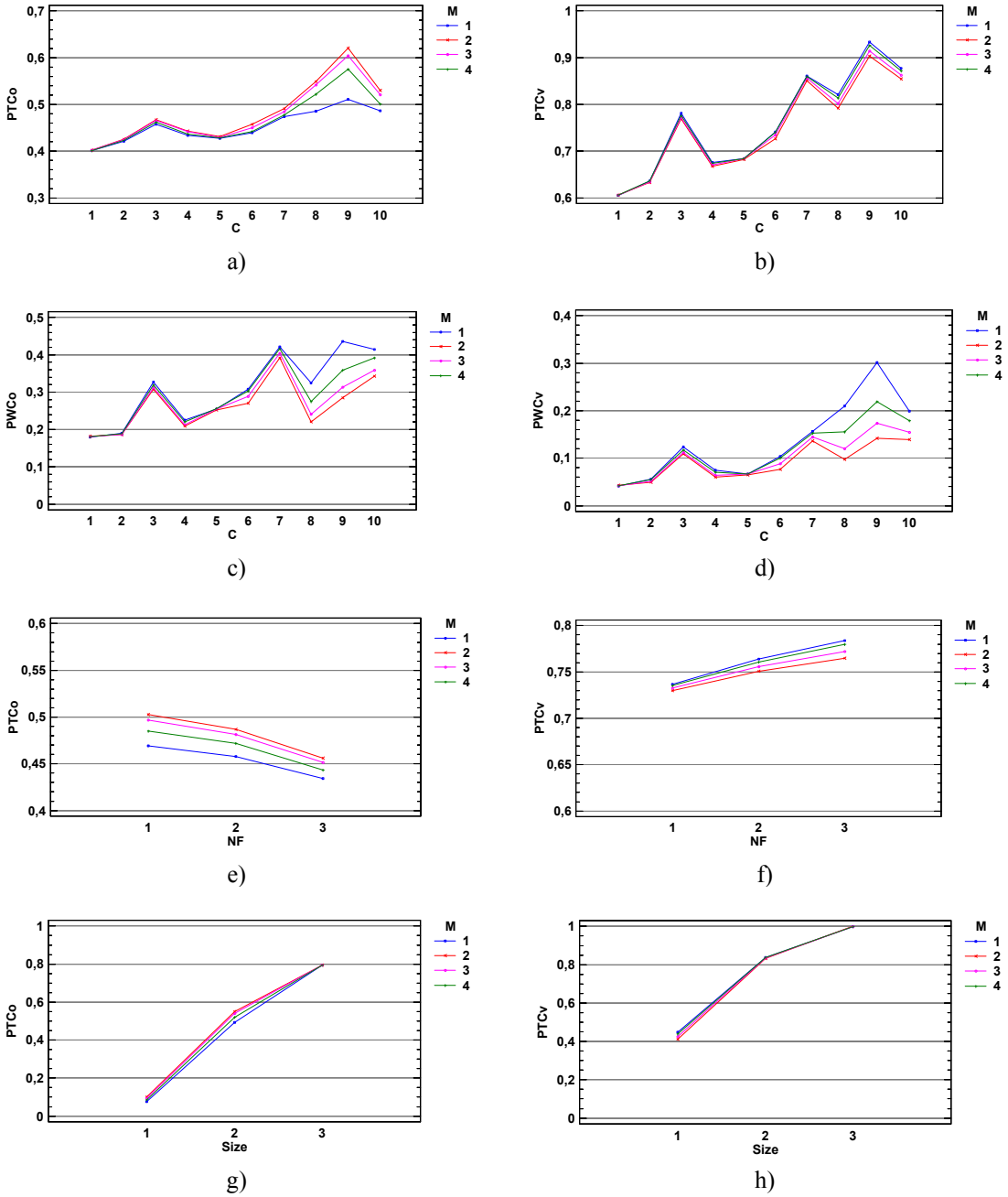

FIGURE 6.6: Interaction plot covariance × method ; NF × method; size × method with α=5% α_{terms} = 5%
Methods: M1: MTY; M2: MTY1 h_{first}/h_{second}=1.5; M3: MTY1 h_{first}/h_{second}=2; M4: MTY1 h_{first}/h_{second}=3
Method × covariance structure ⇒ a) PTC_0 , b) PTC_v , c) PWC_0 and d) PWC_v
Method × NF (Number of faulty variables) ⇒ e) PTC_0 and f) PTC_v
Method × size of fault (1-Small; 2-Medium; 3-Large) ⇒ g) PTC_0 and h) PTC_v

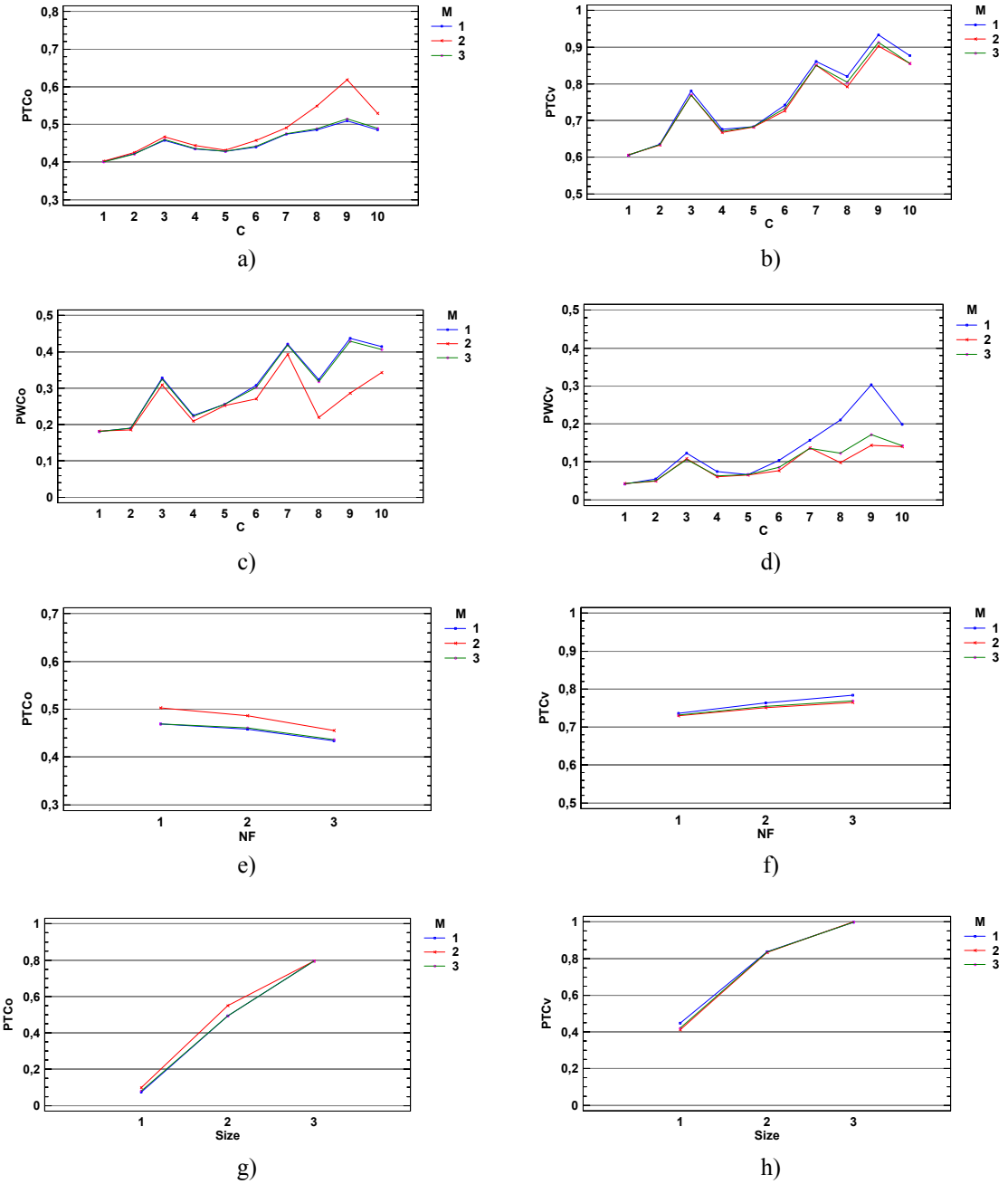

FIGURE 6.7: Interaction plot covariance × method ; NF × method; size × method with α=5% α_{terms} = 5%
Methods: M1: MTY; M2: MTY1 h_{first}/h_{second}=1.5; M3: MTY2
Method × covariance structure ⇒ a) PTC_0 , b) PTC_v , c) PWC_0 and d) PWC_v
Method × NF (Number of faulty variables) ⇒ e) PTC_0 and f) PTC_v
Method × size of fault (1-Small; 2-Medium; 3-Large) ⇒ g) PTC_0 and h) PTC_v

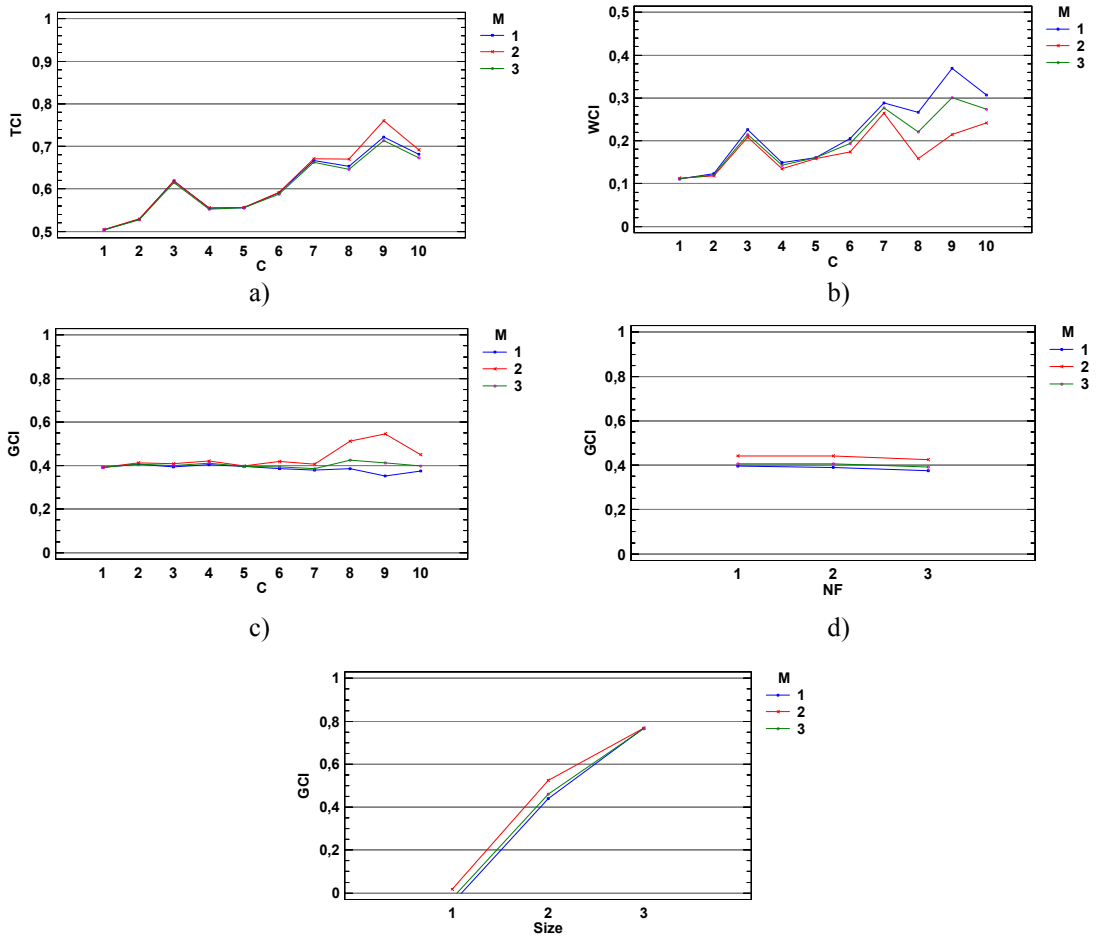

FIGURE 6.8: Interaction plots for the combined indices *TCI*, *WCI* and *GCI* in MTY´s Methodology
Methods: M1: MTY; M2: MTY1 h_{first}/h_{second}=1.5; M3: MTY2
Method × covariance structure ⇒ a) *TCI*, b) *WCI* and c) *GCI*
Method × NF (Number of faulty variables)) ⇒ d) *GCI*
Method × size of fault (1-Small; 2-Medium; 3-Large) ⇒ e) *GCI*

The combined indices confirm these results. Figure 6.8 shows that MTY1 performs better in *TCI* (large values) and *WCI* (small values) than methods MTY and MTY2 in scenarios with high correlations (C8 to C10). In relation to the number of variables involved in the fault, the MTY1 gives better results in *GCI* for 1, 2 or 3 variables faults. The MTY1 also has better results in small and medium-sized faults than the others. For large-sized faults the performance is similar in the three methods.

The above results let us to conclude that in our simulation the MTY1 outperforms the other methods (MTY, and MTY2) specially due to a better performance in high correlation scenarios.

6.2.2 Hawkins´ methodology

6.2.2.1 FRH and RH variants performance

An analysis of variance (ANOVA) was performed considering the factors: Method (4 levels: Hawkins, HSVM, RH and FRH); correlation structure, C (10 levels, see Table 6.1); number of faulty variables, N_f (3 levels: 1, 2 and 3 faulty variables); and size of the fault (3 levels: small, medium or large faults). The ANOVA results (see Appendix 6.2) show that all the factors and most of their interactions are statistically significant (p-value< 0.05) for all the performance indices.

Figure 6.9 shows that the original Hawkins´ methodology (H) yields good results in the PTC_v index but that unfortunately they are accompanied by a high rate of false positives (PWC_v and PWC_0) in strong or negative correlations scenarios (C3). The poor results in PWC_v and PWC_0 accounts for the bad performance in PTC_0 in these scenarios. The recursive (RH) and the pre-filtered recursive (FRH) Hawkins variants successfully reduce the number of false positives and therefore outperform the original algorithm (H) in the PTC_0 index.

In the case of one single variable faults the RH and FRH methods give excellent results in PTC_0 and PTC_v which are similar to the results of the Hawkins' one single variable method (HSVM). An advantage of the RH and FRH methods is that they can also be applied to diagnose multiple variable faults with good results. Figure 6.9 also shows that the FRH variant give slightly better results for PTC_0 than the RH variant in faults involving more than one single variable and large-sized faults.

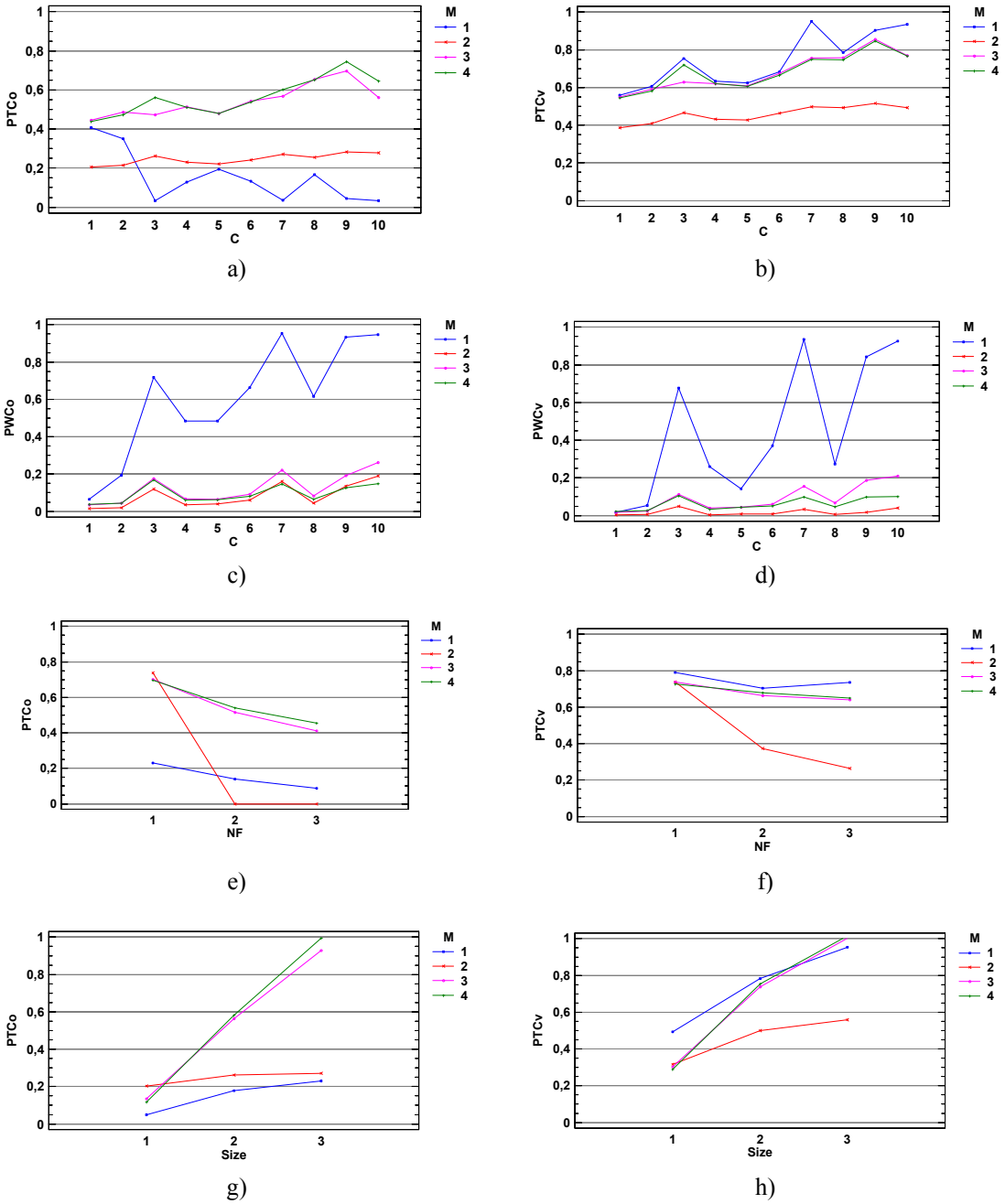

FIGURE 6.9: Interaction plot covariance × method; NF × method; size × method with α=5% α_{terms} = 5%
Methods: M1: H; M2: HSVM; M3: RH; M4: FRH
Method × covariance structure ⇒ a) PTC_0, b) PTC_v, c) PWC_0 and d) PWC_v
Method × NF (Number of faulty variables) ⇒ e) PTC_0 and f) PTC_v
Method × size of fault (1-Small; 2-Medium; 3-Large) ⇒ g) PTC_0 and h) PTC_v

The above results let us to conclude:

- The recursive variants of Hawkins, RH and FRH give better classification results than the standard Hawkins´ method and the Hawkins´ one single variable method.

- The results of the FRH are slightly better than the RH results.
- Despite the original Hawkins method gives the best results in PTC_v it finally yield a poor classification performance as a consequence of the bad results in PWC_0 and PWC_v

6.2.2.2 T2FRH and T2RH variants performance

As commented in Section 5.2.3 in the T2RH and T2FRH variants, after the Hotelling´s T^2 statistic has detected a fault, the significance of the Hawkin´s $\hat{z}$ residuals is checked by comparison against the corresponding threshold limits. Different thresholds (α_{terms}) has been tested and the results demonstrate that the classification performance in the RH and FRH is affected by the introduction of a Hotelling´s T^2 trigger mechanism for fault detection.

In order to select an appropriate value for the α_{terms}, the results on the combined indices *TCI*, *WCI* and *GCI* for α_{terms} equal to 1%, 5% and Bonferroni´s adjusted are compared. Figure 6.10 shows that for the *GCI* index the T2RH with α_{terms} equal to 1% and Bonferroni´s adjusted outperforms the 5% adjustment. The bad performance in the case of a 5% adjustement is explained by the large value in the *WCI* index (false positives). Figure 6.10 also shows that the T2RH has a better performance in *GCI* for high correlation scenarios than the RH.

Figure 6.11 shows that the *GCI* index in the T2FRH with α_{terms} equal to 1% and Bonferroni´s adjusted also outperform the 5% adjustment. But in this case the FRH gives slightly better results than the corresponding Hotelling T^2 variant.

In figure 6.12 and 6.13 the T2RH and T2FRH with the best selection for α_{terms} (1%) are compared to the RH and FRH. They show that T2FRH has slight better results in the PTC_0 and PTC_v indices than the T2RH. It can be seen that the PWC_v in large correlation scenarios in the T2RH is larger than in the case of the T2FRH. Figure 6.12 shows that

there are not important differences between T2FRH and FRH results in PTC_0 and PTC_v. Similarly, the T2RH has close results to the RH in the PTC_0 index but gives slightly better results for the PTC_v.

According to the number of variables involved in the fault (Figure 6.13), the T2RH give similar results to the RH, and the T2FRH in 2 and 3 variables faults has better results than the FRH in PTC_0 and PTC_v.

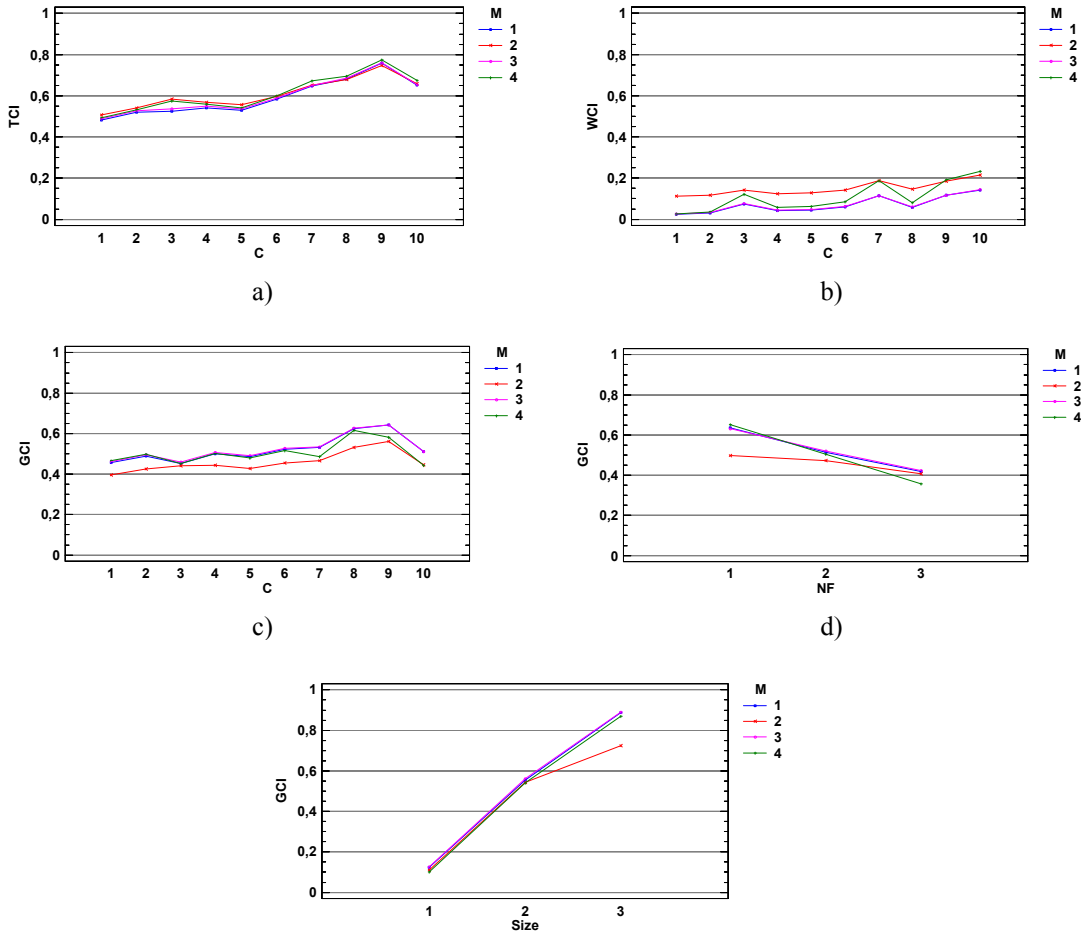

FIGURE 6.10: Interaction plots for the combined indices *TCI*, *WCI* and *GCI*
Methods: M1: T2RH Bonferroni α_{terms}; M2: T2RH α_{terms} = 5% ; M3: T2RH α_{terms} = 1%; M4: RH;
Method × covariance structure ⇒ a) *TCI* , b) *WCI* , c) *GCI*
Method × NF (Number of faulty variables) ⇒ d) *GCI*
Method × Size of fault (1-Small; 2-Medium; 3-Large) ⇒ e) *GCI*

In the *PND* there are only small differences in the RH. The T2RH and T2FRH have a certain levels of lack of power (*PNF*) while this problem does not exist in the RH and FRH. The *PNF* in the T2RH is slightly larger than in the FRH and the worst results are

associated to the C3 correlation scenario where negative correlations are involved. A part of the out-of-control observations classified as *PND* in the RH or FRH are now detected as *PNF* in the T2RH and T2FRH. The fact that these variants use different trigger mechanisms in detection accounts for the *PND* to *PNF* conversion. Even if the T^2 based variants were exactly adjusted to the same overall Type I risk of the others, the

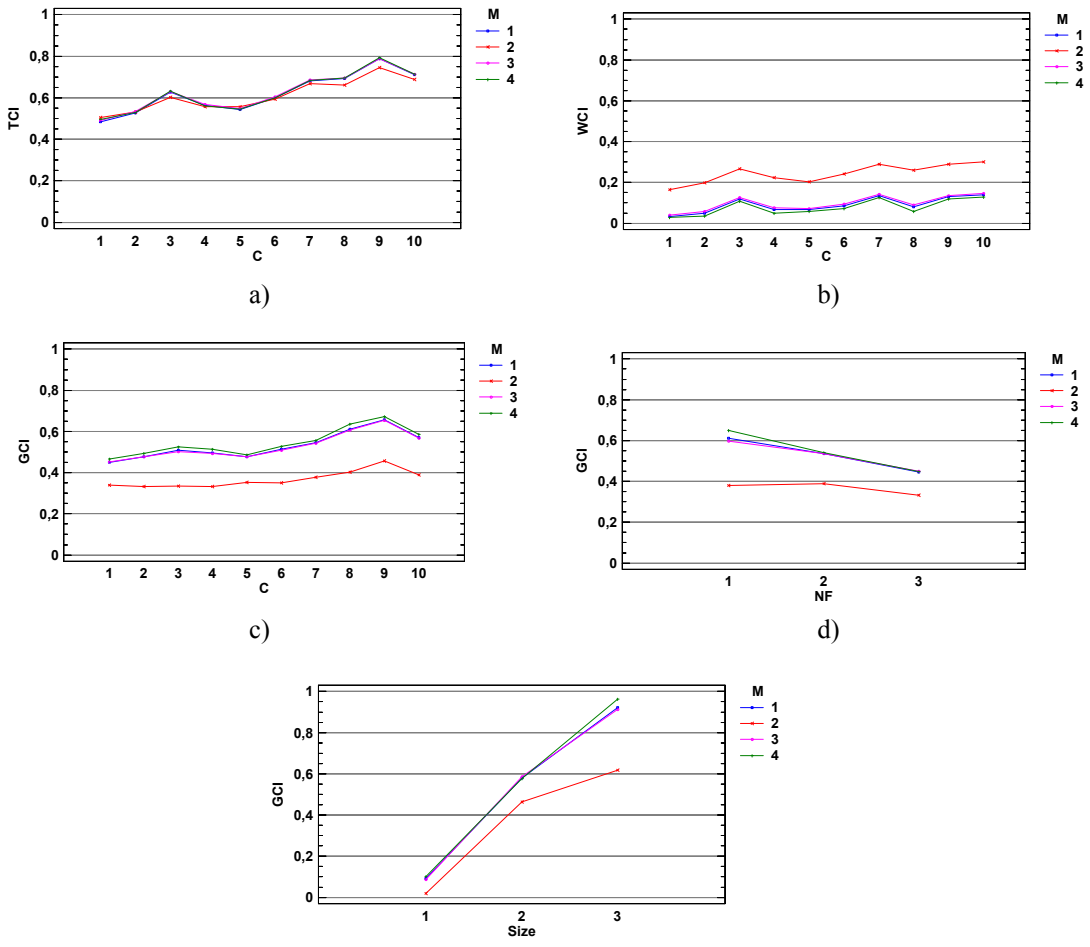

FIGURE 6.11: Interaction plots for the combined indices *TCI*, *WCI* and *GCI*
Methods: M1: T2FRH Bonferroni α_{terms}; M2: T2FRH α_{terms} = 5% ; M3: T2FRH α_{terms} = 1%; M4: FRH
Method × covariance structure ⇒ a) *TCI* , b) *WCI* , c) *GCI*
Method × NF (Number of faulty variables) ⇒ d) *GCI*
Method × Size of fault (1-Small; 2-Medium; 3-Large) ⇒ e) *GCI*

methods would present some small discrepancies in *PND* and *PNF* since the sets of detected out-of-control observations are not necessarily identical.

The above results let us to conclude:

- T2RH performs better for high correlation scenarios than the RH.

- The T2FRH has similar results to the FRH
- Part of the out-of-control observations classified as *PND* in the RH or FRH are detected as *PNF* in the T2RH and T2FRH.
- The T2RH and T2FRH are alternatives to the RH and FRH. One of the advantages of these T^2 variants is that the type I risk can be adjusted in a straightforward way since the monitored statistic for fault detection follows a known Snedecor-F distribution.

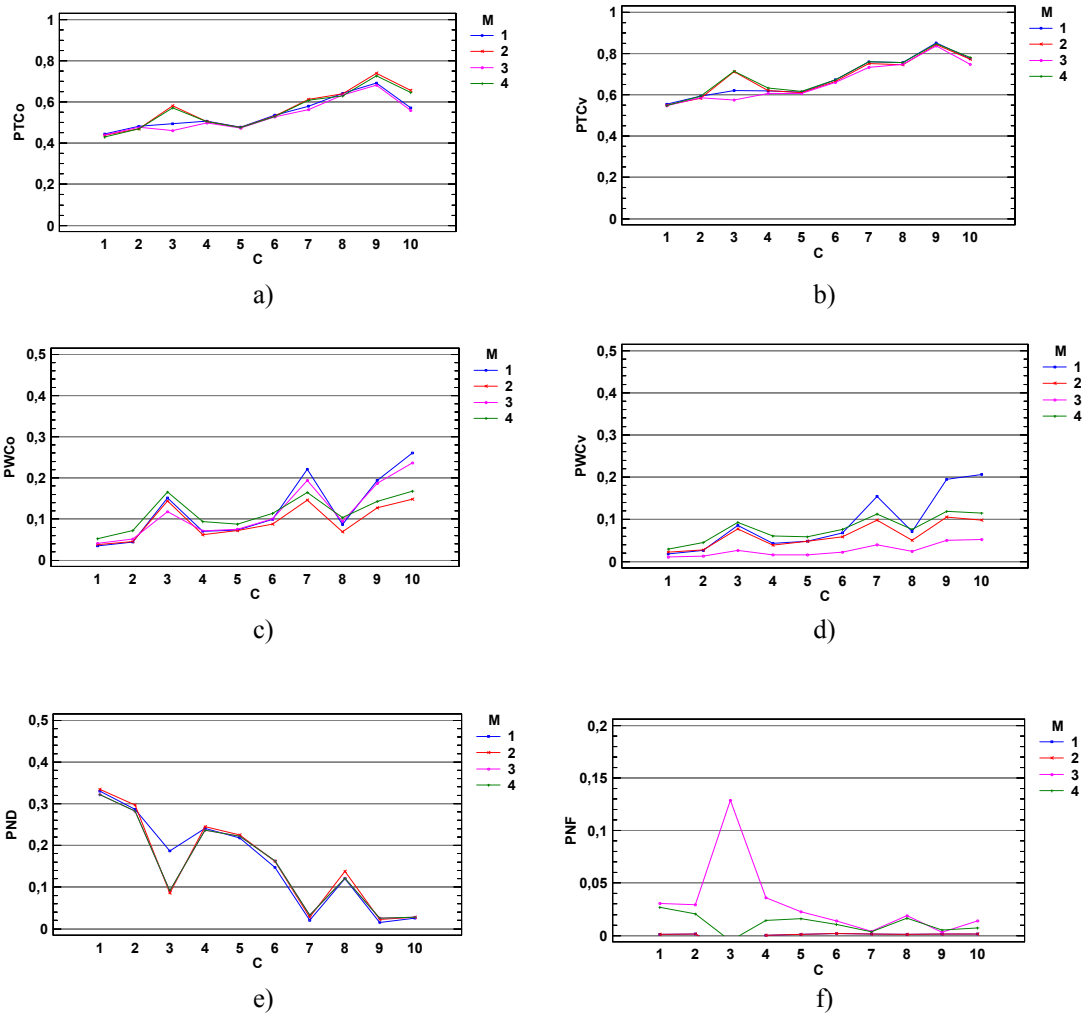

FIGURE 6.12: Interaction plot covariance × method ; NF × method; size × method with α=5%
Methods: M1: RH; M2: FRH; M3: T2RH α_{terms} = 1%; M4: T2FRH α_{terms} = 1%
Method × covariance structure ⇒ a) PTC_0, b) PTC_v, c) PWC_0, d) PWC_v, e) *PND* and f) *PND*

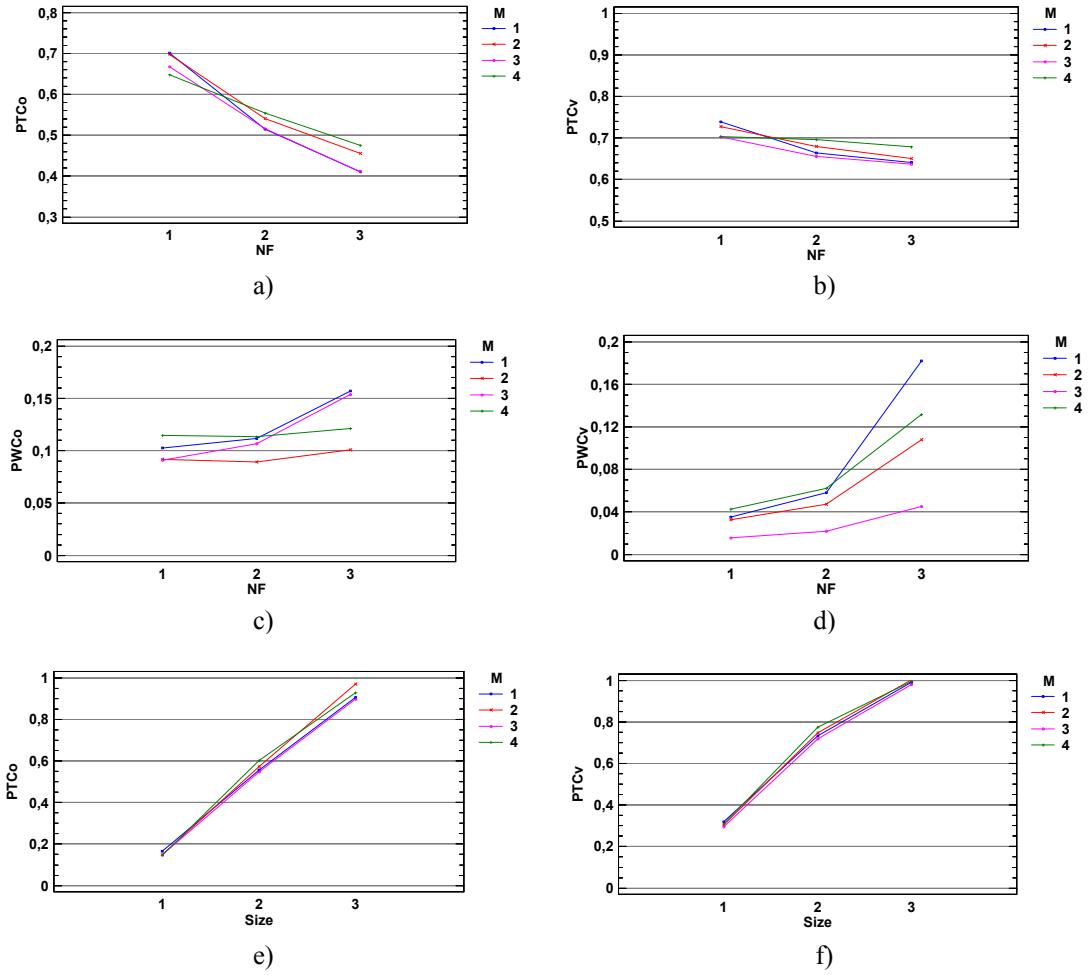

FIGURE 6.13: Interaction plot NF × method; size × method with α=5%
Methods: M1: RH; M2: FRH; M3: T2RH α_{terms} = 1%; M4: T2FRH α_{terms} = 1%
Method × NF (Number of faulty variables) $\Rightarrow$ a) PTC_0, b) PTC_v, c) PWC_0 and d) PWC_v
Method × size of fault (1-Small; 2-Medium; 3-Large) $\Rightarrow$ e) PTC_0, f) PTC_v

6.2.3 Murphy´s methodology

An analysis of variance (ANOVA) was performed considering the factors: Method (3 levels: M, T2M and FT2M); correlation structure, C (10 levels, see Table 6.1); number of faulty variables, N_f (3 levels: 1, 2 and 3 faulty variables); and size of the fault (3 levels: small, medium or large faults). The ANOVA results (see Appendix 6.3) show that all the factors and most of their interactions are statistically significant (p-value< 0.05) for all the performance indices.

Figure 6.14 shows that Murphy´s methodology has similar problems to the Hawkins´ methodology. Despite this method gives good results in the PTC_v, it presents serious problems with high rates of false positives (PWC_v and PWC_o) in scenarios of strong or negative correlations which ruin the performance in the PTC_0 index. The proposed variants T2M and FT2M (Variants of the Murphy´s algorithm explained in section 6.4) achieve better results in PTC_o than the original Murphy´s algorithm.

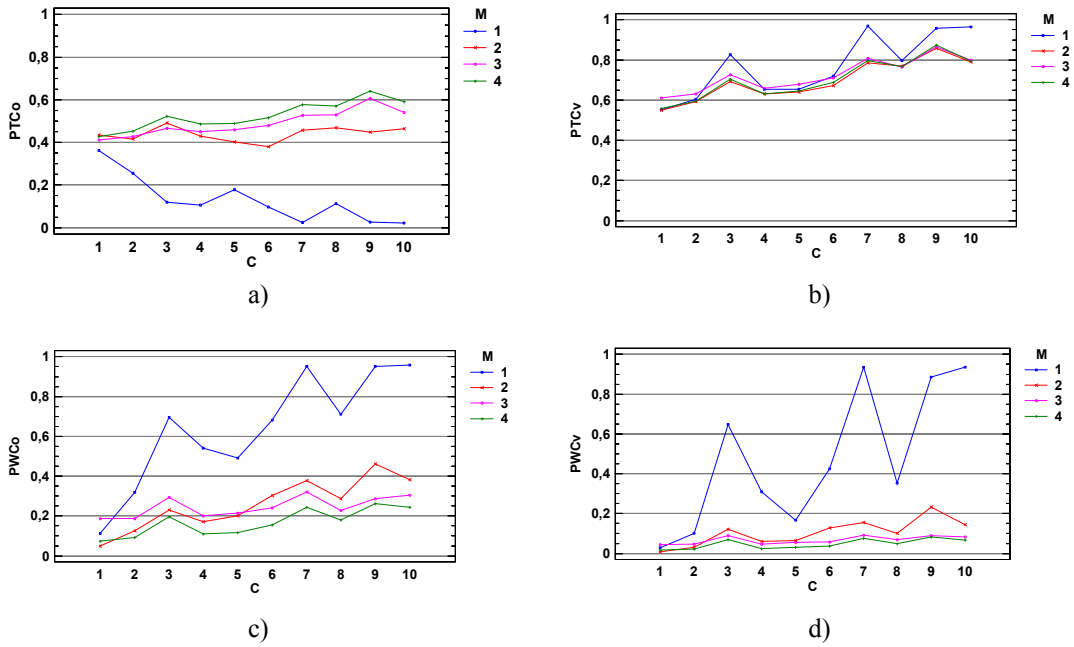

FIGURE 6.14: Interaction plot covariance × method with α=5% α_{terms} = 5%
Methods: M1: M; M2: T2M; M3: FT2M $\alpha_{prefilt.}$ = 5%; M4: FT2M $\alpha_{prefilt.} = \alpha_{Bonf}$
Method × covariance structure $\Rightarrow$ a) PTC_0, b) PTC_v, c) PWC_0, and d) PWC_v

Figure 6.14 shows that the FT2M (Pre-Filtered T^2-Hotelling Murphy´s Methodology) clearly outperforms the T2M (T^2-Hotelling Murphy´s Methodology) and the original Murphy´s algorithm. Figure 6.15 shows that the T2M has serious problems of false positives for large and medium-sized faults and 2 or 3 variables faults in moderated and strong correlation scenarios. It can be seen that T2M only has similar performance to the FT2M when one single variable faults are considered.

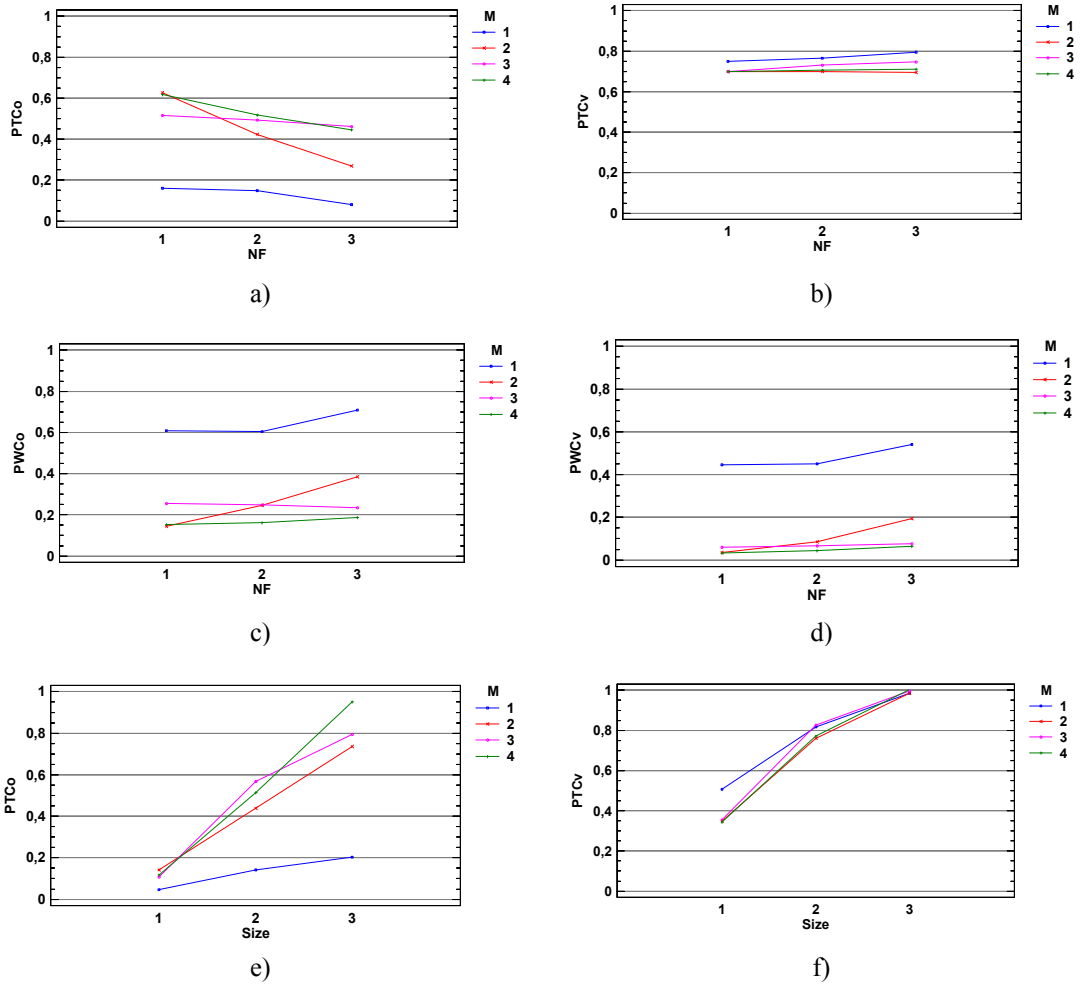

FIGURE 6.15: Interaction plot NF × method; size × method with α=5% α_{terms} = 5%
Methods: M1: M; M2: T2M; M3: FT2M $\alpha_{prefilt.}$ = 5%; M4: FT2M $\alpha_{prefilt.}$ = α_{Bonf}
Method × NF (Number of faulty variables) $\Rightarrow$ a) PTC_0, b) PTC_v, c) PWC_0 and d) PWC_v
Method × size of fault (1-Small; 2-Medium; 3-Large) $\Rightarrow$ e) PTC_0, f) PTC_v

Figure 6.16 shows that the combined indices confirm this results. The WCI shows that the original Murphy´s method has a serious problem of false positives. The FT2M performs better than the T2M in WCI. This results are transferred to the other combined indices so that the FT2M results in the GCI and TCI indices are better than the results in the T2M method.

In relation to the α_{terms} adjustment, Figure 6.16 shows that FT2M with Bonferroni´s adjusted α_{terms} gives better results than with the 5%. It also shows that the large-sized faults

and a reduced number (1 or 2) of variables involved in the fault accounts for this difference.

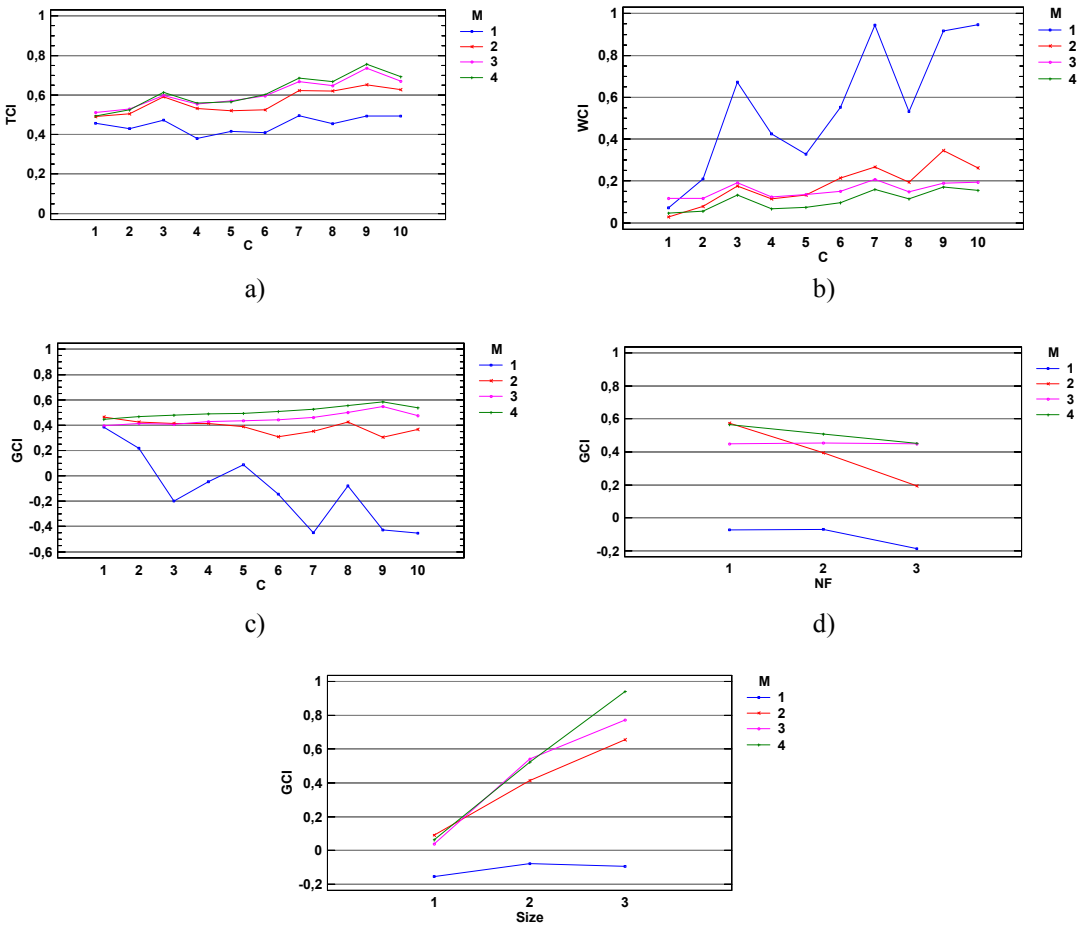

FIGURE 6.16: Interaction plots for the combined indices *TCI*, *WCI* and *GCI*
Methods: M1: M; M2: T2M; M3: FT2M $\alpha_{\text{prefilt.}} = 5\%$; M4: FT2M $\alpha_{\text{prefilt.}} = \alpha_{\text{Bonf}}$
Method × covariance structure $\Rightarrow$ a) *TCI* , b) *WCI* , c) *GCI*
Method × NF (Number of faulty variables) $\Rightarrow$ d) *GCI*
Method × Size of fault (1-Small; 2-Medium; 3-Large) $\Rightarrow$ e) *GCI*

The above results let us to conclude:

- The Murphy´s method has a poor classification performance as a consequence of the bad results in PWC_0 and PWC_v .
- The T2M and FT2M give better classification results than the standard Murphy´s method.

- FT2M perfoms better than the T2M. The T2M has problems of false positives for large and medium-sized faults and 2 or 3 variables faults in moderated and strong correlation scenarios.
- FT2M with Bonferroni´s adjusted α_{terms} gives better results than with the 5%. The large-sized faults and a reduced number of variables involved in the fault accounts for this difference.

6.2.4 Montgomery and Runger´s Methodology

An analysis of variance (ANOVA) was performed considering the factors: Method (5 levels: MM, RM, FRM, MUSE and FMUSE); correlation structure, *C* (10 levels, see Table 6.1); number of faulty variables, N_f (3 levels: 1, 2 and 3 faulty variables); and size of the fault (3 levels: small, medium or large faults). The ANOVA results (see Appendix 6.4) show that all the factors and most of their interactions are statistically significant (*p*-value< 0.05) for all the performance indices.

Figure 6.17 shows that the original Montgomery´s method (MM) has similar problems to Hawkins´ and Murphy´s methodologies with a high rate of false positives (PWC_v and PWC_0) in strong or negative correlations scenarios that account for the bad performance in the PTC_0 index. The results in PTC_0 of the RM (Recursive Montgomery and Runger´s methodology) clearly outperform the MUSE (Montgomery and Runger´s Method under a sequential extraction methodology) and the MM. The PTC_0 results of the RM are similar to the results of the pre-filtered variants, FMUSE and FRM. The high PWC_0 and PWC_v indices in MM and MUSE account for their bad diagnosis performance. The FMUSE and FRM give better results in the PTC_v index than the RM. Figure 6.18 shows that the RM results in PTC_0 and PTC_v decay for 2 and 3 variables faults. Figure 6.18 and 6.19 show that the RM has a certain level of lack of diagnosis power (*PNF)*

which do not exist in the others methods and this level increases in the case of small size faults and 2 or 3 variables faults .

So it can be concluded that the pre-filtered versions FMUSE and FRM improved the classification performance of MUSE and RM and clearly outperform the MM reducing the number of false positives in strong or negative correlations scenarios. Figure 6.20 shows that the FRM presented the best results on the different combined indices.

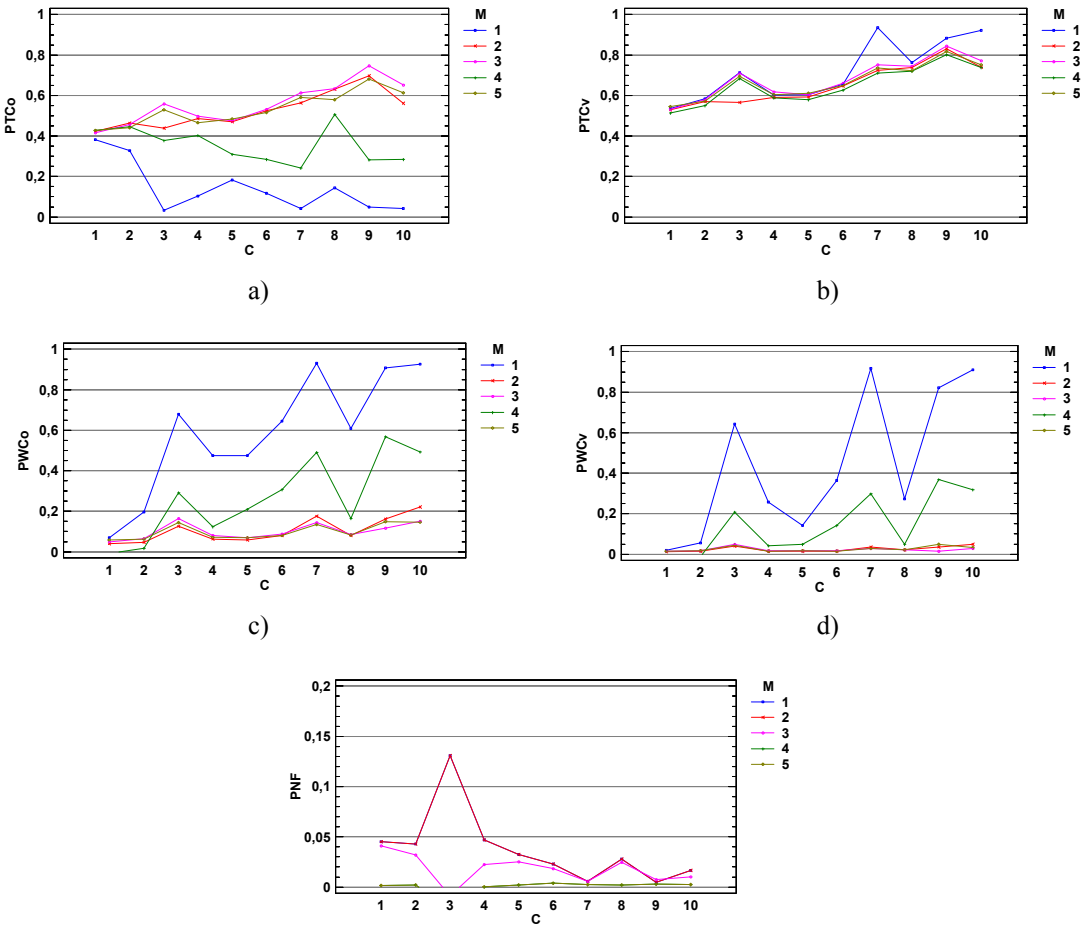

FIGURE 6.17: Interaction plot covariance × method with α=5% $\alpha_{terms} = \alpha_{Bonf}$
Methods: M1: MM; M2: RM; M3: FRM; M4: MUSE; M5: FMUSE
method × covariance structure ⇒ a) PTC_0, b) PTC_v, c) PWC_0, d) PWC_v and e) PNF

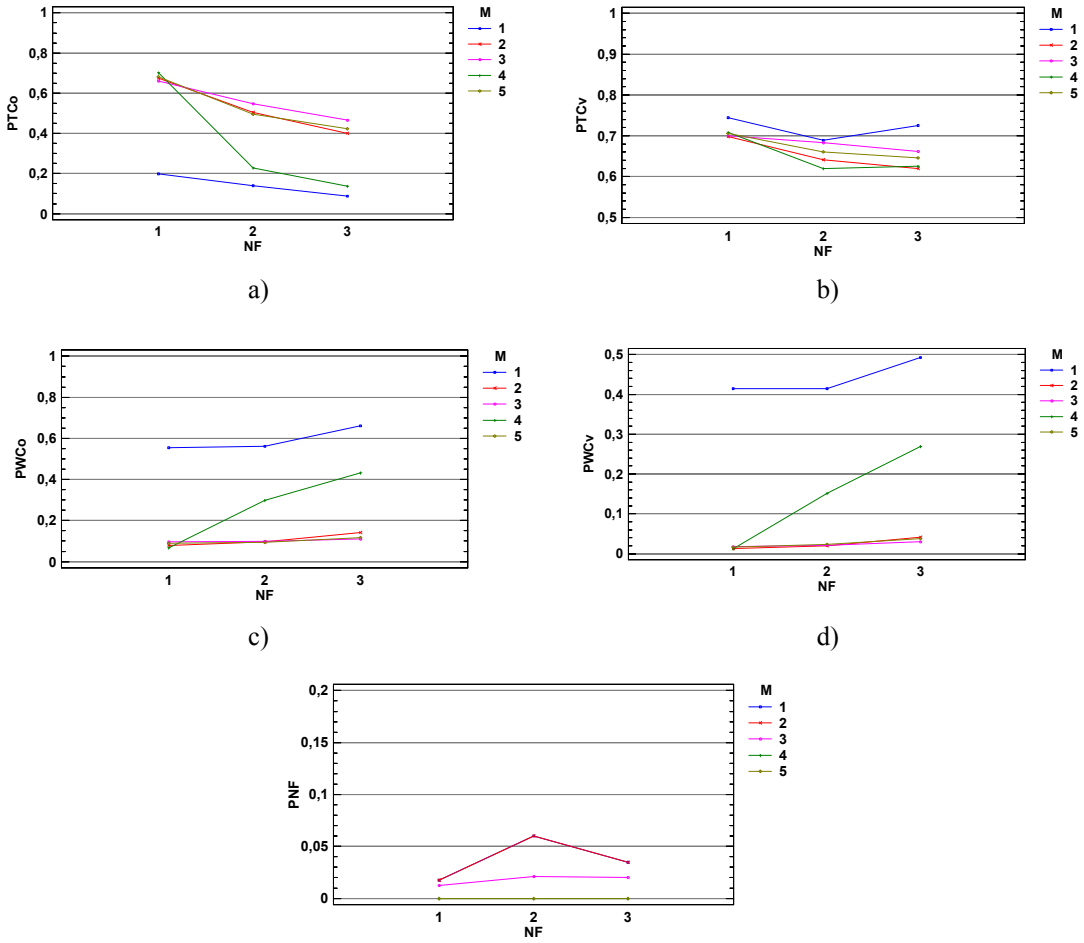

FIGURE 6.18: Interaction plot NF × method with α=5% $\alpha_{terms} = \alpha_{Bonf}$
Methods: M1: MM; M2: RM; M3: FRM; M4: MUSE; M5: FMUSE
Method × NF (Number of faulty variables) $\Rightarrow$ a) PTC_0, b) PTC_v, c) PWC_0, d) PWC_v and e) PNF

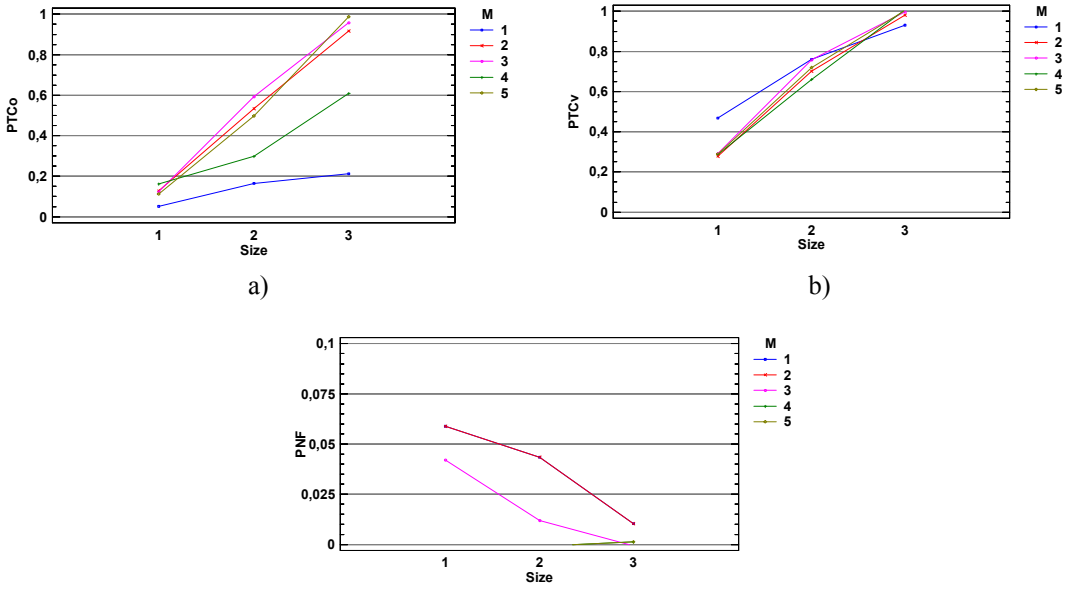

FIGURE 6.19: Interaction plot size × method with α=5% $\alpha_{terms} = \alpha_{Bonf}$
Methods: M1: MM; M2: RM; M3: FRM; M4: MUSE; M5: FMUSE
Method × size of fault (1-Small; 2-Medium; 3-Large) $\Rightarrow$ a) PTC_0, b) PTC_v and c) PNF

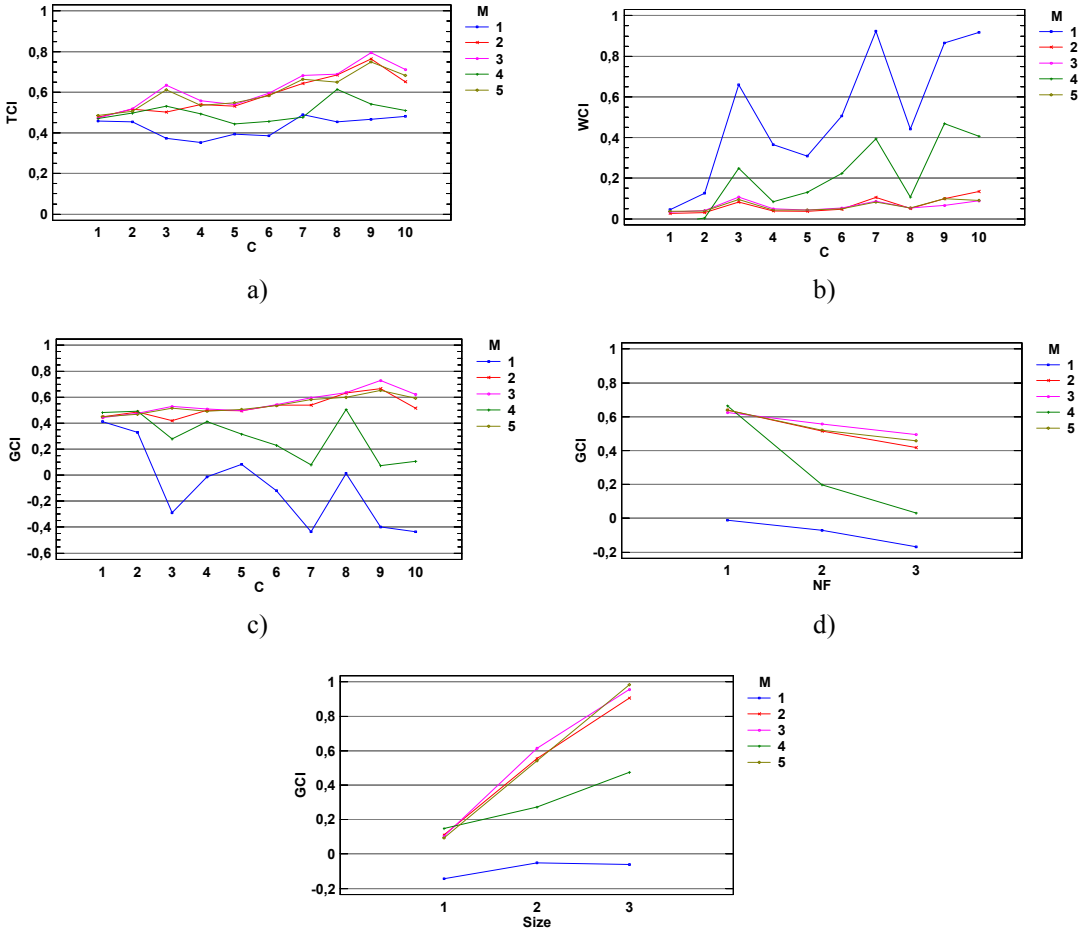

FIGURE 6.20: Interaction plots for the combined indices *TCI*, *WCI* and *GCI*
Methods: M1: MM; M2: RM; M3: FRM; M4: MUSE; M5: FMUSE with α=5% $\alpha_{terms} = \alpha_{Bonf}$
Method × covariance structure ⇒ a) *TCI*, b) *WCI*, c) *GCI*
Method × NF (Number of faulty variables) ⇒ d) *GCI*
Method × Size of fault (1-Small; 2-Medium; 3-Large) ⇒ e) *GCI*

6.2.5 Performance comparison

In this section we are going to compare the performance of the Mason *et al.* original algorithm (MTY), which is the most commonly used for diagnosis in multivariate quality control, with the most promising variants according to the previous sections: MTY1 ratio h_{first}/h_{second}=1.5, Hawkins T2FRH α_{Bonf}, Murphy FT2M $\alpha_{prefilt.} = \alpha_{Bonf}$ and Montgomery and Runger´s FRM α_{Bonf}. An analysis of variance (ANOVA) was performed considering the factors: Method (5 levels: MTY, MTY1 h_{first}/h_{second} =1.5, Hawkins T2FRH, Murphy FT2M and Montgomery and Runger´s FRM); correlation structure, C (10 levels, see Table 6.1); number of faulty variables, N_f (3 levels: 1, 2 and 3 faulty variables); and size of the fault (3 levels: small, medium or large faults). The ANOVA results (see Appendix 6.5) show that all the factors and most of their interactions are statistically significant (p-value< 0.05) for all the performance indices.

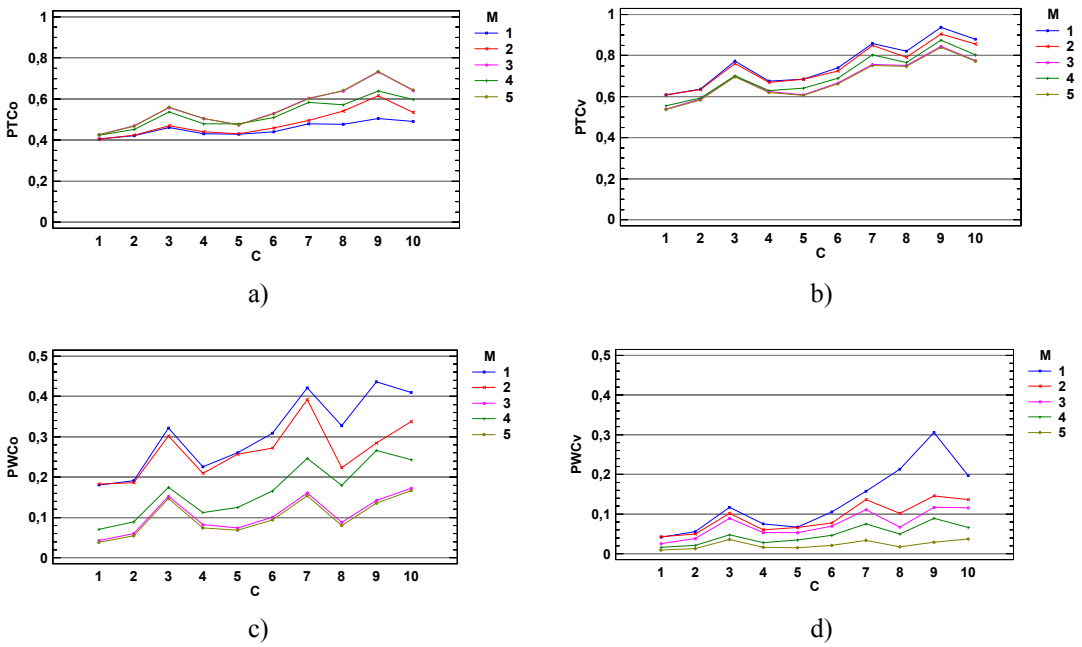

FIGURE 6.21: Interaction plot covariance × method with α=5%
Methods: M1: Mason; M2: Mason h_{first}/h_{second}=1.5; M3: T2FRH α_{Bonf}; M4: FT2M $\alpha_{prefilt.} = \alpha_{Bonf}$; M5: FRM α_{Bonf}
Method × covariance structure ⇒ a) PTC_0, b) PTC_v, c) PWC_0, and d) PWC_v

Figure 6.21 shows that all the proposed variants outperform the MTY results in PTC_0. The Hawkins T2FRH and the Montgomery FRM reach the top results in PTC_0 in all the correlation scenarios. The MTY1 also outperforms the original MTY in all the correlation scenarios.

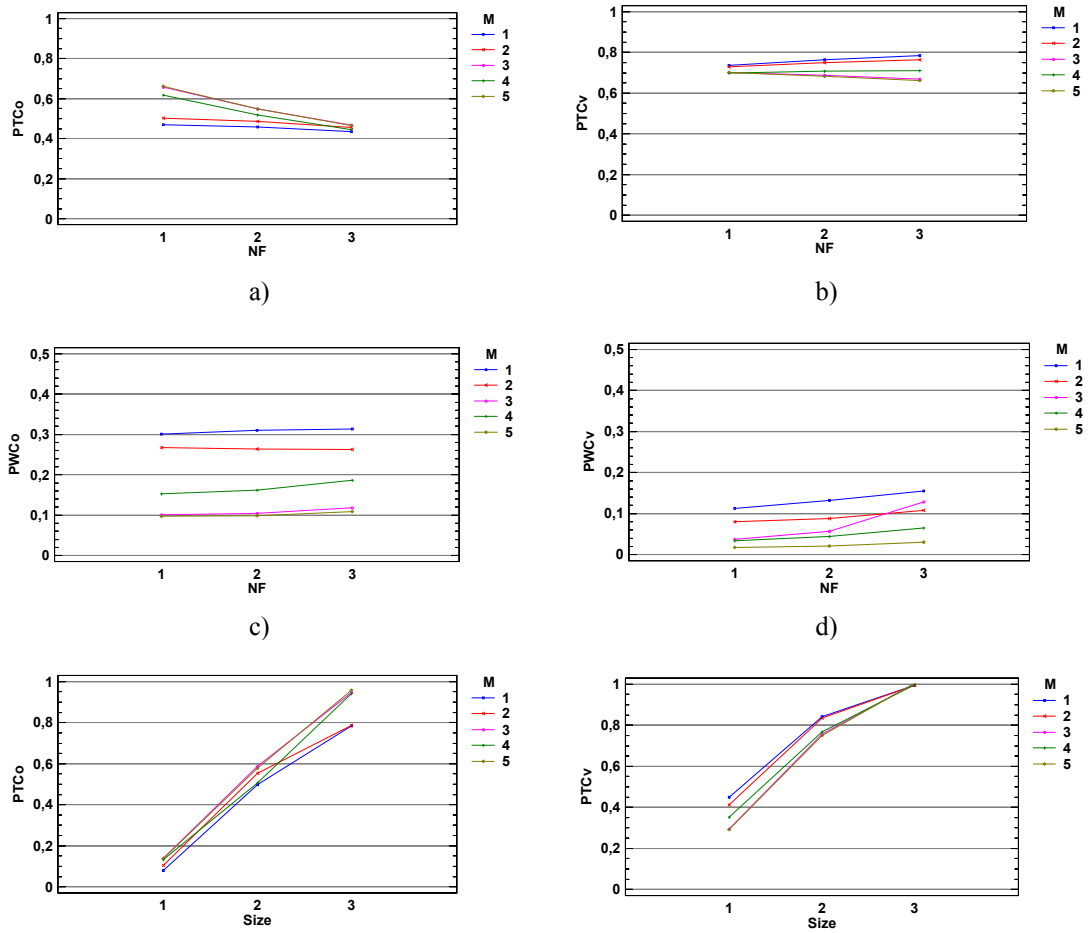

FIGURE 6.22: Interaction plot NF × method; size × method with α=5%
Methods: M1: Mason; M2: Mason h_{first}/h_{second}=1.5; M3: T2FRH α_{Bonf}; M4: FT2M $\alpha_{prefilt.} = \alpha_{Bonf}$; M5: FRM α_{Bonf}
Method × NF (Number of faulty variables) $\Rightarrow$ a) PTC_0, b) PTC_v, c) PWC_0 and d) PWC_v
Method × size of fault (1-Small; 2-Medium; 3-Large) $\Rightarrow$ e) PTC_0, f) PTC_v

In PTC_v the results are completely reversed and the MTY outperforms all the proposed variants. The MTY gives the worst results in PWC_0 and PWC_v in strong correlation scenarios. Figure 6.22 shows that these results are consistent for all the fault sizes and faults involving different number of variables (1 to 3). Figure 6.23 shows the results in

the new combined indices which try to measure an overall classification performance. It shows that in the *TCI* index, the Montgomery FRM and the Hawkins T2FRH outperform the others methods in strong correlation scenarios. In the *WCI* index, the MTY had the worst results in strong correlation scenarios and the Montgomery FRM had the best results. In the global performance index *GCI* all the proposed variants outperform the MTY in strong correlation scenarios. The Hawkins T2FRH and the Montgomery FRM give excellent results not only in strong correlation scenarios but also in weak correlation scenarios.

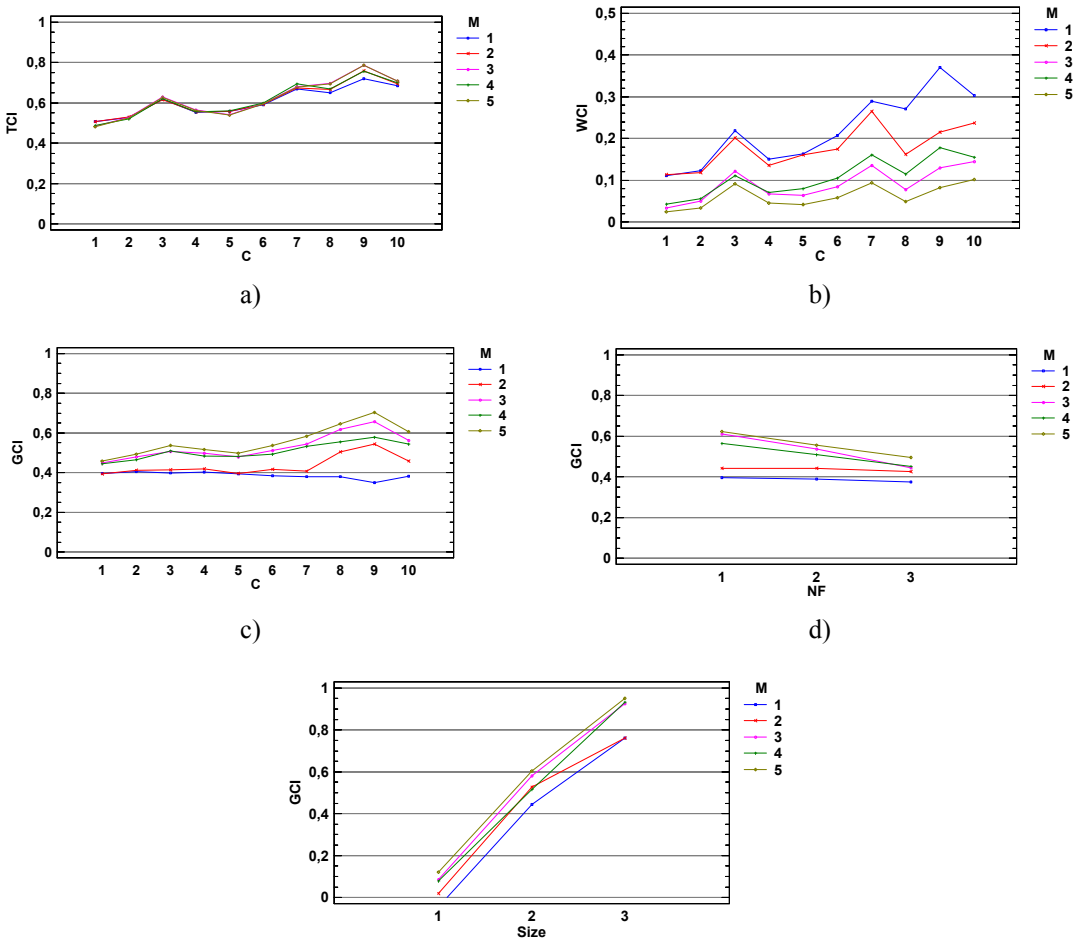

FIGURE 6:23: Interaction plots for the combined indices *TCI*, *WCI* and *GCI*
Methods: M1: Mason; M2: Mason h_{first}/h_{second}=1.5; M3: T2FRH α_{Bonf}; M4: FT2M $\alpha_{prefilt.} = \alpha_{Bonf}$; M5: FRM α_{Bonf}
Method × covariance structure ⇒ a) *TCI*, b) *WCI*, c) *GCI*
Method × NF (Number of faulty variables) ⇒ d) *GCI*
Method × Size of fault (1-Small; 2-Medium; 3-Large) ⇒ e) *GCI*

Hawkins T2FRH and Mongomery FRM close results can be explained by the relation between the Montgomery´s statistics *D* and the Hawkins´s residuals $\hat{z}$ (see section 5.3.1). and that in both the fault detection is based in the Hotelling´s T^2 statistic.

$$T^2_{k|1,2,\ldots k\text{-}1\ldots k+1\ldots K} = c_k^2 = D_k = \hat{z}_k^2 \qquad (6.4)$$

The T2FRH performance also seems to be slightly affected by the number of variables in the fault.

6.3 Performance in the pasteurization process

To compare the methods described in the previous sections in a real context, we use data from the pilot plant of a pasteurization process described in section 3.1.1. There are 13 variables involved in this process as described in Table 6.4.

TABLE 6.4. Variables measured in the pasteurization model

Nr	Variable	Description
X_1	Tank Level	Level of the water in the tank at the beginning of the process. If it drops below a certain limit, the tank is refilled.
X_2	T^a_1	Temperature of the product after flowing through the curved pipe. This temperature defines whether or not we have a good product.
X_3	T^a_2	Temperature of the heating water. This is the water which has to heat the product.
X_4	T^a_3	Temperature of the final product. This is the temperature of the product when it leaves the system.
X_5	T^a_4	Temperature of the product immediately after heating, *i.e.* before entering the curved pipe.
X_6	T^a_5	Temperature of the product after preheating the new product. This temperature defines whether or not the product needs further cooling down.
X_7	Flow	Speed with which the product flows through the system.
X_8	SPFlow	Setpoint of the flow.
X_9 X_{10} X_{11}	Power 1 Power 2 Power 3	These variables measure the power used to heat the heating water.
X_{12}	Pump 1	Percentage that pump 1 is opened. Pump 1 controls the flow speed of the product.
X_{13}	Pump 2	Percentage that pump 2 is opened. Pump 2 controls the flow speed of the heating water.

From this model we got several data sets. To start, we collected data under normal operating conditions. For this process that means that we have a value of 140, 160, 180 or 200 ml/min for the setpoint of the flow and that the product is not cooled down at the end of the process in any case. The setpoint for the temperature of the heating water is 60C^{o} and the product is assumed to be good if the temperature T_1 is larger than 48C^{o}, while the setpoint for T^a_1 is 50C^{o}. While taking this reference data, the product produced was good. Next to these data sets we also produced data sets in which we initialized faults. We kept track of where we initialized which fault, so we can compare the different methods to see which one finds the fault fastest and also which one is most accurate in naming the cause of the fault. We generated two kinds of faults, sensor faults and process faults. A sensor fault means that for one variable a different value is registered than the real value, due to we are dealing with an automatic process this eventually may become a process fault. We generated the following sensor faults:

- Flow: the setpoint of the flow was changed to 0 (Fault 1) or to 1500 (Fault 2). The sensor fault in the flow will make Pump 1 work more (or less). This will cause the temperatures T^a_4, T^a_1, T^a_5 and T^a_3 to decrease (or increase), because the water has less (or more) time to heat. So this sensor fault will change into a process fault. The expected signals immediately after the fault are X_7 (Flow sensor) and X_{12} (Pump 1) as a result of the loop control activation.
- T^a_2 (Fault 3), the value for T^a_2 was set to 0. For T^a_2 the sensor fault will lead to a higher temperature of the heating water. Because the process thinks that the value for T^a_2 is 0, it will start heating more to reach the setpoint for the temperature of the heating water (Pump 2). This also leads to higher temperatures for T^a_1, T^a_3, T^a_4 and T^a_5, so this sensor fault will also influence the process. The expected signal immediately after the fault is X_3 (T^a_2 sensor)

On the other hand, a process fault means that a part of the process stops working or starts working when it is not supposed to do so. We generated the following process faults:

- Pump 1 (Fault 4), the pump stops working. All the pump failures influence the whole process. They will change the temperatures and because of the loop controls this will change almost everything in the process. The expected signals immediately after the fault are signals in the whole process.
- Test for good product (Fault 5), the system throws away good product. When the process starts to throw away good product (and also when it starts to throw away bad product) this will influence several things. The flow will be influenced, because now the product is sent through another pipe, with a different length. This change in the flow will result in a change in Pump 1. Also T^a_3 and T^a_5 will be influenced. These temperatures will go down, because the product in the pipes, where the temperatures are measured, is not flowing anymore, so no new warm product is coming in. The expected signals immediately after the fault are signals in X_7 (Flow sensor), X_{12} (Pump 1), X_4 (T^a_3 sensor)and X_6 (T^a_5 sensor).

Table 6.5 shows the expected fault signals in the different types of faults and the variables that were actually detected as responsible in the different methodologies. The results in Table 6.5 shows show that in the pasteurization process Hayter´s and DFT methods with its variants were successful in the detection and identification of faulty sensors but they got poor results when diagnosing process faults**.** The Step-down method could not be implemented as there were faults that shared common variables, and the Hawkins´ one single variable method gave bad results in process faults since they

involved more than one variable. In fact these methods aimed to the same variables for the sensors faults and the process faults (X_7 and X_{12}). These methods do not account for correlations breakage among variables and, consequently, had more difficulties to assign the root causes of a process fault.

The original Hawkins´, Montgomery and Runger´s and Murphy´s methods gave too excessive signals which caused an excessive false positive rate in fault diagnosis. On the contrary, the Hawkins´ one single fault method signalled only the X_7 variable in the faults F_1, F_2, F_4 and F_5, and the X_3 in the fault F_3 and, consequently, as only one variable was signaled the diagnosis of the process faults was difficult.

The MTY method was more successful in the fault diagnosis than the previous methods. The MTY and MTY1 $h_{first}/h_{second}=1.5$ had similar results in F_2, F_3, F_4 and F_5 but the MTY1 outperformed the original MTY in the case of the fault F_1. In the observation 506 for fault F_1 the MTY1 detected a dominant variable and could signal to the X_7 as responsible, while the MTY could only signal to 10 different variables. In the case of the fault F_2 both methods signaled the X_7 and X_{12} as responsible variables and both signaled the X_3 in the case of fault F_3. In the process fault F_4, the MTY and MTY1 found significant the unconditional terms for X_7 and X_{12} and a large quantity of conditional terms related to X_4, X_6, X_8, X_{10}, X_{11} and X_{13} variables. The significant unconditional terms aim to a problem in the flow or the pump 1. The number of terms and variables involved in the significant conditional terms shows that this fault influence the whole process, as it can be expected for a pump 1 fault. In the case of the process fault F_5, both methods found significant the unconditional terms for X_7 and X_{12} and the conditional terms related to the pairwise variables (X_4, X_6) and (X_{13}, X_3). The MTY significant terms match with the expected result for this kind of fault. Additionally the MTY provides an easy interpretability of the terms and relationships between variables

classifying the cases of out of control in situations that may break or not the correlation structure between the variables. In the case of the pasteurization process the easy interpretability of the terms allowed to correctly diagnoses the process fault F_4

In the pasteurization process the results of the T^2-prefiltered recursive Hawkins´method (T2FRH) were similar to the prefiltered recursive Montgomery and Runger´s method (FRM). The use of the Hotelling´s T^2 as trigger mechanism for detection makes unnecessary to apply the recursive methodology to all the observations, but only to the observations which has been previously detected as out-of-control. An interesting option is to implement these methods in addition to the MTY1. Given that the conditional or unconditional terms of Mason *et al´s* methodology provides an easy interpretability of the terms and relationships between variables classifying the out-of-control cases in situations that may break or not the correlation structure between the variables, the use of the modified Mason et *al´s* method MTY1 in addition to one of the methods T2FRH or FRM would improve the interpretability of the detected signals.

TABLE 6.5. Responsible variables for F_1 F_2 F_3 F_4 and F_5 faults according to the different fault diagnosis methods

Faults	Expected Fault Signals	Hawkins	Hawkins 1 S.V	Hawkins Chi-Filter Rec (T2FRH)	Hayter	Murphy	FTM Murphy
F_1: X_7: Sensor Flow →0 X_7:182→ 147→ 55 Obs(506) Obs(507) Obs(506) ======= Obs(507)	X_7 X_{12}	X_7 X_8 ========= X_7 X_{12} ---------- X_5X_8 $X_{11}X_{13}$	X_7 ========= X_7	Recursive X_7 ========= Prefilter:X_7 Recursive: X_{12}	No Detection ========== X_7 X_{12}	X_3 X_7 X_8 ===== X_7 X_8 X_{12} X_5 $X_{13}X_{11}X_4$ X_{10} X_1 X_2	Prefilter: - Recursive: X_3 X_7 ======= Prefilter: X_7 Recursive: X_{12}
F_2 Sensor Flow 1500 Obs (902)	X_7 X_{12}	X_7 X_8 ---------- $X_1X_3X_4X_5X_6$ $X_9X_{10}X_{11}$	X_7	Prefilter:X_7 Recursive:$X_{12}X_3$	X_7 X_{12}	X_7 X_8 X_{13} X_5 X_4 X_1 X_3 X_{10} X_{11} X_6 X_9 X_{12} X_2	Prefilter: X_7 Recursive: X_3 X_{13} X_9 X_6 X_5 X_4 X_{12}
F_3 Sensor T_2 Obs(199)	X_3	X_3 ---- X_1 X_2 X_4 X_5 X_6 X_7 X_8 X_9 X_{10} X_{11} X_{12} X_{13}	X_3	Prefilter:X_3 Recursive:X_4	X_3	X_3 X_8 X_2 X_{11} X_{13} X_4 X_1 X_5 X_6 X_9 X_{12} X_7 X_{10}	X_3
F_4 Pump 1 Obs(1571)	X_7 X_{12} influence the whole process.	X_7 X_8 X_{12} ---------- X_5 X_6 X_{11} X_{13}	X_7	Prefilter: X_7 X_{12} Recursive: X_6	X_7 X_{12}	X_7 X_8 X_{12} X_5 X_{13} X_6 X_{11} X_{10}	Prefilter: X_7 X_{12} Recursive: X_9 X_{10} X_6
F_5 Good product thrown away Obs(3053) ========= Obs(3054)	X_{12} X_7 X_4 X_6	X_7 X_8 ---------- X_{12} ========== X_7 X_{12} ---------- X_5 X_6 X_{11} X_{13}	X_7 === X_7	Prefilter: X_7 ====== Prefilter: X_7 X_{12} Recursive: X_6	'X7' === X_7 X_{12}	X_7 X_8 X_{12} X_{11} X_4 ========== X_7 X_{12} X_5 X_{13} X_6 X_9X_2 X_{11}	Prefilter: X_7 ========== Prefilter: X_7 X_{12} Recursive: X_3 X_{13}

TABLE 6.5. Responsible variables for F_1 F_2 F_3 F_4 and F_5 faults according to the different fault diagnosis methods

Faults	**DFT (Bonf Ksim 0.80)**	**DFT(Bonf Ksim 0.95)**	**DFT (Holm Ksim 0.8)**	**DFT (Holm Ksim 0.95)**	**DFT (Hochberg Ksim 0.8)**	**DFT (Hochberg Ksim 0.95)**	**DFT (Hommel Ksim 0.8)**	**DFT (Hommel Ksim 0.95)**	**DFT TCH (Ksim 0.8)**	**DFT TCH (Ksim 0.95)**	**DFT DAP (Ksim 0.8)**	**DFT DAP (Ksim 0.95)**
F_1: X_7: Sensor Flow →0 X_7:182→ 147→ 55 Obs(506) Obs(507) Obs(506) ======== Obs(507)	Detected but no variable found =========== X_7 X_{12}	Detected but no variable found =========== X_7	Detected but no variable found ========== X_7 X_{12}	Detected but no variable found =========== X_7	Detected but no variable found ========== X_7 X_{12}	Detected but no variable found ========== X_7	Detected but no variable found ========== X_7 X_{12}	Detected but no variable found ========== X_7	Detected but no variable found ========== X_7 X_{12}	Detected but no variable found ========== X_7 X_{12}	Detected but no variable found ========== X_7 X_{12}	Detected but no variable found ========== X_7 X_{12}
F_2 Sensor Flow 1500 Obs (902)	X_7 X_{12}	X_7 X_{12}	X_7 X_{12}	X_7 X_{12}	X_7 X_{12}	X_7 X_{12}	X_7 X_{12}	X_7 X_{12}	X_7 X_{12}	X_7 X_{12}	X_7 X_{12}	X_7 X_{12}
F_3 Sensor T_2 Obs(199)	X_3	X_3	X_3	X_3	X_3	X_3	X_3	X_3	X_3	X_3	X_3	X_3
F_4 Pump 1 Obs(1571)	X_7 X_{12}	X_7 X_{12}	X_7 X_{12}	X_7 X_{12}	X_7 X_{12}	X_7 X_{12}	X_7 X_{12}	X_7 X_{12}	X_7 X_{12}	X_7 X_{12}	X_7 X_{12}	X_7 X_{12}
F_5 Good product thrown away Obs(3053) ========= Obs(3054)	X_7 === X_7 X_{12}	X_7 ==== X_7 X_{12}	X_7 ===== X_7 X_{12}	X_7 ===== X_7 X_{12}	X_7 ===== X_7 X_{12}	X_7 ===== X_7 X_{12}	X_7 ===== X_7 X_{12}	X_7 ===== X_7 X_{12}	X_7 ===== X_7 X_{12}	X_7 ===== X_7 X_{12}	X_7 ===== X_7 X_{12}	X_7 ===== X_7 X_{12}

TABLE 6.5. Responsible variables for F_1 F_2 F_3 F_4 and F_5 faults according to the different fault diagnosis methods

Faults	Expected Fault Signals	Montgomery	FRM Montgomery	MTY	MTY1 1.5h
F_1: X_7: Sensor Flow →0 X_7:182→ 147→ 55 Obs(506) Obs(507) Obs(506) ======= Obs(507)	X_7 X_{12}	X_7 X_8 --- X_1 X_3 X_{12} ===== X_7 X_{12} --- X_1 X_2 X_4 X_5 X_8 X_{10} X_{11} X_{13}	Recursive: X_7 ========= Prefilter:X_7 Recursive: X_{12}	Terms : '$T_{3\|13}$' '$T_{3\|4}$' '$T_{3\|6}$' '$T_{3\|7}$' '$T_{3\|8}$' '$T_{3\|12}$' '$T_{4\|3}$' '$T_{4\|7}$' '$T_{6\|3}$' '$T_{6\|7}$' '$T_{7\|3}$' '$T_{7\|4}$' '$T_{7\|6}$' '$T_{7\|13}$' '$T_{7\|8}$' '$T_{7\|9}$' '$T_{7\|10}$' '$T_{7\|11}$' '$T_{7\|12}$' '$T_{8\|3}$' '$T_{8\|7}$' '$T_{9\|7}$' '$T_{10\|7}$' '$T_{11\|7}$' '$T_{12\|7}$' '$T_{13\|3}$' '$T_{13\|7}$' Variables: (Conditional terms) 3 4 6 7 8 9 10 11 12 13 ========== Térms : 'T_7' 'T_{12}' Variables: X_7, X_{12}	Terms : '$T_{3\|13}$' '$T_{3\|4}$' '$T_{3\|6}$' '$T_{3\|7}$' '$T_{3\|8}$' '$T_{3\|12}$' '$T_{4\|3}$' '$T_{4\|7}$' '$T_{6\|3}$' '$T_{6\|7}$' '$T_{7\|3}$' '$T_{7\|4}$' '$T_{7\|6}$' '$T_{7\|13}$' '$T_{7\|8}$' '$T_{7\|9}$' '$T_{7\|10}$' '$T_{7\|11}$' '$T_{7\|12}$' '$T_{8\|3}$' '$T_{8\|7}$' '$T_{9\|7}$' '$T_{10\|7}$' '$T_{11\|7}$' '$T_{12\|7}$' '$T_{13\|3}$' '$T_{13\|7}$' Variables: X_7 (dominant variable loop 2) ========== Térms : 'T_7' 'T_{12}' Variables: X_7, X_{12}
F_2 Sensor Flow 1500 Obs (902)	X_7 X_{12}	X_7 X_8 --- X_1 X_3 X_4 X_5 X_6 X_9 X_{10} X_{11} X_{12} X_{13}	Prefilter:X_7 Recursive:$X_{12}X_3$	Terms = 'T_7' 'T_{12}' (Unconditional terms) Variables: X_7, X_{12}	Terms = 'T_7' 'T_{12}' (Unconditional terms) Variables: X_7, X_{12}
F_3 Sensor T_2 Obs(199)	X_3	X_3 X_{13} X_1 X_2 X_4 X_5 X_6 X_7 X_8 X_9X_{10} X_{12}	Prefilter:X_3 Recursive:X_4	Terms : 'T_3' (Unconditional terms) Variable X_3	Terms : 'T_3' (Unconditional terms) Variable X_3
F_4 Pump 1 Obs(1571)	X_7 X_{12} influence the whole process.	X_7 X_{12} --- X_2 X_5 X_6X_8 X_{10} X_{11} X_{13}	Prefilter: X_7 X_{12} Recursive: X_6	Terms: 'T_7' 'T_{12}' '$T_{4\|6}$' '$T_{6\|4}$' '$T_{6\|13}$' '$T_{6\|10}$' '$T_{6\|11}$' '$T_{8\|13}$' '$T_{8\|10}$' '$T_{8\|11}$' '$T_{10\|6}$' '$T_{10\|8}$' '$T_{11\|6}$' '$T_{11\|8}$' '$T_{13\|6}$' '$T_{13\|8}$ (Unconditional terms) Variables X_7, X_{12} (Conditional terms) Variables X_4,X_6, X_8, X_{10}, X_{11}, X_{13}	Terms: 'T_7' 'T_{12}' '$T_{4\|6}$' '$T_{6\|4}$' '$T_{6\|13}$' '$T_{6\|10}$' '$T_{6\|11}$' '$T_{8\|13}$' '$T_{8\|10}$' '$T_{8\|11}$' '$T_{10\|6}$' '$T_{10\|8}$' '$T_{11\|6}$' '$T_{11\|8}$' '$T_{13\|6}$' '$T_{13\|8}$ (Unconditional terms) Variables X_7, X_{12} (Conditional terms) Variables X_4,X_6, X_8, X_{10}, X_{11}, X_{13}
F_5 Good product thrown away Obs(3053) ======= Obs(3054)	X_{12} X_7 X_4 X_6	X_7 X_8 X_{12} --- X_2 X_5 ========== X_7 X_{12} --- X_2 X_5 X_9 X_{10} X_{11} X_{13}	Prefilter: X_7 X_{12} ========== Prefilter: X_7 X_{12} Recursive: X_6	Terms : 'T_7' (Unconditional terms) Variable 7 ========== Terms : 'T_7' 'T_{12}' '$T_{3\|13}$' '$T_{4\|6}$' '$T_{6\|4}$' (Unconditional terms) Variable X_7 X_{12} (Conditional terms) Variables X_3 X_4 X_6 X_{13}	Terms : 'T_7' (Unconditional terms) Variable X_7 ========== Terms : 'T_7' 'T_{12}' '$T_{3\|13}$' '$T_{4\|6}$' '$T_{6\|4}$' (Unconditional terms) Variable X_7 X_{12} (Conditional terms) Variables X_3 X_4 X_6 X_{13}

6.4 Conclusions

According to the results of the simulation shown in Chapter 4 some of the existing methodologies for fault diagnosis in multivariate statistical quality control tend to present a high false positive rate, especially in scenarios with strong correlations among the variables. In this chapter some variants of these methodologies which successfully solve this problem by reducing their false positive rate have been proposed. The proposed variants of the MTY´s algorithm improve the performance of the original MTY´s algorithm in the strong correlation scenarios C8, C9 and C10. The recursive Hawkins variants give excellent results and improve the original Hawkins´s methodology results. The Montgomery´s and Murphy´s variants also improved the performance of the original proposed algorithms. In the 7 variables simulation the best performance was obtained with the pre-filtered recursive versions of Montgomery´s (FRM) and recursive Hawkins´s methodologies (FRHM). Our conclusion is that the use of the modified Mason *et al´s* method (MTY1) in addition to one of the methods T2FRH or FRM would improve the interpretability of the detected signals.

Chapter 6 Appendices

Appendix 6.1

- **ANOVA for the study of the α_{term} in the MTY method**

Analysis of Variance for PTCo - Type III Sums of Squares

Source	*Sum of Squares*	*Df*	*Mean Square*	*F-Ratio*	*P-Value*
MAIN EFFECTS					
A:SIZE	182,948	2	91,4741	49490,52	0,0000
B:NF	0,48971	2	0,244855	132,47	0,0000
C:M (Alpha)	1,50764	2	0,75382	407,84	0,0000
D:C	1,838	9	0,204222	110,49	0,0000
INTERACTIONS					
AB	1,84075	4	0,460187	248,98	0,0000
AC	22,238	4	5,5595	3007,87	0,0000
AD	0,426198	18	0,0236777	12,81	0,0000
BC	0,962376	4	0,240594	130,17	0,0000
BD	0,655461	18	0,0364145	19,70	0,0000
CD	0,486713	18	0,0270396	14,63	0,0000
RESIDUAL	5,50428	2978	0,00184832		
TOTAL (CORRECTED)	319,762	3059			

Analysis of Variance for PTCv - Type III Sums of Squares

Source	*Sum of Squares*	*Df*	*Mean Square*	*F-Ratio*	*P-Value*
MAIN EFFECTS					
A:SIZE (Alpha)	118,312	2	59,1561	7716,95	0,0000
B:NF	0,626175	2	0,313088	40,84	0,0000
C:M	1,0661	2	0,533048	69,54	0,0000
D:C	24,0206	9	2,66896	348,17	0,0000
INTERACTIONS					
AB	0,792972	4	0,198243	25,86	0,0000
AC	1,1585	4	0,289625	37,78	0,0000
AD	22,2495	18	1,23608	161,25	0,0000
BC	0,122599	4	0,0306496	4,00	0,0031
BD	2,89194	18	0,160664	20,96	0,0000
CD	0,582053	18	0,0323363	4,22	0,0000
RESIDUAL	22,8285	2978	0,00766573		
TOTAL (CORRECTED)	258,306	3059			

Analysis of Variance for PWCo - Type III Sums of Squares

Source	*Sum of Squares*	*Df*	*Mean Square*	*F-Ratio*	*P-Value*
MAIN EFFECTS					
A:SIZE (Alpha)	14,2111	2	7,10556	690,56	0,0000
B:NF	0,159349	2	0,0796743	7,74	0,0004
C:M	7,06616	2	3,53308	343,37	0,0000
D:C	19,9883	9	2,22092	215,84	0,0000
INTERACTIONS					
AB	1,47229	4	0,368073	35,77	0,0000
AC	8,37848	4	2,09462	203,57	0,0000
AD	29,0727	18	1,61515	156,97	0,0000
BC	0,411731	4	0,102933	10,00	0,0000
BD	1,9958	18	0,110878	10,78	0,0000
CD	3,79015	18	0,210564	20,46	0,0000
RESIDUAL	30,6421	2978	0,0102895		
TOTAL (CORRECTED)	139,409	3059			

Analysis of Variance for PWCv - Type III Sums of Squares

Source	*Sum of Squares*	*Df*	*Mean Square*	*F-Ratio*	*P-Value*
MAIN EFFECTS					
A:Size	6,85965	2	3,42983	1247,00	0,0000
B:NF	0,715151	2	0,357575	130,01	0,0000
C:M	0,279057	2	0,139529	50,73	0,0000
D:C	13,1048	9	1,45609	529,40	0,0000
INTERACTIONS					
AB	0,394851	4	0,0987126	35,89	0,0000
AC	1,72505	4	0,431263	156,80	0,0000
AD	11,3585	18	0,631026	229,43	0,0000
BC	0,0286039	4	0,00715097	2,60	0,0344
BD	0,888107	18	0,0493393	17,94	0,0000
CD	0,5788	18	0,0321555	11,69	0,0000
RESIDUAL	8,19089	2978	0,00275047		
TOTAL (CORRECTED)	57,0635	3059			

Analysis of Variance for PNF - Type III Sums of Squares

Source	*Sum of Squares*	*Df*	*Mean Square*	*F-Ratio*	*P-Value*
MAIN EFFECTS					
A:Size	0,307145	2	0,153572	337,79	0,0000
B:NF	0,00467091	2	0,00233545	5,14	0,0059
C:M	0,588999	2	0,2945	647,76	0,0000
D:C	0,0575008	9	0,00638898	14,05	0,0000
INTERACTIONS					
AB	0,00509837	4	0,00127459	2,80	0,0244
AC	0,91389	4	0,228472	502,53	0,0000
AD	0,120738	18	0,00670764	14,75	0,0000
BC	0,00935442	4	0,00233861	5,14	0,0004
BD	0,0226642	18	0,00125912	2,77	0,0001
CD	0,177711	18	0,00987281	21,72	0,0000
RESIDUAL	1,35392	2978	0,000454642		
TOTAL (CORRECTED)	3,93125	3059			

Analysis of Variance for PND - Type III Sums of Squares

Source	*Sum of Squares*	*Df*	*Mean Square*	*F-Ratio*	*P-Value*
MAIN EFFECTS					
A:Size	53,5205	2	26,7603	2140,15	0,0000
B:NF	6,5139	2	3,25695	260,47	0,0000
C:M	0	2	0	0,00	1,0000
D:C	22,6847	9	2,52052	201,58	0,0000
INTERACTIONS					
AB	4,73298	4	1,18324	94,63	0,0000
AC	0	4	0	0,00	1,0000
AD	31,2056	18	1,73364	138,65	0,0000
BC	0	4	0	0,00	1,0000
BD	4,91315	18	0,272953	21,83	0,0000
CD	0	18	0	0,00	1,0000
RESIDUAL	37,2367	2978	0,0125039		
TOTAL (CORRECTED)	182,23	3059			

.

- **ANOVA for MTY and MTY1 methods**

Analysis of Variance for PTCo - Type III Sums of Squares

Source	*Sum of Squares*	*Df*	*Mean Square*	*F-Ratio*	*P-Value*
MAIN EFFECTS					
A:Size	234,798	2	117,399	85243,17	0,0000
B:NF	0,959856	2	0,479928	348,47	0,0000
C:M	0,314336	3	0,104779	76,08	0,0000
D:C	7,2976	9	0,810845	588,75	0,0000
INTERACTIONS					
AB	3,53314	4	0,883286	641,35	0,0000
AC	0,308542	6	0,0514237	37,34	0,0000
AD	3,26813	18	0,181563	131,83	0,0000
BC	0,00967816	6	0,00161303	1,17	0,3186
BD	1,70256	18	0,0945867	68,68	0,0000
CD	0,665647	27	0,0246536	17,90	0,0000
RESIDUAL	5,48686	3984	0,00137722		
TOTAL (CORRECTED)	397,768	4079			

Analysis of Variance for PTCv - Type III Sums of Squares

Source	*Sum of Squares*	*Df*	*Mean Square*	*F-Ratio*	*P-Value*
MAIN EFFECTS					
A:Size	158,839	2	79,4194	13289,23	0,0000
B:NF	0,664828	2	0,332414	55,62	0,0000
C:M	0,0690623	3	0,0230208	3,85	0,0091
D:C	28,3388	9	3,14875	526,88	0,0000
INTERACTIONS					
AB	1,14228	4	0,28557	47,78	0,0000
AC	0,154709	6	0,0257848	4,31	0,0002
AD	26,2928	18	1,46071	244,42	0,0000
BC	0,0091153	6	0,00151922	0,25	0,9578
BD	3,86147	18	0,214526	35,90	0,0000
CD	0,0696832	27	0,00258086	0,43	0,9954
RESIDUAL	23,8093	3984	0,00597622		
TOTAL (CORRECTED)	328,996	4079			

Analysis of Variance for PWCo - Type III Sums of Squares

Source	*Sum of Squares*	*Df*	*Mean Square*	*F-Ratio*	*P-Value*
MAIN EFFECTS					
A:Size	13,5072	2	6,75359	955,26	0,0000
B:NF	0,0132694	2	0,00663472	0,94	0,3913
C:M	0,74168	3	0,247227	34,97	0,0000
D:C	15,2621	9	1,69579	239,86	0,0000
INTERACTIONS					
AB	1,54425	4	0,386064	54,61	0,0000
AC	0,661113	6	0,110186	15,59	0,0000
AD	28,8847	18	1,60471	226,98	0,0000
BC	0,020703	6	0,00345049	0,49	0,8177
BD	2,33016	18	0,129453	18,31	0,0000
CD	1,36635	27	0,0506054	7,16	0,0000
RESIDUAL	28,1666	3984	0,00706992		
TOTAL (CORRECTED)	109,442	4079			

Analysis of Variance for PWCv - Type III Sums of Squares

Source	*Sum of Squares*	*Df*	*Mean Square*	*F-Ratio*	*P-Value*
MAIN EFFECTS					
A:Size	5,83109	2	2,91555	1962,24	0,0000
B:NF	0,714281	2	0,35714	240,36	0,0000
C:M	0,671424	3	0,223808	150,63	0,0000
D:C	7,71137	9	0,856819	576,66	0,0000
INTERACTIONS					
AB	0,431385	4	0,107846	72,58	0,0000
AC	0,515733	6	0,0859554	57,85	0,0000
AD	8,5721	18	0,476228	320,51	0,0000
BC	0,0178877	6	0,00298129	2,01	0,0614
BD	1,03021	18	0,0572337	38,52	0,0000
CD	1,51861	27	0,0562447	37,85	0,0000
RESIDUAL	5,91953	3984	0,00148583		
TOTAL (CORRECTED)	42,0248	4079			

- **ANOVA for MTY variants; MTY1 and MTY2**

Analysis of Variance for PTCo - Type III Sums of Squares

Source	*Sum of Squares*	*Df*	*Mean Square*	*F-Ratio*	*P-Value*
MAIN EFFECTS					
A:Size	177,715	2	88,8576	62097,24	0,0000
B:NF	0,611249	2	0,305624	213,58	0,0000
C:C	3,81496	9	0,423884	296,23	0,0000
D:M	0,339078	2	0,169539	118,48	0,0000
INTERACTIONS					
AB	2,38556	4	0,596389	416,78	0,0000
AC	1,29987	18	0,0722148	50,47	0,0000
AD	0,353679	4	0,0884198	61,79	0,0000
BC	1,14775	18	0,0637641	44,56	0,0000
BD	0,0121034	4	0,00302585	2,11	0,0764
CD	0,704553	18	0,0391418	27,35	0,0000
RESIDUAL	4,26135	2978	0,00143094		
TOTAL (CORRECTED)	295,824	3059			

Analysis of Variance for PTCv - Type III Sums of Squares

Source	*Sum of Squares*	*Df*	*Mean Square*	*F-Ratio*	*P-Value*
MAIN EFFECTS					
A:Size	120,721	2	60,3603	10160,20	0,0000
B:NF	0,45432	2	0,22716	38,24	0,0000
C:C	20,8008	9	2,3112	389,03	0,0000
D:M	0,063393	2	0,0316965	5,34	0,0049
INTERACTIONS					
AB	0,843852	4	0,210963	35,51	0,0000
AC	19,0943	18	1,0608	178,56	0,0000
AD	0,143431	4	0,0358578	6,04	0,0001
BC	2,90138	18	0,161188	27,13	0,0000
BD	0,0087465	4	0,00218663	0,37	0,8315
CD	0,0663146	18	0,00368415	0,62	0,8869
RESIDUAL	17,6919	2978	0,00594086		
TOTAL (CORRECTED)	248,061	3059			

Analysis of Variance for PWCo - Type III Sums of Squares

Source	*Sum of Squares*	*Df*	*Mean Square*	*F-Ratio*	*P-Value*
MAIN EFFECTS					
A:Size	11,213	2	5,60649	760,40	0,0000
B:NF	0,00465245	2	0,00232622	0,32	0,7294
C:C	12,9806	9	1,44229	195,62	0,0000
D:M	0,802583	2	0,401292	54,43	0,0000
INTERACTIONS					
AB	1,04116	4	0,260291	35,30	0,0000
AC	22,9041	18	1,27245	172,58	0,0000
AD	0,68122	4	0,170305	23,10	0,0000
BC	1,70359	18	0,0946437	12,84	0,0000
BD	0,0143239	4	0,00358097	0,49	0,7463
CD	1,48538	18	0,0825213	11,19	0,0000
RESIDUAL	21,957	2978	0,00737307		
TOTAL (CORRECTED)	89,0972	3059			

Analysis of Variance for PWCv - Type III Sums of Squares

Source	*Sum of Squares*	*Df*	*Mean Square*	*F-Ratio*	*P-Value*
MAIN EFFECTS					
A:Size	3,80792	2	1,90396	1334,32	0,0000
B:NF	0,420584	2	0,210292	147,37	0,0000
C:C	5,46117	9	0,606796	425,25	0,0000
D:M	0,684874	2	0,342437	239,98	0,0000
INTERACTIONS					
AB	0,255428	4	0,0638571	44,75	0,0000
AC	5,59211	18	0,310673	217,72	0,0000
AD	0,522501	4	0,130625	91,54	0,0000
BC	0,595897	18	0,0331054	23,20	0,0000
BD	0,0132503	4	0,00331258	2,32	0,0546
CD	1,50662	18	0,0837011	58,66	0,0000
RESIDUAL	4,24936	2978	0,00142692		
TOTAL (CORRECTED)	29,3187	3059			

Appendix 6.2

- **ANOVA for Hawkins´ method and its variants**

Analysis of Variance for PTCo - Type III Sums of Squares

Source	*Sum of Squares*	*Df*	*Mean Square*	*F-Ratio*	*P-Value*
MAIN EFFECTS					
A:Size	107,298	2	53,649	2875,40	0,0000
B:NF	45,5102	2	22,7551	1219,59	0,0000
C:M	90,2703	3	30,0901	1612,72	0,0000
D:C	3,22521	9	0,358357	19,21	0,0000
INTERACTIONS					
AB	2,81527	4	0,703817	37,72	0,0000
AC	87,4671	6	14,5779	781,32	0,0000
AD	16,7904	18	0,9328	49,99	0,0000
BC	27,1633	6	4,52722	242,64	0,0000
BD	1,58906	18	0,0882809	4,73	0,0000
CD	26,8957	27	0,996135	53,39	0,0000
RESIDUAL	74,3332	3984	0,0186579		
TOTAL (CORRECTED)	614,047	4079			

Analysis of Variance for PTCv - Type III Sums of Squares

Source	*Sum of Squares*	*Df*	*Mean Square*	*F-Ratio*	*P-Value*
MAIN EFFECTS					
A:Size	134,459	2	67,2294	3574,09	0,0000
B:NF	11,1891	2	5,59457	297,42	0,0000
C:M	32,9573	3	10,9858	584,03	0,0000
D:C	21,5907	9	2,39896	127,54	0,0000
INTERACTIONS					
AB	0,75208	4	0,18802	10,00	0,0000
AC	26,417	6	4,40283	234,07	0,0000
AD	20,524	18	1,14022	60,62	0,0000
BC	11,1495	6	1,85826	98,79	0,0000
BD	8,55385	18	0,475214	25,26	0,0000
CD	6,58231	27	0,243789	12,96	0,0000
RESIDUAL	74,9399	3984	0,0188102		
TOTAL (CORRECTED)	452,578	4079			

Analysis of Variance for PWCo - Type III Sums of Squares

Source	*Sum of Squares*	*Df*	*Mean Square*	*F-Ratio*	*P-Value*
MAIN EFFECTS					
A:Size	0,159761	2	0,0798803	2,87	0,0571
B:NF	2,11714	2	1,05857	37,97	0,0000
C:M	133,909	3	44,6364	1601,00	0,0000
D:C	36,9593	9	4,10659	147,29	0,0000
INTERACTIONS					
AB	0,0884309	4	0,0221077	0,79	0,5296
AC	15,7038	6	2,6173	93,88	0,0000
AD	5,42728	18	0,301516	10,81	0,0000
BC	0,938757	6	0,156459	5,61	0,0000
BD	4,55531	18	0,253073	9,08	0,0000
CD	44,5652	27	1,65056	59,20	0,0000
RESIDUAL	111,076	3984	0,0278804		
TOTAL (CORRECTED)	437,149	4079			

Analysis of Variance for PWCv - Type III Sums of Squares

Source	*Sum of Squares*	*Df*	*Mean Square*	*F-Ratio*	*P-Value*
MAIN EFFECTS					
A:Size	0,177053	2	0,0885266	4,31	0,0134
B:NF	4,65518	2	2,32759	113,43	0,0000
C:M	82,1506	3	27,3835	1334,51	0,0000
D:C	35,4626	9	3,94029	192,03	0,0000
INTERACTIONS					
AB	0,0520432	4	0,0130108	0,63	0,6382
AC	8,39187	6	1,39865	68,16	0,0000
AD	1,96549	18	0,109194	5,32	0,0000
BC	1,61915	6	0,269858	13,15	0,0000
BD	3,72273	18	0,206819	10,08	0,0000
CD	74,1977	27	2,74806	133,92	0,0000
RESIDUAL	81,7501	3984	0,0205196		
TOTAL (CORRECTED)	348,192	4079			

Appendix 6.3

- **ANOVA for Murphys´ method and its variants**

Analysis of Variance for PTCo - Type III Sums of Squares

Source	*Sum of Squares*	*Df*	*Mean Square*	*F-Ratio*	*P-Value*
MAIN EFFECTS					
A:Size	149,686	2	74,8431	3430,54	0,0000
B:NF	11,5123	2	5,75613	263,84	0,0000
C:C	1,06058	9	0,117842	5,40	0,0000
D:M	68,4715	3	22,8238	1046,16	0,0000
INTERACTIONS					
AB	1,68154	4	0,420386	19,27	0,0000
AC	16,1889	18	0,899383	41,22	0,0000
AD	45,7772	6	7,62954	349,71	0,0000
BC	1,27448	18	0,0708042	3,25	0,0000
BD	5,38618	6	0,897697	41,15	0,0000
CD	17,8577	27	0,661395	30,32	0,0000
RESIDUAL	86,9177	3984	0,0218167		
TOTAL (CORRECTED)	515,872	4079			

Analysis of Variance for PTCv - Type III Sums of Squares

Source	*Sum of Squares*	*Df*	*Mean Square*	*F-Ratio*	*P-Value*
MAIN EFFECTS					
A:Size	175,106	2	87,5532	8597,17	0,0000
B:NF	0,251661	2	0,125831	12,36	0,0000
C:C	29,6047	9	3,28941	323,00	0,0000
D:M	2,1434	3	0,714465	70,16	0,0000
INTERACTIONS					
AB	0,795823	4	0,198956	19,54	0,0000
AC	25,5504	18	1,41947	139,38	0,0000
AD	4,33764	6	0,72294	70,99	0,0000
BC	2,75131	18	0,152851	15,01	0,0000
BD	0,254925	6	0,0424875	4,17	0,0003
CD	3,82727	27	0,141751	13,92	0,0000
RESIDUAL	40,5729	3984	0,0101839		
TOTAL (CORRECTED)	375,772	4079			

Analysis of Variance for PWCo - Type III Sums of Squares

Source	*Sum of Squares*	*Df*	*Mean Square*	*F-Ratio*	*P-Value*
MAIN EFFECTS					
A:Size	0,0647115	2	0,0323558	1,06	0,3457
B:NF	4,54887	2	2,27444	74,68	0,0000
C:C	42,0696	9	4,6744	153,49	0,0000
D:M	93,9981	3	31,3327	1028,84	0,0000
INTERACTIONS					
AB	0,195993	4	0,0489982	1,61	0,1691
AC	10,9626	18	0,609034	20,00	0,0000
AD	22,3479	6	3,72465	122,30	0,0000
BC	4,03636	18	0,224242	7,36	0,0000
BD	4,90529	6	0,817548	26,85	0,0000
CD	33,2028	27	1,22973	40,38	0,0000
RESIDUAL	121,33	3984	0,0304543		
TOTAL (CORRECTED)	401,712	4079			

Analysis of Variance for PWCv - Type III Sums of Squares

Source	*Sum of Squares*	*Df*	*Mean Square*	*F-Ratio*	*P-Value*
MAIN EFFECTS					
A:Size	1,19423	2	0,597115	36,20	0,0000
B:NF	3,53007	2	1,76503	107,00	0,0000
C:C	31,9297	9	3,54774	215,07	0,0000
D:M	86,6656	3	28,8885	1751,24	0,0000
INTERACTIONS					
AB	0,105968	4	0,026492	1,61	0,1699
AC	2,78752	18	0,154862	9,39	0,0000
AD	9,34879	6	1,55813	94,45	0,0000
BC	2,95016	18	0,163898	9,94	0,0000
BD	1,97736	6	0,329559	19,98	0,0000
CD	70,3836	27	2,6068	158,03	0,0000
RESIDUAL	65,7204	3984	0,0164961		
TOTAL (CORRECTED)	332,634	4079			

Appendix 6.4

- **ANOVA for Montgomery and Runger´s method and its variants**

Analysis of Variance for PTCo - Type III Sums of Squares

Source	*Sum of Squares*	*Df*	*Mean Square*	*F-Ratio*	*P-Value*
MAIN EFFECTS					
A:Size	223,449	2	111,724	4885,72	0,0000
B:NF	35,5619	2	17,781	777,56	0,0000
C:C	5,32549	9	0,591722	25,88	0,0000
D:M	86,2649	4	21,5662	943,09	0,0000
INTERACTIONS					
AB	6,20175	4	1,55044	67,80	0,0000
AC	36,1585	18	2,00881	87,85	0,0000
AD	67,6837	8	8,46046	369,98	0,0000
BC	5,65709	18	0,314283	13,74	0,0000
BD	11,9099	8	1,48874	65,10	0,0000
CD	36,1127	36	1,00313	43,87	0,0000
RESIDUAL	114,109	4990	0,0228676		
TOTAL (CORRECTED)	812,874	5099			

Analysis of Variance for PTCv - Type III Sums of Squares

Source	*Sum of Squares*	*Df*	*Mean Square*	*F-Ratio*	*P-Value*
MAIN EFFECTS					
A:Size	256,609	2	128,305	7769,56	0,0000
B:NF	1,54451	2	0,772253	46,76	0,0000
C:C	32,8048	9	3,64497	220,72	0,0000
D:M	2,16588	4	0,54147	32,79	0,0000
INTERACTIONS					
AB	0,626814	4	0,156704	9,49	0,0000
AC	24,103	18	1,33905	81,09	0,0000
AD	9,51185	8	1,18898	72,00	0,0000
BC	8,04888	18	0,44716	27,08	0,0000
BD	0,752452	8	0,0940564	5,70	0,0000
CD	5,15565	36	0,143213	8,67	0,0000
RESIDUAL	82,4037	4990	0,0165138		
TOTAL (CORRECTED)	566,03	5099			

Analysis of Variance for PWCo - Type III Sums of Squares

Source	*Sum of Squares*	*Df*	*Mean Square*	*F-Ratio*	*P-Value*
MAIN EFFECTS					
A:Size	0,680175	2	0,340088	10,36	0,0000
B:NF	7,3868	2	3,6934	112,53	0,0000
C:C	47,7293	9	5,30326	161,58	0,0000
D:M	125,63	4	31,4075	956,91	0,0000
INTERACTIONS					
AB	0,782128	4	0,195532	5,96	0,0001
AC	3,15169	18	0,175094	5,33	0,0000
AD	30,5274	8	3,81593	116,26	0,0000
BC	6,10142	18	0,338968	10,33	0,0000
BD	8,16538	8	1,02067	31,10	0,0000
CD	54,4009	36	1,51114	46,04	0,0000
RESIDUAL	163,781	4990	0,0328218		
TOTAL (CORRECTED)	550,512	5099			

Analysis of Variance for PWCv - Type III Sums of Squares

Source	*Sum of Squares*	*Df*	*Mean Square*	*F-Ratio*	*P-Value*
MAIN EFFECTS					
A:Size	2,74342	2	1,37171	74,95	0,0000
B:NF	3,88795	2	1,94398	106,22	0,0000
C:C	33,8282	9	3,75869	205,37	0,0000
D:M	90,2125	4	22,5531	1232,27	0,0000
INTERACTIONS					
AB	0,435235	4	0,108809	5,95	0,0001
AC	2,20043	18	0,122246	6,68	0,0000
AD	13,4958	8	1,68698	92,17	0,0000
BC	3,21265	18	0,17848	9,75	0,0000
BD	4,46277	8	0,557847	30,48	0,0000
CD	83,58	36	2,32167	126,85	0,0000
RESIDUAL	91,3273	4990	0,0183021		
TOTAL (CORRECTED)	397,723	5099			

Appendix 6.5

- **ANOVA for best methods**

Analysis of Variance for PTCo - Type III Sums of Squares

Source	*Sum of Squares*	*Df*	*Mean Square*	*F-Ratio*	*P-Value*
MAIN EFFECTS					
A:Size	340,539	2	170,269	43360,85	0,0000
B:NF	8,20443	2	4,10222	1044,67	0,0000
C:C	15,9169	9	1,76854	450,38	0,0000
D:M	6,05737	4	1,51434	385,64	0,0000
INTERACTIONS					
AB	8,57647	4	2,14412	546,02	0,0000
AC	11,7037	18	0,650207	165,58	0,0000
AD	5,35867	8	0,669834	170,58	0,0000
BC	2,49	18	0,138333	35,23	0,0000
BD	2,36598	8	0,295747	75,32	0,0000
CD	2,72464	36	0,0756845	19,27	0,0000
RESIDUAL	19,5947	4990	0,0039268		
TOTAL (CORRECTED)	639,756	5099			

Analysis of Variance for PTCv - Type III Sums of Squares

Source	*Sum of Squares*	*Df*	*Mean Square*	*F-Ratio*	*P-Value*
MAIN EFFECTS					
A:Size	245,741	2	122,87	20441,25	0,0000
B:NF	0,0123855	2	0,00619277	1,03	0,3570
C:C	32,2028	9	3,57809	595,27	0,0000
D:M	3,71077	4	0,927692	154,33	0,0000
INTERACTIONS					
AB	0,914106	4	0,228527	38,02	0,0000
AC	23,6654	18	1,31474	218,73	0,0000
AD	3,97778	8	0,497223	82,72	0,0000
BC	3,99779	18	0,222099	36,95	0,0000
BD	0,625118	8	0,0781397	13,00	0,0000
CD	0,377585	36	0,0104885	1,74	0,0039
RESIDUAL	29,9944	4990	0,0060109		
TOTAL (CORRECTED)	482,177	5099			

Analysis of Variance for PWCo - Type III Sums of Squares

Source	*Sum of Squares*	*Df*	*Mean Square*	*F-Ratio*	*P-Value*
MAIN EFFECTS					
A:Size	12,8512	2	6,4256	1068,65	0,0000
B:NF	0,146965	2	0,0734824	12,22	0,0000
C:C	11,9678	9	1,32976	221,15	0,0000
D:M	24,11	4	6,02749	1002,44	0,0000
INTERACTIONS					
AB	0,684322	4	0,171081	28,45	0,0000
AC	17,763	18	0,986832	164,12	0,0000
AD	2,26813	8	0,283517	47,15	0,0000
BC	1,89609	18	0,105338	17,52	0,0000
BD	0,115674	8	0,0144592	2,40	0,0138
CD	2,85528	36	0,0793134	13,19	0,0000
RESIDUAL	30,0039	4990	0,00601281		
TOTAL (CORRECTED)	129,49	5099			

Analysis of Variance for PWCv - Type III Sums of Squares

Source	*Sum of Squares*	*Df*	*Mean Square*	*F-Ratio*	*P-Value*
MAIN EFFECTS					
A:Size	3,27724	2	1,63862	921,67	0,0000
B:NF	1,20901	2	0,604505	340,01	0,0000
C:C	4,05852	9	0,450946	253,64	0,0000
D:M	4,98126	4	1,24531	700,44	0,0000
INTERACTIONS					
AB	0,424403	4	0,106101	59,68	0,0000
AC	4,13551	18	0,229751	129,23	0,0000
AD	1,54207	8	0,192758	108,42	0,0000
BC	0,708777	18	0,0393765	22,15	0,0000
BD	0,633616	8	0,079202	44,55	0,0000
CD	3,50275	36	0,0972987	54,73	0,0000
RESIDUAL	8,87168	4990	0,00177789		
TOTAL (CORRECTED)	40,9285	5099			

Appendix 6.6

TABLE 1: Selection of the number of standard deviations (*nd*) to use in the construction of the UCL in Recursive Hawkins´ Methodology (RH) in order to get an overall Type I risk $\alpha_{overall}=0.05$ in the 10 correlation matrix scenarios. The final selection is in **bold** font.

	nd														
Mcorr (Ci)	2.36	2.38	2.39	2.50	2.51	2.6	2.61	2.62	2.63	2.64	2.65	2.66	2.67	2.68	2.69
C1	0.1214	0.1153	0.1128		0.0816	0.0638	0.0617	0.06	0.0584	0.0568	0.0552	0.0535	0.0518	**0.0502**	0.0487
C2	0.1196	0.1138	0.1108		0.0804	0.0629	0.0614	0.0597	0.0578	0.056	0.0545	0.0529	0.0513	**0.0501**	0.0485
C3	**0.0495**	0.0472	0.0462		0.034	0.0272	0.0262	0.0255	0.0247	0.024	0.0234	0.0226	0.0221	0.0217	0.0211
C4	0.1067	0.1017	0.0994		0.0728	0.0572	0.0554	0.0537	0.0523	0.0511	**0.0499**	0.0487	0.0475	0.0461	0.0446
C5	0.1126	0.1072	0.1046		0.076	0.0586	0.057	0.0555	0.0541	0.0527	0.0512	**0.0495**	0.0482	0.0466	0.0453
C6	0.1046	0.0994	0.0968		0.0692	0.0539	0.0523	0.051	**0.0495**	**0.0481**	0.047	0.0457	0.0446	0.0433	0.042
C7	0.0522	**0.05**	0.0487		0.0361	0.0283	0.0276	0.0269	0.0263	0.0255	0.0248	0.0242	0.0236	0.0231	0.0226
C8	0.1105	0.1048	0.1022		0.0744	0.0583	0.0567	0.0553	0.054	0.0526	0.0511	**0.0495**	0.0482	0.0471	0.0456
C9	0.0731	0.0699	0.0683	**0.05**	**0.0495**	0.0385	0.0375	0.0365	0.0356	0.0346	0.0337	0.0328	0.0319	0.0312	0.0304
C10	0.0526	**0.0501**	**0.049**		0.0357	0.0282	0.0274	0.0266	0.0259	0.0254	0.0248	0.0241	0.0232	0.0223	0.0215

TABLE 2: Selection of the number of standard deviations (*nd*) to use in the construction of the UCL in Prefiltered Recursive Hawkins´ Methodology (FRH) in order to get an overall Type I risk ($\alpha_{overall}=0.05$) in the 10 correlation matrix scenarios. The final selection is in **bold** font.

	nd																	
Mcorr	**2.7**	**2.71**	**2.72**	**2.73**	**2.74**	**2.75**	**2.76**	**2.77**	**2.78**	**2.79**	**2.8**	**2.81**	**2.82**	**2.83**	**2.84**	**2.85**	**2.89**	**2.9**
C1	0.0565	0.0551	0.0533	0.052	0.0503	**0.049**	0.0475	0.0461	0.0448	0.0435	0.042	0.0407	0.0396	0.0388	0.0374	0.0363	0.0322	0.0313
C2	0.0699	0.0684	0.0665	0.0648	0.0631	0.061	0.0593	0.0576	0.0558	0.0542	0.0527	**0.0512**	**0.0498**	0.0486	0.0471	0.0457	0.0409	0.0397
C3	0.0642	0.0625	0.0607	0.0592	0.0575	0.056	0.0545	0.0532	0.0515	**0.0499**	0.0485	0.0471	0.0455	0.0441	0.0427	0.0413	0.0369	0.0355
C4	0.0748	0.0731	0.0713	0.0694	0.0676	0.0657	0.0641	0.0624	0.0604	0.0586	0.0572	0.0553	0.0539	0.0525	**0.051**	0.0495	0.0445	0.0431
C5	0.061	0.0592	0.0575	0.0557	0.0543	0.0524	0.0509	**0.0491**	0.0478	0.0463	0.0452	0.044	0.043	0.0415	0.0404	0.0393	0.0348	0.0339
C6	0.0683	0.0667	0.0648	0.0628	0.061	0.0595	0.0574	0.0558	0.0546	0.053	0.0517	**0.0504**	0.0487	0.0473	0.046	0.0445	0.0394	0.0383
C7	0.062	0.0604	0.0585	0.0568	0.0552	0.0535	0.0521	**0.0508**	**0.0494**	0.0482	0.0468	0.0456	0.0439	0.0426	0.0415	0.0402	0.0359	0.0348
C8	0.0719	0.0705	0.069	0.0672	0.0656	0.0639	0.0621	0.0606	0.0586	0.0571	0.0554	0.0541	0.0527	**0.0509**	**0.0494**	0.0481	0.0423	0.041
C9	0.0583	0.0566	0.0554	0.0536	0.0522	**0.0508**	**0.0495**	0.0481	0.0468	0.0457	0.0443	0.043	0.0418	0.0405	0.0394	0.0382	0.0338	0.0329
C10	0.0606	0.0589	0.0573	0.0555	0.0542	0.0525	0.0511	**0.0495**	0.0482	0.0469	0.0452	0.0438	0.0427	0.0415	0.0401	0.0389	0.0347	0.0336

Part III

Fault diagnosis in latent-based multivariate statistical process control (Lb-MSPC)

The second part, including chapters 7 to 9, is concerned with the Multivariate Statistical Process Control (MSPC). In this part we are going to consider data rich environments (scenario 3 described in section 2.3.2**)** where the MSPC is the preferred option for monitoring the process. The methods discussed in this thesis are defined in the latent variables space and perform reasonably well when there is a great number of correlated process variables with an ill-conditioned covariance matrix.

Our research in this part has produced the following results:

Conferences

- "A comparative study of different methodologies for supervised fault diagnosis in multivariate statistical process control". *Proceedings of the 12th Annual Conference of the European Network for Business and Industrial Statistics 2013 (ENBIS) Linz, Austria*
- "Fingerprints contribution plot: A new approach for fault diagnosis in multivariate statistic process control" *11th International Conference on Chemometrics in Analytical Chemistry (CAC 2008) Montpellier, France.*
- "Diagnóstico de fallos basado en una estrategia combinada: PLS Discriminante SIMCA" *XXX Congreso Nacional de Estadística e Investigación Operativa" 2007 (SEIO) Valladolid, Spain*
- "Fault diagnosis in the on-line monitoring of a pasteurisation process: a comparative study of different strategies". *Proceedings of the 5th Annual Conference of the European Network for Business and Industrial Statistics 2005 (ENBIS), Newcastle, UK.*

Chapter 7: Fault diagnosis methods in MSPC

This chapter gives a description of the most common methods used for fault diagnosis in supervised MSPC. The chapter describes the rationale of the different methods and shows the requirements for their implementation, their strong points and their drawbacks.

7.1 Introduction

At the end of the last century initiated a great technological revolution enabled by the explosive innovations in electronics and communication determining that computers, sensors and measure devices have become increasingly cheaper. This has been traduced into a growing automatization of the industrial processes. It has also permitted to record on line a large quantity of process variables stored at a frequency of milliseconds. This improved process information can be added to the information provided by productivity and quality variables, which are measured at a much lower frequency (usually off-line) and frequently requiring costly laboratory testing. The real challenge nowadays is how to manage such a big quantity of correlated information. To use only the quality variables to monitor the processes would lose a lot of information about the process and would certainly make more difficult to identify the root causes of the different faults affecting the processes. Thus the inclusion of process variables in the monitoring scheme is a key step in the adaptation of the statistical process control to modern highly automated environments. The on-line measurements of process variables characterised by high sample rate, reduced cost (compared to diagnostic *laboratory testing*) and greater sensitivity than process anomalies, contribute to reduce the reaction speed and helps the diagnosis of the root causes.

In this data rich environments specific and adapted statistical tools are required. The classical statistical tools present some difficulties when they are applied in this context. The first problem is the data dimensionality. The matrices of data in continuous processes have a large dimensionality. In continuous processes it is frequent to measure hundreds or even thousands of variables every few seconds and dozens of quality variables every few hours. Moreover, the advances in measuring technology are allowing to measure quality variables on-line (every few minutes). A second problem is the collinearity. The

real dimensionality of what is happening in our processes is much lower than the apparent high dimensionality of the collected data. The common causes of variability are controlled by a much lower number of independent latent variables (not explicitly measurable) which express themselves through the hundreds or thousands of measured variables and, consequently, causes a strong correlation among them. A third problem is the noise. All the variables (process or quality variables) are measured with error (sampling error, measuring error, …). As they are measured under normal operating conditions is logical to have a small signal-to-noise ratio in each variable given that the objective of the operators is to keep the process on the target trajectory. A fourth problem is the missing data. The high automatization is the cause of the abundance of missing data in the collected data bases (sometimes even to a 20%). These missing data are due to sensors malfunctions, sensor maintenance and delays in the analysis of laboratory. In addition to all these problem there is another important problem, the ill-conditioning of the covariance matrix. The classical methods need to invert the covariance matrix and this becomes a big problem when this matrix is so ill-conditioned.

To overcome all of these problems is necessary a new set of statistical tools able to manage this type of data. The use of latent variable models (PCA, PLS) for monitoring and fault diagnosis in this context has been proved superior. Thus a great number of successful applications has been proposed in the last decade (MacGregor *et al*. 1991 and 1994, MacGregor and Kourti 1995 and Kourti and MacGregor 1996). In particular, the contribution plot (MacGregor *et al.*1994 and Miller *et al.* 1993) (described in Section 1.3.2) on scores and the square prediction error *(SPE)* are excellent options, particularly when there is no information about the different types of fault. The contribution plots is the most widespread unsupervised diagnosis method in Lb_MSPC. It must be noted that the unsupervised methods only decide which variables are involved in the fault and then

the process engineers have to search for the root causes of the fault. The existence of available information about the different types of faults make possible the use of a new set of tools or methods for fault diagnosis that incorporate the available information in their diagnosis procedures. These methods, are known as supervised fault diagnosis methodologies and it must be noted that these methods can address directly the root causes in the diagnosis stage. These methods are the focus of our research in the second part of this thesis. As it was commented in the *state of the art (*Chapter 1), the USPC and classical MSPC do not work in the context of rich environments. It is in rich environments context where a multivariate statistical process control (Lb_MSPC), based on statistical techniques that use the projection to latent structures such as Principal Component Analysis (PCA) (Jackson 1991) and the Partial Least Squares, (PLS) (Geladi and Kowalski 1986), (Wold *et al.* 1987) become interesting options *i.e*. Moreover, these methods work well in data rich environments, do not require first principle models and are widely implanted in the industry.

Although we have limited our study to methods based on Lb_MSPC, it is important to point out that the list of methods used remains quite extensive (Section 1.1.2.2). In my thesis I have prioritized methods widely referenced and successfully applied in different contexts (Qin 2012, Russell *et al.* 2012 and MacGregor and Cinar 2012)

In Chapter I review the following methods for supervised fault diagnosis in Lb_MSPC: a) classification techniques based on the use of PLSDA (partial least squares discriminant analysis) (Sjöström *et al.* 1985), b) fault signatures (Yoon and MacGregor 2001), c) fault reconstruction methodology (Dunia and Qin 1998), and d) fault reconstruction using a single combined index that integrates the *SPE* and T^2_A (Yue and Qin 2001).

7.2 Fault detection on a latent based model

Based on the PCA model an observation vector $\mathbf{x}$ $(K \times 1)$ can be decomposed into a modeled $(\hat{\mathbf{x}})$ and $(\tilde{\mathbf{x}})$ unmodeled part so that $\mathbf{x} = \hat{\mathbf{x}} + \tilde{\mathbf{x}}$ where $\hat{\mathbf{x}}$ is the projection of $\mathbf{x}$ in the principal component subspace (S_{model}) of dimension $A \leq K$ and $\tilde{\mathbf{x}}$ is the projection of $\mathbf{x}$ in the residual subspace ($S_{residual}$) of dimension K-A:

$$\hat{\mathbf{x}} = \mathbf{Pt} = \mathbf{PP^T x} = \mathbf{Cx} \in S_{model} \in \tag{7.1}$$

where $\mathbf{P} \in \Re^{KxA}$ is the loading matrix with A ≥ 1, $\mathbf{t} \in \Re^{A}$ is the score vector and A is the number of principal components (PCs) retained in the PCA model. The matrix $\mathbf{C} = \mathbf{PP}^{T}$ is called the projection matrix.

The residual portion $\tilde{\mathbf{x}}$ can be obtained according to the following expression:

$$\tilde{\mathbf{x}} = (\mathbf{I}\text{-}\mathbf{PP}^{T})\mathbf{x} = (\mathbf{I}\text{-}\mathbf{C})\mathbf{x} = \tilde{\mathbf{C}}\mathbf{x} \in S_{residual} \subset \Re^{K} \tag{7.2}$$

where $\tilde{\mathbf{C}}$ is the projection matrix on the residual subspace. Consequently, $\hat{\mathbf{x}}$ and $\tilde{\mathbf{x}}$ are orthogonal with $\hat{\mathbf{x}}^{T} \cdot \tilde{\mathbf{x}} = 0$

Abnormal values of $\hat{\mathbf{x}}$ are associated to changes affecting the variable correlations which violate the energy balances, mass balances or operational restrictions of the process which have been captured or modeled by the PCA model. A typical statistic to detect that situation is the square prediction error ($SPE = \|\tilde{\mathbf{x}}\|^2$). The process is considered normal if $SPE < \delta^2$ where δ^2 is a confidence limit or threshold for the SPE according to Jackson and Mudholkar (1979) or Box (1954) proposals (Section 1.3.1.3).

Additionally, abnormal values of $\hat{\mathbf{x}}$ can also be due to faults which projections are mainly in the S_{model} or normal changes in the process with a displacement of the operating point that keep the correlation structure. The mostly used statistic to detect that situations

is the Hotelling T^2_{A} (Section 1.3.1.3). The Hotelling´s T^2 statistic expressed in terms of the principal components is :

$$T^2_{\mathrm{A}} = \sum_{a=1}^{A} \frac{t^2_{a,\mathrm{new}}}{s^2_a} \tag{7.3}$$

It can be expressed alternatively as $T^2_{\mathrm{A}} = \mathbf{t}^T \boldsymbol{\Lambda}^{-1} \mathbf{t}$ where $\boldsymbol{\Lambda} = \mathrm{diag}\{\lambda_1 \lambda_2 ..... \lambda_{\mathrm{A}}\}$ is the diagonal matrix with the A largest eigenvalues of the covariance matrix of $\mathbf{x}$, or the correlation matrix if the data are mean centered and scaled to unit variance. These eigenvalues are equal to the variance s^2_a of the different latent components.

7.3 Fault diagnosis methodologies

It is assumed that there exist a database of reference patterns, each corresponding to a known fault. In this situation, the fault detection is performed by testing whether the behavior of current measurement data is consistent with past in-control behavior captures by a PCA or PLS model. The fault isolation is implemented by referencing signatures of the current fault against a database of the reference fault signatures. Existing fault diagnosis methods differ in the type of signatures used to characterize the faults and in the manner of comparing them against the reference signature bank.

7.3.1 PLS-DA

The PLS-DA consists in a classical regression where the PLS algorithm has been modified for classification. Classification techniques can be viewed as aiming to find a relationship between a multivariate independent vector **x** and a qualitative vector of responses. Accordingly, if a suitably designed dummy response vector is introduced, traditional regression methods can be used also to tackle with classification problems

The model is used to predict the class to which belong the new faulty observations. The new faulty observation is assigned to the class with a prediction much closer to one as it is shown in Figure 7.1. In our study we used a single PLS-DA model for all the classes. In the literature there are other proposals with multiple models but we considered that a single model was a good choice.

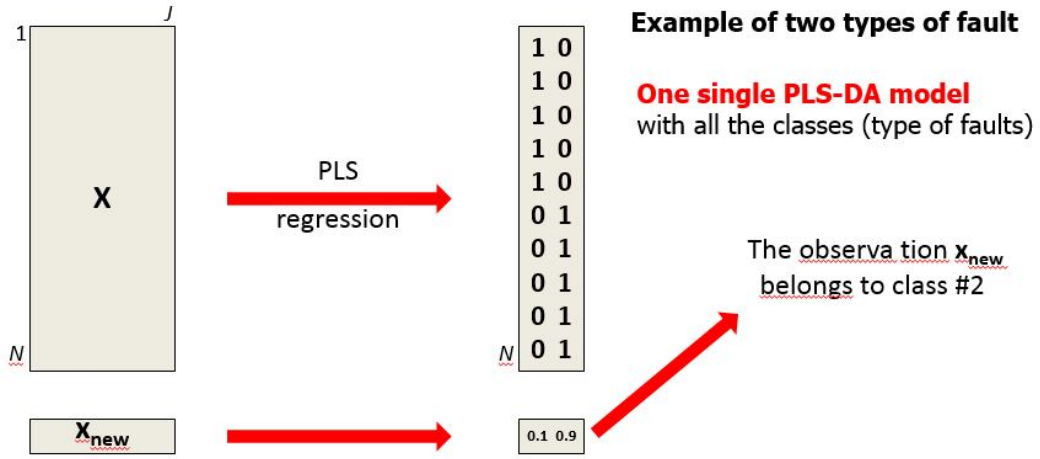

FIGURE 7.1: PLS-DA Model for 2 types of faults

7.3.2 Fault Signatures

Yoon and Macgregor (2001) propose the fault signature methodology. This method uses the PCA already built for fault detection based on common-cause variation *i.e.* from normal operating condition (NOC) data. Fault isolation is then based on the projection of the fault history on this model (scores) and its movement in the orthogonal residual space. As long as the projected scores of a fault form a data cluster in the principal component space one can apply pattern recognition methods. A complex fault has: initial fault signature, a time varying trajectory and steady state fault signature. The initial fault signature may provide a good and prompt source for the fault diagnosis since it is not affected by the fault propagation. However the initial fault signature can be easily missed

by any fault detection scheme and then the transient behavior and final steady state vector of measurements are generally used as an alternative to the initial fault signature to characterize the complex fault signature. The PCA model built from NOC data can be used to develop signatures of past faults from the final steady state or the transient trajectories arising from the faults. An isolation delay is inevitable and a false isolation may arise if the transient fault directionality is very different from the steady state one. The authors focus on the use of the steady state fault signatures. The resulting method appear to work well in many applications even during the transient periods. In our research we will apply this method to observations just immediately after the fault.

By using these relationships, faults and disturbances can be decomposed into two vectors, which explain the fault effects in both the principal component model space and the residual space. Fault signatures are then developed for these faults based on the PCA/PLS model built from normal common-cause data. A fault signature consists of the directions of the movements of the process in both the model space and in the orthogonal residual space during the period immediately following the fault detection.

Let the sample vector of measurements for normal operation condition just prior to a fault be denoted by $\mathbf{x}^*$. In the presence of a fault i the sample vector $\mathbf{x}$ can be represented using an additive fault vector, $\mathbf{f}_i$ according to the following expression $\mathbf{x} = \mathbf{x}^* + \mathbf{f}_i$, then the vector for the fault i $\mathbf{f}_i$ can be decomposed using the PCA model in two components, one ($\widehat{\mathbf{f}}_i$) lying in the model space and the other ($\widetilde{\mathbf{f}}_i$) lying in the residual space as follows:

$$\mathbf{f}_i = \widehat{\mathbf{f}}_i + \widetilde{\mathbf{f}}_i = \mathbf{C}\mathbf{f}_i + (\mathbf{I}\text{-}\mathbf{C})\,\mathbf{f}_i = \mathbf{C}\mathbf{f}_i + \widetilde{\mathbf{C}}\,\mathbf{f}_i \tag{7.4}$$

where $\mathbf{C} = \mathbf{P}\mathbf{P}^T$ is the projection matrix of the PCA model built from NOC data and $\widetilde{\mathbf{C}}$ is the projection matrix on the residual subspace.

These vector components are normalized to be insensitive to their magnitudes. That is,

$$\hat{\mathbf{f}}_i^0 = \frac{\hat{\mathbf{f}}_i}{\|\hat{\mathbf{f}}_i\|} \qquad \tilde{\mathbf{f}}_i^0 = \frac{\tilde{\mathbf{f}}_i}{\|\tilde{\mathbf{f}}_i\|} \tag{7.5}$$

Where it is assumed that $\|\hat{\mathbf{f}}_i\| \neq 0$ and $\|\tilde{\mathbf{f}}_i\| \neq 0$.

A fault signature library consists of all known fault signature vectors (j = 1,2 ……. J) as follows:

$$\hat{\mathbf{F}} = \left[\hat{\mathbf{f}}_1^0 \ \hat{\mathbf{f}}_2^0 \ \ldots \ \hat{\mathbf{f}}_J^0\right] \qquad \tilde{\mathbf{F}} = \left[\tilde{\mathbf{f}}_1^0 \ \tilde{\mathbf{f}}_2^0 \ldots \tilde{\mathbf{f}}_J^0\right]$$

These two fault signature matrices include all known fault information in both the modeled and the unmodeled spaces about the J faults. The fault signature bank or catalog would simply contain the collection of these fault signatures that are available to date. There will be many unknown fault signatures which can be added after detecting a new type of fault.

Once a new fault occurs its signature is compared with those in the fault bank in order to identify the most likely cause. The new faulty observation is decomposed in two components and the two components are normalized as follows:

$$\begin{gathered} \hat{\mathbf{x}}_{new}=\mathbf{C}\hat{\mathbf{x}}_{new} \quad \text{and} \quad \tilde{\mathbf{x}}_{new}=(\mathbf{I}-\mathbf{C})\tilde{\mathbf{x}}_{new} \\ \hat{\mathbf{x}}_0 = \frac{\hat{\mathbf{x}}_{new}}{\|\hat{\mathbf{x}}_{new}\|} \qquad \tilde{\mathbf{x}}_0 = \frac{\tilde{\mathbf{x}}_{new}}{\|\tilde{\mathbf{x}}_{new}\|} \end{gathered} \tag{7.6}$$

The method continue by obtaining the angles measures and using a joint plot for isolation. The angle measures between the known fault signatures (libraries $\hat{\mathbf{F}}$ and $\tilde{\mathbf{F}}$) and the new observation vector signature $\hat{\mathbf{x}}_0$ and $\tilde{\mathbf{x}}_0$ are used for the fault isolation. The cosine value between the new observation vector and one of the known fault signatures gives the relative measure of the collinearity between them. The angle measure in the model space and in the residual space between the fault signature of the new observation and the known fault signature of fault j can be calculated through the scalar product: $\cos\hat{\theta}_j =$

$\hat{\mathbf{x}}_0^{\mathrm{T}} \cdot \hat{\mathbf{f}}_{j_0}$ and $\cos\tilde{\theta}_j = \tilde{\mathbf{x}}_0^{\mathrm{T}} \cdot \tilde{\mathbf{f}}_{j_0}$. When the cosine value is close to one, it means that the new observation vector is near collinear to the fault direction. Then, the fault can be tentatively isolated as the one whose cosine value is closest to one or is the maximum among the row vector cosines components as follows

$$\begin{aligned} \max_j[\hat{\mathbf{x}}_0^{\mathrm{T}} \cdot \hat{\mathrm{F}}] &= \max_j[\,\hat{\mathbf{x}}_0^{\mathrm{T}} \cdot \hat{\mathbf{f}}_{1_0} \quad \hat{\mathbf{x}}_0^{\mathrm{T}} \cdot \hat{\mathbf{f}}_{2_0} \;\cdots\; \hat{\mathbf{x}}_0^{\mathrm{T}} \cdot \hat{\mathbf{f}}_{J_0}\,] \\ \max_j[\tilde{\mathbf{x}}_0^{\mathrm{T}} \cdot \tilde{\mathrm{F}}] &= \max_j[\,\tilde{\mathbf{x}}_0^{\mathrm{T}} \cdot \tilde{\mathbf{f}}_{1_0} \quad \tilde{\mathbf{x}}_0^{\mathrm{T}} \cdot \tilde{\mathbf{f}}_{2_0} \;\cdots\; \tilde{\mathbf{x}}_0^{\mathrm{T}} \cdot \tilde{\mathbf{f}}_{J_0}\,] \end{aligned} \tag{7.7}$$

However the starting point of the model component of the fault signature must not be taken as the origin point of the score space but rather as the normal operating point ($\mathbf{x}^*$) just before the fault is detected. As shown in Figure 7.2, when the model components of their fault directions are considered with respect to the origin O of the model (average in-control operating point) vectors OA^F and OB^F in Figure 7.2 look different even though both faults are the same. This is due to the starting point of the fault vectors. Thus the starting point must be the point where the fault is initiated. So the components model directions AA^* and BB^* and the residual component directions A^*A^F and B^*B^F becomes quite similar.

Note that the isolation could be misleading if the initial direction of the fault is very different form its final direction due to nonlinearity

Authors propose the joint cosine plot to perform the fault diagnosis (Figure 7.3). In this type of plot one single observation is represented by *J* dots where *J* is the number of faults in the fault signature library. Each dot represents the pair of cosines $(\cos\hat{\theta}_j, \cos\tilde{\theta}_j)$ for a particular observation with a particular type of fault. When the number of different types of faults in the library increases and particularly when the signal is monitored during a whole period of time, these plots become very difficult to interpret. It must be noted that

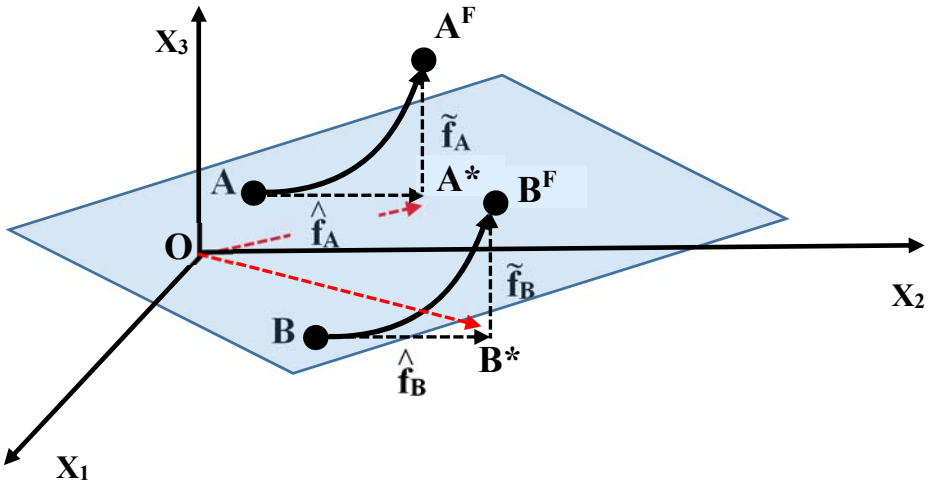

FIGURE 7.2: Fault signatures for the same type of fault in two points (A and B) of the operating space

if we consider only a particular instant of time, then this plot can be replaced for a bar plot displaying the distance to the vertex [+1 +1], with one bar assigned to each fault signature in the library.

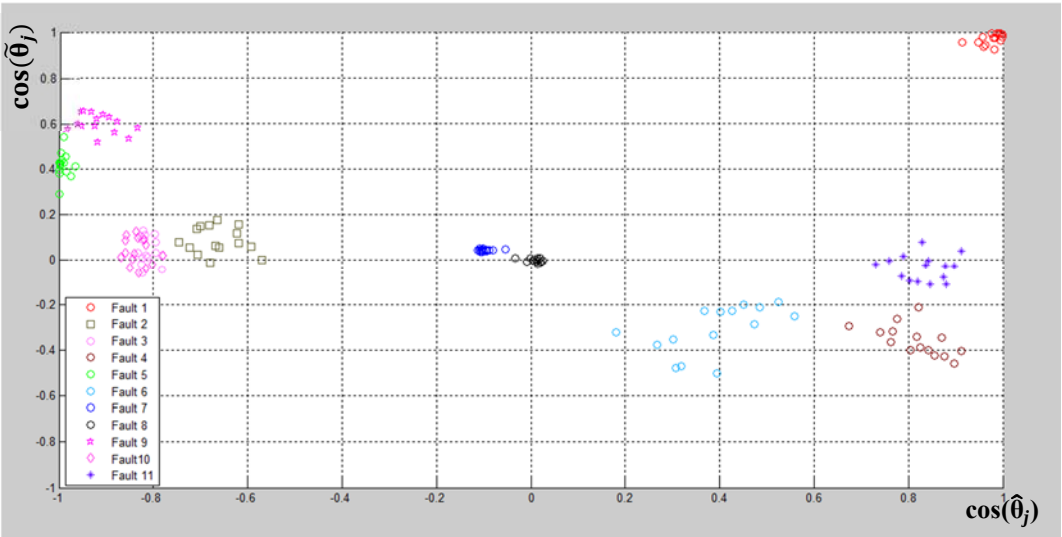

FIGURE 7.3: example of cosine join plot for fault $\mathbf{f}_1$ data set

Figure 7.3 shows the dots corresponding to the pair of cosines of all the observations of fault f_1 in the training data set of the pasteurization process (Table 9.1). The red dots located close to the vertex [+1,+1] are the pair of cosines corresponding to the comparison

of each observation in f_1 test data set to the f_1 signature. As the actual fault is f_1, cosines in the model space and the residual space are close to +1 and consequently the dot is located close to vertex [+1,+1]. The other dots in different colors are the pair of cosines of the comparison of each observation in f_1 test data set to the other types of fault signatures. As there are no other dots close to the vertex [+1,+1] of a different color it is concluded that the fault f_1 can be successfully isolated from the others.

Figure 7.4 represents the cosine join plot corresponding to all the observations of fault f_7 in pasteurization process training data set. The f_7 fault is the fault of a sensor that records a temperature (T_5) which is lower than the real temperature. The fault f_8 is the opposite recording temperatures (T_5) higher than real temperature values. The Figure 7.4 shows that if the minimum distance to vertex [+1 +1] and vertex [-1 -1] is used to diagnose the faults then a sensor or process faults of different sign to the fault signature would not be properly isolated *i.e.* f_7 that is the actual fault would not be successfully isolated of fault f_8. On the contrary, if we consider only the minimum distance to vertex [+1 +1] in order to diagnose the faults, then faults of different sign (f_7 and f_8) can be successfully isolated.

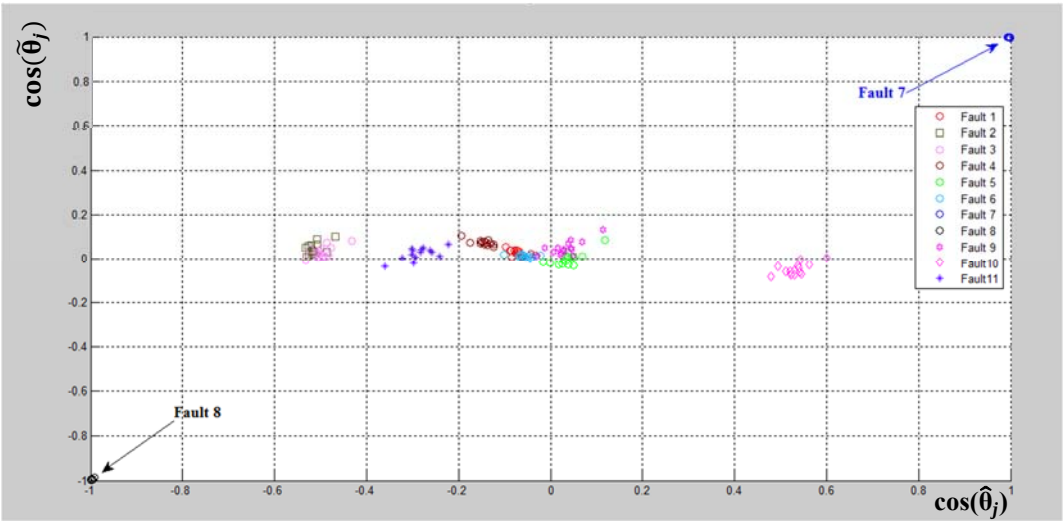

FIGURE 7.4 Example of cosine join plot for $\mathbf{f_7}$ data set

In addition, unknown fault signatures can be added to the library after detecting a new type of fault.

7.3.3 Fault reconstruction methodologies

In these methods the diagnosis of the faults is performed through the reconstruction of different statistics (*SPE*, T^2_A, combined indices) in the faulty observations.

7.3.3.1 Sensor faults reconstruction method

Wise and Ricker (1991) proposed a fault isolation method based on reconstructing each variable using PCA/PLS models that used the remaining variables. Any variable whose reconstruction error was large was considered to be a faulty sensor. However a fundamental assumption behind this approach is that the fault only affects the variable being reconstructed, and does not affect any of the other variables being used to reconstruct it. It effectively limits this approach to the detection of simple faults. Complex faults cannot in general be isolated based on projection models built from in-control data. Such models are non-causal and have no ability to account for the propagated causal effect of the fault into other variables.

Dunia and Qin (1998) (a) proposed the Sensor Validity Index (SVI) to isolate faults sensors . Due to the assumption that the fault effect is not propagated into the other variables the use of the SVI is again limited to the simple sensor fault situation. The approach also examines only the behavior of the fault in the residual space and does not consider the movement that is also included in the PCA model space.

7.3.3.2 Dunia and Qin´s method (SPE Reconstruction Index)

Dunia and Qin (1998 b) presented a unified approach to process and fault sensor detection identification, and reconstruction via principal components analysis. The algorithm used to obtain the PCA model does not only consider the best model for fault reconstruction but also provides the dimension of the fault subspace. In this method the fault reconstruction methodology is adapted to the multidimensional fault case.

In addition, this method allows to study some interesting aspect about the faults diagnosis capability given a particular model and specific fault data set:

- Detectability: Represents the capability of the model to detect the presence of a fault.
- Reconstructability: is the property that assures the estimation of the in-control sample vector using the corrupted sample vector and the model.
- Identifiability: Refers to the ability to find the true fault from a set of possible candidates.
- Isolability: Makes faults capable of being distinguished from one another by means of the model and fault direction.

Fault Detectability

The proposed methodology allows to study the fault detectability. Let S_i be the subspace of fault type i and fault $f_i \in \{\mathbf{F}_j; j = 1.....J\}$ be the set of all possible faults. The dimension of S_i is $l_i \leq K$ and $S_i \in \Re^K$. A set of orthonormal bases for S_i can be represented as columns of the matrix Ξ_i of dimension $K \times l_i$.

The vector for normal operating conditions $\mathbf{x}^*$ when a fault occurred is unknown. In the presence of a fault f_i the sample vector can be represented by the following expression: $\mathbf{x} = \mathbf{x}^* + \boldsymbol{\Xi}_\mathbf{i}\mathbf{f}$ where $\|\mathbf{f}\|$ represents the magnitude of the fault.

The fault subspace matrix $\boldsymbol{\Xi}_\mathrm{i}$ can be projected onto the subspaces S_{model} and $S_{residual}$

$$\boldsymbol{\Xi}_\mathrm{i} = \hat{\boldsymbol{\Xi}}_\mathrm{i} + \widetilde{\boldsymbol{\Xi}}_\mathrm{i} \tag{7.8}$$

where $\hat{\boldsymbol{\Xi}}_\mathrm{i} = \mathbf{C}\boldsymbol{\Xi}_\mathrm{i}$ and $\widetilde{\boldsymbol{\Xi}}_i = \widetilde{\mathbf{C}}\boldsymbol{\Xi}_i$

The matrix $\boldsymbol{\Xi}_\mathrm{i}$ is full rank but the projected matrices are not necessarily full rank.

The projection of the sample vector on the residual subspace becomes:

$$\tilde{\mathbf{x}} = \tilde{\mathbf{x}}^* + \widetilde{\boldsymbol{\Xi}}_i\mathbf{f} \tag{7.9}$$

Using singular valued decomposition (SVD) it is possible to obtain an orthonormal matrix $\widetilde{\boldsymbol{\Xi}}_i^\mathrm{o}$ from $\widetilde{\boldsymbol{\Xi}}_i$

$$\widetilde{\boldsymbol{\Xi}}_i = \left[\widetilde{\mathbf{U}}_i \widetilde{\mathbf{U}}_i^{\perp}\right] \begin{bmatrix} \widetilde{\mathbf{D}}_i & \\ & 0 \end{bmatrix} \left[\widetilde{\mathbf{V}}_i \widetilde{\mathbf{V}}_i^{\perp}\right] = \widetilde{\mathbf{U}}_i \widetilde{\mathbf{D}}_i \widetilde{\mathbf{V}}_i^T = \widetilde{\boldsymbol{\Xi}}_i^o \widetilde{\mathbf{D}}_i \widetilde{\mathbf{V}}_i^T \tag{7.10}$$

where $\widetilde{\mathbf{D}}_i$ has $l_i \times l_i$ dimensions and contains non zero singular values of $\widetilde{\boldsymbol{\Xi}}_i$ and, therefore, $\widetilde{\boldsymbol{\Xi}}_i^\mathrm{o}$ represents nonvanishing directions and $\widetilde{\mathbf{U}}_\mathrm{i}^{\perp}$ the vanishing directions when $\boldsymbol{\Xi}_i$ is projected onto $S_{residual}$.

According to this, equation 7.10 can be rewritten as:

$$\tilde{\mathbf{x}} = \tilde{\mathbf{x}}^* + \widetilde{\boldsymbol{\Xi}}_\mathrm{i}^\mathrm{o} \widetilde{\mathbf{D}}_\mathrm{i} \widetilde{\mathbf{V}}_\mathrm{i}^\mathrm{T} \mathbf{f} = \tilde{\mathbf{x}}^* + \widetilde{\boldsymbol{\Xi}}_\mathrm{i}^\mathrm{o} \tilde{\mathbf{f}} \tag{7.11}$$

where: $\tilde{\mathbf{f}} = \widetilde{\mathbf{D}}_\mathrm{i} \widetilde{\mathbf{V}}_\mathrm{i}^\mathrm{T} \mathbf{f}$ and $\|\tilde{\mathbf{f}}\| = \|\widetilde{\boldsymbol{\Xi}}_\mathrm{i}^\mathrm{o} \tilde{\mathbf{f}}\| = \|\widetilde{\boldsymbol{\Xi}}_\mathrm{i} \mathbf{f}\|$ represents the fault displacement proyected on S_residual. $\widetilde{\boldsymbol{\Xi}}_i^o$ and $\widetilde{\boldsymbol{\Xi}}_i$ span the same subspace $\widetilde{S}_i$ but the use of $\widetilde{\boldsymbol{\Xi}}_i^o$ eliminates the possibility of linear dependence of the fault basis projected onto S_residual

Therefore the *SPE* can be represented according to the following expression:

$$SPE = \left\| \tilde{\mathbf{x}}^* + \tilde{\boldsymbol{\Xi}}_i \mathbf{f} \right\|^2 = \left\| \tilde{\mathbf{x}}^* + \tilde{\boldsymbol{\Xi}}_i^{\mathrm{o}} \tilde{\mathbf{f}} \right\|^2 \tag{7.12}$$

And, consequently, the necessary condition for detectability is that the direction of a particular type of fault has a projection in the residual space. Therefore if $\tilde{\boldsymbol{\Xi}}_i = 0$ which implies that $S_{\mathrm{i}} \subseteq S_{\mathrm{model}}$ the fault is not detectable no matter what magnitude **f** is. If $\tilde{\boldsymbol{\Xi}}_i \neq 0$ but $\tilde{\boldsymbol{\Xi}}_i$ is rank deficient, the fault is not detectable if $\tilde{\mathbf{f}} = 0$. In this case the displacement caused by $\boldsymbol{\Xi}_i \mathbf{f} \in S_{\mathrm{model}}$. It must be noted that even if $\left\| \tilde{\mathbf{f}} \right\| \neq 0$, it should be large enough to make *SPE* exceeds the confidence limit. Authors demonstrate that the sufficient condition for detectability is $\left\| \tilde{\mathbf{f}} \right\| > 2\delta$. Otherwise the fault may be detected, but not guaranteed detectable. According to this, increasing the number of components of the model reduce the value of δ and it can serve to improve the chances of detection of small faults but it also reduces the value of $\left\| \tilde{\mathbf{f}} \right\|$ so there is a trade off to determine the optimum number of components in the model.

Fault subspace extraction

In sensor faults the fault direction matrix is easily obtained. In the case of process faults Yue and Qin (2001) and Valle *et al* (2001) propose to extract the fault direction using singular value decomposition (SVD) on historical fault data.

A new observation with a fault j is $\mathbf{x}_{\mathrm{new}} = \mathbf{x}^*_{\mathrm{new}} + \boldsymbol{\Xi}_j \mathbf{f}_j$. The matrix of fault data $\mathbf{X}_j$ collected under f_j fault is $\mathbf{X}_j^{\mathrm{T}} = \boldsymbol{\Xi}_j$ [($\mathbf{f}(1)$ ….. $\mathbf{f}(J)$]. According to this, the columns of $\mathbf{X}_j^{\mathrm{T}}$ and $\boldsymbol{\Xi}_j$ span the same subspace. Then it is possible to perform singular value decomposition on $\mathbf{X}_j^{\mathrm{T}} \Rightarrow \mathbf{X}_j^T = \mathbf{U}_j \mathbf{D}_j \mathbf{V}_j^T$ to obtain the matrices $\mathbf{U}_{\mathrm{j}}$, $\mathbf{D}_j$ and $\mathbf{V}_j$, where $\mathbf{D}_j$

contains the nonzero singular values in descending order. Finally the fault matrix direction $\boldsymbol{\Xi}_j = \mathbf{U}_j$ is obtained.

In practice, it is often difficult to differentiate between zero and nonzero singular values. Authors propose a method of determining the dimension of the fault subspace. Starting from the singular vector of the largest singular value $\mathbf{U}j(:, 1)$ as the fault direction and performing reconstruction. If the reconstructed sample $\mathbf{x}j$ is within the normal region, then $\mathbf{U}j(:, 1)$ can adequately represent and reconstruct the fault. Otherwise, the next singular vector is added until the reconstructed sample ($\mathbf{x}_j$) is within the normal region.

Fault reconstruction

The reconstruction of process faults consists of estimating the reconstructed sample vector $\mathbf{x}_i$ by eliminating the effect of the fault *i* that we assume as the actual fault. The reconstruction using the PCA model of the normal portion $\mathbf{x}^*$ of the observation $\mathbf{x}$ which now is a corrupted observation vector is conducted bringing $\mathbf{x}_i$ back to the S_{model} along the direction $\boldsymbol{\Xi}_i$ following the expression $\mathbf{x}_i = \mathbf{x} - \boldsymbol{\Xi}_i \mathbf{f}_i$ as it is shown in Figure 7.5.

where $\mathbf{f}_i$ is an estimate of the fault magnitude $\mathbf{f}$ and $\boldsymbol{\Xi}_i$ an orthonormal base that span the subspace of the fault S_i. The projection of $\mathbf{x}_i$ in the residual subspace $S_{residual}$ follows:

$$\tilde{\mathbf{x}}_i = \tilde{\mathbf{x}} - \tilde{\boldsymbol{\Xi}}_i \mathbf{f}_i \;\Rightarrow\; \tilde{\mathbf{x}}_i = \tilde{\mathbf{x}} - \tilde{\boldsymbol{\Xi}}_i^o \tilde{\mathbf{f}}_i \tag{7.13}$$

where $\tilde{\mathbf{f}}_i = \tilde{\mathbf{D}}_i \tilde{\mathbf{V}}_i^T \mathbf{f}_i$

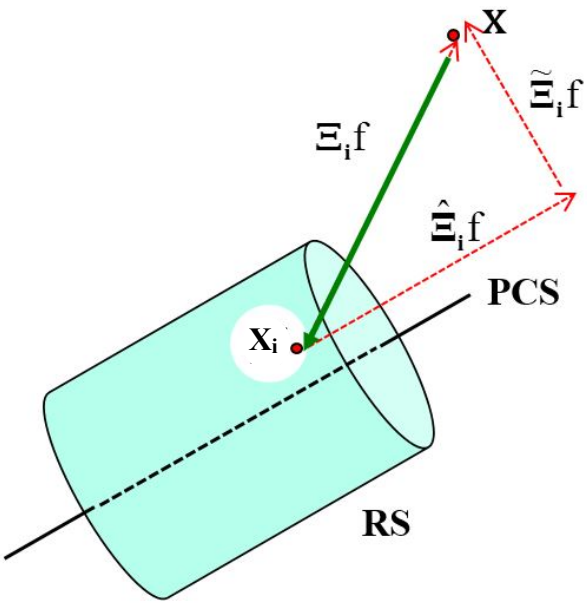

FIGURE 7.5: Fault reconstruction according to the fault f_i

The best estimate of $\mathbf{x}^*$ is found by minimizing the distance from $\mathbf{x}_i$ to the $S_{residual}$

$$\mathbf{f}_i = \arg\min \left\| \tilde{\mathbf{x}} - \tilde{\Xi}_i \mathbf{f}_i \right\|^2 = \left(\tilde{\Xi}_i^T \tilde{\Xi}_i \right)^{-1} \tilde{\Xi}_i^T \tilde{\mathbf{x}}_i \qquad (7.14)$$

Complete reconstructability	Partial reconstructability
▪ $\dim\{\tilde{S}_i\} = \dim\{S_i\} = l_i$ ▪ $S_i \cap S_{model} = \phi$ ▪ $\tilde{\Xi}_i$ is full column rank ▪ The smallest singular value of $\tilde{\Xi}_i$ is major than 0	▪ $\dim\{\tilde{S}_i\} \neq 0$ ▪ $S_i \not\subset S_{model}$ ▪ $\tilde{\Xi}_i \neq 0$ ▪ The largest singular value of $\tilde{\Xi}_i$ is major than 0
Reconstructed vector: $\mathbf{x}_i = (\mathbf{I} - \Xi_i (\tilde{\Xi}_i^T \tilde{\Xi}_i)^{-1} \tilde{\Xi}_i^T)\mathbf{x}$	Reconstructed vector: $\mathbf{x}_i = (\mathbf{I} - \Xi_i \tilde{\Xi}_i^+)\mathbf{x}$
Projection of the reconstructed vector: $\tilde{\mathbf{x}}_i = (\mathbf{I} - \tilde{\Xi}_i (\tilde{\Xi}_i^T \tilde{\Xi}_i)^{-1} \tilde{\Xi}_i^T)\tilde{\mathbf{x}}$	Projection of the reconstructed vector: $\tilde{\mathbf{x}}_i = (\mathbf{I} - \tilde{\Xi}_i^o \tilde{\Xi}_i^{oT})\tilde{\mathbf{x}}$ where $\tilde{\Xi}_i^+ = \tilde{\mathbf{V}}_i \tilde{\mathbf{D}}_i^{-1} \tilde{\Xi}_i^{oT}$ is the Moore-Penrose pseudoinverse

Reliability of the reconstruction procedure

The reliability of the fault reconstruction is the criterion proposed by the authors to determine the best number of components to use in the PCA model. For a fault F_i the reconstruction of the whole set of measurements $\mathbf{x}^*$ using the fault space basis $\boldsymbol{\Xi}_i$ has an unreconstructed portion $\mathbf{x}^* - \mathbf{x}_i$ and the part of this unreconstructed portion in the subspace S_i is $\boldsymbol{\Xi}_i^T(\mathbf{x}^* - \mathbf{x}_i)$. According to this, the *unreconstructed mean* is $\omega_i = \mathcal{E}\left\{\boldsymbol{\Xi}_i^T(\mathbf{x}^* - \mathbf{x}_i)\right\}$ and the *unreconstructed variance* is $u_i = \mathcal{E}\left\{\left\|\boldsymbol{\Xi}_i^T(\mathbf{x}^* - \mathbf{x}_i) - \omega_i\right\|^2\right\}$

As the corrupted observation is $\mathbf{x} = \mathbf{x}^* + \boldsymbol{\Xi}_i\mathbf{f}$ and the reconstructed observation is $\mathbf{x}_i = \mathbf{x} - \boldsymbol{\Xi}_i\mathbf{f}_i$ by substitution $\Rightarrow \quad \mathbf{x}_i + \boldsymbol{\Xi}_i\mathbf{f}_i = \mathbf{x}^* + \boldsymbol{\Xi}_i\mathbf{f} \Rightarrow \mathbf{x}^* - \mathbf{x}_i = \boldsymbol{\Xi}_i(\mathbf{f}_i - \mathbf{f})$

then

$$\begin{aligned} \omega_i &= \mathcal{E}\left\{\boldsymbol{\Xi}_i^T(\mathbf{x}^* - \mathbf{x}_i)\right\} = \mathcal{E}\left\{\boldsymbol{\Xi}_i^T\boldsymbol{\Xi}_i(\mathbf{f}_i - \mathbf{f})\right\} = \mathcal{E}\left\{\mathbf{f}_i - \mathbf{f}\right\} \\ \mathrm{u}_i &= \mathcal{E}\left\{\left\|\boldsymbol{\Xi}_i^T(\mathbf{x}^* - \mathbf{x}_i) - \omega_i\right\|^2\right\} = \mathcal{E}\left\{\left\|\boldsymbol{\Xi}_i^T\boldsymbol{\Xi}_i(\mathbf{f}_i - \mathbf{f}) - \omega_i\right\|^2\right\} = \mathcal{E}\left\{\left\|\mathbf{f}_i - \mathbf{f} - \omega_i\right\|^2\right\} \end{aligned} \tag{7.15}$$

For partial reconstruction authors demonstrate that $\omega_i = (\widetilde{\boldsymbol{\Xi}}_i^+\boldsymbol{\Xi}_i - \mathbf{I})\mathbf{f}$ and so that if $\boldsymbol{\Xi}_i$ is rank deficient then $\mathbf{x}_i$ is a biased estimation of $\mathbf{x}^*$. In the case of complete reconstruction $\omega_i = 0$ the reconstruction is unbiased. Authors also demonstrate that $\mathrm{u}_i = Trace\left\{\widetilde{\boldsymbol{\Xi}}_i^+\mathbf{R}\widetilde{\boldsymbol{\Xi}}_i^{+T}\right\}$ and therefore the unreconstructed variance does not depend on the magnitude of the fault.

Number of principal components for best reconstruction

The criterion proposed for the authors is to choose the number of principal components which minimize the variance reconstruction. The variance reconstruction can be divided in two parts $\mathrm{u}_i = \tilde{\mathrm{u}}_i + \hat{\mathrm{u}}_i$ where $\tilde{u}_i$ is the variance of $\mathbf{f}_i$ projected on S_{residual} and $\hat{u}_i$ is the variance of $\mathbf{f}_i$ projected on S_{model}.

$$\begin{aligned}\tilde{u}_i &= \mathcal{E}\left\{\left\|\tilde{\Xi}_i \mathbf{f}_i\right\|^2\right\} = \mathcal{E}\left\{\left\|(\tilde{\mathbf{x}}^* - \tilde{\mathbf{x}}_i\right\|^2\right\} \\ \hat{u}_i &= \mathcal{E}\left\{\left\|\hat{\Xi}_i \mathbf{f}_i\right\|^2\right\} = \mathcal{E}\left\{\left\|(\hat{\mathbf{x}}^* - \hat{\mathbf{x}}_i\right\|^2\right\}\end{aligned} \tag{7.16}$$

Authors demonstrate that $\tilde{u}_i = trace\left\{\tilde{\Xi}_i^{oT}\mathbf{R}\tilde{\Xi}_i^{o}\right\}$, $\hat{u}_i = trace\left\{\hat{\Xi}_i\tilde{\Xi}_i^{+}\mathbf{R}\tilde{\Xi}_i^{+T}\hat{\Xi}_i^{T}\right\}$ and that u_i has a minimum respect to *the number of components of the model A.* The calculation of a *minimum* u_i by choosing A improves reconstruction and identification of f_i. They propose to minimize a linear combination of all possible unreconstructed variances with respect to the number of principal components of the model:

$$\min_A \mathbf{q}^T\mathbf{u} = \min_A\left(\mathbf{q}^T\tilde{\mathbf{u}} + \mathbf{q}^T\hat{\mathbf{u}}\right) \quad (8.20)$$

where $\mathbf{u}$ represent the vector of unreconstructed variances for all $f_i \in \{\mathbf{F}_j\}$ and $\mathbf{q}$ is a weighting vector with positive entries. Such a vector allows one to adjust the model depending on how critical each fault is to process operation.

Inclusion of faults and variables

Despite the authors recommend to study how reliable the reconstructed sample vector are for different sets of sensors and number of principal components we have considered only the number of principal components in our study. If there is a lack of correlation among all variables, however it is possible that the best reconstruction is not better than the sample mean $\bar{\mathbf{x}}_i$. Authors propose to calculate the unreconstructed variance based on the sample mean and compare it with u_i

$$\rho_i = \mathcal{E}\left\{\left\|\Xi_i^T\left(\mathbf{x}^* - \bar{\mathbf{x}}^*\right)\right\|^2\right\} = \mathrm{var}\left\{\Xi_i^T\mathbf{x}^*\right\} = trace\left\{\Xi_i^T\mathbf{R}\Xi_i\right\} \tag{7.17}$$

In case $u_i > \rho_i$ the authors propose to reduce the variance of u_i by dropping out insignificant singular values of $\tilde{\Xi}_i$ that tend to introduce large reconstruction variance. In

this case we have imposed the restriction to maintain at least one singular value for each considered fault. If after previous step $u_i > \rho_i$ authors state the fault f_i cannot be reliably reconstructed using the PCA model and the best reconstruction is the sample mean. They also consider that if the fault f_i is a sensor fault that cannot be reliably reconstructed, that sensor has little correlation with others and should be removed from the PCA model. In our study in order to compare the diagnosis performance of this method with the others we decided to maintain all the sensors and faults in the model. We detected that in processes where correlations were not strong the method tends to exclude most of the sensors and process faults. Indeed it achieved reasonably good results in diagnosis when sensors and faults were not excluded from the model.

Fault identification

The objective is to identify a fault from a set of possible faults $\{\mathbf{F}_j; j = 1.....J\}$. The identification is carried out by assuming each fault f_j in turn and performing reconstruction. When the actual fault f_i is assumed, the reconstructed sample vector $\mathbf{x}_i$ is closest to the S_{model} and the *SPE* of $\mathbf{x}_i$ is brought into the normal confidence region. $SPE_{i|i} = \|\tilde{\mathbf{x}}_i\|^2 \le \delta_i^2$. Due to the fact that reconstruction is involved in $SPE_{i|i} \Rightarrow \delta_i^2 \neq \delta^2$ where no reconstruction is involved. Authors define $SPE_{j|i} = \|\tilde{\mathbf{x}}_j\|^2$ for a reconstruction in the direction Ξ_j^o when the actual fault is f_i and demonstrate that $\delta_i^2 = \delta^2 - \tilde{u}_i$. An alternative way is defining a threshold for δ_i^2 using fault free data. Or if it is assumed that $\tilde{u}_i$ is small compared to δ^2, one can use δ^2 as an approximation to δ_i^2.

Situations:

i) Reconstructing f_j while the actual fault is f_i then $SPE_{j|i} = SPE - \left\|\tilde{\mathbf{f}}_j\right\|^2$ the larger fault the magnitude the larger is the *SPE* and thus $SPE_{j|i}$. So small $\left\|\tilde{\mathbf{f}}_j\right\|^2$ and large *SPE* are desirable for the identification. That is, to make $SPE_{j|i} > \delta_j^2$ and that f_i can be identified from $\{\mathbf{F}_j; j = 1,2....J\}$.

ii) Reconstructing f_i which is the actual fault, then $SPE_{i|i} \le \delta_i^2$ nevertheless, it is possible that that $SPE_{j|i} \le \delta_j^2$; in this case f_i and f_j are not isolatable. Authors define an identification index for f_j :

$$\eta_j^2 = \frac{SPE_j}{SPE} = 1 - \frac{\left\|\tilde{\mathbf{f}}_j\right\|^2}{SPE} \tag{7.18}$$

where $\eta_j^2 \in [0 \quad +1] \Rightarrow$ if f_j is the actual fault $\eta_j^2 \to 0$

Fault isolability

Fault isolability measures the possibility of identifying the actual fault f_i from the set $\{\mathbf{F}_j; j = 1.....J\}$. If only one index η_j^2 is close to zero, the η_i^2, then the fault is uniquely identifiable. If some candidates are close to zero then the unique identification is impossible. Another fault f_j is rejected as the possible cause of the actual fault f_i if $SPE_{j|i} > \delta_j^2$

According to the relation between both faults subspaces f_i and f_j :

a) if $\tilde{S}_i \cap \tilde{S}_j = \phi$ the projections of both subspaces in the S_{residual} subspace do not overlap and the two faults are completely isolatable.

b) if $\widetilde{S}_i \cap \widetilde{S}_j \neq \phi$ or $\widetilde{S}_j \subset \widetilde{S}_i$ the projections of both subspaces in the S_{residual} subspace partially overlap and the isolatability depends on the magnitude and direction of **f**

c) if $\widetilde{S}_{\mathrm{i}} \subseteq \widetilde{S}_{\mathrm{j}}$ the two faults are not isolatable.

Authors also derive the conditions for complete isolatability:

f_i is completely isolatable from f_j if there is no $\widetilde{\mathbf{f}} \neq 0$ which verifies $\widetilde{\boldsymbol{\Xi}}_{\mathrm{i}}^{o}\widetilde{\mathbf{f}} \in \Re\left\{\widetilde{\boldsymbol{\Xi}}_{\mathrm{j}}^{o}\right\}$

Which supposes that there is no nonzero common vector between $\widetilde{S}_{\mathrm{i}}$ and $\widetilde{S}_{\mathrm{j}}$ and consequently $\widetilde{S}_{\mathrm{i}} \cap \widetilde{S}_{\mathrm{j}} = \phi$. It also supposes that $(\mathbf{I} - \boldsymbol{\Xi}_j^{o}\boldsymbol{\Xi}_j^{o^T})\boldsymbol{\Xi}_i^{o}$ has full column rank as none of the directions of $\boldsymbol{\Xi}_{\mathrm{i}}^{o}$ vanish when projecting onto $\widetilde{S}_j^{\perp}$.

7.3.3.3 Yue and Qin´s method (Combined Reconstruction Index)

Yue and Qin (2001) extend the reconstruction based in the SPE method of Dunia and Qin (1998) to incorporate both indices: the *SPE* and Hotelling´s T^2_{A} statistic, so that the identification is formulated in terms of both indices. A fault is identified if the indices after reconstruction are within the normal region.

Fault detection using a Combined Index φ

Authors propose a combined index to simplify the fault detection task:

$$\varphi = \frac{SPE(\mathbf{x})}{\delta^2} + \frac{T_A^2(\mathbf{x})}{\chi_A^2} = \mathbf{x}^T\boldsymbol{\Phi}\mathbf{x} \tag{7.19}$$

where the operator $\boldsymbol{\Phi} = \dfrac{\mathbf{P}\boldsymbol{\Lambda}^{-1}\mathbf{P}^T}{\chi_A^2} + \dfrac{\mathbf{I} - \mathbf{P}\mathbf{P}^T}{\delta^2}$ is symmetric and positive definite. The distribution of the combined index φ can be approximated using a $g\chi_h^2$ distribution

where $g = \frac{Tr(\mathbf{S\Phi})^2}{Tr(\mathbf{S\Phi})}$ and $h = \frac{[Tr(\mathbf{S\Phi})]^2}{Tr(\mathbf{S\Phi})^2}$. A fault is detected by the combined index if $\varphi \geq g\chi_h^2(\alpha) = \xi^2$, where $\chi_h^2(\alpha)$ is the (1-α)th percentile of the χ_h^2 distribution.

Fault reconstruction

In this method the reconstruction consists on estimating the normal values **x*** using the PCA model of the process by eliminating the effect of the actual fault f_i on both the *SPE* and the T^2_A assuming a true fault direction f_i. A reconstruction $\mathbf{x}_j$ is an adjustment of the sample vector **x** along a given fault direction $\mathbf{\Xi}_j$ where $\mathbf{f}_j$ is the estimated fault magnitude such that $\mathbf{x}_j$ is closest to the normal region. Authors propose the following criterion: $\min_{f_j}\left\{\frac{SPE(\mathbf{x}_j)}{\delta^2} + \frac{T_A^2(\mathbf{x}_j)}{\chi_A^2}\right\}$. The use of $\delta^2$and χ_A^2 as weighting factors make sures that both índices are minimized to the same extent with respect to their control limits. Authors derive the following expression for the fault magnitude $\mathbf{f}_j = \left(\mathbf{\Xi}_j^T\mathbf{\Phi\Xi}_j\right)^{-1}\mathbf{\Xi}_j^T\mathbf{\Phi x}$. Then the observation can be reconstructed according to the fault $f_j \Rightarrow \mathbf{x}_j = \mathbf{x} - \mathbf{\Xi}_j\mathbf{f}_j$ and $\varphi_j = \frac{SPE(\mathbf{x}_j)}{\delta^2} + \frac{T_A^2(\mathbf{x}_j)}{\chi_A^2} = \mathbf{x}_j^T\mathbf{\Phi x}_j$

Regarding the reconstruction error $\mathbf{x}^* - \mathbf{x}_j$, if the true fault direction is reconstructed $\mathbf{x}_i = \mathbf{x} - \mathbf{\Xi}_i\mathbf{f}_i$, the reconstruction can always bring the index back to the normal region. If $\mathbf{\Xi}_j \neq \mathbf{\Xi}_i$ the reconstruction error depend on the fault magnitude and the fault subspace $\mathbf{\Xi}_j$. A large enough fault **f** will make $\varphi_j > \xi^2$ which can be useful for fault identification.

Fault Identification using a Combined Index φ

We identify faults on the basis of whether reconstruction can bring the combined index back to the normal region defined by both the *SPE* and the T^2_A. Then f_j is considered the true fault if $\varphi_j \le \xi^2$. The reconstructed combined index has the same control limits as the detection indices. If there is only one identified fault then the fault is uniquely identified and if there is more than one fault that satisfies the identification criterion then unique identification is not possible.

Chapter 8: Fingerprints Contribution Plots (FCP)

This chapter introduces a novel fault diagnosis approach called the Fingerprints Contribution Plot (FCP) methodology (Vidal-Puig and Ferrer, 2008) for fault diagnosis in MSPC. This novel method tries to extend the use of the contribution plots, which is widely used as an unsupervised method for fault diagnosis, to the supervised case in which there is information about the different types of fault. This chapter describes the rationale of this method and its full detail implementation in the case of the pasteurization process example.

8.1 Introduction

The contribution plots proposed by Miller *et al*. (1998) points to the original variables which account for the large value of the signalling monitoring statistic. From a different approach Dunia and Qin (1998) and Qin (2000) introduced a fault diagnosis methodology which is based in the reconstruction of the fault (Section 7.3.3.2). When compared to the contribution plots, Qin´s methodology and others supervised methodologies becomes more difficult to implement since they can only be applied when there is enough information available to characterise the different types of faults. One of the advantages of the contribution plots is that this methodology does not require additional information about the different types of faults in order to be successfully applied on the other hand, some authors state that when this information is available, supervised methods such as Qin´s methodology outperforms the diagnosis results of the contribution plots.

In this chapter we introduce a novel fault diagnosis approach called the Fingerprints contribution plot methodology (FCP). This is an extension of the contribution plots methodology that combines the available information about the different types of faults with the traditional contribution plots methodology. The FCP can only be applied in a supervised context, it is to say when different sets of faulty observations for all the known types of faults are available. The idea is to use the average contribution plot for each type of fault as a fingerprint. The FCP assumes that different signals recorded for one type of fault will produce a similar shape in the contribution plots. According to this, the methodology assumes that when a fault change in size the contribution plot will keep the shape and the relationships among the contributions of the measured variables. In other words, a fault with a smaller size than the one used to create its fingerprint will produce smaller contributions for all the variables, but it will maintain the shape of the fingerprint contribution plot. Additionally the FCP methodology makes possible to study the

consistency of the fingerprints, the isolability of the different types of faults, and the time evolution of the signals for the different types of faults which determine the speed of degradation of the fault isolation capability of the method.

The measurement of the consistency of the fingerprints is important because it determines if this methodology can be successfully applied to the process under study. The contribution plots of different signals for the same type of fault must keep a similar shape if they are to be used in the construction of a fingerprint.

The isolation capability of the method for the different types of faults will rely upon the similitude degree among the different fingerprints.

The degradation of the signal becomes an important issue in regulated process environments. Despite the signals of the different types of faults may be very different at the initial point of the faults, the actuators may change the signals quickly and lead to a situation where the contribution plot for every type of fault may differ largely of its own fingerprint, and indeed it could become similar to the fingerprints of other types of faults. In the FCP the speed of the signal degradation for the different types of faults can be easily measured.

8.2 Fingerprints contribution plot: construction

The fingerprints contribution plot (FCP) measures the similitude degree between the contribution plot of a signalling observation and the fingerprints (average contribution plots) of the battery of different types of fault considered in the process. This plot will consist of a barchart in which the number of bars will match the number of the different types of faults and the size of every bar will depend on the similitude degree index (*SDI*) for every type of fault. The *SDI* measures the similitude degree between the contribution

plot of the signalling observation and the fault fingerprint corresponding to one of the faults of the battery.

8.2.1 Similitude degree index (SDI)

In order to compare the similitude degree of different contribution plots four criteria have been considered: i) the similitude degree of the bar sizes (I_s), ii) the similitude degree in the composition of the set of variables with significant contributions (I_{sc}), iii) the similitude degree in the sign of the significant contributions (I_{ss}) and, finally, iv) the similitude degree in the order of the contributions sorted by size (I_o).

The *SDI* for the fault *j*-th follows the next expression:

$$SDI_j = \alpha I_s^j + \beta I_{sc}^j + \gamma I_{ss}^j + \theta I_o^j \tag{8.1}$$

The weighting coefficients (α, β, γ and θ) of the four criteria in the *SDI* may be selected according to an optimization process as illustrated in Section 8.2.2.2 In order to calculate the *SDI*, the contribution of each original variable to the value of the signalling statistic is computed as a percentage of the total sum of contributions for all the original variables. In case that only the significant contributions would be considered, the contributions will be computed as the percentage of the total sum of significant contributions. This scale transformation in the value of the contributions was also applied to the contributions plots which were used in the construction of the fingerprints database containing the information about of the different types of fault which may affect the process.

- I_s : *Size of bars similitude index*

For every type of fault *j* the difference in the value of each original variable *k* scaled contribution to the signalling statistic (c_k) and the corresponding scaled contribution of variable *k* to the fault *j* fingerprint (c_k^j) are computed. These differences are computed

taking into account the sign of the contributions and then the absolute value d_k^j of these differences is used to compute the I_s index according to the following expressions:

$$d_k^j = \left| c_k - c_k^j \right|$$
$$I_s^j = 1 - \frac{d_1^j + d_2^j ..... d_K^j}{200} \tag{8.2}$$

The index value becomes 1 when the scaled contributions in the new observation are the same to the scaled contributions in the fault *j* fingerprint for all the variables. In that situation the contribution plot for the new faulty observation and the fingerprint for the considered type of fault have the same shape. On the contrary, the index value becomes 0 when there is not any coincidence between them since the maximum value of the sum of differences d_k^j is 200. As indicated in Section 1.3.2 we will use a definition of the contributions to the *SPE* that maintains the information related to the sign of the differences. So the length of the bars (scaled to 100% contributions) in the FCP plot covers the *SPE* range from +100% to -100% . Consequently the difference between the length of the bars of a fault with a positive contribution of 100% related to a fingerprint with a negative contribution of 100% adds up to the 200%.

Figure 8.1 a) shows an example of the fingerprint for fault *j* in a case with 13 measured variables. In that fingerprint the contributions are represented as the percentage of the total sum of the significant contributions. Figure 8.1 b) and Figure 8.1 c) display the contribution plots for two new faulty observations: obs 1 and obs 2.

When the contribution values of obs 1 and 2 are changed into percentages of the total sum of significant contributions it can be appreciated that these two new observations completely match with the fingerprint for fault *j* presenting the same FCP shape despite the original contribution bars may have different sizes before being scaled.

a)

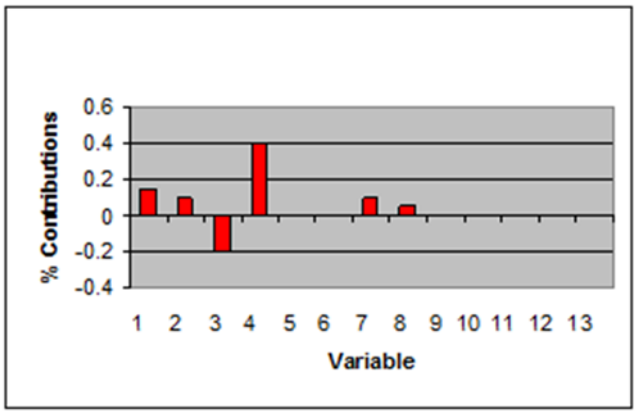

b) c)

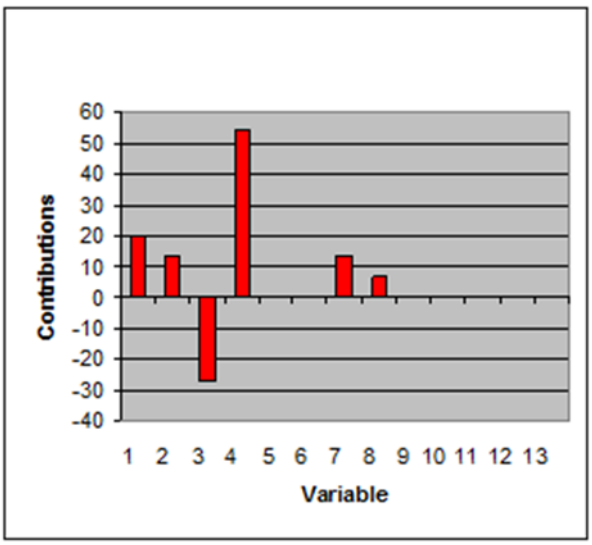

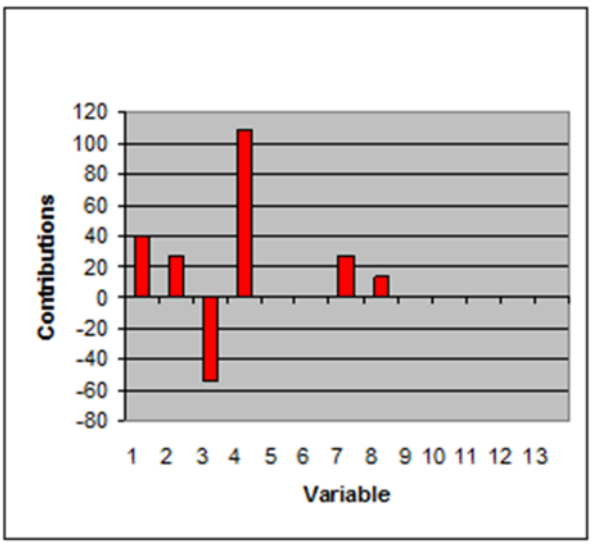

FIGURE 8.1: a) *j*-th fault fingerprint b) Obs 1 contribution plot c) Obs 2 contribution plot

- I_{sc} : *Set of significant contributions similitude index*

This index measures the degree of coincidence between the set of variables with significant contributions (according to Section 8.2.2.1) in the *j*-th fault fingerprint and the set of variables with significant contributions in the new faulty observation. In fact this information is partially and indirectly measured by the I_s index, as the only way to get a value of 100% in the I_s index is when the list of significant contributions in the two cases match perfectly. This index may serve to adjust the final weight of this similarity feature in the *SDI*.

For every type of fault *j* the number of discrepancies n_D^j between both sets (the set of variables with significant contributions in the *j*-th fault fingerprint and the set of variables with significant contributions in the new faulty observation) will be computed. The index I_{sc} for the type of fault *j* can be expressed according to the following expression:

$$I_{sc}^j = 1 - \frac{n_D^j}{K} \tag{8.3}$$

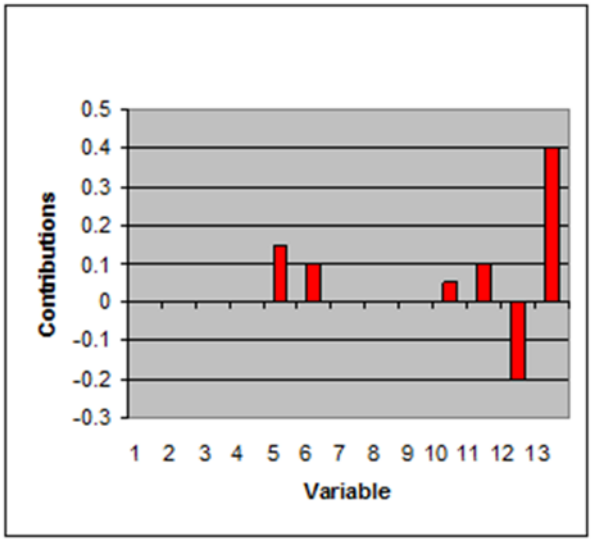

FIGURE 8.2: Obs 3 contribution plot

For instance, between the fingerprint of Figure 8.1 a) and the faulty observation in Figure 8.1 b) there are no discrepancies as they have the same set of variables with significant contributions: variables {1,2,3,4,7,8}. Then $n_D^j = 0$ and with a number of measured variables *K*=13, the expression would lead to a $I_{sc}^j = 1$. On the contrary, between the fingerprint of figure 8.1 a) and the faulty observation (obs 3) in figure 8.2 there is near full discrepancy. The set of variables with significant contributions in the fingerprint for fault *j*: {1,2,3,4,7,8} is completely different to the set of variables with significant contributions in the faulty observation 3 {5,6,10,11,12,13}. So, there is discrepancy in 12 variables, $n_D^j = 12$, the expression would lead to a $I_{sc}^j = 0.08$. The index is not exactly zero because in both sets variable 9 is classified as non significant.

- I_{ss} : *Sign of contributions similitude index*

This index measures the degree of coincidence in the sign of the significant contributions between the *j*-th fault fingerprint and the new faulty observation. This information is also partially measured by the I_s index, because a value of 1 in the I_s will require a complete coincidence in the sign of the significant contributions. But this index may also serve to adjust the final weight of this similarity feature in the *SDI*.

For every type of fault *j*, the number of discrepancies in the sign of the contribution n_{DS}^{j} between the two sets (the set of variables with significant contributions in the *j*-th fault fingerprint and the set of variables with significant contributions in the new faulty observation) will be computed.

The index I_{ss} for the fault *j* will be computed according to the following expression:

$$I_{\mathrm{ss}}^{j} = 1 - \frac{n_{\mathrm{DS}}^{j}}{K} \tag{8.4}$$

When a contribution is significant in only one of the sets it will count as a discrepancy in the sign. Despite these situations are fully captured by the index I_{sc}, this situation is considered as a discrepancy to avoid some problems. For example, when comparing the scaled contributions for the faulty observation 3 in Figure 8.2 with the fingerprint for the fault *j* (Fig 8.1 a), the indices $I_s = 0$ and $I_{sc} = 0.08$ show successfully that there is a great discrepancy between them. In the case that the aforementioned situation would not be considered as a discrepancy, then the indice I_{ss} would become equal to 1 and would lead to a misinterpretation.

- I_o : *Contribution size order similitude index*

This index measures the degree of similarity in the order of the sorted by size scaled contributions of the original variables between the fault *j*-th fingerprint and the new faulty observation.

In order to compute this index we introduce a new type of matrix, the *contribution size order matrix* (**OM**). There will be a different matrix for every type of fault. These matrices are computed according to the corresponding fault fingerprint and its size becomes $K \times K$. The columns of this matrix are assigned to the different original variables and the rows of this matrix are used to record the order number of the sorted contributions in the fingerprint for a particular fault. Each column of these matrices show the size order position of the contribution for the variable assigned to that column. For instance if variable 1 is the 5th highest contribution then the value for the 1st column and 5th row of the **OM** will be 1 and the rest of the column will be zero. A modified **OM** where the contributions size order is adjusted by a window range can be a good solution when the size of the contributions for different variables are similar or situations in which several contributions may be 0 (if only significant contributions are taken into account). In this new matrix $\mathbf{OM}_w$ the size order position of the contribution may not be unique and, therefore, the columns of these matrices may include several 1 values.

Figure 8.3 shows the sorted scaled contributions for fault *j* fingerprint. With a 5% window range variable 4 has the highest contribution and there is no other variable contribution inside its 5% range window. Thus in the 4th column of the $\mathbf{OM}_w^j$ there will be a 1 in the first row and a 0 is assigned to the rest of the 4th column. Variable 1 is the 2nd contribution in size and there are two others variable contributions, variable 2 (3rd position) and variable 7 (4th position), inside its 5% range window.

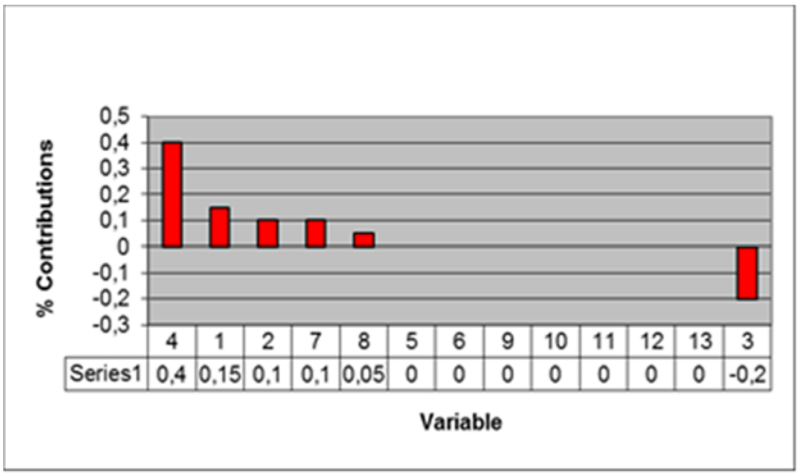

FIGURE 8.3: Sorted fingerprint for fault *j*

According to this, in the 1st column of the $\mathbf{OM}_w^j$ there will be a 1 in rows 2, 3 and 4. The $\mathbf{OM}_w^j$ matrix for the fault *j* obtained by proceeding this way for all of the variable contributions follows:

$$\mathbf{OM}_w^j = \begin{bmatrix} 0 & 0 & 0 & 1 & 0 & 0 & 0 & 0 & 0 & 0 & 0 & 0 & 0 \\ 1 & 1 & 0 & 0 & 0 & 0 & 1 & 0 & 0 & 0 & 0 & 0 & 0 \\ 1 & 1 & 0 & 0 & 0 & 0 & 1 & 1 & 0 & 0 & 0 & 0 & 0 \\ 1 & 1 & 0 & 0 & 0 & 0 & 1 & 1 & 0 & 0 & 0 & 0 & 0 \\ 0 & 0 & 0 & 0 & 1 & 1 & 0 & 1 & 1 & 1 & 1 & 1 & 1 \\ 0 & 0 & 0 & 0 & 1 & 1 & 0 & 1 & 1 & 1 & 1 & 1 & 1 \\ 0 & 0 & 0 & 0 & 1 & 1 & 0 & 1 & 1 & 1 & 1 & 1 & 1 \\ 0 & 0 & 0 & 0 & 1 & 1 & 0 & 1 & 1 & 1 & 1 & 1 & 1 \\ 0 & 0 & 0 & 0 & 1 & 1 & 0 & 1 & 1 & 1 & 1 & 1 & 1 \\ 0 & 0 & 0 & 0 & 1 & 1 & 0 & 1 & 1 & 1 & 1 & 1 & 1 \\ 0 & 0 & 0 & 0 & 1 & 1 & 0 & 1 & 1 & 1 & 1 & 1 & 1 \\ 0 & 0 & 0 & 0 & 1 & 1 & 0 & 1 & 1 & 1 & 1 & 1 & 1 \\ 0 & 0 & 1 & 0 & 0 & 0 & 0 & 0 & 0 & 0 & 0 & 0 & 0 \end{bmatrix}$$

Following this procedure to all the types of faults, a database of $\mathbf{OM}_w^j$ matrices for each type of fault is constructed. In a new faulty observation, the positions of the sorted scaled contributions will be checked against the OM_w^j for every type of fault *j*. The index I_o for the fault *j* will be computed according to the following expression:

$$I_{\mathrm{sc}}^{j} = 1 - \frac{n_{\mathrm{DO}}^{j}}{K} \tag{8.5}$$

where n_{DO}^{j} is the number of discrepancies in the contribution size order.

8.2.2 FCP implementation

8.2.2.1 Data generation and PCA model of the process

In order to explain the FCP method we have applied it to the pasteurization process described in chapter 2. In this case a slightly changed normal operation condition data set with only one value for the set point of the flow (in our case 160) was considered. Table 8.1 shows the 12 measured variables. In addition to this data set we also produced data sets in which we initialized the different types of faults (Table 8.2). We kept track of the moment in which every type fault was initialized, so we could check the performance of the fault diagnosis methodology.

TABLE 8.1 Variables measured in the pasteurization model

Nr	Variable	Description
X_1	Tank Level	Level of the water in the tank at the beginning of the process. If it drops below a certain limit, the tank is refilled.
X_2	T^a_1	Temperature of the product after flowing through the curved pipe. This temperature defines whether or not we have a good product.
X_3	T^a_2	Temperature of the heating water. This is the water which has to heat our product.
X_4	T^a_3	Temperature of the final product. This is the temperature of the product when it leaves the system.
X_5	T^a_4	Temperature of the product immediately after heating, so before entering the curved pipe..
X_6	T^a_5	Temperature of the product after preheating the new product. This temperature defines whether or not the product needs further cooling down.
X_7	Flow	Speed with which the product flows through the system.
X_8 X_9 X_{10}	Power 1 Power 2 Power 3	These variables all measure some aspect of the power used to heat the heating water.
X_{11}	Pump 1	Opening percentage of pump 1. Pump 1 controls the flow speed of the product.
X_{12}	Pump 2	Opening percentage of pump 2. Pump 2 controls the flow speed of the heating water.

In order to apply the fingerprint contribution plot methodology (FCP), the NOC and the different types of fault data sets were generated. According to the results of a PCA study on the NOC file, a two component model was selected for monitoring the process.

TABLE 8.2 Types of fault

Number	Type	Fault
f_1	Process Fault	Set Point T_1 (Uncontrolled change)
f_2	Process fault	Failure in Pump 1 (Feeding)
f_3	Process fault	Decay of 30% in Pump 1 (Feeding)
f_4	Sensor fault	Sensor Flow (Down)
f_5	Sensor fault	Sensor T_1 (Down)
f_6	Sensor fault	Sensor T_1 (Up)
f_7	Sensor fault	Sensor T_2 (Down)
f_8	Sensor fault	Sensor T_3 (Up)
f_9	Sensor fault	Sensor T_4 (Down)
f_{10}	Sensor fault	Sensor T_4 (Up)
f_{11}	Sensor fault	Sensor T_5 (Down)
f_{12}	Sensor fault	Sensor T_5 (Up)
f_{13}	Process fault	Failure of the valve which divert the wrong product
f_{14}	Process Fault	Set Point Flow (Down to 110)
f_{15}	Process Fault	Set Point Flow (Up to 200)

Training and test data sets were generated for every fault defined in Table 8.2. As the pasteurization process is regulated (*i.e.* it has some control loops), whenever a fault is generated it normally takes some time to drive the process back to the NOC conditions. Due to this problem the data bases on the different faults were not very extense. Every type of fault was generated 5 times. The training set was composed of the first 6 observations after the fault in the first two runs while the test set was composed of the first 3 observations after the fault in the last three runs.

The FCP selects a number of components of the PCA model that gives the best fault diagnosis performance calculated over all the different types of faults. It must be noted that the number of components considered to ensure best diagnosis is not necessarily the same number required for process monitoring (*i.e.* some components of the model not considered when monitoring the process because of its small weight may be critical for the purpose of diagnosis of some specific type of faults).

Only the significant contributions are considered in our study. The threshold limits determining significant contributions when considering individual variable contributions to the Hotelling´s T_A^2 or SPE can empirically be obtained from extensive NOC data sets and/or alternatively using the theoretical distributions described in Section 1.3.1.3.

In the case of the *SPE* we preferred to use the square root values of these contributions in order to maintain the sign of the contributions.

8.2.2.2 SDI and Minor Difference Between Faults (MDBF) index

For every type of fault the contribution plots corresponding to a sequence of faulty observations and its corresponding fingerprint based on the information contained in all of them were obtained. Finally, the *SDI* and a new index, the *MDBF* (Minor Difference Between Faults) for the different faulty observations, were calculated in order to assess the diagnosis performance of the methodology.

As commented previously, the *SDI* measures the similitude degree between the scaled contributions in every fault signal and a fault fingerprint. In addition, obtaining the *SDI* for the sequence of different fault signals generated for every type of fault serve to measure the variability of the signals in relation to its corresponding fingerprint. The sequence of *SDI* values determines the homogeneity of the observations for each type of fault.

The *MDBF* (Minor Difference Between Faults) for a faulty observations is the difference between the *SDI* calculated for the real type of fault and the maximun *SDI* obtained when considering all the other types of faults. This is defined for a faulty observation f_n and a real type of fault *i* as:

$$MDBF_n = SDI(\hat{f}_n, \hat{f}_i) - max\ SDI(\hat{f}_n, \hat{f}_j) \qquad \forall j \neq i \tag{8.6}$$

Where $\hat{f}_j$ is the fingerprint for the type of fault *j*, $\hat{f}_i$ the fingerprint for the real type of fault and $\hat{f}_n$ the fingerprint for the new faulty observation.

Following its own definition, this index is related to the identifiability of the fault. Moreover, a higher MDBF of the faulty observation is associated with better diagnosis performance results. It must be noted that observations with high *SDI* can have small *MDBF*. In this case it would be concluded that the fault is similar to at least two fingerprints and consequently that the diagnosis performance will be affected. Thus a high *SDI* values are not a guarantee of a correct classification.

This *MDBF* is calculated for each individual faulty observation and it is used to assess the performance in the fault diagnosis.

The parameters: α, β, γ and θ of the *SDI* index, were optimized to achieve the best fault diagnosis performance given the selected number of components in the model. The parameters to be used for computing the *SDI* in the Hotelling´s T_A^2 and *SPE* statistics were optimized on an individual basis

Parameter´s optimization

Two methods were used for performing the optimization:

- Optimization using the fingerprint

The optimization process works with the fingerprints data base that previously were obtained from the training set. It looks for the best number of components of the model and the best values for the four parameters (α, β, γ and θ) in order to maximize the average *MDBF* (Minor Difference Between Faults) obtained for all the types of faults.

$$MDBF = \sum_{i=1}^{F} MDBF_i \Big/ J \tag{8.7}$$

where, J is the number of different types of faults, and for each fault i the $MDBF_i$ is computed according to the expression :

$$MDBF_i = SDI(\hat{f}_i, \hat{f}_i) - max\ SDI(\hat{f}_i, \hat{f}_j) = 1 - max\ SDI(\hat{f}_i, \hat{f}_j) \quad \forall j \neq i \qquad (8.8)$$

- Optimization using the training set observations

It looks for the best number of components of the model and the best values for the four parameters (α, β, γ and θ) in order to maximize the average percentage of true fault classification in the training set of the faults.

In this method, the situations where the *SDI* for the real fault in an observation of the training set become less than the 50% and situations where the monitoring statistics do not signal were penalised with a negative weight.

In the optimization process it was required that the coefficient α would be greater or equal to 0.5. The main reason for this is primarily that the *SDI* contains the most consistent information about the faults. Small values for the coefficient α usually were accompanied by a bad fault diagnosis performance in the test set accompanied by inconsistency with the results in the training sets.

8.2.2.3 FCP fingerprints, fault isolability, homogeneity and signal degradation:

FCP fingerprints

Figure 8.4 shows an example of a fingerprints in the FCP. The fingerprints were obtained using the training set.

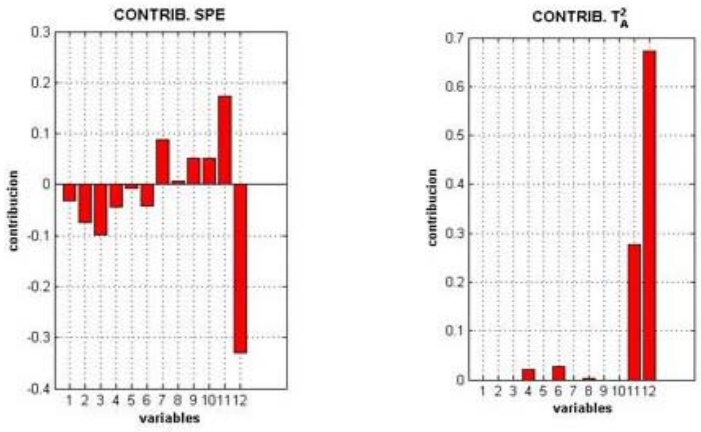

Fingerprint of Fault 1

FIGURE 8.4: Example of fingerprint for fault f_1 in the FCP:

Faults isolability

Isolability in the SPE

Table 8.3 shows that in the case of the *SPE*, the only cases in which the *SDI* between each pair of fingerprints is higher than 50% are between the fingerprints of the faults f_2 and f_4 (90.20%),f_3 and f_{15} (72.25%), f_1 and f_{13} (55.31%).

	f1	f2	f3	f4	f5	f6	f7	f8	f9	f10	f11	f12	f13	f14	f15
f1	1	0,3228	0,354	0,2721	0,2245	0,2354	0,2165	0,2607	0,1737	0,2202	0,196	0,2693	**0,5531**	0,0641	0,3712
f2		1	0,3839	**0,9020**	0,1612	0,4077	0,1863	0,1788	0,1970	0,1743	0,3112	0,1780	0,1584	**0,3131**	0,1276
f3			1	0,405	0,1436	0,3208	0,1273	0,1621	0,1528	0,1443	0,347	0,1676	0,4139	0	**0,7225**
f4				1	0,1778	**0,4163**	0,2165	0,1749	0,1926	0,1953	**0,3834**	0,1697	0,1347	0,2658	0,1276
f5					1	0	0,2681	0,2632	0,2984	0,1536	**0,323**	0,264	0,1977	0,2752	0,106
f6						1	0,182	0,342	0,1543	**0,3205**	0,2311	0,3369	0,1883	0,1297	0,2075
f7							1	0,1892	0,2856	0,1375	0,2606	0,1824	**0,3555**	0,1663	0,0328
f8								1	0,1638	0,2673	0,267	**0,4721**	0,2017	0,2859	0,1274
f9									1	0	0,2576	0,1614	0,3126	0,143	0,0627
f10										1	0,158	0,2647	0,0582	0,1158	0,1378
f11											1	0	0,1696	0,1394	0,1607
f12												1	0,2078	0,2891	0,1417
f13													1	0,0642	0,4323
f14														1	0
f15															1

TABLE 8.3: Similitude degree index (*SDI*) among the *SPE* fingerprints
Bold numbers correspond to the highest *SDI* for every fault or cases with a *SDI* > 50%

-

- Isolability in the T^2_A:

	f_1	f_2	f_3	f_4	f_5	f_6	f_7	f_8	f_9	f_{10}	f_{11}	f_{12}	f_{13}	f_{14}	f_{15}
f_1	1	0,3113	0,3127	0,2822	0,0308	0,004	0,0022	0,0223	0,0046	0,005	0,0266	0,0266	0,2941	**0,3262**	0,316
f_2		1	0,3844	**0,9632**	0,0041	0,0015	0,0002	0,0157	0,0022	0,005	0,018	0,0182	0,3055	**0,6267**	0,4813
f_3			1	0,3924	0,0294	0,004	0,0003	0,0002	0,0048	0,0045	0,0099	0,0098	**0,4376**	**0,5731**	**0,898**
f_4				1	0,0041	0,0015	0,001	0,0019	0,0016	0,0037	0,0019	0,002	0,3221	**0,6125**	0,4671
f_5					1	**0,9707**	0,0001	0,0002	0,0048	0	0,0002	0,0001	0,0161	0,0041	0,0041
f_6						1	0,0001	0,0002	0,0028	0	0,0002	0,0001	0,004	0,0015	0,0015
f_7							1	0	0,0001	0	0,0004	0	**0,2269**	0,0022	0
f_8								1	0,0002	0,0005	0	0,0001	0,0002	0,103	0,0164
f_9									1	**0,9933**	0,0002	0,0001	0,0048	0,0003	0,0003
f_{10}										1	0,0045	0,0045	0	0,005	0,005
f_{11}											1	**0,9996**	0,0004	0,113	0,0222
f_{12}												1	0,0001	0,113	0,0223
f_{13}													1	0,4251	0,4229
f_{14}														1	**0,6751**
f_{15}															1

TABLE 8.4: Similitude degree index (*SDI*) among the T^2_A fingerprints
Bold numbers correspond to the highest *SDI* for every fault or cases with a SDI > 50%

Table 8.4 shows that in the case of the T^2_A, the highest similitude degree index (*SDI*) are between the fingerprints of the faults f_9 and f_{10} (99.33%), f_{11} and f_{12} (99.96%) and f_5 and f_6 (97.07%). Despite it seems difficult to distinguish between these pairs of faults in the T^2_A, they can be clearly distinguished in its *SPE* fingerprints as shown in Table 8.3 Each pair of these faults corresponds to a fault in the same temperature sensor increasing or decreasing its normal measurement. Table 8.4 also shows that the similitude degree index (*SDI*) between the faults f_2 (flow sensor fault) and f_4 (pump 1 fault) is 96.32%. As shown in Tables 8.3, in the *SPE* the *SDI* between the faults f_2 and f_4 is also high: 90.20%. Other cases where the *SDI* for the T^2_A is higher than 50% are between the fingerprints of the faults f_2 and f_{14} (62.67%), f_3 and f_{14} (57.31%) f_3 and f_{15} (89.08%) f_4 and f_{14} (61.25%) and f_{14} and f_{15} (67.51%) .

The minor difference between faults (*MDBF*) is an index that can be useful to determine the isolability of the different types of faults. This index is obtained by applying the *SDI* to the fingerprints in expression (8.*7)* as if they were new observations

$$MDBF_i = SDI(\hat{f}_i, \hat{f}_i) - max\ SDI(\hat{f}_i, \hat{f}_j) = 1 - max\ SDI(\hat{f}_i, \hat{f}_j) \quad \forall j \neq i$$

TABLE 8.5: Minor difference between faults (*MDBF*) calculated over the fingerprints

	SPE		T^2_A	
	MDBF	Fault	*MDBF*	Fault
f_1	0.4469	f_{13}	0.6738	f_{14}
f_2	0.0980	f_4	0.0368	f_4
f_3	0.2775	f_{15}	0.102	f_{15}
f_4	0.0980	f_2	0.3249	f_{15}
f_5	0.6770	f_{11}	0.0293	f_6
f_6	0.5837	f_4	0.0293	f_5
f_7	0.6445	f_{13}	0.7731	f_{13}
f_8	0.5279	f_{12}	0.897	f_{14}
f_9	0.6874	f_{13}	0.0067	f_{10}
f_{10}	0.6795	f_6	0.0067	f_9
f_{11}	0.6166	f_4	0.0004	f_{12}
f_{12}	0.5279	f_8	0.0004	f_{11}
f_{13}	0.4469	f_1	0.5627	f_3
f_{14}	0.6869	f_2	0.3249	f_{15}
f_{15}	0.2775	f_3	0.102	f_3

This parameter can be easily obtained from Tables 8.3 and 8.4 and it clearly confirms the results obtained from the *SDI*.

Following the results in Table 8.5, faults f_2 and f_4 are the most difficult to isolate since they have a *MDBF* that is smaller than 10% in the two monitoring statistics. In the case of the *SPE* the *MDBF* for all the other faults fingerprints is always higher than 25 % . In the case of T^2_A the *MDBF* is very small for the three pairs of faults f_5- f_6, f_9- f_{10} and f_{11}-f_{12} which correspond to faults involving the same sensors T_1,T_4 and T_5 (see Table 8.2), respectively, but they can be easily isolated in the *SPE*. The only faults which had T^2_A signals not accompanied by *SPE* signals while monitoring, were the faults f_1, and f_{13} which had both a *MDBF* in T^2_A above the 25%

Table 8.6 and figure 8.5 show that the *MDBF* results computed from the training set match perfectly the isolability results obtained by the analysis of the *SDI* of the faults fingerprints (represented in Tables 8.3 and 8.4). In fact, measuring the *SDI* between a pair of fingerprints is equivalent to measuring the isolability of that pair of faults. Conversely

TABLE 8.6: Minor difference between faults (*MDBF*) obtained from the training set

	SPE	T^2_A
	MDBF	*MDBF*
f_1		0.6599
f_2	0.0560	
f_3	0.2012	
f_4	0.0354	
f_5	0.6527	
f_6	0.5806	
f_7	0.6332	
f_8	0.5255	
f_9	0.4389	
f_{10}	0.6773	
f_{11}	0.5920	
f_{12}	0.5215	
f_{13}		0.3270
f_{14}	0.5963	
f_{15}	0.2316	

measuring the MDBF for each type of fault is a comparative measure of the isolability between the fault analysed and the most similar fault present in the fault data base. It must be noted that the faults fingerprints are obtained from the training set so that this was an expected result

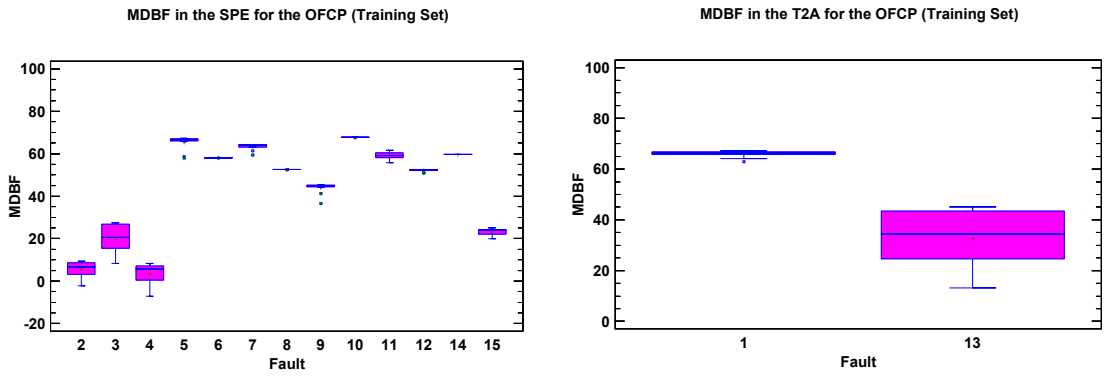

FIGURE 8.5 **:** *MDBF* for the *SPE* and T^2_A

- **Fault homogeneity**

The homogeneity of the fingerprints of the observations in each fault data set around its corresponding overall fingerprint is an important issue to consider before concluding that the proposed methodology is going to give good results in the isolation of the different types of faults. To measure the homogeneity we calculate the variable *difference of the SDI* from $Target = 1 - SDI(f_i, \hat{f}_i)$ where $\hat{f}_i$ is the fingerprint for type fault *i* and f_i is the fingerprint for each observation of the corresponding fault data set. Yet, this value is computed for all the observations in the training and test sets corresponding to each type of fault *i* and following this, the mean and standard deviation of these values are obtained. Tables 8.7 and 8.8 (and Figures 8.6 and 8.7) display the mean and the standard deviation of the discrepancy of the *SDI* among the observations of the different sets of faults for the two monitoring statistics *SPE* and T^2_A. These tables show that the majority of the faults have a high degree of homogeneity with a small standard deviation. These tables and figures show that the sensor faults had better results in the *SDI* than the process faults as it can be concluded from their smaller values in the mean of $1 - SDI(f_i, \hat{f}_i)$. These results were also confirmed in the test sets. Sensor faults also had more homogeneity in the fingerprint signal with smaller standard deviation in the *SDI* than the process faults.

TABLE 8.7 : Signal stability for the *SPE*

Fault *i*	$1-SDI(f_i,\hat{f}_i)$			
	Training Set		Test Set	
	mean	σ	mean	σ
f_1 (Process fault)	---	---	---	---
f_2 (Process fault)	0.0891	0.0533	0.1342	0.0618
f_3 (Process fault)	0.1199	0.0793	0.1342	0.0618
f_4 (Sensor fault)	0.0862	0.0626	0.1323	0.0344
f_5 (Sensor fault)	0.0244	0.0303	0.0359	0.0350
f_6 (Sensor fault)	0.0031	0.0024	0.0037	0.0033
f_7 (Sensor fault)	0.0115	0.0153	0.0235	0.0204
f_8 (Sensor fault)	0.0028	0.0007	0.0027	0.0004
f_9 (Sensor fault)	0.0106	0.0146	0.0065	0.0015
f_{10} (Sensor fault)	0.0022	0.0021	0.0050	0.0050
f_{11} (Sensor fault)	0.0244	0.0123	0.0402	0.0477
f_{12} (Sensor fault)	0.0225	0.0423	0.0055	0.0013
f_{13} (Process fault)	---	---	0.3388	0.1670
f_{14} (Process fault)	---	---	---	---
f_{15} (Process fault)	0.0373	0.0525	0.1030	0.1081
Average $1-\mathrm{SDI}(f_i,\hat{f}_i)$	0.0362	0.0306	0.0743	0.0421
Sensor faults: Average $1-SDI(f_i,\hat{f}_i)$	0.0209	0.0203	0.0284	0.0166
Process faults: Average $1-SDI(f_i,\hat{f}_i)$	0.0821	0.0617	0.1105	0.0997

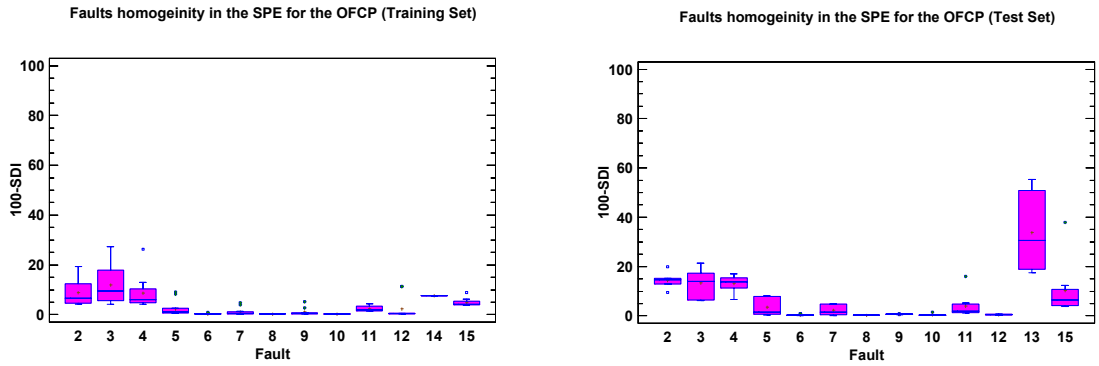

FIGURE 8.6 **:** Signal stability for the *SPE*

Fault *i*	$1-SDI(f_i,\hat{f}_i)$			
	Training Set		Test Set	
	media	σ	media	σ
f_1 (Process fault)	0.0139	0.0071	0.0488	0.0547
f_2 (Process fault)	---	---	---	---
f_3 (Process fault)	---	---	---	---
f_4 (Sensor fault)	---	---	---	---
f_5 (Sensor fault)	---	---	---	---
f_6 (Sensor fault)	---	---	---	---
f_7 (Sensor fault)	---	---	---	---
f_8 (Sensor fault)	---	---	---	---
f_9 (Sensor fault)	---	---	---	---
f_{10} (Sensor fault)	---	---	---	---
f_{11} (Sensor fault)	---	---	---	---
f_{12} (Sensor fault)	---	---	---	---
f_{13} (Process fault)	0.2310	0.1121	0.3183	0.0121
f_{14} (Process fault)	---	---	---	---
f_{15} (Process fault)	---	---	---	---
Average $1-\mathrm{SDI}(f_i,\hat{f}_i)$	0.1225	0.0596	0.1836	0.0334
Sensor faults: Average $1-\mathrm{SDI}(f_i,\hat{f}_i)$	---	---	---	---
Process faults: Average $1-\mathrm{SDI}(f_i,\hat{f}_i)$	0.1225	0.0596	0.1836	0.0334

TABLE 8.8 : Signal stability for the T^2_A

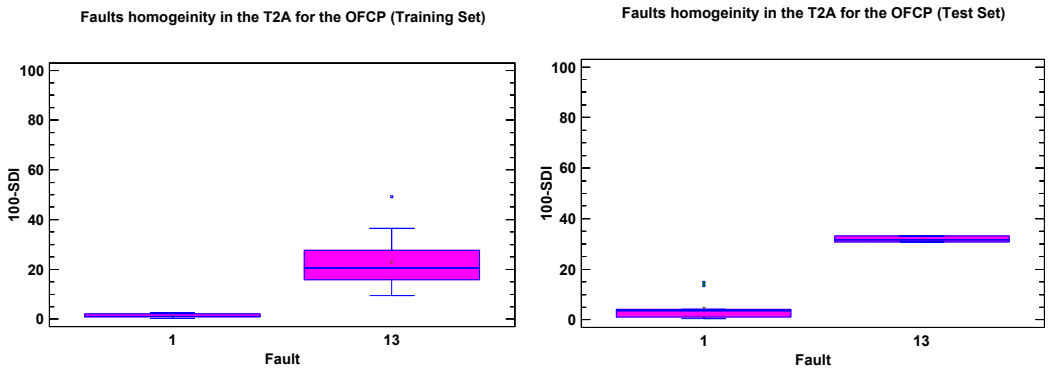

FIGURE 8.7 **:** Signal stability for the T^2_A

The previous results can be confirmed through an analysis of variance (ANOVA) on the FCP data. The analysis of variance (ANOVA) in the FCP for the *SDI* with factors: Set (training, test) and Type of fault, show that the two factors and the interaction were statistically significant (*p-value* < 0.05) for the two statistics: *SPE* and T^2_A

TABLE 8.9: ANOVA for the *SDI* on the *SPE*

Análisis de Varianza para SDI - Suma de Cuadrados Tipo III

Fuente	*Suma de Cuadrados*	*Gl*	*Cuadrado Medio*	*Razón-F*	*Valor-P*
EFECTOS PRINCIPALES					
A:Fault	4735,49	11	430,499	26,38	0,0000
B:Set	99,8458	1	99,8458	6,12	0,0141
INTERACCIONES					
AB	225,907	11	20,537	1,26	0,2502
RESIDUOS	3672,39	225	16,3217		
TOTAL (CORREGIDO)	8683,39	248			

Todas las razones-F se basan en el cuadrado medio del error residual

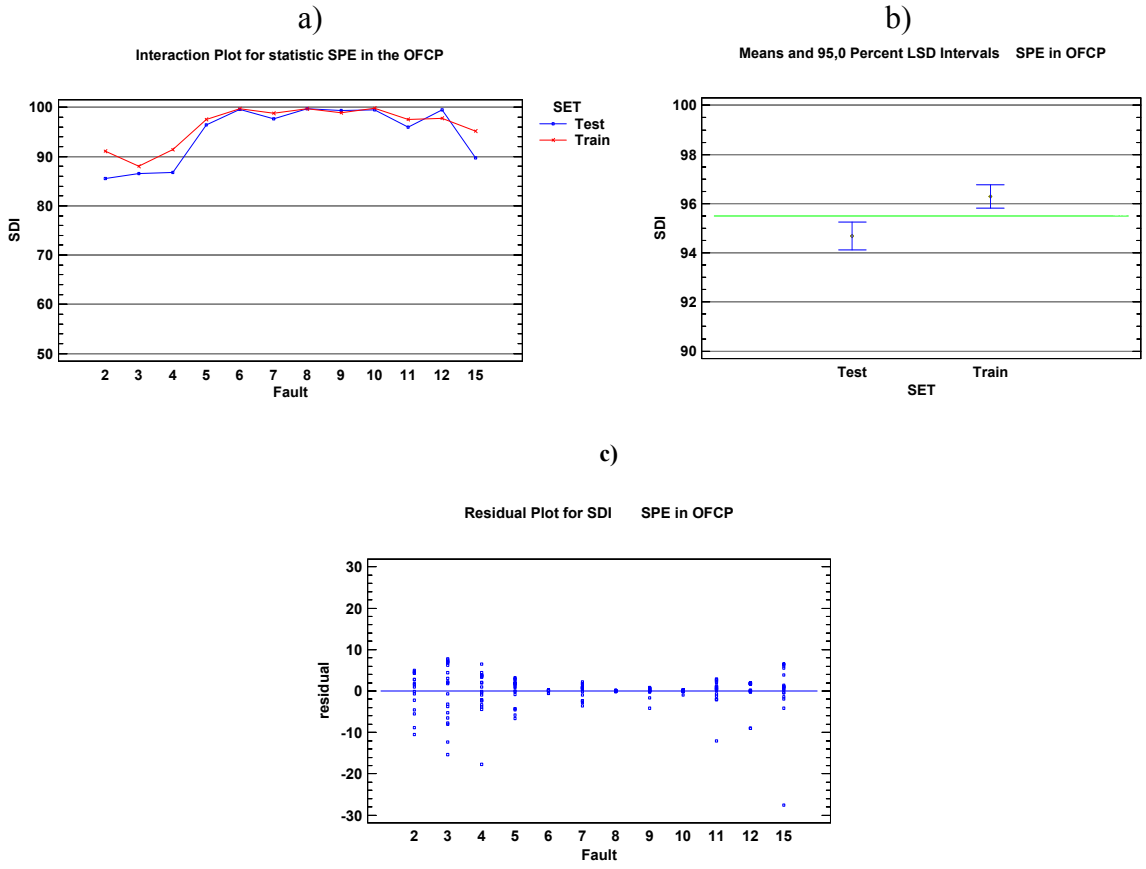

FIGURE 8.8 ANOVA plots for the *SDI* on the *SPE*

Table 8.9 and 8.10 show that the factor Set is statistically significant, yielding on average better results (higher *SDI*) in the training set than in the test set. Note that the training set was employed in the construction of the fingerprints. The residuals in Figures 8.8 and 8.9 c) provides similar information to the box whisker plot for the *SPE* in Figure 8.6 where it can be observed that fault f_{13} has low homogeneity in the fingerprint and that there is an observation which differ notably of the other observations of the test set in fault f_{15}.

TABLE 8.10: ANOVA for the *SDI* on the T^2_A

Analysis of Variance for SDI - Type III Sums of Squares T^2_A

Source	*Sum of Squares*	*Df*	*Mean Square*	*F-Ratio*	*P-Value*
MAIN EFFECTS					
A:Fault	3873,6	1	3873,6	76,08	0,0000
B:SET	244,32	1	244,32	4,80	0,0359
INTERACTIONS					
AB	44,8721	1	44,8721	0,88	0,3549
RESIDUAL	1629,2	32	50,9126		
TOTAL (CORRECTED)	6093,54	35			

All F-ratios are based on the residual mean square error.

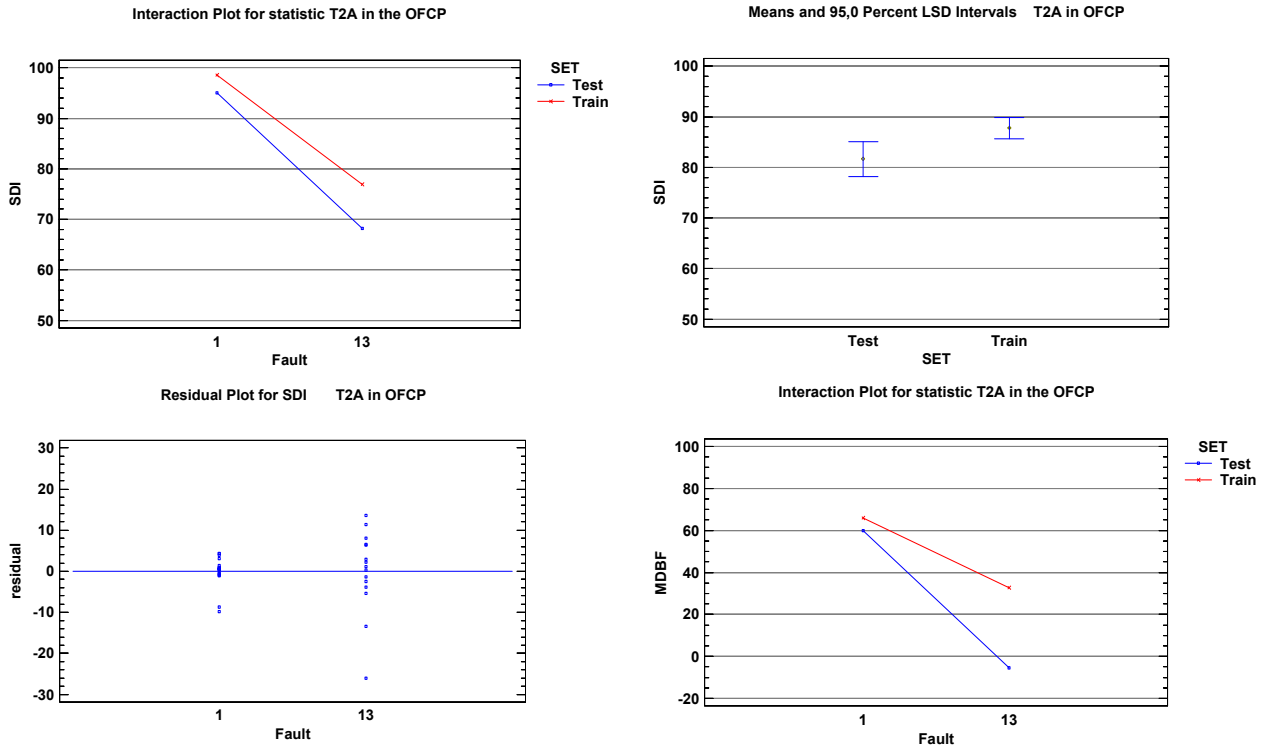

FIGURE 8.9 ANOVA plots for the *SDI* on the T^2_A

Table 8.10 and figure 8.9 a) and b) show that for the T^2_A the factor Set is also significant, yielding on average better results in the training set than in the test set. The anova residuals in figure 8.9 c) shows that fault f_{13} has the lowest homogeneity in the fingerprint.

Signal degradation in FCP

A question to study in a closed loop process is how the contributions evolve after the fault detection. It makes possible to study if the isolation capability of the method is degrading or not after the initial detection. This study is important since it could happen that the methodology yield only good diagnosis results in early detection. In order to study the signal degradation, we proceed to study the evolution of the *SDI* in the sequence of observations following the first signal of fault.

Table 8.11 shows the number of observations until the *SDI* decreases under 70%, until the *MDBF* decreases under 10% and until there is a wrong fault diagnosis.

This table shows that all the sensor faults are detected specially by the *SPE* and there is no problem of isolation with faults f_5, f_6, f_7, f_8, f_9, f_{10}, f_{11} and f_{12}. All these faults have a *SDI* up the 70% and keep a *MDBF* > 0.1 for a long sequence of observations after the fault is diagnosed for the first time.

The only sensor fault that had some isolation problem was the f_4 that could not be appropriately isolated from the process fault f_2. Bearing in mind that the f_4 is a fault in the flow sensor and the f_2 is a fault in the pump 1 which affects in a straight way the flow rate explains why these two types of faults can not be successfully isolated.

In relation to the isolation in the process faults, the fault f_1 is detected in the T^2_A and has a *SDI* up the 70% and keep a *MDBF* < 0.1 for a long sequence of observations,

the fault f_{12} (failure of the valve which divert the wrong product) has no problem of misclassification in a long sequence of observations after the fault is diagnosed for the first time, and finally the faults f_{14} and f_{15} (changes in the set point of the flow) are also successfully diagnosed. The only problem with the f_{14} (Set Point Flow Down to 110) is that the signal takes 6 to 8 observations to be detected for the first time and then the signal ends after 5 to 7 observations. So in this case it is more a problem of lack of detection that a problem of misdiagnosis.

In some of the data sets *MDBF* < 0.1 or *SDI* up a 70% was not successfully achieved for a long sequence of observations but it must be noted that this fact was not necessarily accompanied by misclassification.

TABLE 8.11. Signal degradation for all the types of fault.

Fault f_1	Training 1	Training 2	**Fault f_2**	Training 1	Training 2
	T^2_A	T^2_A		*SPE*	*SPE*
SDI <0.7	23	18	SDI <0.7	16	15
MDBF <0.1	28	28	MDBF <0.1	1 (f_4)	1 (f_4)
Diagnosed other fault	>30	30	Diagnosed other fault	3 (f_4)	24(f_{14})

Fault f_3	Training 1	Training 2	**Fault f_4**	Training 1	Training 2
	SPE	*SPE*		*SPE*	*SPE*
SDI <0.7	>20	>20	SDI <0.7	>20	>20
MDBF <0.1	7 (f_{15})	6 (f_{15})	MDBF <0.1	1 (f_2)	1(f_2)
Diagnosed other fault	19(f_{15})	11(f_{15})	Diagnosed other fault	11(f_2)	1(f_2)

Fault f_5	Training 1	Training 2	**Fault f_6**	Training 1	Training 2
	SPE	*SPE*		*SPE*	*SPE*
SDI <0.7	>20	>20	SDI <0.7	>15	>15
MDBF <0.1	>20	>20	MDBF <0.1	>15	>15
Diagnosed other fault	>20	>20	Diagnosed other fault	>15	>15

Fault f_7	Training 1	Training 2	**Fault f_8**	Training 1	Training 2
	SPE	*SPE*		*SPE*	*SPE*
SDI <0.7	>20	>20	SDI <0.7	>20	>20
MDBF <0.1	>20	>20	MDBF <0.1	>20	>20
Diagnosed other fault	>20	>20	Diagnosed other fault	>20	>20

Fault f_9	Training 1	Training 2	**Fault f_{10}**	Training 1	Training 2
	SPE	*SPE*		*SPE*	*SPE*
SDI <0.7	>20	>20	SDI <0.7	>19	>20
MDBF <0.1	>20	>20	MDBF <0.1	>19	>20
Diagnosed other fault	>20	>20	Diagnosed other fault	>19	>20

Fault f_{11}	Training 1	Training 2	**Fault f_{12}**	Training 1	Training 2
	SPE	*SPE*		*SPE*	*SPE*
SDI <0.7	>20	>20	SDI <0.7	>20	>20
MDBF <0.1	>20	>20	MDBF <0.1	>20	>20
Diagnosed other fault	>20	>20	Diagnosed other fault	>20	>20

Fault f_{13}	Training 1		Training 2		**Fault f_{14}**	Training 1	Training 2
	T^2_A	*SPE*	T^2_A	*SPE*		*SPE*	*SPE*
SDI <0.7	>29	>29	3	>28	SDI <0.7	5*	6*
MDBF <0.1	28 ($f_3 f_{15}$)	>29	>27(f_3)	>28	MDBF <0.1	5*	6*
Diagnosed other fault	>29	>29	>27(f_3)	>28	Diagnosed other fault	5*	6*

Fault f_{15}	Training 1	Training 2
	SPE	*SPE*
SDI <0.7	>34	>33
MDBF <0.1	10(f_3)	>33
Diagnosed other fault	>34	>33

8.2.2.4 FCP monitoring results

The objective of this section is to provide an example of the monitoring tools and plots in order to detect and diagnose the faults under the FCP methodology. Figures 8.15 displays the monitoring results in the *SPE* and T^2_A of the test set corresponding to fault f_7 . A representative fingerprint contribution plot (FCP) for one single observation of the test set in this type of fault is also shown. The FCP plot is a barchart with so many bars as different types of faults are included in a fault data base. Each bar of the plot has a size which corresponds to the measured *SDI* (similitude degree index) between the fingerprint

of the new faulty observation and the corresponding fault fingerprint in the fault data base.

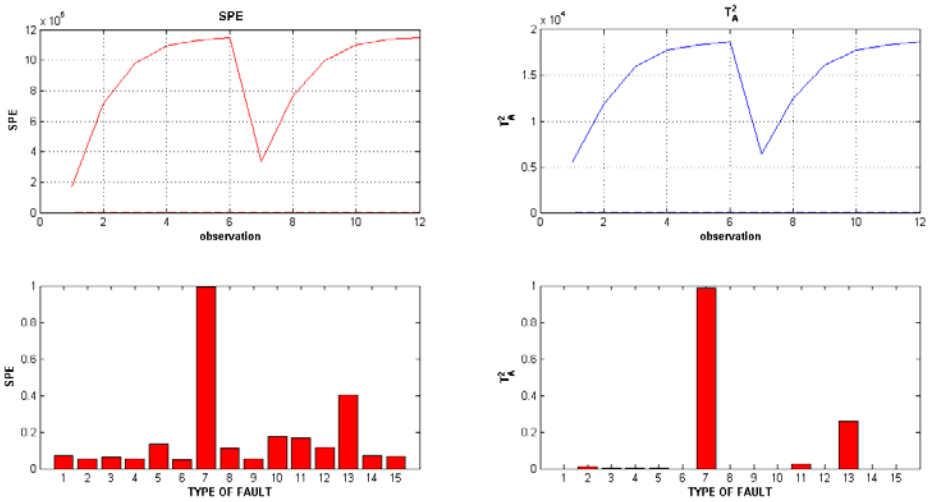

FIGURE 8.15 Fault 7: a) T^2_A, and SPE chart for the test set; b) Example of a FCP

8.3 FCP: Final considerations

The fingerprints methodology provides a successful set of complementary plots to be added to the traditional contribution plots and the T^2_A and *SPE* monitoring plots. This methodology allows the incorporation of information about the different types of faults to the diagnosis stage. The fingerprints methodology also provides information about fault isolability, fault homogeneity and fault signal degradation. The traditional contribution plots used in the non-supervised methods can be easily extended to a supervised diagnosis method in the case that we have information of the different types of faults by only including the fingerprint contribution plots (FCP plots). Additionally, the supervised method allows the addition of new types of fault to the fault data set in a sequential way as soon as they will be detected and studied. It would only require the computation of the new fingerprints and the corresponding optimization in a regular basis. These new types of faults can be easily detected if they can be distinguished from the

others as it supposes that all the *SDI* values will be small and this will be a clear indication that a new type of fault has happened. If the new faults can not be distinguished from the others then the only solution would be to measure new process variables that allow a successful isolation of this new type of fault.

Chapter 9: Diagnosis performance in MSPC

In this chapter we proceed to compare the diagnosis performance of different fault diagnosis methodologies in MSPC discussed in Chapter 8. The methods are tested using two processes data sets corresponding to a pasteurization process and a distillation process. The evaluation of the performance of these methods tries to highlight the strong and weak points of the different methods under study.

9.1 Diagnosis performance indices

It is well established that the sensitivity and specificity indices allows comparison of the classification results of different methodologies applied to a test comparing only two classes (effective against ineffective product) evaluated using the results of a single test. In the case of the fault diagnosis, where the number of classes (different types of faults) tend to be more than two, the measurement of the performance of the different methods is not so well established.

In the first part of this thesis we evaluated the performance of the methods in MSQC using an analysis of the variance (ANOVA) and a group of indices: PTC_0, $PTCv$, PWC_0, $PWCv$, PND and PNF that were explained in Section 4.1.2. In this second part we are going to use the average sensitivity and average specificity indices calculated over all the considered types of faults as a way to compare efficiently the performance of different diagnosis methods in MSPC studied in this thesis.

9.1.1 Average sensitivity and average specificity

The sensitivity for a fault F_i is the proportion of the real faults (F_i) that are correctly identified by the diagnosis method. The specificity for a fault F_i is the proportion of the real "no F_i faults" that are correctly identified by the diagnosis method. Both indices are calculated according to the expressions in figure 9.1 .

Then, the average values for the sensitivity and specificity are computed on the complete set of different types of faults:

$$\text{Average sensitivity} = \sum_{j=1}^{J} \frac{\text{Sensitivity}_j}{J} \;;\; \text{Average specificity} = \sum_{j=1}^{J} \frac{\text{Specificity}_j}{J}$$

where J is the number of different types of faults.

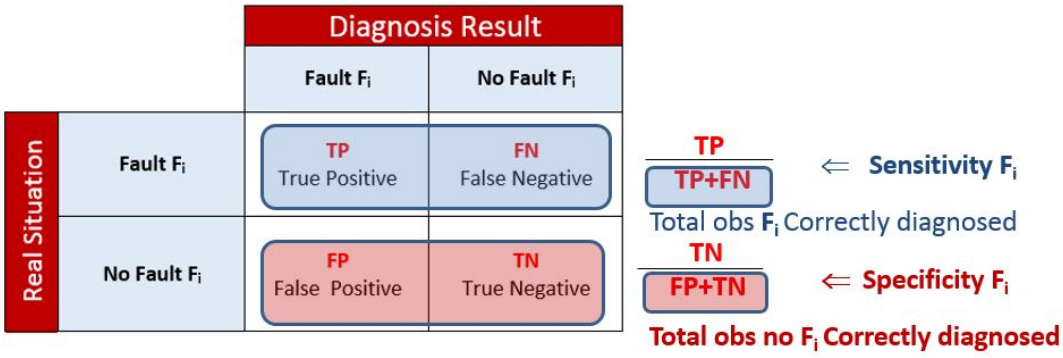

FIGURE 9.1 Calculation of the Sensitivity and Specificity

9.1.2 Fault diagnosis criteria

Another important issue is which criterion we use to assign the observed fault to a particular class of fault. In our study we are going to use two criteria:

- C1: In this criterion, fault diagnosis methodologies always signal only one type of fault which corresponds to the most suspected fault.
- C2: In this criterion the method signal all the types of fault that reach a significance threshold. This criterion is particularly interesting to detect new types of fault.

a) **Fault signature methodology:** in C1 we assign the new observed fault to the class with a projection in the cosine plot that is closest to vertex [+1, +1]. In the case of C2 we assign it to all the types of fault with a projection inside a semicircle defined by an empirical threshold r (distance from vertex [+1,+1]) and centred in vertex [+1,+1] as it is shown in figure 9.2.

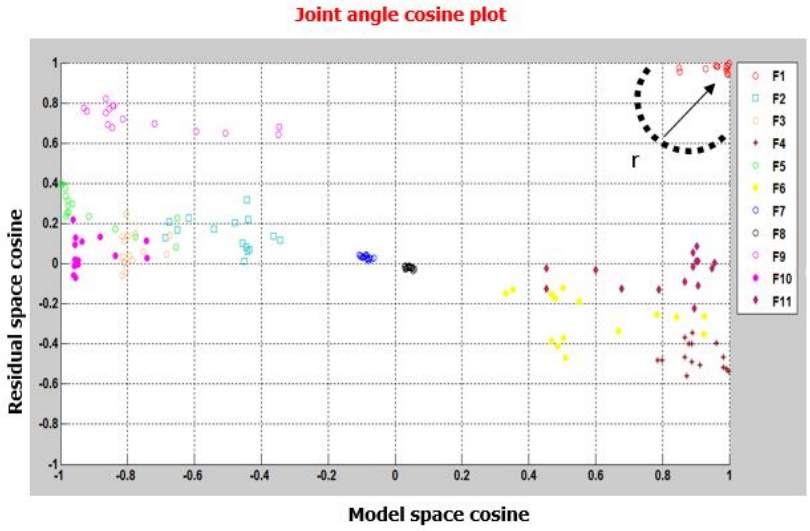

FIGURE 9.2 Empirical threshold r for the calculation of C2 in the Fault signature methodology

b) **Fault reconstruction methodology on SPE (FR_SPE) and the combined index (FR_Index):** in C1 we assign the new observed fault to the class with a best reconstruction and in the case of C2 we assign it to all the types of faults that after reconstruction get the minimum value of the considered statistic below a significance threshold.

c) **Discriminant partial least squares (PLS-DA)**: in C1 we assign the new observed fault to the class which best fit to the fault observation (Y prediction closest to 1) and in the case of C2 we assign it to all the types of faults with prediction higher than a significance threshold.

c) **Fingerprints (FCP)**: in C1 we assign the new observed fault to the class which best fit to the fault observation (SDI closest to 1) and in the case of C2 we assign it to all the types of faults with SDI higher than an empirical threshold.

9.1.3 Diagnosis and model windows

Model window:

In the model building stage it has been considered the use of three different window sizes in the training set replicates. The main purpose of this decision is to make it possible to study the effect of the size of the model window in the diagnosis performance and, consequently, its effect in the early and late diagnosis performance in the different methodologies.

In the pasteurization process we selected windows of 1 observation (W=1), 6 observations (W=6) and a large windows of 12 observations (W=12), while in the case of the distillation process a window of 1 observation (W=1), 30 observations (W=30) and a large window (W=120) were chosen. Figure 9.3 shows an example about how the training fault data set for modelling with a window size W=6 is built up from the complete fault data sets.

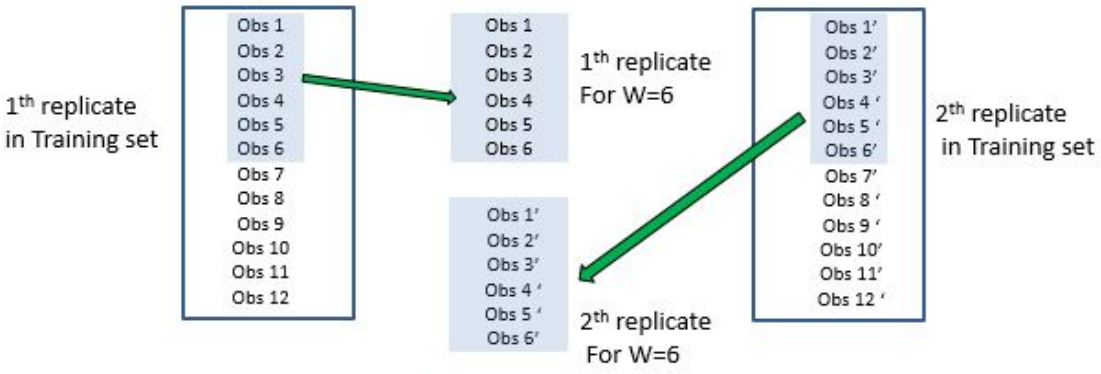

FIGURE 9.3 Fault data set construction for a selected model window size

The different availability of data and the diverse nature of the processes and the type of faults determined the size of the model windows that we finally decided to test in each process (*i.e.* in the pasteurization process a protection system can even provoke a shutdown of the plant. Similarly some faults, if maintained for some time, could require a long period of time to achieve the steady state conditions).

- **Diagnosis window:**

In the diagnosis stage it has been considered the use of a range of different windows sizes for diagnosis in the test set. The main purpose of this decision is to make it possible to study the evolution of the diagnosis performance in the different methodologies as we move away from the moment in which the fault is detected.

In the pasteurization process we selected a range of diagnosis windows from 1 to 12 observations and in the case of the distillation process a range of diagnosis windows from 1 to 120 observations.

Figure 9.4 shows an example about how the fault data set for fault diagnosis is built up according to different fault diagnosis windows.

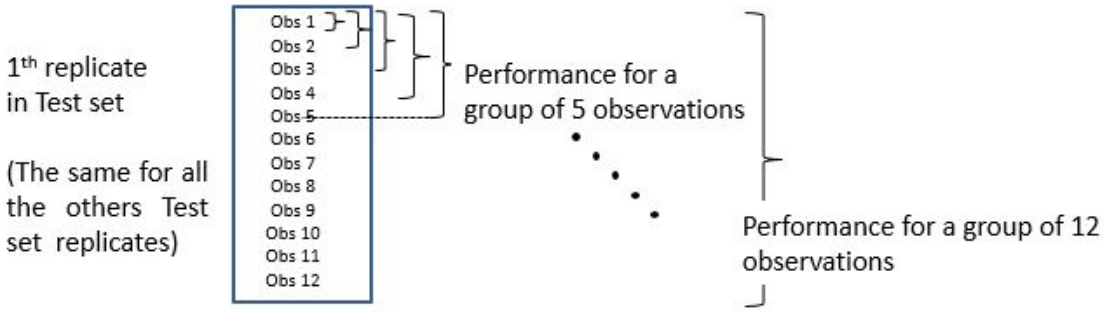

FIGURE 9.4 Fault data set construction for a selected diagnosis window size

9.1.4 Pre-calibration of the performance indices

In order to compare the performance of the methodologies in C2 we use the training set to calibrate all the methods with the same average specificity. In order to do this, the threshold limits of the different methods are conveniently selected to achieve the required fixed average specificity in the diagnosis of the training set. In doing so, the average sensitivity in the diagnosis results of the different methodologies are directly comparable in C2.

On the contrary in C1 as the criterion forces to signal a fault there is no need for such calibration given that the average sensitivity becomes similar to the average specificity differing only in the scale and, consequently, the average sensitivity in the diagnosis results of the different methodologies are directly comparable in C1.

9.2 Fault diagnosis performance comparison

9.2.1 Data sets

The fault diagnosis methods were tested in two process data sets which correspond to a pasteurization process and a distillation process. These data sets (registered variables and types of faults) are fully described in chapter 3. In the performance comparison described in this chapter the following subset of types of faults in each data set has been considered:

- Pasteurization process

TABLE 9.1 Types of fault

Number	Type	Fault description
f_1	Process fault	Uncontrolled change of the Set Point T_1
f_2	Process fault	Decay of 30% in Pump 1 (Feeding)
f_3	Sensor fault	Sensor Flow (Down)
f_4	Sensor fault	Sensor T_1 (Up)
f_5	Sensor fault	Sensor T_2 (Down)
f_6	Sensor fault	Sensor T_4 (Up)
f_7	Sensor fault	Sensor T_5 (Down)
f_8	Sensor fault	Sensor T_5 (Up)
f_9	Process fault	Failure of the valve which divert the wrong product
f_{10}	Process fault	Set Point Flow (Down to 110)
f_{11}	Process fault	Set Point Flow (Up to 200)

- Distillation process

Some of the faults were related to changes in feed parameters (F, Z_F and T_F) and the other types of faults were related to regulatory control (changes in controllers)

TABLE 9.2 Type of faults

Number	Type	Fault
$\mathbf{f_1}$	Process fault	Change in feed parameter F
$\mathbf{f_2}$	Process fault	Change in feed parameter Z_F
$\mathbf{f_3}$	Process fault	Change in feed parameter T_F
$\mathbf{f_4}$	Process fault	Change in controllers
$\mathbf{f_5}$	Process fault	Change in controllers

9.2.2 Implementation of the methods

The performance indices were pre-calibrated in all the methods to yield an average specificity in C2 equal to 95% in the case of the pasteurization process and 85% in the case of the distillation process.

9.2.2.1 Fault signature methodology (FS)

The empirical threshold *r* is adjusted to accomplish the pre-calibration objective. The results in both data sets and the two selected model windows is shown in Table 9.3:

TABLE 9.3 Selected empirical threshold *r*

	Model window W=1	Model window W=6	model window W=12
Pasteurization process	$r = 0.25$	$r = 0.86$	$r = 0.987$

	Model window W=1	Model window W=30	model window W=120
Distillation Process	$r = 1.18$	$r = 0.766$	$r = 0.924$

As indicated in Section 7.3.2 the Fault signature methodology was defined by its authors to work with model windows of size W=1. In this case wider windows models were selected in order to be able to compare it with the other methodologies.

We used 5 different procedures in the construction of the fault signature library:

- **M1**: uses the first observation after the fault and then the average is calculated on the different repetitions
- **M2**: uses the average of the vector direction calculated for the selected window and then the average is calculated on the different repetitions
- **M3**: uses the vector direction of the average observation for the selected window and then the average calculated on the different repetitions
- **M4**: uses the single value decomposition (SVD) on the fault data sets to obtain the fault signature. It was applied to a pool of observations collected from several repetitions of each type of fault. The observations are selected according to the size of the selected window and in all of them the value of the observation immediately before the fault is subtracted.
- **M5**: uses the single value decomposition (SVD) on the fault data sets to obtain the fault signature. It is similar to M4 but in this case there is no subtraction of the value of the observation immediately before the fault.

The average distance to vertex [+1,+1] in the cosine plot of the training set of the whole set of faults was used to decide which one of the five proposed methods give more accurate fault signatures. In the case of the pasteurization process, Figure 9.5 shows that procedures M2 and M3 performed better than the others in the extraction of the fault signatures. It can be noted that the M1, which uses only the information contained in the first observation after the fault detection, performs increasingly worse as the size of the

window increases. Procedure M5 based on the use of the SVD gives slightly worse results than M2 and M3.

Figure 9.5 a) shows that in the case of a model window equal to 1 methods 1, 2, 3 and 5 becomes equivalent. These results were consistent in the other data base (distillation process. Accordingly, in the study we will use the procedure M3 to obtain the fault signatures. .

a)

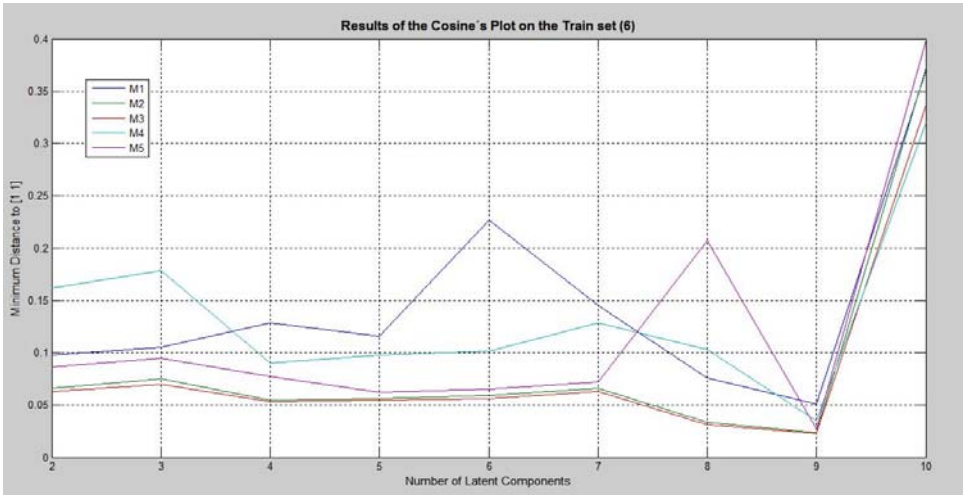

b)

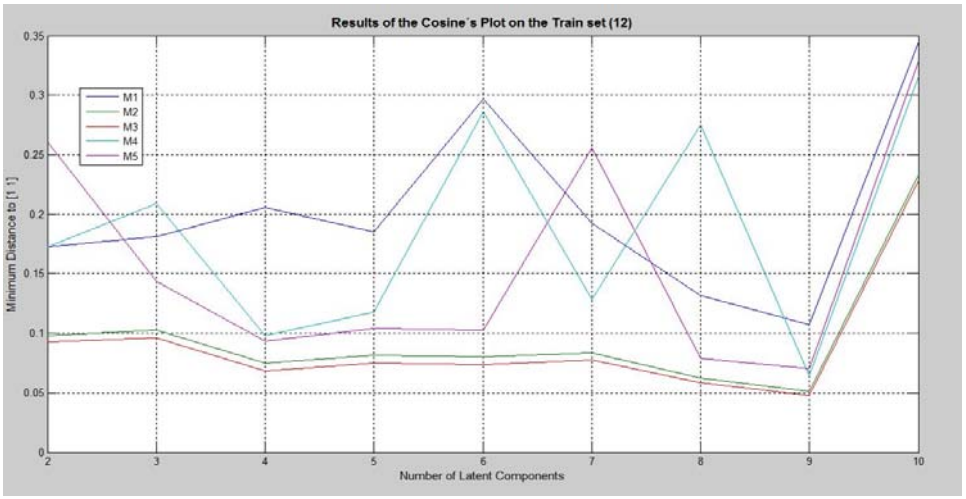

FIGURE 9. 5: Distance to vertex [+1,+1] in the Cosine´s plot in the pasteurization process training set in PCA models with a number of components ranging from 2 to 12: a) w=6 b) w=12

In relation to the selection of the number of PCs, our decision was based on the C1 and C2 performance results in the training set. In accordance with this, 8 PCs were selected for the pasteurization process and 7 PCs for the distillation process.

9.2.2.2 Fault reconstruction methodology (FR_SPE)

In accordance with the unreconstructed variance criterion we selected a 3 PCs model for both processes.

a) b)

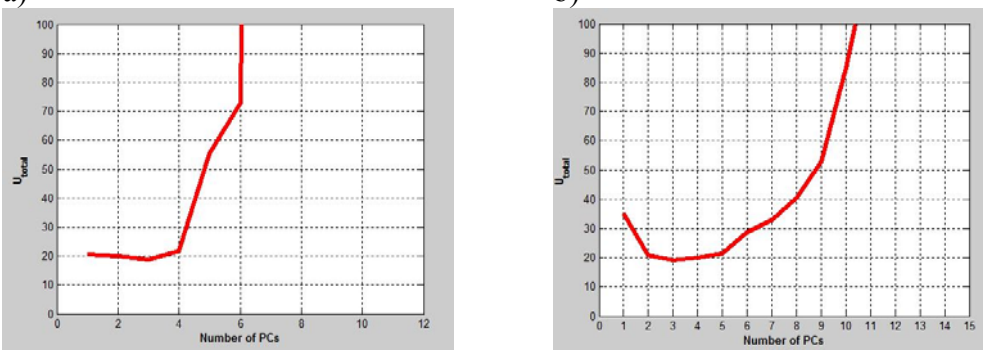

FIGURE 9.6 Unreconstructed variance a) Pasteurization process b) Distillation Process

The *SPE* threshold was adjusted to accomplish the pre-calibration objective. The results in both data sets and the two selected model windows is shown in Table 9.4:

TABLE 9.4 Selected *SPE* threshold

	Model window W=1	**Model window W=6**	**Model window W=12**
Pasteurization process	*SPE* = 96%	*SPE* = 93%	*SPE* = 98.5%

	Model window W=1	**Model window W=30**	**Large model window W=120**
Distillation Process	*SPE* = 60%	*SPE* = 92.87%	*SPE* = 95.75%

9.2.2.3 Fault reconstruction methodology (FR_Index)

In relation to the selection of the number of PCs, our decision was based on the C1 and C2 performance results in the training set. In accordance with this, it was selected 2 PCs were selected for both processes.

The combined index φ threshold was adjusted to accomplish the pre-calibration objective. The results in both data sets and the two selected model windows is shown in Table 9.5:

TABLE 9.5 Selected φ threshold

	Model window W=1	**Small model window W=6**	**Large model window W=12**
Pasteurization process	φ = 85%	φ = 83.1%	φ = 87.5%

	Model window W=1	**Small model window W=30**	**Large model window W=120**
Distillation Process	φ = 31.8%	φ = 60.5%	φ = 77.3%

9.2.2.4 Discriminant partial least squares (PLS-DA)

The number of latent variables of the discrimination models obtained by PLS-DA were set according to the outcomes resulting from the analysis of the training set (see Table 9.6, which also contains the average specificity percentage calculated by predicting the class membership of the test observations after having adjusted the corresponding significance threshold in the pre-calibration step).

TABLE 9.6 Adjust in C2 in the test set

	Pasteurization process	
	n° LV	**Adjustment in C2 (test set)**
C1 (W=1)	7	-
C1 (W=6)	11	-
C1 (W=12)	11	-

C1 (W=1)	4	93.5%
C2 (W=6)	7	95.2%
C2 (W=12)	7	93.4%

	Distillation process	
	n° LV	**Adjustment in C2 (test set)**
C1 (W=30)	8	-
C1 (W=30)	7	-
C1 (W=120)	7	-
C2 (W=30)	1	82.1%
C2 (W=30)	4	84.8%
C2 (W=120)	5	84.4%

9.2.2.5 Fingerprints contribution plots (FCP)

In this case, the selection of the number of PCs and FCP indices is based on the diagnosis performance results in the training set. In accordance with this, the number of PC components and the FCP indices for the SPE fingerprints are shown in Table 9.6

	Model window W=1	**Model window W=6**	**Model window W=12**
Pasteurization process	*Nº Comp =1* I_s=65; I_{sc}=0; I_{ss}=35 I_o=0	*Nº Comp =1* I_s=50; I_{sc}=0; I_{ss}=0; I_o=50	*Nº Comp =2* I_s=50; I_{sc}=0; I_{ss}=25; I_o=25

	Model window W=1	**Model window W=30**	**Model window W=120**
Distillation Process	*Nº Comp =2* I_s=50;I_{sc}=0;I_{ss}=0; I_o=50	*Nº Comp =3* I_s=50;I_{sc}=40;I_{ss}=0;I_o=10	*Nº Comp =3* I_s=55; I_{sc}=5; I_{ss}=40; I_o=0

TABLE 9.6 Selected number of components and SPE-FCP indices

9.2.3 Diagnosis performance results

Results in average sensitivity and specificity

In our study we decided to study the impact of the selected size of the "model window" (number of observations of the training sets used to build the models) for the

performance of the specific diagnosis methodologies. It must be noted that it cannot be assumed that by using a wider model window models would necessarily have poor performance in diagnosing the first observations immediately after fault detection (early diagnosis). To study the diagnosis performance of the models, once obtained with different model windows, they were used to diagnose "diagnosis windows" that progressively increased their size until they could be considered a large diagnosis window (late diagnosis) *i.e.* 120 in the case of the distillation process and 12 in the case of the pasteurization process. The objective of the plots in Figure 9.7 is to determine how the performance of the methodologies evolves as we move farther from the instant of the fault detection. In the plots it is measured the average sensitivity and specificity of the methods in progressively growing in size "diagnosis windows". Starting with the case of considering a diagnosis window of size equal to 1 (only one observation after the fault in all the test sets is considered for diagnosis), then considering a diagnosis window of size equal to 2 (two observations after that fault in all the test sets is considered for diagnosis) and so on.

According to the Figure 9.7 the following results follow:

- **Fault signature (FS):** This is the best method when all the methods are forced to build the models with only one single observation after the fault. Figure 9.7i and 9.7ii shows that FS has the best results in C1 and C2 for model windows (W=1) in the case of the distillation process. FS clearly outperforms the other methods. It must be noted that this statement does not mean that the best early diagnosis is obtained by this method. In figure 9.7i it is showed that other methods like Fingerprints or FR-SPE using wider model windows (*i.e.* W=30) obtain better results (higher sensitivities in C1 and C2) in early diagnosis as it can be appreciated in the value of sensitivity in the first diagnosis windows. It must be

taken into account that, as already commented, FS was defined by its authors to work with model windows of size W=1 and in this thesis we have forced this methodology to work also with of larger size model windows in order to be able to compare it with the others.

- **Fault reconstruction based on the SPE (FR.SPE):** This method has best performance when the diagnosis window is not too small. In the case of the distillation process, good results in C1 particularly during early diagnosis were obtained for W=30. This methodology was only outperformed by the Fingerprints methodology. FR.SPE also achieved good results in early diagnosis in C2 and only was outperformed by the FR-INDEX. When the diagnosis model is increased in size the results worsen in comparison with the results obtained with other methods. So FR.SPE has a poor performance in late diagnosis.
- **Fault reconstruction based on combined index (FR.C.INDEX):** This also yields better results when the diagnosis window is not too small. Results in C2 of the distillation process clearly outperformed the others in W=30 and W=120 in the first diagnosis window. When the diagnosis window is increased in size the results worsen but their decay is more gradual than in the case of the FR-SPE. So compared to the other methods **FR.C.INDEX** has poor performance in late diagnosis.
- **Fingerprints Contribution Plot (FCP_SPE):** The Fingerprints contribution plots on the SPE showed different performance in both data sets. In the pasteurization setting it yielded good results in C2. In the case of the distillation process, the method presented a singular performance in C2 that was similar to the performance of the FS method. It must be noted that the FCP_SPE behaves

differently to the FS in C1. FCP_SPE presented better results in C1 in the distillation process, especially in early diagnosis.

- **Partial Least Squares (PLS-DA):** This method achieved better results when the model window is not small. In addition it has also some limitations for early diagnosis and there are other methods that clearly outperform the PLS-DA. By conversely, when large diagnosis windows are considered, the diagnosis result improves. Indeed with large model windows and large diagnosis windows, this method clearly outperforms the others in late diagnosis.

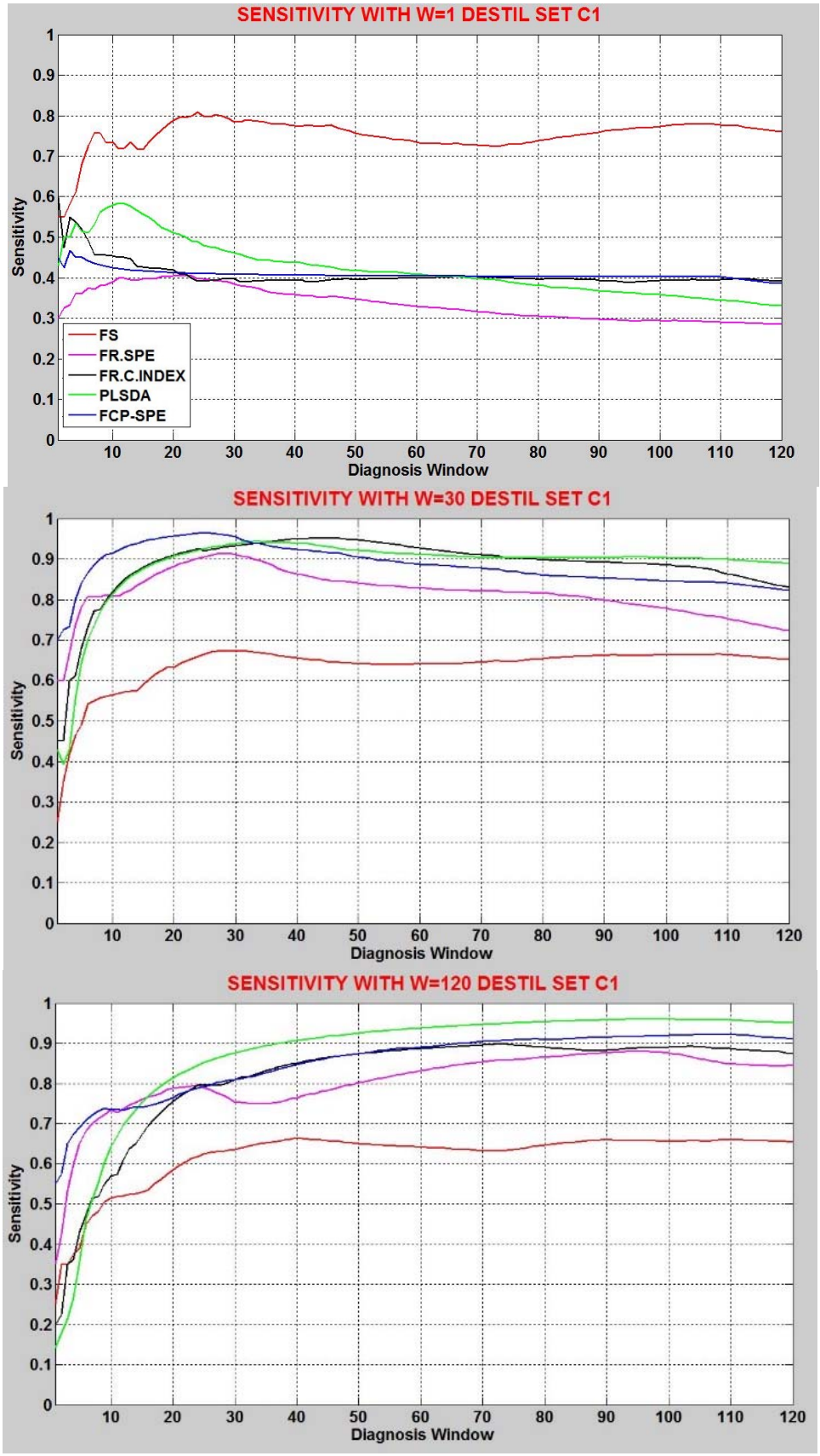

FIGURE 9.7 i) Average sensitivity for the distillation process in C1
a) W=1; b) W=30; c) W=120

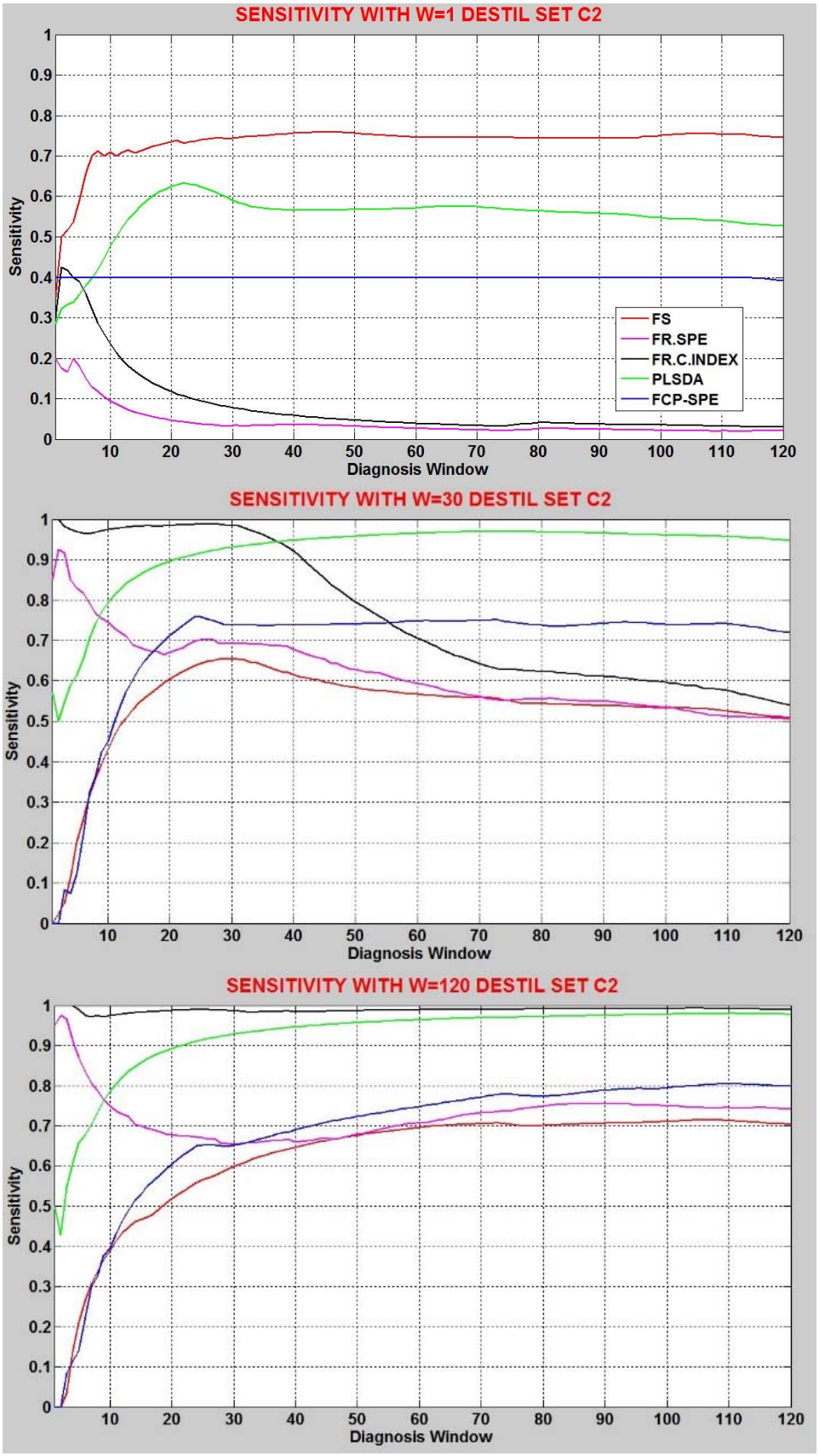

FIGURE 9.7 ii) Average sensitivity for the distillation process in C2
a) W=1; b) W=30; c) W=120

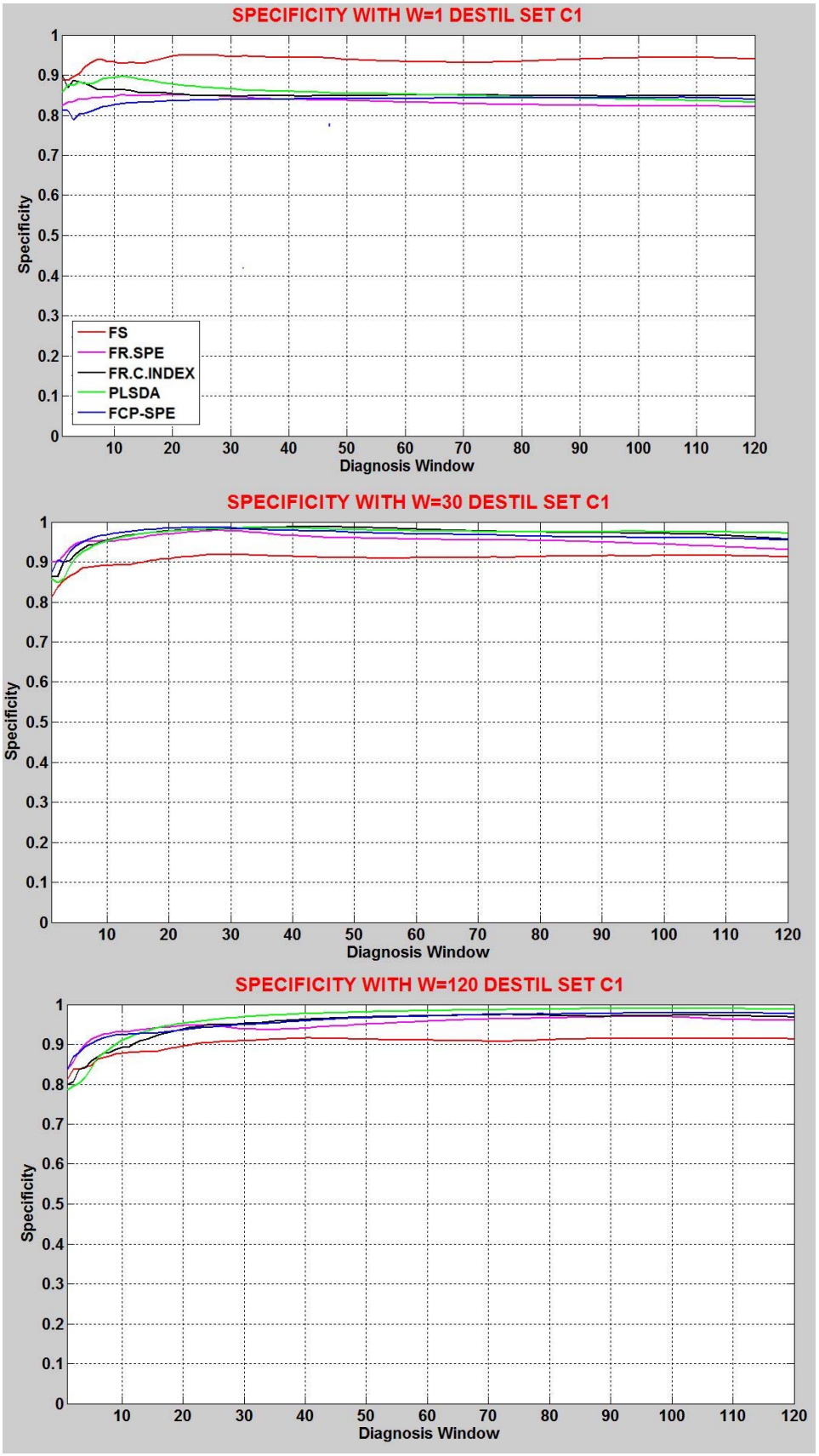

FIGURE 9.7 iii) Average specificity for the distillation process in C1
a) W=1; b) W=30; c) W=120

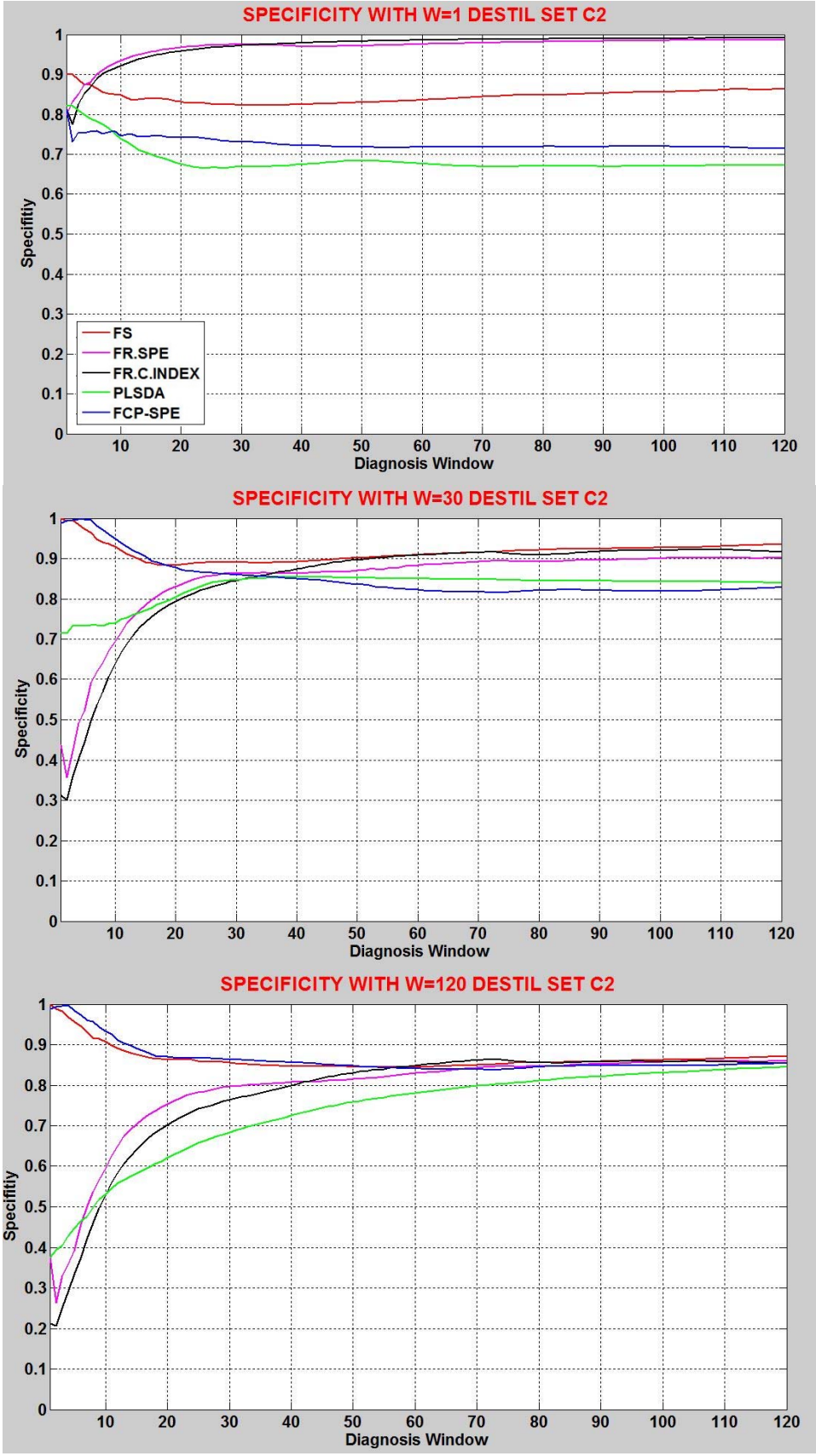

FIGURE 9.7 iv) Average specificity for the distillation process in C2
a) W=1; b) W=30; c) W=120

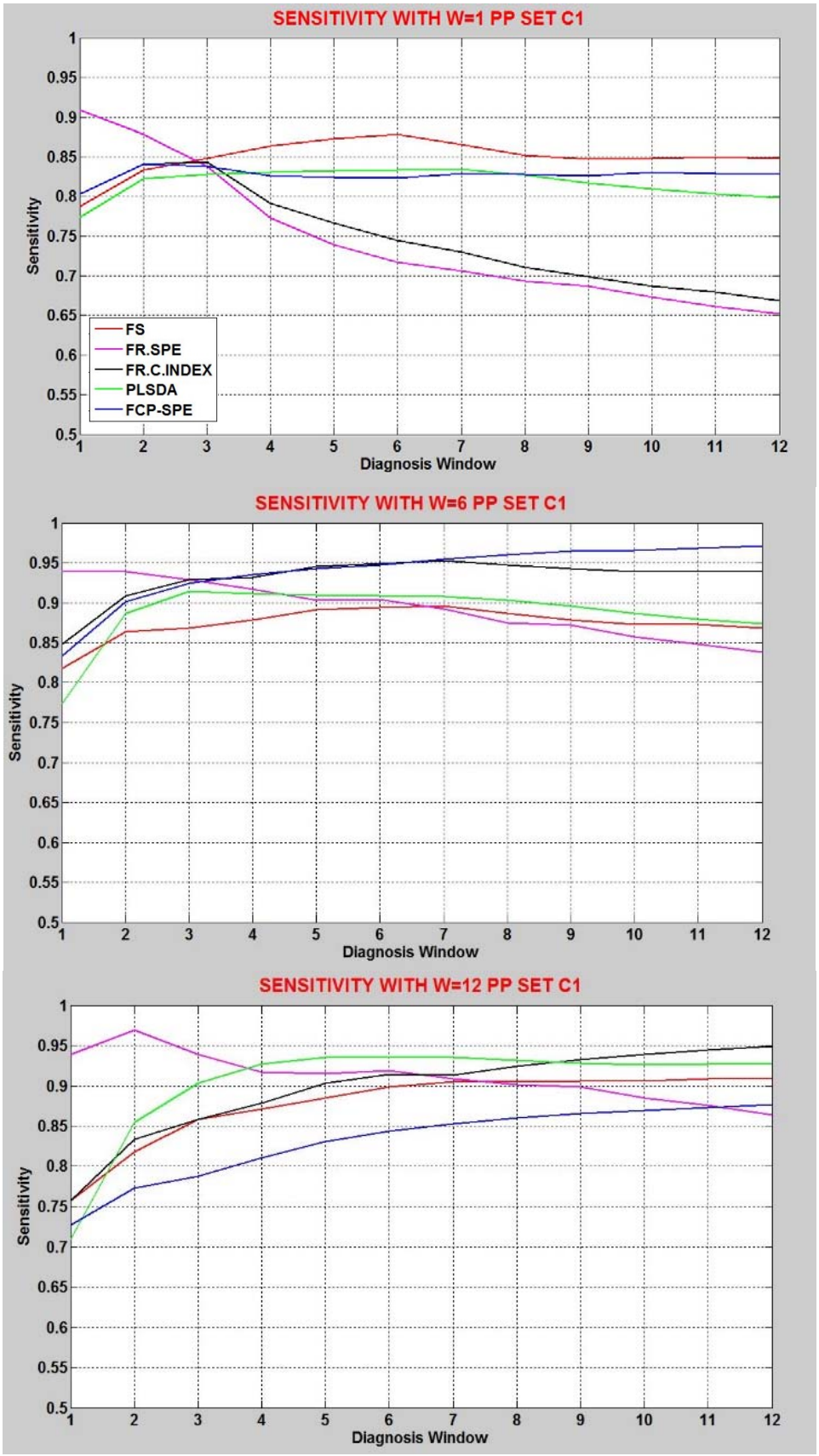

FIGURE 9.7 v) Average sensitivity for the pasteurization process in C1
a) W=1; b) W=6; c) W=12

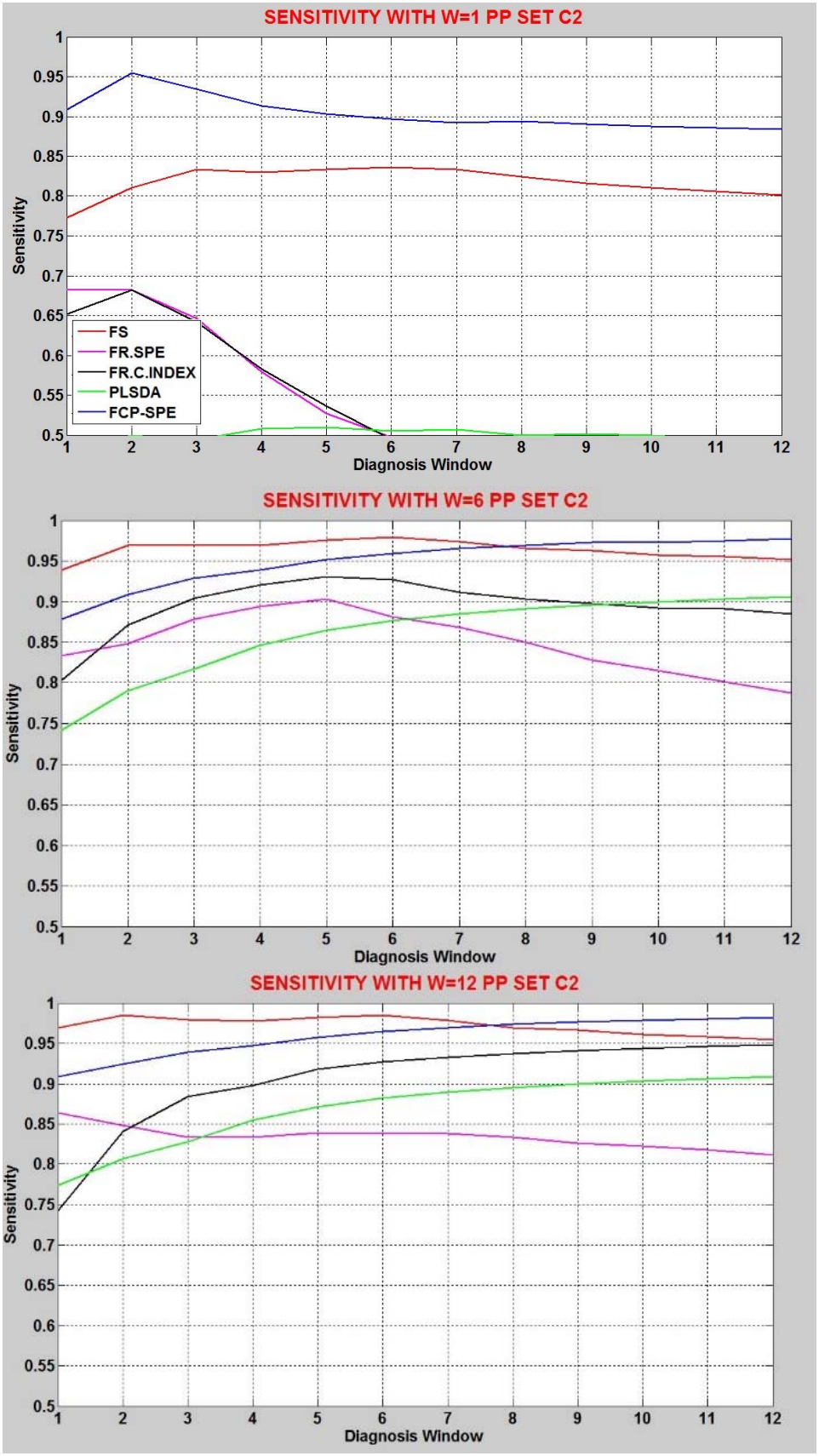

FIGURE 9.7 vi) Average sensitivity for the pasteurization process in C2
a) W=1; b) W=6; c) W=12

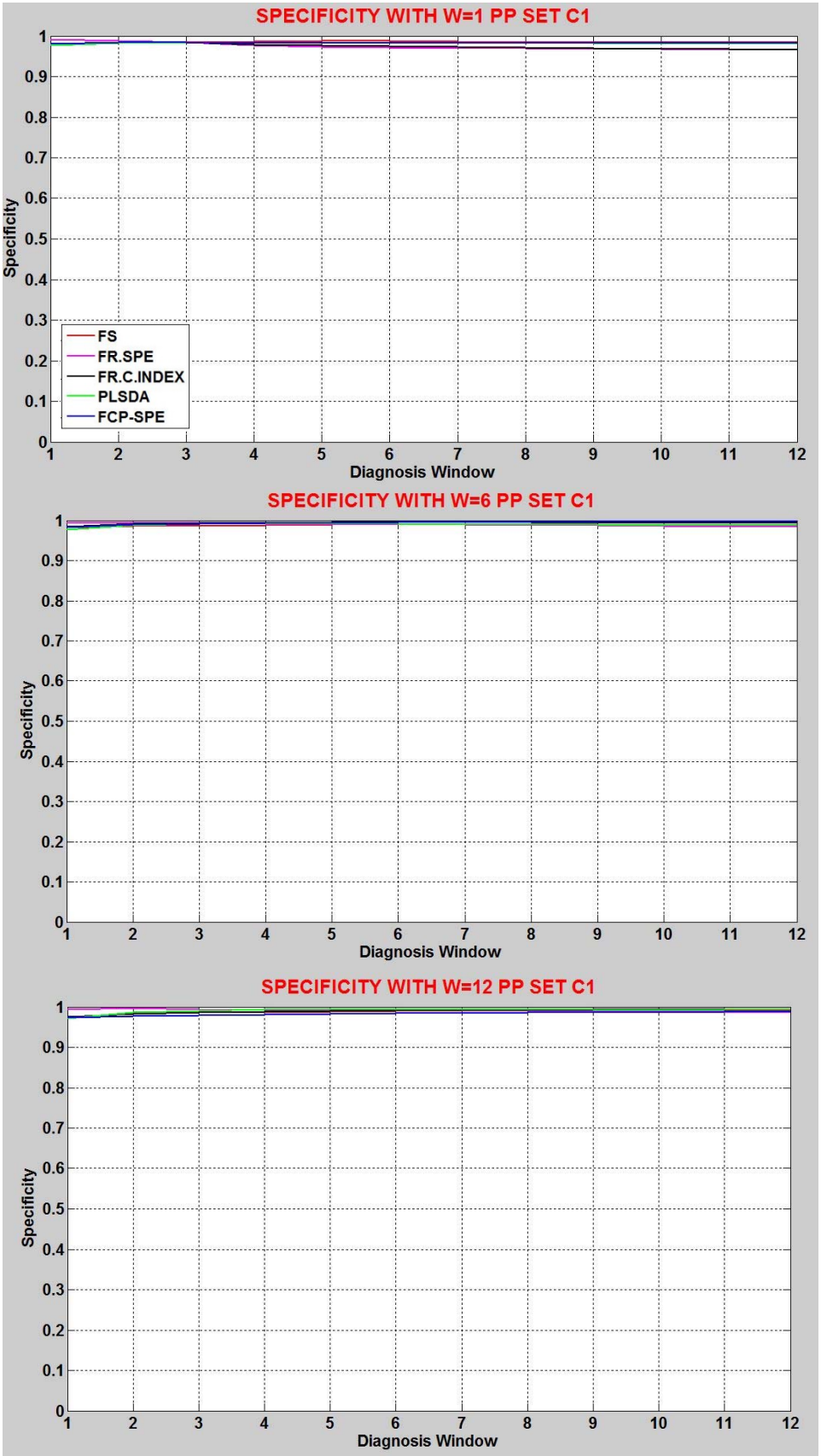

FIGURE 9.7 vii) Average specificity for the pasteurization process in C1
a) W=1; b) W=6; c) W=12

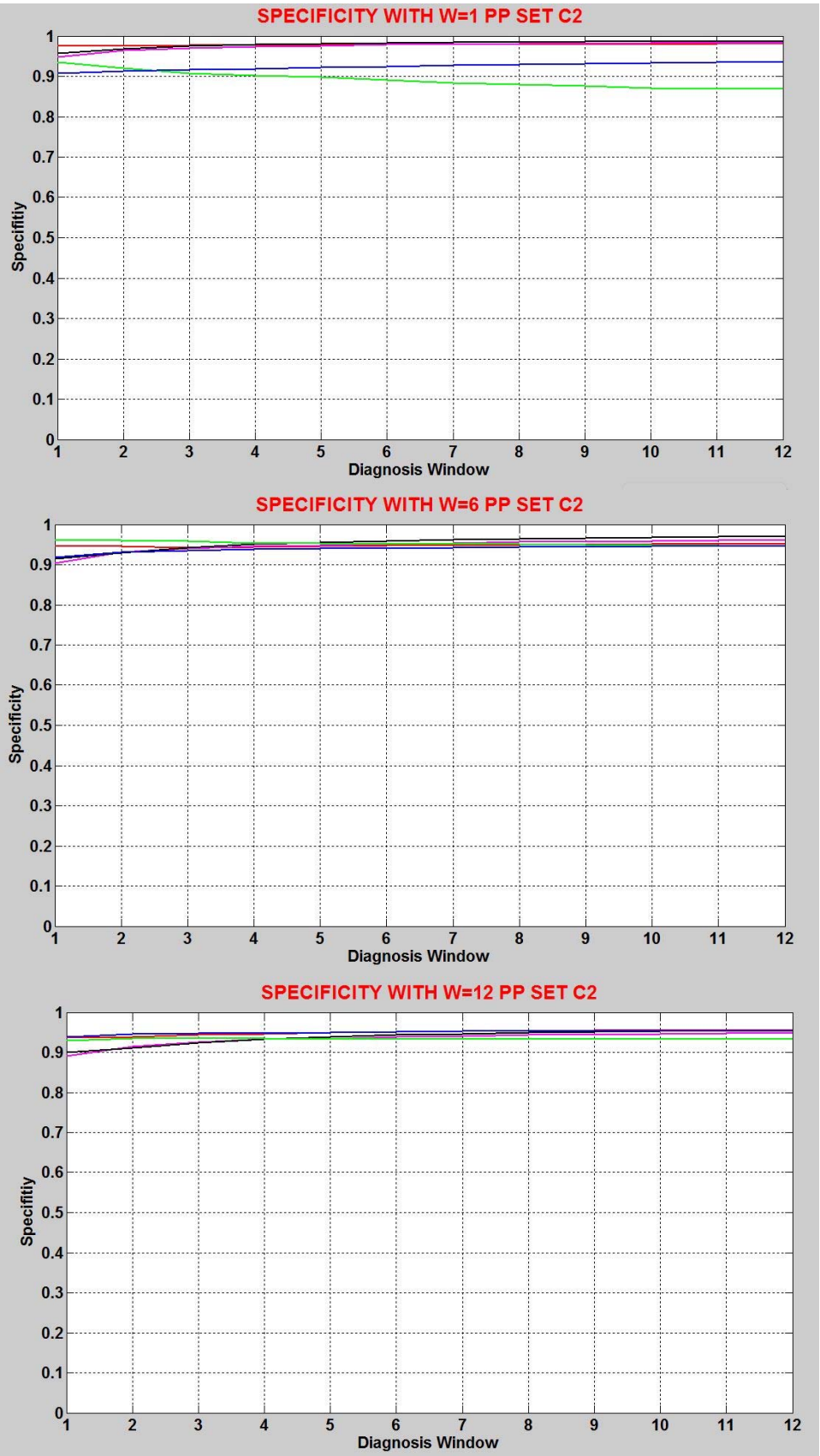

FIGURE 9.7 viii) Average specificity for the pasteurization process in C2
a) W=1; b) W=6; c) W=12

9.2.4 Conclusions

- The methods used exhibited different diagnosis performance. Fault signature methodology yielded better results when used to build models with small model windows (FS) . The other methods required larger model windows to improve their performance. These models also demonstrated different performance depending whether early or late fault diagnosis were considered. It was proved that the size of the model windows affects the performance of the different methodologies and that the use of small model windows does not guarantee a better early diagnosis performance. Indeed there are methods that require larger model windows to build models that perform reasonably well in early diagnosis.
- The new proposed method (FCP) exhibited comparable diagnosis performance to the most widespread fault diagnosis methods. It must be highlighted the excellent results of the FCP method in the case of C1 and early diagnosis.
- These results show that a mixed strategy based on the use of methods that are good for early diagnosis (fault reconstruction methodologies, the fingerprints or the fault signature) combined with methods that are good for late diagnosis (PLS-DA) can be an interesting option. In this case the second model would act to back the first, helping in the diagnosis particularly when the early diagnosis is not succesful.

Part V

Conclusions and future areas of research

Chapter 10: Conclusions and future areas of research

10.1 Conclusions

This thesis is devoted to the study and comparison of different methodologies proposed for fault diagnosis in a multivariate context. In our study we have differentiated between methodologies commonly used in Multivariate Statistical Quality Control (MSQC) and methodologies used in Latent-based Multivariate Statistical Process Control (Lb-MSPC). First, a detailed description of the methods was performed in order to understand the differences and relationships among the different methodologies. The diagnosis performance of the methods was tested in two process data bases (a pasteurization process and a distillation process) and two numerical simulations. Finally, new diagnosis methods and different variants of the former methodologies were considered in order to improve their diagnosis performance.

Here the main conclusions of the work are summarized, organized according to the objectives presented at the beginning of the document:

- **Clarify the relationships and the requirements for the implementation in practice of the most important data driven diagnosis methods in MSQC and Lb-MSPC and highlight their key weaknesses and strengths:** The methods and algorithms were described in full detail and also the most relevant considerations about their implementation (*i.e.* different algorithm schemes) and relationships (*i.e.* relationships among Hawkins´ residuals and the MTY conditional terms in Appendix 3.7).

- **Develop new efficient ways of comparing the performance of the different diagnosis methods:** In part II of this thesis we evaluated the performance of the different methods in MSQC using an analysis of the variance (ANOVA) and a group of indices: PTC_0, *PTCv*, PWC_0, *PWC*v, *PND* and *PNF*. In part III of the thesis we used the average sensitivity and average specificity indices calculated over all the considered types of fault in order to compare the performance of the diagnosis methods in Lb-MSPC. In the model building stage of the Lb-MSPC methods the use of different window sizes in the training set replicates to study the effect of the size of the model window in the diagnosis performance was considered. The later allows us to study the early and late diagnosis performance in the different methodologies.

  Both strategies to measure the diagnosis performance were successfully applied to situations were a large number of different types of faults is considered.

- **Test and compare the performance of different diagnosis methods in MSQC:** Our study showed that the MTY method presented the best diagnosis performance and provided an easy interpretation of the significant terms. Hawkins´, Murphy´s and Montgomery´s methods do not perform well in the case of strong correlations and exhibit an excessive number of false positives. The DFT method and its variants have problems of "lack of power in fault isolation" (PNF). The ad hoc methods D/AP and TCH show better power in fault isolation than the Bonferroni´s variant. Finally, the Step-down method with profile 1-1-1-1 and the Hawkins´ method for faults in one single variable yield the best results in the case of one single variable faults but it must be noted that they cannot be used to diagnose faults in which there are more than one responsible variable.

- **Propose and test new improved variants of the diagnosis methods in MSQC:** In the thesis some new variants of Mason, Tracy and Young´s, Hawkins´, Murphy´s and Runger and Montgomery´s algorithms were proposed. The proposed variants of the MTY´s algorithm improve the performance of the original MTY´s algorithm in the strong correlation scenarios. The recursive Hawkins variants give excellent results and improve the original Hawkins´s methodology results. The Montgomery´s and Murphy´s variants also improve the performance of the original proposed algorithms. In the simulations the best performance was obtained with the pre-filtered recursive versions of Montgomery´s (FRM) and Hawkins´s methodologies (FRHM). Our conclusion is that the use of the modified MTY method (MTY1) in addition to these methods would serve to improve the interpretability of the detected signals.

- **Propose and test new diagnosis methods in Lb-MSPC:** In the thesis a new diagnosis method called the Fingerprints contribution plot (FCP), is proposed. This method tries to extend the use of the contribution plots, which is widely used as an unsupervised method for fault diagnosis, to the supervised case in which there is information about the different types of fault. The method is described in full detail and implemented in the case of the pasteurization process example.

- **Test and compare the performance of different diagnosis methods in Lb-MSPC:** The diagnosis methods exhibited different diagnosis performance. Fault signature methodology yield better results when used to build a model using small model windows. The other methods required larger model windows to improve their performance. Fault reconstruction methodologies requires not too small

model windows and performed well for early diagnosis in C2. The Fingerprints also requires not too small model windows and perform well for early diagnosis in C1. The PLS-DA requires large model windows and outperform the others in late diagnosis whilst has a poor performance in early diagnosis.

To sum up the results show that a mixed strategy based in the use of a method for the early diagnosis combined with other for the late diagnosis can be an interesting option. In this case the first model is aimed to the early diagnosis and the second is backing the first, helping in the diagnosis when the early diagnosis is not successful.

10.2 Future areas of research

This thesis opens several areas of research for future work amongst which the following could be outlined:

- Related to comparative performance analysis of the fault diagnosis methodology efficiency:
    - To extend the comparative analysis by including a broader spectrum of techniques including those from the diverse focus described as part of the review included Chapter 1. More specifically I consider of particular relevance the comparative analysis of methodology involving neuronal networks (NN) and methods based on independent component analysis (ICA), known to produce interesting results in specific fields.
    - To extend the comparative analysis and applications of the Lb-SPC methodologies that we have applied to continuous processes in this thesis, to batch processes.

- Related to the Fingerprints methodology:
    - To determine the classification performance of the fingerprints methodology to new and diverse conditions. *E.g.* application to well known benchmarks (Tennessee Eastman process) o usage of new simulation data characterised by specific latent variable structures selected according the algorithm of Arteaga and Ferrer (2010)
    - To improve the algorithm required to obtain SDI index parameters and the optimum number of components required for fault diagnosis. A priori the modified algorithm should allow for different number of components in the modelling of different types of faults.

Part V

Appendices

References

Alcala, C. F., Qin, S. J. (2009). "Reconstruction-based contribution for process monitoring". *Automatica,* 45(7), 1593–1600.

Anderson, T.W. (1984). "An Introduction to Multivariate Statistical Analysis". 2nd Wiley & Sons

Armitage, P., Parmar, M. (1986) "Some Approaches to the Problem of Multiplicity in Clinical Trials". *Proceedings of the XII th International Biometrics Conference Seattle*

Arteaga, F., Ferrer, A. (2002). "Dealing with missing data in MSPC: several methods, different interpretations, some examples". *Journal of Chemometrics* 16, 408-418.

Arteaga, F. , Ferrer, A. (2003). "Monitorización de procesos multivariantes con datos faltantes mediante análisis de componentes principales". *27 Congreso Nacional de Estadística e Investigación Operativa*. Lleida.

Arteaga, F., Ferrer, A. (2010). "How to simulate normal data sets with the desired correlation structure". *Chemometrics and Intelligent Laboratory Systems,* 101 ,1. 38-42

Barker, M., Rayens, W. (2003). "Partial Least Squares for discrimination". *Journal of Chemometrics* 17, 166-173.

Box, G. (1954). "Some theorems on quadratic forms applied in the study of analysis of varian ce problems, I. Effect of in equality of variance in the one-way classification". *The Annals of Mathematical Statistics,* 25, 290–302.

Box, G., Luceño, A. (1997). "Statistical Control by Monitoring and Feedback Adjustment". Wiley & Sons.

Bro, R., Kjeldahl, K., Smilde, K., Kiers, H.A.L (2008). "Cross-validation of component models: A critical look at current methods". *Analytical Bioanalytical Chemistry* 390, 1241-1251.

Camacho J., Ferrer, A. (2014) "Crossvalidation in PCA models with the element-wise K-fold(ekf) algorith: practical aspects. *Chemolab* 131, 37-50.

Chester, D., Lamb, D., Dhurjati, P. (1984). "Rule-based computer alarm analysis in chemical process plants". *In Proceedings of 7th Micro-Delcon* 22 -29.

Cheung, J. T, Stephanopoulos, G. (1990). "Representation of process trends part I. A formal representation framework". *Computers and Chemical Engineering* 14 (4 -5), 495-510.

Dayal, B., MacGregor, J.F., Taylor, P.A., Kildaw, R., Marcikic, S. (1994). "Application of feedforward neural networks and partial least squares regression for modelling Kappa number in a continuous Kamyr digester". *Pulp Paper Canada* 95, (1), 7-13.

Doganaksoy, N., Faltin, F. W., Tucker, W. T. (1991)." Identification of out of control quality characteristics in a multivariate manufacturing environment". *Communications in Statistics – Theory and Methods* 20(9):2775–2790.

Dubey, S.D. (1985). "Adjustment of p-values for Multiplicities of Intercorrelating Symptoms", *Proceedings of the VIth International Society for Clinical Biostatisticians, Germany*

Dunia, R., Qin, S.J. (1998) (a). "A unified geometric approach to process and sensor fault identification and reconstruction:the unidimensional fault case". *Computers Chem. Eng* 44 927-943

Dunia, R., Qin, S.J. (1998). (b). "Subspace approach to multidimensional fault identification and reconstruction". *AIChE Journal* Vol 44 pp. 1813-1831

Ferrer, A. (2007). "Multivariate statistical process control based on principal components analysis (MSPC-PCA): some reflections and a case study in an autobody assembly process". *Quality Engineering*, 19, pp. 311-325.

Ferrer, A. (2014). "Latent structures-based multivariate statistical process control: a paradigm shift". *Quality Engineering*, 26:1, pp. 72-91.

Frank, P. M. (1987). "Advanced fault detection and isolation schemes using nonlinear and robust observers". *10th IFACWorld Congress*, Munich, Germany.

Fuchs, C., Benjamini, Y. (1994). "Multivariate Profile Charts for Statistical Process Control". *Technometrics,* 36 pp. 182-195.

Geladi, P., Kowalski, B.R. (1986). "Partial Least-Squares Regression: A Tutorial". *Analytica Chimica Act,* 185, 1-17.

Geladi, P. (1989). "Analysis of Multi-way (Multi-mode) Data". *Chemometrics and Intelligent Laboratory Systems,* 7, 11-30.

Gertler, J., Singer D. (1990). "A new structural framework for parity equations based failure, detection and isolation". *Automatica, 26 (2)*. 381-388.

Gertler, J. (1998). "Fault Detection and Diagnosis in Engineering Systems". Marcel Dekker, Inc., New York.

Hawkins, D. M., Olwell, D.H (1988). "Cumulative sum charts and charting for quality improvement". 2th ed. Springer, New York

Hawkins, D. M. (1991). "Multivariate quality control based on regression- adjusted variables". *Technometrics* 33:61–75.

Hawkins, D. M. (1993). "Regression adjustment for variables in multivariate quality control". *Journal of Quality Technology* 25(3):170–182.

Hayter, A. J., Tsui, K. L. (1994). "Identification and quantification in multivariate quality control Problems". *Journal of Quality Technology* 26(3):197–207.

Henley, E.J. (1984). "Application of expert systems to fault diagnosis". *In AIChE annual meeting* San Francisco, CA.

Hochberg, Y. (1988). "A Sharper Bonferroni Procedure for Multiple Test of Significance". *Biometrika*, 75, pp. 800-802.

Holm, S. (1979). "A Simple Sequentially Rejective Multiple Test Procedure". *Scandinavian Journal of Statistics*, 6, pp. 65-70.

Hommel, G. (1988). "A Comparison of Two Modified Bonferroni Procedures". *Biometrika,* 75, pp. 383-386.

Hoskins J. C., Kaliyur, K. M., D. M. Himmelblau (1991). "Fault diagnosis in complex chemical plants using artificial neural networks" . *AICHE J.* 37(1),137-141.

Hunter J. S. (1986). "Exponentially weighted moving average" . *Journal of Quality Technology".* 18, pp. 97-102.

Iri, M., Aoki, K., O'Shima, E., Matsuyama, H. (1979). " An algorithm for diagnosis of system failures in the chemical process". *Computers and Chemical Engineering* 3, 489-493.

Jackson J.E. (1991) A User´s Guide to Principal Components. Wiley & Sons.

Jackson, J.E., Mudholkar, G.S. (1979). "control procedures for residuals associated with principal component analysis". *Technometrics* 21,341-349

Janusz, M., Venkatasubramanian, V. (1991). "Automatic generation of qualitative description of process trends for fault detection and diagnosis". *Engineering Applications of Artificial Intelligence* 4 (5), 329 -339.

Jionghua, J., Jianjun, S. (2008) "Causation-Based T2 Decomposition for Multivariate Process Monitoring and Diagnosis". *Journal of Quality Technology* 40, 1, pp. 46-58.

Jolliffe, I.T (2002) . "Principal Component Analysis", Series: Springer Series in Statistics. Springer, NY

Kourti, T., Lee, J. ; MacGregor, J.F. (19 96). "Experiences with Industrial Applications of Projections Methods for Multivariate Statistical Process Control". *Computers in Chemical Engineering* 20 Suppl., 745-750.

Kourti, T., MacGregor, J.F. (1996). "Multivariate SPC Methods for Process and Product Monitoring". *Journal of Quality Technology* 28, (4), 409-428.

Lucas, J. M., Saccucci, M. S. (1990). "Exponentially weighted moving average control schemes: Properties and enhancements", *Technometrics 32*, 1-29.

MacGregor, J. F., Marlin, T. E., Kresta, J., Skagerberg, B. (1991). "Multivariate statistical methods in process analysis and control". *In Y. Arkun & W. H. Ray (Eds.), Chemical process control*/CPCIV* (pp. 79_/100). *CACHE-AIChE*.

MacGregor, J.F., Jaeckle, C., Kiparissides, C., Koutoudi, M. (1994): "Process monitoring and diagnosis by Multiblock PLS Methods". *AIChE Journal* 40, (5), 826-838.

MacGregor, J. F., Kourti, T. (1995). "Statistical process control of multivariate processes". *Control Engineering Practice* 3 (3), 403-414.

MacGregor, J.F. (1996). "Using On-Line Process Data to Improve Quality. Is there a Role for Statisticians?. Are They Up for the Challenge?". *ASQC Statistics Division Newsletter,* 16, 2, 6-13.

MacGregor, J.F., Cinar, A. (2012). "Monitoring, fault diagnosis, fault-tolerant control and optimization: Data driven methods". *Computers and Chemical Engineering*

Mason, R. L., Tracy, N. D., Young, J. C. (1995a). "Multivariate control charts for individual observations". *Journal of Quality Technology* 24(2):88–95.

Mason, R. L., Tracy, N. D., Young, J. C. (1995b). "Decomposition of T^2 for multivariate control chart interpretation". *Journal of Quality Technology* 27(2):99–108.

Mason, R. L., Tracy, N. D., Young, J. C. (1997). A practical approach for interpreting multivariate T^2 control chart signs. *Journal of Quality Technology* 29(4):396–406.

Mason, R.L, Young, J.C. (1999). "Improving the Sensitivity of the T^2 statistic in Multivariate Process Control". *Journal of Quality Technology* 31 (2), pp. 155-165.

Miller, P., Swamson, R. E., Heckler, C.F. (1993). "Contribution plots: The missing link in multivariate quality control" *presented at Annual Fall Technical Conference of the American Society for Quality Control (Milwakee WI) and the American Statistical Association (Alexandria VA)*

Murphy, B. J. (1987). "Selecting out of control variables with the T^2 multivariate quality procedure".*The Statistician* 36:571–583.

Nelson, P.P.C., Taylor, P.A., MacGregor, J.F. (1996). "Missing data methods in PCA and PLS: Score calculations with incomplete observations". *Chemometrics Intell. Lab. Sist.* 35, 45-65.

Nelson, P.P.C. (2002). "Treatment of missing measurements in PCA and PLS models", *M. Eng. Thesis*. Department of Chemical Engineering, McMaster University. Hamilton, Ontario, Canada.

Niida, K. (1985). "Expert system experiments in processing engineering". *In Institution of chemical engineering symposium series* pps.529 -583.

Nomikos, P., MacGregor, J.F. (1995). "Multivariate SPC Charts for Monitoring Batch processes".*Technometrics* 37, (1), 41-59.

O'Reilly, J. (1983) "Observers for Linear Systems". Academic Press.

Page, E. S. (1961). "Cumulative sum control charts". *Technometrics 3*(1), pps.1- 9.

Patton, R. J. ; Chen J. (1997). "Observer-based fault detection and isolation: Robustness and applications" . *Contr. Eng. Practice* 5(5), 671- 682.

Qin, S.J., Valle, S., Piovoso, M.J. (2001). "On unifying multiblock analysis with application to decentralized process monitoring". *Journal of Chemometrics* 15, 715-742.

Qin, S.J. (2012). "Survey on data-driven industrial process monitoring and diagnosis". *Annual reviews in control* 36, 220-234.

Roy, J. (1958). "Step-down procedures in multivariate analysis". *The Annals of Mathematical Statistics* 29:1177–1187.

Raich, A., Cinar, A. (1996). "Statistical process monitoring and disturbance diagnosis in multivariable continuous processes". *American Institute of Chemical Engineers Journal* 42 (4), 995 -1009.

Rencher, A. C. (1993). "The contribution of individual variables to Hotelling´s T^2, Wilks´ Λ and R^2. *Biometrics,* 49 .pp.479-489.

Rengaswamy, R., Venkatasubramanian, V. (1995). "A syntactic pattern-recognition approach for process monitoring and fault diagnosis". *Engineering Applications of Artificial Intelligence* 8 (1), 35 -51.

Rengaswamy, R., Hagglund, T., Venkatasubramanian, V. (2001). "A qualitative shape analysis formalism for monitoring control loop performance". *Engineering Applications of Artificial Intelligence* 14 (1), 23-33.

Roberts. S. (1959). "Control charts tests based on geometric moving averages". *Technometrics,* Vol 42(1) pp. 97-102.

Runger, G. C., Montgomery, D. C. (1996). "Contributors to a multivariate statistical process control chart signal". *Communications in Statistics – Theory and Methods* 25(10):2203–2213.

Russell, E. L., Chiang, L. H., Braatz, R. D. (2012). "Data-driven methods for fault detection and diagnosis in chemical processes". Springer Science & Business Media.

Sankoh, A.J., Huque, M.F., Dubey, S.D. (1997). "Some Comments on Frequently Used Multiple Endpoint Adjustment Methods in Clinical Trials". *Statistics in Medicine* , 16, 2529-2542.

Sarle, W.S. (1994). "Neural networks and statistical models". *Proceedings of the 19th Annual SAS Group conference*, Cary, NC. 1538-1550.

Shewhart, W. A. (1931). "Economic control of quality of manufactured product". New York: D. Van Nostrand Company. 501

Smith, M. (1993). "Neural networks for statistical modelling". Van Nostrand Reinhold. N.Y.

Sjöström, M., Wold, S., Söderström, B. (1985), "PLS discriminant plots". *Proceedings of PARC in Practice,* Amsterdam, Elsevier Science Publishers B.V.,North-Holland pp. 19–21.

Skogestad, S. (1996). "MATLAB Distillation Column Model ("Column A")." Retrieved from: http://www.nt.ntnu.no/users/skoge/book/matlab_m/cola/cola.htm

Tano, K., Samskog, P.O., Andreasson, B. (1995). "Mathematical modelling in mining industry increases both quality and quantity!.- multivariate modelling and on-line data presentation for process optimization at LKAB. Presented at the *International Federation of Automatic Control Symposium on Automation in Mining Mineral and Metal Processing.* Sun City. South Africa.

Tracy, N. D., Young, J. C., Mason, R. L. (1992), "Multivariate Control Charts for Individual Observations." *Journal of Quality Technology*, 24, 88–95.

Tukey, J.W., Ciminera, J.L., Heyse, J.F. (1985). "Testing the Statistical Certainty of a Response to Increasing Doses of a Drug". *Biometrics ,* 45, pp.295-301.

Ungar, L. H., Powell, B. A., Kamens, S. N. (1990). "Adaptive networks for fault diagnosis and process control". *Computers and Chem. Eng.* 14(4-5), 561-572.

Valle, C. S., Qin, S. J., Piovoso, M. J., Bachmann, M., Mandakoro, N. (2001). "Extracting fault subspaces for fault identification of a polyester film process". *Proc. American Control Conference,* Arlington, VA, 4466-4471.

Venkatasubramanian, V., Chan, K. (1989). "A neural network methodology for process fault diagnosis". *American Institute of Chemical Engineers Journal* 35 (12), 1993 -2002.

Venkatasubramanian, V., Rengaswamy, R., Yin, K., Kavuri, S. N. (2003). "A review of process fault detection and diagnosis Part I: Quantitative model-based methods". *Computers and Chemical Engineering* 27, 293-311

Venkatasubramanian V., Rengaswamy R., Yin K.; Kavuri, S. N. (2003). "A review of process fault detection and diagnosis Part II: Qualitative models and search strategies". *Computers and Chemical Engineering* 27, 313-326

Venkatasubramanian, V., Rengaswamy R., Yin K. ; Kavuri S. N. (2003). "A review of process fault detection and diagnosis Part III: Process history based methods". *Computers and Chemical Engineering* 27, 327-346

Vidal-Puig S., Janssen, P.M.A, Sanchis J. and Ferrer A. (2005). "Fault diagnosis in the on-line monitoring of a pasteurization process: a comparative study of different strategies". *5th Annual Conference of the European Network for Business and Industrial Statistics (ENBIS) Newcastle (U.K)*

Vidal-Puig S., Ferrer, A. (2008) "Fingerprints contribution plot: A new approach for fault diagnosis in multivariate statistic process control", *11th International Conference on Chemometrics in Analytical Chemistry 27-31, Montpellier (France)*

Villaba, P.M. (2012). "Multivariate statistical process monitoring of a distillation column". *Master Thesis Universidad Politécnica de Valencia.*

Watanabe K., Matsura I., Abe M., Kubota M., Himmelblau D. M. (1989). "Incipient fault diagnosis of chemical processes via artificial neural networks". *AICHE J.* 35(11), 1803-1812.

Wierda, S.J. (1993) "Papers 557", Groningen State, Institute of Economic Research

Westerhuis, J.A., Kourti, T., MacGregor, J.F. (1998a). "Analysis of multiblock and hierarchical PCA and PLS models. *Journal of Chemometrics* 12, 301-321.

Wise, B. M., Ricker, N. L.(1991) "Recent advances in multivariate statistical process control: Improving robustness and sensitivity". *In Proceedings of the IFAC, ADCHEM Symposium ,* 125-130.

Wold, H. (1985). "Partial least squares". In Kotz, Samuel; Johnson, Norman L. Encyclopedia of statistical sciences 6. New York: Wiley. pp. 581–591.

Wold, S. (1978). "Cross-Validatory Estimation of the Number of Components in Factor and Principal Component Models. *Technometrics* 20, 397-405.

Wold S.; Albano C.; Dunn WJ III.; Esbensen K.; Hellberg S.; Johansson E.; Sjöström M.(1983). "Pattern recognition: finding and using patterns in multivariate data". I*n: H. Martens and H. Russwurm, Jr., Editors, Food Research and Data Analysis,Applied Science Publ., London,* pp. 147–188.

Wold, S., Geladi, P., Esbensen, K., Öhman, J. (1987). "Multi-Way Principal Components-and PLS Analysis". *Journal of Chemometrics* 1, 41-56.

Wold, S., Kettaneh. N., Tjessem, K. (1996). "Hierarchical multiblock PLS and PC models for easier model interpretation and as an alternative to variable selection". *Journal of Chemometrics* 10, 463-482.

Yoon, S., MacGregor, J.F. (2001). "Fault diagnosis with multivariate statistical model parts I: using steady state fault signatures". *Journal of Process Control* Vol 11, 387-400

Yue, H., Qin, S.J. (2001). "Reconstruction based fault identification using a combined index". *Ind. Eng. Chem. Res*. Vol 40 pp. 4403-4414.

Zarzo, M., Ferrer, A., Romero, R. (2002a). "Fault detection by PLS to improve the quality of batch PPOX production". *3rd International Chemometrics Research Meeting* ICRM2002. Veldhoven (Holanda).

Zarzo, M., Ferrer, A., Romero, R. (2002b). "Multivariate process control to improve the quality of batch PPOX production". *2nd Annual Conference on Business and Industrial Statistics*. Rimini (Italia).

Glossary

The sense in which one should understand some of the terms and acronyms used in this document is as follows:

- **ANOVA**: ANalysis of VAriance.
- **ARL:** Average Run Length.
- **CUSUM:** CUmulative SUM.
- **D/AP:** Dubey, Armitage and Parmar procedure (ad hoc variant of DFT)
- **DFT:** Doganaksoy Faltin and Tucker´s method.
- **EWMA:** Exponentially Weighted Moving Average.
- **FDI:** Fault Diagnosis and Isolation.
- **FMUSE:** pre-Filtered Montgomery and Runger´s method Under a Sequential. Extraction
- **FRH:** pre-Filtered Recursive Hawkins´method.
- **FRM:** pre-Filtered Recursive Montgomery and Runger´s metho.d
- **FT2M:** pre-Filtered T2-Murphy´s method.
- **GCI:** Global Classification Index.
- **HM:** Hawkin´s method.
- **Lb-MSPC:** Latent based Multivariate Statistical Process Control.
- **LCL:** Lower Control Limit.
- **M:** Murphy´s method.
- **MCUSUM:** Multivariate CUSUM.
- **MEWMA**: Multivariate EWMA.
- **MR:** Montgomery and Rungers´method.
- **MSE:** Mean Square Error.
- **MSPC:** Multivariate Statistical Process Control.
- **MSQC:** Multivariate Statistical Quality Control.
- **MTY:** Mason Tracy and Young´s method.
- **MTY1:** Variant 1 of Mason Tracy and Young´s method.
- **MTY2:** Variant 2 of Mason Tracy and Young´s method.
- **MUSE:** Montgomery and Rungers´method Under a Sequential Extraction.

- **NIPALS:** Non-Linear Iterative Partial Least Squares.
- **NN:** Neural Network.
- **NOC:** Normal Operation Conditions.
- **PCA:** Principal Components Analysis.
- **PLC:** Progammable Logic Controller.
- **PLS:** Partial Least Squares.
- **PLS-DA**: Partial Least Square Discriminant Analysis.
- **RH**: Recursive Hawkins´method.
- **RM:** Recursive Montgomery and Runger´s method.
- **SDG:** Signed Digraph.
- **SIMCA**: Soft Independent Modelling Class Analogy.
- **SPC:** Statistical Process Control.
- **SPE:** Square Predicction Error.
- **SVD:** Singular Valued Decomposition.
- **TCH**: Tukey, Ciminera and Heyse procedure (ad hoc variant of DFT).
- **TCI:** True Classification Index
- **T2M:** T2-Hotelling Murphy´s methodology.
- **T2RH:** Recursive Hawkin´s methodology with a Hotelling´s T2 trigger mechanism.
- **T2FRH:** pre-Filtered Recursive Hawkins with a Hotelling´s T2 trigger mechanism.
- **UCL:** Upper Control Limit.
- **USPC:** Univariate Statistical Process Control.
- **WCI:** Wrong Classification Index.

Notation

The mathematical notation used in this document is the following: bold capital letters for matrices, bold lower case letters for vectors and cursive letters for scalars.